Bioresponsive Polymer-Phospholipase A_2 Conjugates as Novel Anti-cancer Agents

Elaine Lesley Ferguson
MRPharmS

A thesis submitted to Cardiff University in partial fulfilment of the requirements for the degree of Doctor of Philosophy

Centre for Polymer Therapeutics
Welsh School of Pharmacy
Cardiff University
United Kingdom

ProQuest LLC
789 East Eisenhower Parkway
P.O. Box 1346
Ann Arbor, MI 48106-1346

Acknowledgements

First and foremost, I would like to express my sincere gratitude to my supervisor, Prof. Ruth Duncan, for her insight, support and enthusiasm. I am also grateful to Dr. Dirk Schmaljohann, who has aided me with technical and intellectual matters. I greatly appreciate having the opportunity to contribute to such an exciting field of research and would also like to recognise Cardiff University and the Centre for Polymer Therapeutics for funding my PhD studentship.

I would also like to acknowledge all my friends and colleagues in the Centre for Polymer Therapeutics: new members (Monerah, Ed), past members (Saly, Zeena, Tom), visiting scientists (Marjan, Davide, Verena, Lorella, Benjaporn), and nanomedicine platform collaborators (Alison, Alison, Matt, Simon, Arwyn). Special thanks go to Catherine, Joe, Helena, Fran, Karen, Sian, Philipp, Chris, Danielle, Neal, Wendy, Jan and Jo for offering me friendship, support, assistance and entertainment! Finally, an extra big thank you goes to Lucile, Kerri and Sam who have been with me every step of the way- the past 3 years wouldn't have been half as rewarding, fun and worthwhile without them! Thank you!

Additional passion and vitality for this research was provided externally through my involvement in several social activities. Thus, Cardiff Triathletes provided me with light relief during the tough times and gave me the opportunity to meet many good friends (Sally, Kat, Rachel, James, Hannah, Claire, Julia, Jen...). Special thanks go to Dave, who has been a star during the last months of this PhD and I thank him for his encouragement, patience and distraction!

In addition, I wish to acknowledge my best friends- Jessica, Matthew, Ed, Rebecca and Laura- for their friendship, phone calls, faith in my abilities and genuine interest in my studies. Thank you for always being there!

Finally, the completion of this PhD would also not have been possible without the love, support and infinite belief of my whole family, but especially Mum, Dad, Victoria, Heather, Guy and Markus. Words cannot express my gratitude for their contribution to this work! I love you!

'Dulcius ex Asperis'

Abstract

Increasingly sophisticated new treatments such as trastuzumab (Herceptin®) and Bevacizumab (Avastin®) have contributed to reduced mortality from breast cancer over recent years, nevertheless 40-60 % of those affected still die from metastatic disease. Thus there remains an urgent need for novel therapies for breast cancer. As PLA_2 (crotoxin) has proven anticancer activity but its use is limited by non-specific toxicity, and polymer-drug and polymer-protein conjugates are finding growing use as anticancer agents, the aim of this thesis was to explore the potential of polymer-PLA_2 conjugates as a new treatment for breast cancer. Polymer conjugation has previously been shown to reduce systemic toxicity of proteins, prolong their plasma half-life and promote tumour-specific targeting by the enhanced permeability and retention (EPR) effect.

First, the synthesis and characterisation methods were optimised using trypsin as a model. After these studies highlighted dextrin as the best polymer for conjugation, dextrin-PLA_2 (*Apis mellifera* venom) conjugates were prepared. Dextrin was chosen for conjugation as it can be used to mask protein activity in the protein masked-unmasked polymer therapy (PUMPT) concept. Such conjugates retained 36 % enzyme activity compared to free PLA_2, and moreover, unmasking by α-amylase degradation of dextrin regenerated full enzyme activity. However, while free PLA_2 was found to be very haemolytic, dextrin-PLA_2 displayed no haemolytic activity, and unmasking by α-amylase degradation of dextrin did not reinstate this activity. The conjugate displayed significant toxicity towards several tumour cell lines, including human breast cancer. Indirect evidence that epidermal growth factor receptor (EGFR) status and tyrosine kinase activity of the receptor influences PLA_2-induced anti-proliferative activity were shown. Uptake studies have revealed that conjugation of dextrin to PLA_2 reduces non-specific binding to breast cancer cells. In a further study, dextrin-PLA_2's ability to burst DaunoXome® using the polymer-enzyme liposome therapy (PELT) concept was assessed. Here, it was seen that the conjugate released liposomally encapsulated drug and the combination caused enhanced cytotoxicity in MCF-7 cells.

These studies confirm the potential of dextrin-PLA_2 as a novel anticancer agent and/or as trigger for liposomal drug release and highlight the feasibility of developing a candidate for further *in vivo* pharmacokinetic and activity studies.

Index

Figures List

Table List

Abbreviations

ADEPT	Antibody-directed enzyme prodrug therapy
ALL	Acute lymphoblastic leukaemia
ANOVA	Analysis of variance
AP	Ammonium persulfate
ATCC	American type culture collection
B16F10	Murine melanoma cell line
BAEE	benzoyl L-arginine ethyl ester
BCA	Bicinchoninic acid
BSA	Bovine serum albumin
^{13}C	Carbon-13
Ca^{2+}	Calcium
Cont	Continued
$cPLA_2$	Cytoplasmic phospholipase A_2
CRC	Colorectal cancer
ddH_2O	Double distilled water
DMAP	4-dimethylaminopyridine
DMF	N,N-imethylformamide
DMSO	Dimethyl sulphoxide
ε	Extinction coefficient
EC_{50}	Effective concentration to achieve 50 % maximal response
ECACC	European collection of cell cultures
EDTA	ethylenediaminetetraaceticacid
EDC	1-ethyl-3(3-dimethylaminopropyl)carbodiimide
EEA1	Early endosome antigen 1
EGF	Epidermal growth factor
EGFR	Epidermal growth factor receptor
Enz	Enzyme
EPR	Enhanced permeability and tention effect
Eq.	Equivalent
ER	Endoplasmic reticulum
ESF	European Science Foundation
FACS	Fluorescence-activated cell sorting
FBS	Foetal bovine serum
FDA	US Food and Drug Administration
FITC	fluorescein isothiocyanate
FPLC	Fast protein liquid chromatography
FT-IR	Fourrier transform infrared spectroscopy
GCSF	Granulocyte colony stimulating factor
GDEPT	Gene-directed enzyme prodrug therapy
Gly	Glycine
GPC	Gel permeation chromatography
^{1}H	Hydrogen-1
HCl	Hydrochloric acid
HER	Human epidermal growth factor receptor
HPMA	N-(2-hydroxypropyl)methacrylamide
HI FBS	Heat-inactivated foetal bovine serum

HT29	Colon carcinoma cell line
IC_{50}	Concentration which inhibits cell growth by 50 %
IL2	Interleukin-2
IFNα	Interferon-α
IP	Inter-peritoneal
IR	Infra-red
IM	Intramuscular
IU	International units
IV	Intravenous
K_{cat}	Turnover rate
K_m	Affinity constant
L-BAPNA	$_N$-Benzoyl-$_L$-arginine-$_p$-Nitroanilide
LDH	Lactase dehydrogenase
LAMP-1	lysosome-associated membrane protein-1)
LE/L	Late endosome/lysosome
LEAPT	Lectin-directed enzyme prodrug therapy
Leu	Leucine
Lys	Lysine
mAb	Monoclonal antibody
MCF-7	Breast adenocarcinoma cancer cell line
mPEG	Monomethoxy-PEG
MSH	Melanocyte stimulating hormone
MTT	3-(4,5-dimethylthiazol-2-yl)-2,5-diphenyl-2H-terazoliumbromide
MW	Molecular weight (weight average)
MWCO	Molecular weight cut-off
N_2	Nitrogen
NA	Not applicable
NaOH	Sodium hydroxide
NAp	p-Nitroanilide
NCS	Neocarzinostatin
ND	Not determined
NMR	Nuclear magnetic resonance
NS	Not stated/ not significant
NSCLC	Non-small cell lung cancer
OG	Oregon green
ONp	p-nitrophenol
p-gp	p-glycoprotein
PAMAM	Polyamidoamine dendrimer
PBS	Phosphate buffered saline
PC	Phosphatidylcholine
PDEPT	Polymer-directed enzyme prodrug therapy
PE	Phosphatidylethanolamine
PDI	Polydispersity index
PEG	Polyethylene glycol
PEI	Polyethylenimine
PELT	Polymer Enzyme Liposome Therapy
PGA	Poly-L-glutamic acid
Phe	Phelnylalanine

PI	Phosphatidylinositol
pI	Isoelectric point
pKa	Acid dissociation constant
PLA_2	Phospholipase A_2
PLC	Phospholipase C
PS	Phosphatidylserine
PUMPT	Polymer masking UnMasking Protein Therapy
R	Receptor
RBC	Red blood cell
RES	Reticuloendothelial system
RI	Refractive index
RPMI	Rose park memorial institute (cell culture medium)
RT	Room temperature
S	Substrate concentration
SCID	Severe combined immunodeficiency disease
SD	Standard deviation
SDS	Sodium dodecyl sulphate
SDS PAGE	Sodium dodecyl sulphate polyacrylamide gel electrophoresis
SEC	Size exclusion chromatography
SEM	Standard error of the mean
SM	Sphingomyelin
SMA	Styrene-co-maleic anhydride
SMANCS	Styrene-co-maleic anhydride-neocarzinostatin
$sPLA_2$	Secretory phospholipase A_2
SU	Sigma units
Sulfo-NHS	N-hydroxysulfosuccinimide
TEM	Transmission electron microscopy
TEMED	N,N,N,N'-tetra-methyl-ethylenediamine
TK	Tyrosine kinase
TKI	Tyrosine kinase inhibitor
TLC	Thin layer chromatography
TMPEG	Tresylated monomethoxy polyethylene glycol
TNBS	2,4,6-trinitrobenzenesulfonate
TR	Texas red
UKCCCR	United Kingdom coordinating committee on cancer research
UV	Ultraviolet
V	Velocity
V_b	Bed volume
V_{max}	Maximum velocity
V_o	Void volume
VDEPT	Virus-directed enzyme prodrug therapy

Chapter One

General Introduction

1.1 Introduction

Cancer is defined as a collection of life-threatening diseases, which are characterised by uncontrolled division of abnormal cells (National Cancer Institute, 2005). It currently affects one in three British people, and one in four people die from it. While mortality associated with other major diseases, such as heart disease and infections, has improved since 1950, cancer mortality has shown little such progress and became the most common cause of death in Britain since 1969 in women, and 1995 in men (Office for National Statistics, 2004). Meanwhile, recent research has shown that 50 % of cancers could be prevented by lifestyle changes such as smoking cessation, sensible eating and drinking, and increased exercise (Cancer Research UK, 2005).

Therefore, the aim of this study was to synthesise dextrin-phospholipase A_2 (PLA_2) conjugates to investigate the potential of a polymer-PLA_2 conjugate, either as an anti-cancer agent or for use as a trigger to promote release of liposome-encapsulated drug, in the context of Polymer Enzyme Liposome Therapy (PELT).

The traditional options available for the management of cancers include surgery, radiotherapy, cytotoxic drugs, immunotherapy and hormonal agents. The aims of treatment vary from curative to prolonging life or palliating symptoms. It has become an increasingly common practice to combine two or more treatments for cancer therapy, as they can be selected to achieve a synergistic action by, for example, targeting different points in the cell cycle, or blocking different growth factor receptors (reviewed in Moore, 2007). Most current drugs act by preventing nucleic acid synthesis or mitosis.

Unfortunately, conventional cancer treatments are often restricted by adverse systemic effects. Due to the mechanism of action of many chemotherapeutics, rapidly dividing cells, such as bone marrow, ovaries and testes are particularly sensitive to cytotoxic drugs. Further common adverse effects of chemotherapeutics include hair loss, nausea and vomiting and anaemia. These adverse effects have a limiting effect on the dose, frequency of administration and total cumulative dose, as well as prolonging the patient's stay in hospital and decreasing their quality of life.

Another unfortunate consequence of chemotherapy is the development of resistant tumour cells. Cells exhibit various mechanisms of resistance, including upregulation of p-glycoprotein (p-gp), a membrane transport protein, increased levels of target, for example dihydrofolate reductase, and decreased influx of drug.

Novel approaches to cancer treatment

The search for better cancer treatments is ongoing and research largely falls into two categories; the design of novel tumour-specific molecular targets using genomics and proteomics research and improving drug delivery and tumour targeting. One approach currently showing promise in the fight against cancer is 'nanomedicine', defined by the European Science Foundation (ESF) as 'the science and technology of diagnosing, treating and preventing disease and traumatic injury, of relieving pain, and of preserving and improving human health, using molecular tools and molecular knowledge of the human body' (European Science Foundation, 2005). Nanomedicines have also been defined by the ESF as 'nanometer size scale complex systems, consisting of at least two components, one of which being the active ingredient'.

Polymer therapeutics are nanomedicines that are designed to deliver drug(s) specifically to tumours via the enhanced permeability and retention (EPR) effect, while reducing the exposure of normal tissue, and consequently reducing systemic toxicity, and prolonging drug half-life (reviewed in Duncan, 2006). The term 'polymer therapeutic' was coined by Duncan and describes a class of therapeutic agents comprising of at least two components, including a water soluble polymer covalently attached to an active constituent, such as a drug, protein, gene or peptide (reviewed in Duncan, 2003). Over the past decade, several polymer-protein conjugates have been in routine clinical use, while 11 polymer-drug conjugates have entered clinical development. Of these, N-(2-hydroxypropyl)methacrylamide (HPMA) copolymer-doxorubicin has shown clinical activity in breast cancer (Vasey *et al*, 1999) and HPMA copolymer conjugates containing a combination of chemotherapy and aromatase inhibitors are already showing exciting synergistic activity (Vicent *et al*, 2004).

Concurrently, PLA_2 from snake venom (*Crotalus durissus terrificus)* has demonstrated promising activity in Phase I clinical trials (including breast cancer patients) and is already undergoing Phase II clinical trials as a cancer treatment. PLA_2 is an enzyme that specifically hydrolyses the sn-2 acyl bond of phospholipids releasing fatty acid and lysophospholipid. In Phase I clinical trials crotoxin was administered intramuscularly for 30 consecutive days at doses ranging from 0.03 to 0.22 mg/m^2. Patients with histologically confirmed solid tumours deemed untreatable by surgery, radiation therapy or conventional chemotherapy were selected. Four patients had breast cancer, and the cohort also included patients with gastrointestinal cancer, non-small cell lung cancer, prostate cancer and squamous cervix carcinoma. Results from these studies observing the anti-cancer properties of crotoxin look promising. Of 23 patients, 2 showed greater than 50 % tumour mass reduction, and 1 patient had a complete response to the treatment. However, 13 out of the 23 patients tested displayed some reversible, non-limiting neurotoxicity, including diplopia, palpebral ptosis, nystagmus and anxiety (Costa *et al*, 1998; Cura *et al*, 2002).

Hypothesis of PLA_2 conjugates as novel cancer therapeutics

Therefore, in this project, it is proposed that, by conjugating PLA_2 to a polymer, not only will the neurotoxicity be reduced, but it will also be possible to target the protein specifically to tumours actively, by targeting residues, and passively, by the EPR effect, thus prolonging the plasma circulation (described in more detail in section 1.2).

The two hypotheses for the use of a PLA_2 conjugate are depicted in Figure 1.1. It was postulated that the polymer-protein conjugate would localise in the tumour through the EPR effect and as a result of its selectivity towards cells that over-express the epidermal growth factor receptor (EGFR). Subsequently, the PLA_2 would adhere to the lipid membrane of cancer cells, to exert its enzymatic activity (Figure 1.1a). Figure 1.1b depicts the PELT model, where the liposome-encapsulated drug would accumulate in the tumour interstitium as a result of the EPR. Polymer-PLA_2 would next be administered and would accumulate in the tumour interstitum by the same mechanism, where it can hydrolyse the phospholipid bilayer of the liposomes, resulting in rapid release of the drug load to the cancerous cells.

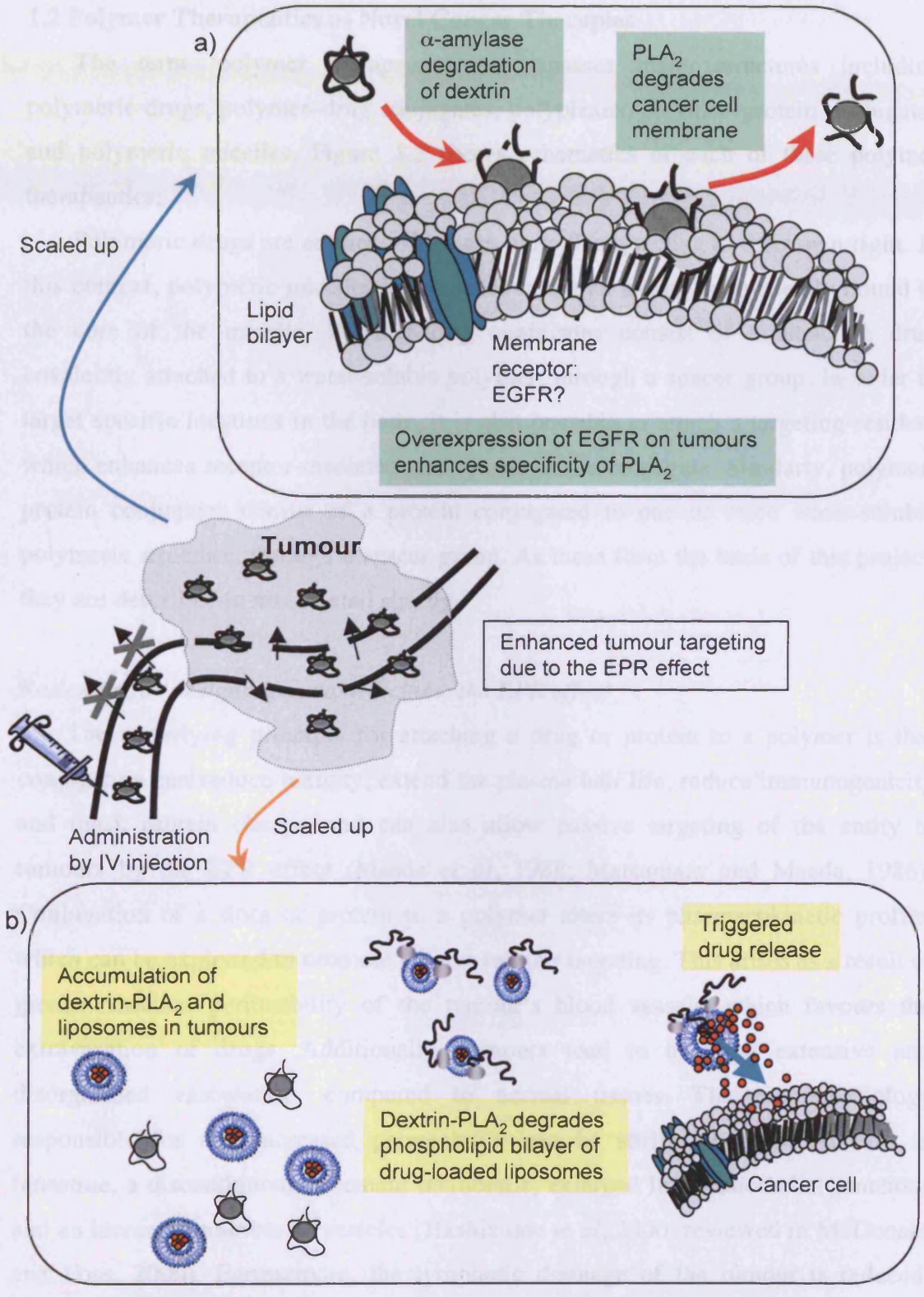

Figure 1.1 Schematic of hypothesised mechanism of action of dextrin-PLA_2. Panel (a) shows dextrin-PLA_2 acting as an active entity, and panel (b) depicts the PELT model.

1.2 Polymer Therapeutics as Novel Cancer Therapies

The term 'polymer therapeutic' encompasses many structures including polymeric drugs, polymer–drug conjugates, polyplexes, polymer–protein conjugates and polymeric micelles. Figure 1.2 shows schematics of each of these polymer therapeutics.

Polymeric drugs are entities, which are biologically active in their own right. In this context, polymeric micelles are micelles in which a drug is covalently bound to the core of the micelle. Polymer-drug conjugates consist of a bioactive drug covalently attached to a water-soluble polymer, through a spacer group. In order to target specific locations in the body, it is also possible to attach a targeting residue, which enhances receptor-mediated pinocytosis of the conjugate. Similarly, polymer-protein conjugates consist of a protein conjugated to one or more water-soluble polymeric structure, through a spacer group. As these form the basis of this project, they are described in more detail shortly.

Rationale for designing nanomedicines: the EPR effect

The underlying principle for attaching a drug or protein to a polymer is that conjugation can reduce toxicity, extend the plasma half life, reduce immunogenicity and mask protein charge, and can also allow passive targeting of the entity to tumours by the EPR effect (Maeda *et al*, 1988; Matsumara and Maeda, 1986). Conjugation of a drug or protein to a polymer alters its pharmacokinetic profile, which can be exploited to promote passive tumour targeting. This arises as a result of greater vascular permeability of the tumour's blood vessels, which favours the extravasation of drugs. Additionally, tumours tend to have an extensive and disorganised vasculature, compared to normal tissues. The pathophysiology responsible for this increased permeability can be attributed to an increase in fenestrae, a discontinuous basement membrane, enlarged inter-endothelial junctions and an increased number of vesicles (Hashizume *et al*, 2000; reviewed in McDonald and Foss, 2000). Furthermore, the lymphatic drainage of the tumour is reduced, resulting in the pooling of circulating polymer-protein conjugates in the tumour interstitium. Thus, the EPR effect can be exploited in the delivery of polymer therapeutics. While conventional, low molecular weight drugs can pass readily

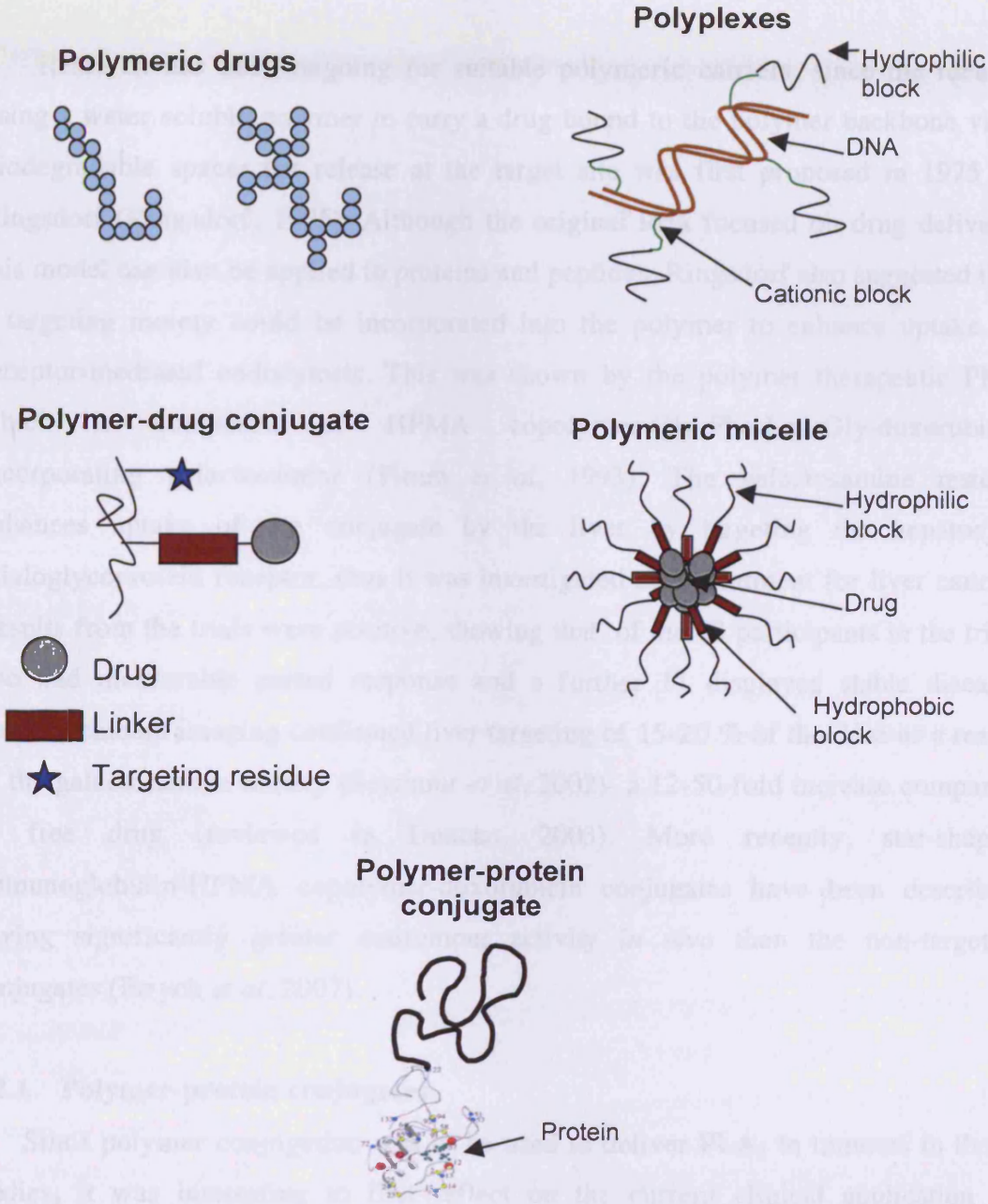

Figure 1.2 Categories of polymer therapeutics including polymeric drugs, polyplexes, polymer-drug conjugates, polymeric micelles and polymer-protein conjugates. (Adapted from Duncan, 2003)

through the bloodstream, into the tissue or to be excreted, polymer therapeutics can accumulate in tumour tissues due to the EPR (reviewed in Reddy, 2005; Seymour *et al*, 2002). A diagram of the EPR effect is shown in Figure 1.3.

Research has been ongoing for suitable polymeric carriers, since the idea of using a water soluble polymer to carry a drug bound to the polymer backbone via a biodegradable spacer for release at the target site was first proposed in 1975 by Ringsdorf (Ringsdorf, 1975). Although the original idea focused on drug delivery, this model can also be applied to proteins and peptides. Ringsdorf also suggested that a targeting moiety could be incorporated into the polymer to enhance uptake by receptor-mediated endocytosis. This was shown by the polymer therapeutic PK2, which is composed of HPMA copolymer-Gly-Phe-Leu-Gly-doxorubicin incorporating galactosamine (Pimm *et al*, 1993). The galactosamine residue enhances uptake of the conjugate by the liver by targeting the hepatocyte asialoglycoprotein receptor, thus it was investigated as a treatment for liver cancer. Results from the trials were positive, showing that, of the 23 participants in the trial, two had measurable partial response and a further 11 displayed stable disease. Gamma camera imaging confirmed liver targeting of 15-20 % of the dose as a result of the galactosamine moiety (Seymour *et al*, 2002)- a 12-50-fold increase compared to free drug (reviewed in Duncan, 2003). More recently, star-shaped immunoglobulin-HPMA copolymer-doxorubicin conjugates have been described having significantly greater antitumour activity *in vivo* than the non-targeted conjugates (Etrych *et al*, 2007).

1.2.1 Polymer-protein conjugates

Since polymer conjugation was to be used to deliver PLA_2 to tumours in these studies, it was interesting to first reflect on the current clinical application of polymer-protein conjugates. Ever since dextran-streptokinase (Streptodekase) was first used clinically (Torchilin *et al*, 1982) polymer therapeutics have become increasingly popular for delivering proteins, peptides and antibody-based therapeutics, with polymer-protein conjugates being the first polymer therapeutics to be used in practice. An ideal polymer-protein conjugate should be stable and usually

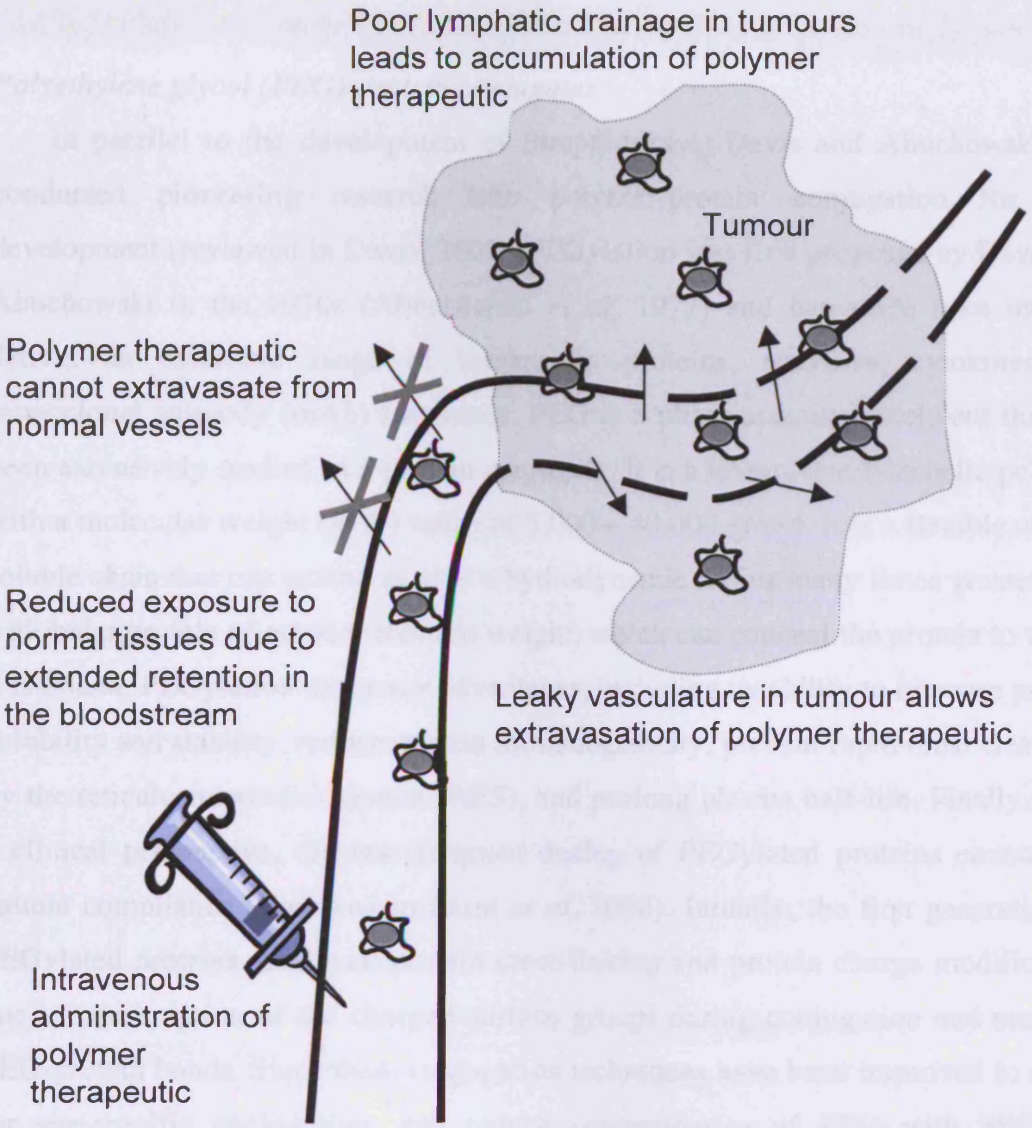

Figure 1.3 Tumour selectivity of polymer therapeutics by the EPR effect. (Adapted from Duncan, 2003)

pharmacologically inactive in the circulation. If required, it could then be specifically taken up by the tumour cells, internalised by endocytosis, and activated by enzymatic or hydrolytic cleavage in the lysosomes. Finally, the polymer needs to be excreted safely after delivering the drug load.

Polyethylene glycol (PEG)-protein conjugates

In parallel to the development of Streptodekase, Davis and Abuchowski also conducted pioneering research into polymer-protein conjugation for drug development (reviewed in Davis, 2002). PEGylation was first proposed by Davis and Abuchowski in the 1970s (Abuchowski *et al*, 1977) and has since been used to deliver an extensive range of therapeutic proteins, enzymes, cytokines and monoclonal antibody (mAb) fragments. PEG is a pharmaceutical excipient that has been extensively studied as a protein conjugate. It is a linear, semitelechelic polymer with a molecular weight (MW) range of 5,000 – 40,000 g/mol. It is a flexible, water-soluble chain that can extend to give a hydrodynamic radius many times greater than a globular protein of equal molecular weight, which can conceal the protein to which it is bound. PEGylation has many advantages, including its ability to increase protein solubility and stability, reduce protein immunogenicity, prevent rapid renal clearance by the reticuloendothelial system (RES), and prolong plasma half-life. Finally, from a clinical perspective, the less frequent dosing of PEGylated proteins encourages patient compliance (reviewed in Pasut *et al*, 2008). Initially, the first generation of PEGylated proteins displayed protein cross-linking and protein charge modification due to consumption of the charged surface groups during conjugation and unstable PEG-protein bonds. Since then, conjugation techniques have been improved to allow for site-specific conjugation, and reduce contamination of PEG with PEG-diol (Brocchini *et al*, 2007).

In 1990, PEG-adenosine deaminase (Adagen®) became the first polymer-protein conjugate to receive US Food and Drug Administration (FDA) approval for the treatment of severe combined immunodeficiency disease (SCID). It acts by replenishing levels of adenosine deaminase which are missing in this disease. Studies have demonstrated improved efficacy and reduced immunogenicity of Adagen®, than

previous therapies involving blood transfusion or administration of native enzyme (Chaffee *et al*, 1992; Hershfield *et al*, 1987). Attempts to use gene therapy for adenosine deaminase replacement in SCID have also shown impressive levels of immune reconstitution, however, vector-related leukaemias have overshadowed this success (Kohn *et al*, 2003).

Shortly after, in 1994, a PEG-L-asparaginase conjugate (Oncaspar®) received approval by the FDA for the treatment of acute lymphoblastic leukaemia (ALL). It is useful in the treatment of leukaemia as leukaemic cells must rely on an external source of asparagine as a result of a defect in asparagine synthetase. The administration of asparaginase degrades asparagine, thus depriving leukaemic cells of asparagine, and hence inhibiting protein biosynthesis (reviewed in Duncan, 2006; reviewed in Pasut *et al*, 2008). Asparaginase is also available in a non-conjugated formulation, but Oncaspar® demonstrates longer retention time in the plasma, reduced immunogenicity and requires only a weekly administration, while unconjugated L-asparaginase requires daily administration and can induce anaphylaxis and other hypersensitivity reactions (reviewed in Duncan, 2006; reviewed in Pasut *et al*, 2008).

PEG has also been used to deliver cytokines, such as interleukin-2 (IL2), recombinant granulocyte colony-stimulating factor (GCSF) and interferon-α (INFα). GCSF is used to promote re-growth of white blood cells following chemotherapy, thereby preventing chemotherapy-induced neutropenia. The PEGylated form of GCSF need only be administered as a single subcutaneous injection while native GCSF requires daily dosing by injection for two weeks to obtain equivalent prevention of neutropenia.

Other polymer-protein conjugates currently used as therapeutics

Maeda and colleagues synthesised SMANCS by covalently linking two styrene maleic anhydride chains (SMA) to neocarzinostatin (NCS), an anti-tumour protein (Maeda and Matsumara, 1989). Previously, NCS had proved to be too toxic for clinical use. However, following conjugation to SMA and subsequent dispersion in Lipiodol, a phase contrast agent, it was possible to administer it specifically to

tumour tissue using visualisation by x-ray, through the hepatic artery for the treatment of liver cancer. SMANCS has shown best results when given as 'patient-individualised treatment', where in a clinical trial 95 % of patients showed a decrease in tumour size, and 86 % of patients had decreased concentration of the biomarker for liver cancer, α-fetoprotein.

1.3 Rationale for design of polymer-PLA_2 conjugates

1.3.1 Choice of polymer model

It was important to select the most appropriate polymer for conjugation to PLA_2, in order to fully achieve the therapeutic aim. Polymers are high molecular weight substances made from one or more small repeating units (monomers). There are many structures of polymers; and size, 3-D shape (including crosslinking) and asymmetry determine the properties of them. Homopolymers are chains of polymers containing one type of repeating monomer. Copolymers contain more than one monomer, and may be an alternating copolymer chain, a block copolymer or a graft copolymer. The structure of the polymer also varies. It may be linear, star, branched or dendrimers.

A number of polymers have been used to prepare polymer-protein conjugates. These are summarised in Table 1.1, including examples of polymer-enzyme conjugates which have previously been described in the literature. An important factor in selecting a suitable polymer for protein conjugation is its ability to produce a conjugate whilst retaining enzymatic activity of the protein. PEG appears to be a very favourable choice for protein conjugation due to its extensive use in many regulatory authority-approved pharmaceutical products, its wide range of molecular weights and its potential for surface modification of proteins (reviewed in Harris and Chess, 2003; reviewed in Pasut *et al*, 2008). However, PEG is not suitable for use in these studies due to its potential for steric hindrance, which could interfere with the enzyme's access to its substrate. In contrast, HPMA copolymers have shown little such effect on substrate specificity and enzyme activity against low molecular weight substrates (Satchi-Fainaro *et al*, 2002). Here, a novel catalytic antibody-polymer conjugate for selective prodrug activation was prepared, which retained 75-81 % of its catalytic activity compared to the free antibody.

Table 1.1 Examples of polymer-protein conjugates in clinical use or development.

	Polymer-protein combination	Indication	FDA approval/ status	Manufacturer
Streptodekase®	Dextran-streptokinase	Anti-thrombolytic	1982	-
Adagen®	PEG-adenosine deaminase	Enzyme replacement therapy for SCID	1990	Enzon
SMANCS®	Polystyrene-co-maleic acid-neocarzinostatin	Hepatocellular carcinoma	1993	-
Oncaspar®	PEG-asparaginase	Acute lymphoblastic leukaemia	1994	Enzon
Neulasta®	PEG-filgrastim/ PEG-GCSF	Chemotherapy-induced neutropenia	2006	Amgen
PEG Intron®	PEG-interferon alfa-2b	Hepatitis C	2004	Schering
		Renal cell carcinoma Advanced melanoma	P III	
		Chronic myeloid leukaemia Gastrointestinal carcinoid tumour Brain and CNS tumour	P II	
Somavert®	Pegvisomant/ PEG-recombinant DNA protein (HGH analogue)	Acromegaly	2003	Pfizer

Table 1.1 Examples of polymer-protein conjugates in clinical use or development. (cont.)

	Polymer-protein combination	Indication	FDA approval/ status	Manufacturer
Pegasys®	PEG-interferon alfa-2a	Hepatitis C	2002	Roche
		Non-melanomatous skin cancer	P I	
		Chronic hepatitis B and C	P III	
Macugen®	Pegapanib (PEG-oligonucleotide)	Age-related macular degeneration	2004	Eyetech Pharmaceuticals/ Pfizer
CDP870	PEG- anti-TNF Fab' fragment	Rheumatoid arthritis	P III	Celltech
CERA (continuous erythropoiesis receptor activator)	PEG-epoetin	Renal anaemia	P III	Roche

The aim was to prepare polymer-enzyme conjugates with one enzyme bound to each polymer chain (1:1). This should create a molecule of sufficient size that it will concentrate efficiently in tumour cells by the EPR effect, but avoid uptake by the reticuloendothelial system (RES). Therefore, two polymers were selected as models for protein conjugation.

HPMA copolymers

The first of these was HPMA copolymer-Gly-Gly-p-nitrophenol (ONp) (5 mol %; ~ 30, 000 g/mol) (Figure 1.4a), which has a linear, random coil structure. HPMA copolymers are commonly prepared by a polymer analogous reaction, based on free radical precipitation co-polymerisation of HPMA monomer and methacryloylated (MA) peptides containing a reactive ONp group. This reaction produces the polymeric intermediate to which drugs, proteins or targeting moieties may be attached either by aminolysis or following further modification to the side chain to obtain the desired functionality (reviewed in Duncan, 2005).

HPMA-Gly-Gly-ONp is available commercially with a monomer feed ratio of HPMA:MA-peptide-ONp (95:5), as used for PK1, and (90:10), as used for PK2. Increasing the content of pendant side chains facilitates incorporation of more than one active agent or targeting group, as well as providing for higher drug loading (reviewed in Duncan, 2005). By selecting a HPMA copolymer with 5 mol % substitution, the possibility of multiple attachments to a single enzyme molecule is minimised, thus reducing the risk of cross-linking and interference with its active site, leading to inactivation of the enzyme. Determining the optimum reaction conditions for the conjugation can further control this.

HPMA copolymer was chosen for this study because it is a water-soluble, non-biodegradable polymer, which is accepted by the FDA for drug use. Furthermore, HPMA copolymers are already undergoing clinical trials, for example PK1 (Vasey *et al*, 1999). HPMA copolymers were originally designed as plasma expanders by Kopecek in the early seventies (Kopecek *et al*, 1973), but were later developed as anti-cancer drug carriers by linking the drug to the polymer to the polymer backbone through a pendant peptide spacer (Kopecek *et al*, 1985a). The –Gly-Gly- linker is a

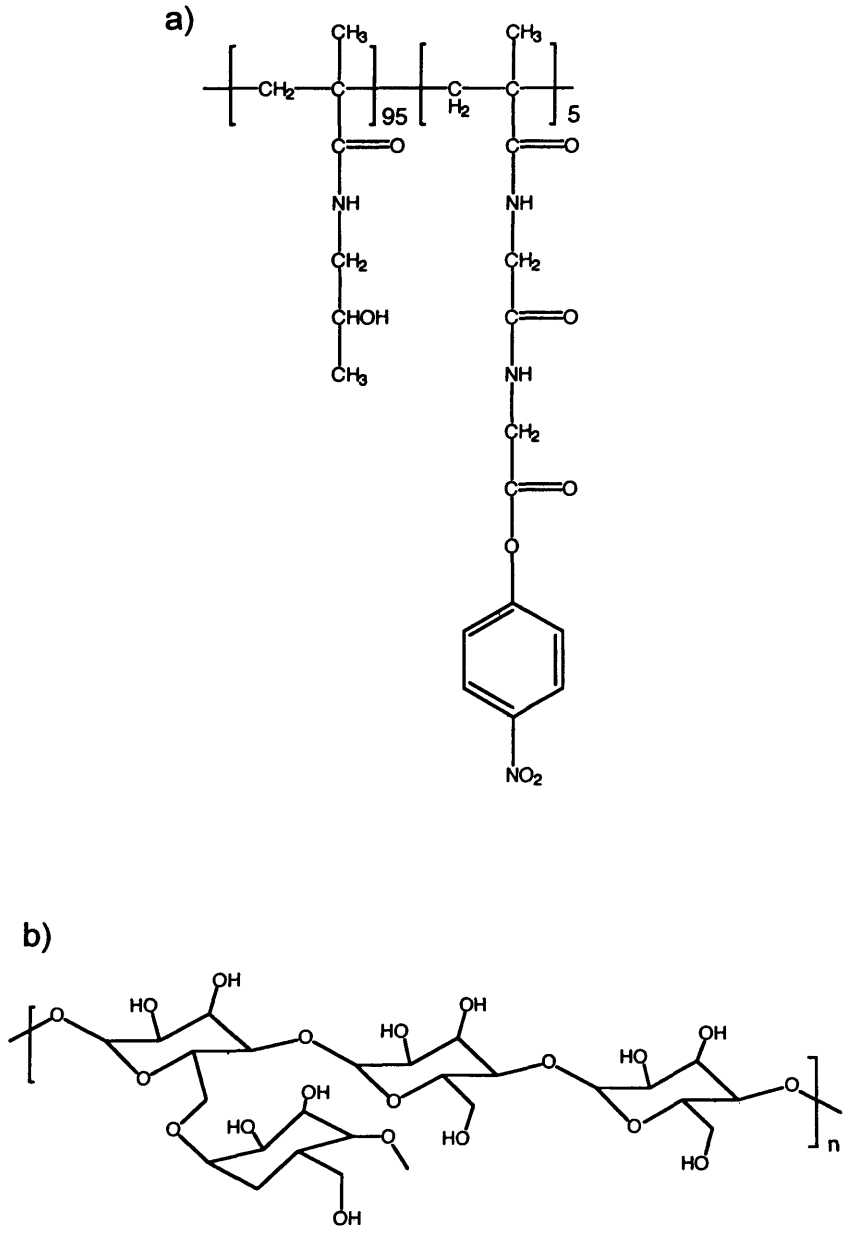

Figure 1.4 Chemical structure of a) HMPA copolymer-Gly-Gly-ONp, and b) dextrin.

short and stable, selectively degradable linker. The ONp group is used as marker of hydrolysis/ aminolysis as it produces a yellow colour when it is released from the polymer as the free p-nitroanilide (NAp), which is detectable quantitatively in the UV spectrophotometer.

Dextrin

The second polymer chosen as a model for this work was dextrin (MW: 51,000 g/mol) (Figure 1.4b), a biodegradable polysaccharide that is produced from the enzymatic hydrolysis of corn starch. Dextrin is a α-1,4 polymer of D-glucose with less than 5 % α-1,6 links, resulting in minimal branching of the polymer. It is rapidly degraded by α-amylase to yield the disaccharides maltose and iso-maltose, in just a few minutes (Hreczuk-Hirst *et al*, 2001a; Hreczuk-Hirst *et al*, 2001b). Studies on α-amylase-mediated degradation of dextrin have revealed that altering the degree of modification to the backbone by succinoylation can control the rate of enzymatic degradation (Hreczuk-Hirst *et al*, 2001a). Interestingly, several cases of elevated α-amylase concentrations in tumours have been reported (Inaji *et al*, 1991; Weitzel *et al*, 1988), where levels up to 85-fold normal have been observed, and this could be exploited for the delivery of anti-cancer proteins.

Dextrin was chosen as a model for these studies because it has been used clinically for many years and is FDA approved, proving it to be non-toxic and non-immunogenic. Caloreen is composed of maltodextrin, and has been used as a dietary supplement in patients with renal and hepatic failure. Following successful clinical safety trials, Icodextrin, a dextrin with a MW of ~ 20,000 g/mol, was approved for routine use as an intraperitoneal dialysis solution for chronic renal failure and is undergoing clinical trials for Kaposi's sarcoma treatment (Thornton *et al*, 1999). Moreover, dextrin has also been used as a carrier for the delivery of 5-fluorouracil to the intraperitoneal cavity (McArdle *et al*, 1994), and recent papers describe its conjugation to various drugs, including doxorubicin, tyrosinamide and biotin (Hreczuk-Hirst *et al*, 2001b).

The main advantages supporting the use of dextrin are its multifunctionality and biodegradability. Multifunctionality allows the polymer to surround the protein and

mask the protein's activity. Furthermore, since it has been shown that succinoylation delays the break down of dextrin, it is possible to tailor the rate of degradation, and consequently the unmasking of protein activity. This concept has recently been coined '**P**olymer masking-**U**n**M**asking **P**rotein **T**herapy' (PUMPT) using dextrin as a model polymer (Duncan *et al*, 2008). The hypothesis is that conjugation of a biodegradable polymer to a biologically active protein can mask activity and enhance stability in the bloodstream, while subsequent regeneration of activity can be achieved by triggered degradation of the polymer at the target site.

Biodegradable polymers for masking/unmasking of PLA_2 activity

Over recent years the concept of using biodegradable polymers for delivery of therapeutic proteins has become increasingly attractive. The use of non- or slowly biodegradable polymers in macromolecular therapeutics for an extended length of time have the potential to cause long term vacuolisation (Bendele *et al*, 1998), development of lysosomal storage disease (Chi *et al*, 2006), and, at high concentrations, could lead to other pathological metabolic changes (Miyasaki, 1975). In response to this, a number of polymers have been investigated as biodegradable carriers, including naturally occurring polysaccharides such as chitosan, dextran, dextrin (Schacht *et al*, 1987), and synthetic polymers including polyals and polyglutamic acid (PGA) (Singer *et al*, 2003). Additionally, biodegradable linkers, such as the peptide Gly-Phe-Leu-Gly found in PK1, have been described to enable drug to be released by enzymatic cleavage inside the lysosomes (Vasey *et al*, 1999).

The aim of coupling a biodegradable polymer to PLA_2 was to create a conjugate, not only able to benefit from the advantages of PEGylation, but also render PLA_2 inactive during transit, yet enable activity to be reinstated at an appropriate rate by triggered polymer degradation.

The ideal biodegradable polymer should be completely degraded at the target site, resulting in the formation of non-toxic, readily clearable or metabolisable products. The advantages of these polymers include the ability to mask the immunogenicity and minimise enzyme activity prior to 'unmasking' of the protein by degradation of the polymer at the site of action. Furthermore, since historically

polymers for protein delivery were usually required to have a molecular weight of < 40,000 g/mol to permit excretion by the kidneys, biodegradable polymers allow the selection of much larger polymers. Altering the type of polymer-protein linkage or degree of modification can additionally be used to vary the degradation profile of the conjugate and its biological properties (Hreczuk-Hirst *et al*, 2001a).

1.4 Rationale for choice of PLA_2 and trypsin models

PLA_2

The active enzyme selected for conjugation was PLA_2. PLA_2s are enzymes that catalyse the hydrolysis of phospholipids at the *sn-2* fatty acyl bond to release free fatty acid and lysophospholipid (Kudo and Murakami, 2002). Phospholipids are polar structures composed of three main portions; a phosphorylated head group, linked to a glycerol moiety, to which two fatty acid chains are linked. There are several known phospholipids occurring in nature, and their abundance varies between the inner and outer layer of the cell membrane. The outer membrane is composed predominantly of phosphatidylcholine (PC), phosphatidylethanolamine (PE) and sphingomyelin (SM), while the inner membrane contains mostly phosphatidylinositol (PI) and phosphatidylserine (PS) (Punnonen *et al*, 1989). The catalysis of phospholipids has many toxic and pharmacological biological functions including lipid digestion, homeostasis of cell membranes, signal transduction and production of eicosanoids (Valentin and Lambeau, 2000).

Many PLA_2s have been characterised, and classified as either secretory ($sPLA_2$) or cytoplasmic ($cPLA_2$) types, based on their cellular localisation. $sPLA_2$s typically have a molecular weight of around 14,000 g/mol while cytoplasmic types are bigger (typically 85,000 g/mol) (Dennis, 1997). To date, 10 distinct groups of mammalian $sPLA_2$s have been identified, based on their primary structure. Phospholipase's selectivity is affected by the nature of the water-soluble head group, and length and extent of saturation of hydrocarbon tail of the phospholipid. They are classified according to their target bond, as shown in Figure 1.5.

Crotoxin, a PLA_2 currently undergoing clinical testing as an anti-cancer agent, is a dimeric $sPLA_2$. Its native form consists of two subunits; where subunit A is non-

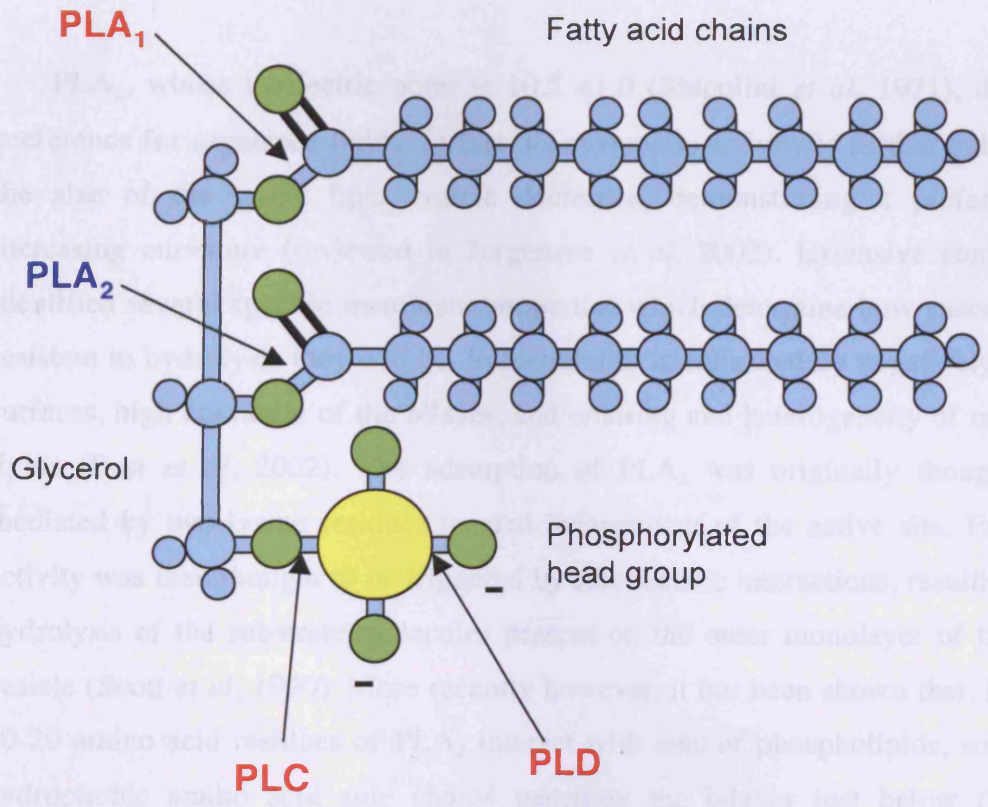

Figure 1.5 Phospholipase classification according to target bond at the phospholipid. Where PLA = phospholipase A, PLC = phospholipase C, and phospholipase D. (Adapted from Invitrogen Molecular Technologies, 2004)

toxic, and displays no enzymatic activity, while subunit B is toxic and is responsible for the enzymatic activity of the PLA_2 (Cura *et al*, 2002; Hanley, 1979). As Figure 1.6 demonstrates, crotoxin is activated by the dissociation of subunits A and B, and subsequent binding of subunit B to the cell membrane. Cura *et al* (2002) propose that subunit A acts as a 'chaperone' to prevent non-specific binding of the active component, as well as having a role in target recognition.

PLA_2, whose isoelectric point is 10.5 ±1.0 (Shipolini *et al*, 1971), displays a preference for organised lipids. In fact, its enzymatic activity is further enhanced as the size of the target lipid vesicle decreases, demonstrating a preference for increasing curvature (reviewed in Jorgensen *et al*, 2002). Extensive studies have identified several specific membrane properties which determine how susceptible or resistant to hydrolysis they will be. Susceptibility is enhanced by negatively charged surfaces, high curvature of the bilayer, and ordering and heterogeneity of membrane lipids (Best *et al*, 2002). The adsorption of PLA_2 was originally thought to be mediated by two lysine residues located independent of the active site. Enzymatic activity was then thought to be triggered by electrostatic interactions, resulting in the hydrolysis of the substrate molecules present on the outer monolayer of the target vesicle (Scott *et al*, 1990). More recently however, it has been shown that, in fact, ~ 10-20 amino acid residues of PLA_2 interact with tens of phospholipids, so that the hydrophobic amino acid side chains penetrate the bilayer just below the polar headgroups and enable hydrolysis of phospholipids at the interface (Bollinger *et al*, 2004).

Polymer-PLA_2 conjugates have previously been synthesised using PLA_2 from *Naja naja naja* (cobra snake) venom, *Bothrops Neuwiedii* (crotalid snake) venom and from bee venom, conjugated to tresilated monomethoxy PEG (TMPEG) (Bianco *et al*, 2002). PLA_2 was conjugated to activated TMPEG via a secondary amine. They performed the reaction in phosphate buffered saline (PBS) at room temperature over 2 h, with a yield of 60 %. Studies found the conjugates retained enzymatic activity toward phospholipid monolayers, though with a reduced specific activity and a greater lag time than the free PLA_2. Bianco *et al* (2002) found that different PLA_2s

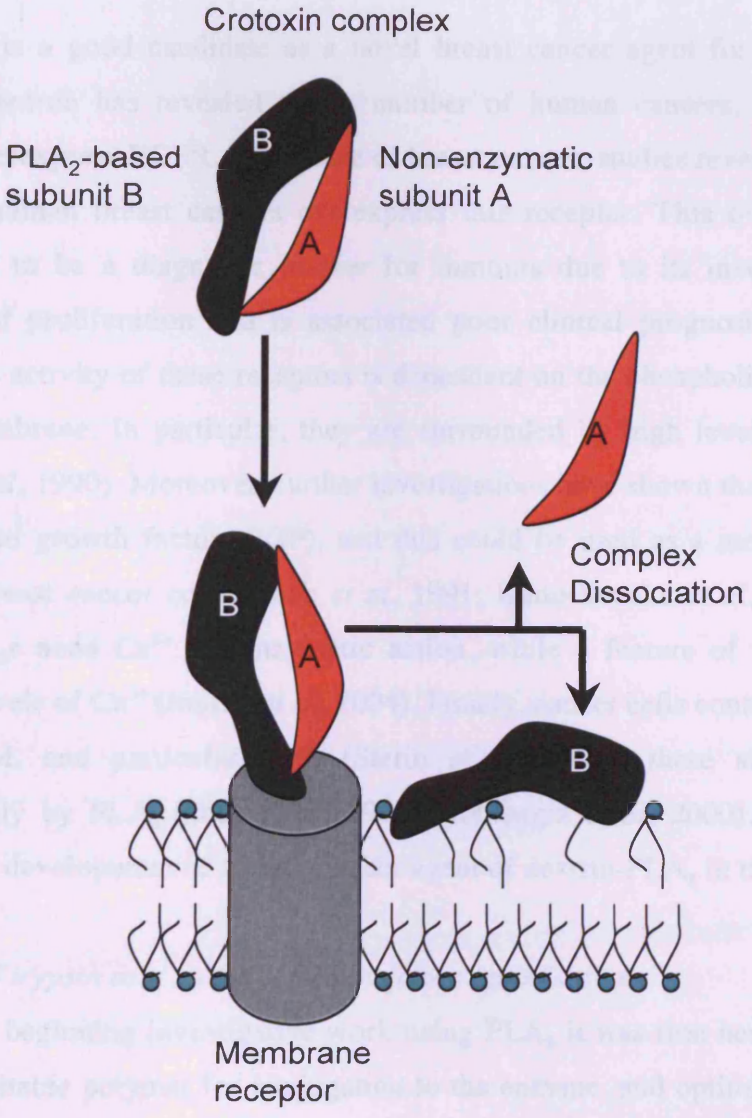

Figure 1.6 Proposed mechanism of action of crotoxin. (Adapted from Ventech Research Inc., 1995)

displayed varying degrees of retention of enzyme activity (10 - 60 % native PLA_2). This was considered to be a consequence of the different isoenzymes having varied distribution of lysine residues on their surface, which are affected to varying extents by conjugation to PEG, and thus affecting the ability of the enzyme to partition/adsorb with the target cell membrane.

PLA_2 is a good candidate as a novel breast cancer agent for several reasons. Firstly, research has revealed that a number of human cancers, including breast cancer, overexpress EGFR. In the case of breast cancer, studies reveal approximately 48 % of human breast cancers overexpress this receptor. This over-expression is considered to be a diagnostic marker for tumours due to its involvement in cell growth and proliferation and is associated poor clinical prognosis (Kumar *et al*, 2001). The activity of these receptors is dependent on the phospholipid environment of the membrane. In particular, they are surrounded by high levels of PE (Kano-Sueoka *et al*, 1990). Moreover, further investigations have shown that PLA_2 can bind to epidermal growth factor (EGF), and this could be used as a means of targeting PLA_2 to breast cancer cells (Hack *et al*, 1991; Kano-Sueoka *et al*, 1990). Further, some PLA_2s need Ca^{2+} for enzymatic action, while a feature of breast cancer is elevated levels of Ca^{2+} (Journe *et al*, 2004). Finally, cancer cells contain higher levels of PC, SM, and particularly PE (Sterin *et al*, 2004); these are all degraded preferentially by PLA_2 (Diez *et al*, 1994; Monteggia *et al*, 2000). These findings support the development of an anti-cancer agent of dextrin-PLA_2 in this study.

Selection of trypsin as a model for conjugation optimisation

Before beginning investigative work using PLA_2 it was first necessary to select the most suitable polymer for conjugation to the enzyme, and optimise the synthesis and characterisation methods.

Trypsin is a serine protease that is produced in the pancreas as an inactive zymogen and activated by the cleavage of trypsinogen at the Lys^6-Ile^7 peptide bond. Trypsin has an isoelectric point of 10.2-10.8 (Malamud and Drysdale, 1978). Enzymatic activity is optimum at pH 7-9 and is dependent on millimolar concentrations of Ca^{2+} and Na^+ as cofactors (ExPASy, 2004). Trypsin catalyses the

hydrolysis of peptides at the C-terminal end of lysine and arginine residues, for example in milk. Trypsin can also hydrolyse the ester and amide bonds of synthetic substances, such as benzoyl L-arginine ethyl ester (BAEE) and Nα-benzoyl-L-arginine p-nitroanilide (L-BAPNA), forming the basis of the enzyme activity assay described later. A number of polymer-trypsin conjugates have been described in the literature (summarised in Table 1.2). Porcine pancreatic trypsin was used in this project.

Porcine trypsin (23,400 g/mol) consists of a single chain polypeptide of 223 amino acids, of which 10 are lysine residues (European Bioinformatics Institute). It is these lysine amino acids that are commonly used for conjugation to polymeric carboxyl functional groups. The number of lysines in a protein's structure can therefore be regarded as an indicator of the number of potential binding sites. While extensive characterisation of trypsin's crystal structure and amino acid sequence has been described, the number of accessible lysines may differ from those calculated. This is due to the tertiary folding of the amino acid chain, leaving some lysine residues buried within the structure, and ultimately inaccessible for polymer conjugation.

Trypsin was chosen as an initial model to synthesise the first conjugates because it is a readily available enzyme that has previously been conjugated to polymers, including HPMA copolymer (Chytry and Kopecek, 1982) and dextrin (Duncan *et al*, 2008), making it an ideal choice for optimisation of synthesis and characterisation methods. Also, since trypsin is inexpensive and has similar molecular weight, isoelectric point and number of lysine groups as PLA_2, it was considered to be a good model enzyme for optimisation of synthesis and characterisation methods.

1.5 Enzyme-prodrug combinations

Since polymer PLA_2 conjugates were also to be investigated as an enzyme-prodrug combination in the PELT model it was useful to explore other existing such combinations. There are several existing enzyme-prodrug combinations currently being explored for delivery of therapeutics to tumours, including Gene-Directed Enzyme Prodrug Therapy (GDEPT), Antibody-Directed Enzyme Prodrug Therapy

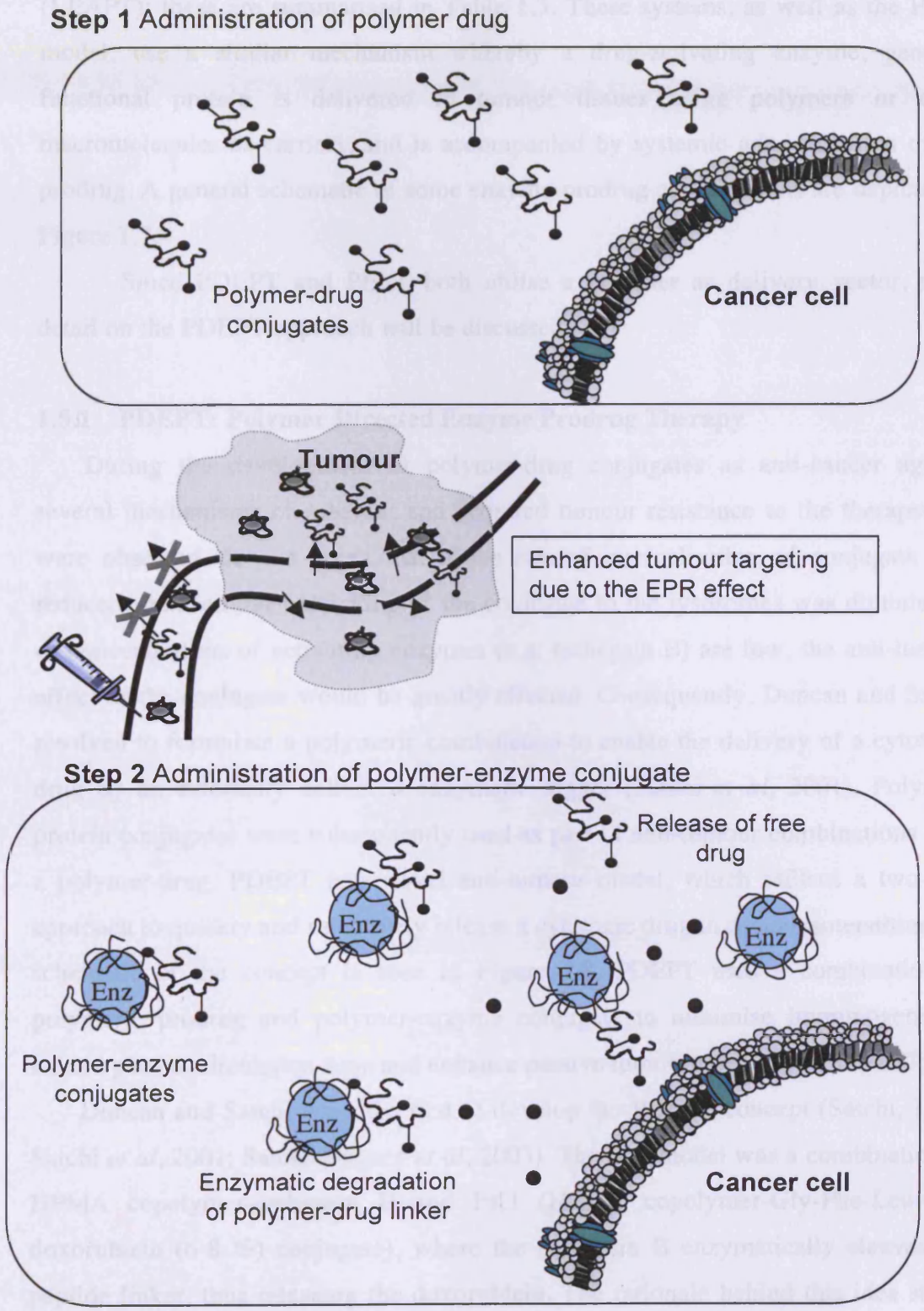

Figure 1.8 Schematic of PDEPT hypothesis. (Adapted from Satchi, 1999)

(ADEPT), Virus-Directed Enzyme Prodrug Therapy (VDEPT), Polymer-Directed Enzyme Prodrug Therapy (PDEPT), and Lectin-Directed Enzyme Prodrug Therapy (LEAPT); these are summarised in Table 1.3. These systems, as well as the PELT model, use a similar mechanism whereby a drug-activating enzyme, gene or functional protein is delivered to tumour tissues using polymers or other macromolecules as carriers, and is accompanied by systemic administration of the prodrug. A general schematic of some enzyme-prodrug combinations are depicted in Figure 1.7.

Since PDEPT and PELT both utilise a polymer as delivery vector, more detail on the PDEPT approach will be discussed.

1.5.1 PDEPT: Polymer Directed Enzyme Prodrug Therapy

During the development of polymer-drug conjugates as anti-cancer agents, several mechanisms of inherent and acquired tumour resistance to the therapeutics were observed. It was noted that if the rate of internalisation of conjugate was reduced, intracellular trafficking of the conjugate to the lysosomes was diminished, or concentrations of activating enzymes (e.g. cathepsin B) are low, the anti-tumour effect of the conjugate would be greatly affected. Consequently, Duncan and Satchi resolved to formulate a polymeric combination to enable the delivery of a cytotoxic drug by an externally delivered enzymatic trigger (Satchi *et al*, 2001). Polymer-protein conjugates were subsequently used as part of anti-tumour combinations with a polymer-drug. PDEPT is a novel anti-tumour model, which utilises a two-step approach to quickly and selectively release a cytotoxic drug in tumour interstitium. A schematic of the concept is seen in Figure 1.8. PDEPT uses a combination of polymeric prodrug and polymer-enzyme conjugate to minimise immunogenicity, extend plasma circulation time and enhance passive tumour targeting by the EPR.

Duncan and Satchi were the first to develop the PDEPT concept (Satchi, 1999; Satchi *et al*, 2001; Satchi-Fainaro *et al*, 2003). The first model was a combination of HPMA copolymer-cathepsin B and PK1 (HPMA copolymer-Gly-Phe-Leu-Gly-doxorubicin (6-8 %) conjugate), where the cathepsin B enzymatically cleaves the peptide linker, thus releasing the doxorubicin. The rationale behind this idea stems from the fact that, after endocytosis, lysosomal enzymes, including cathepsin B,

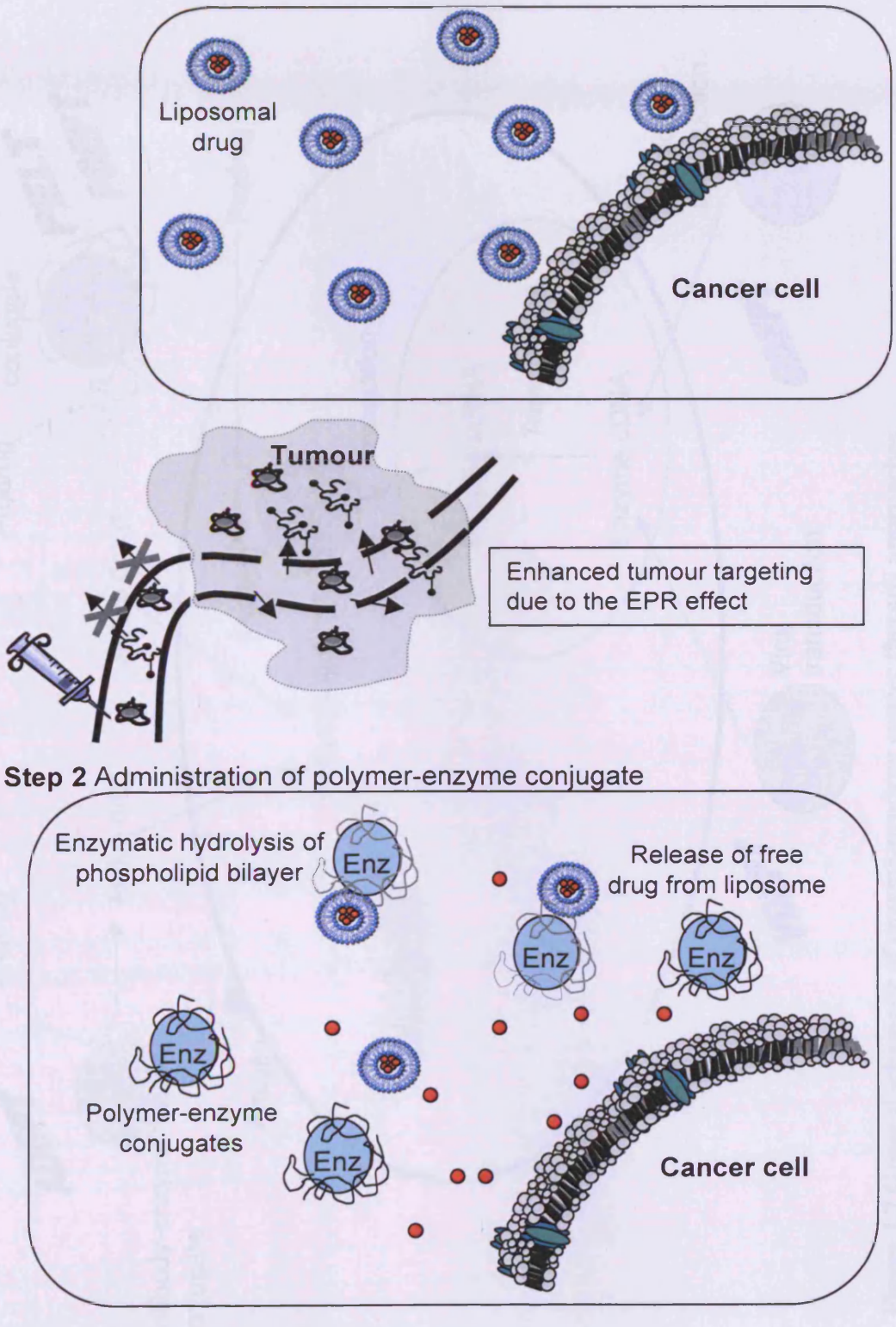

Figure 1.9 Schematic of PELT concept.

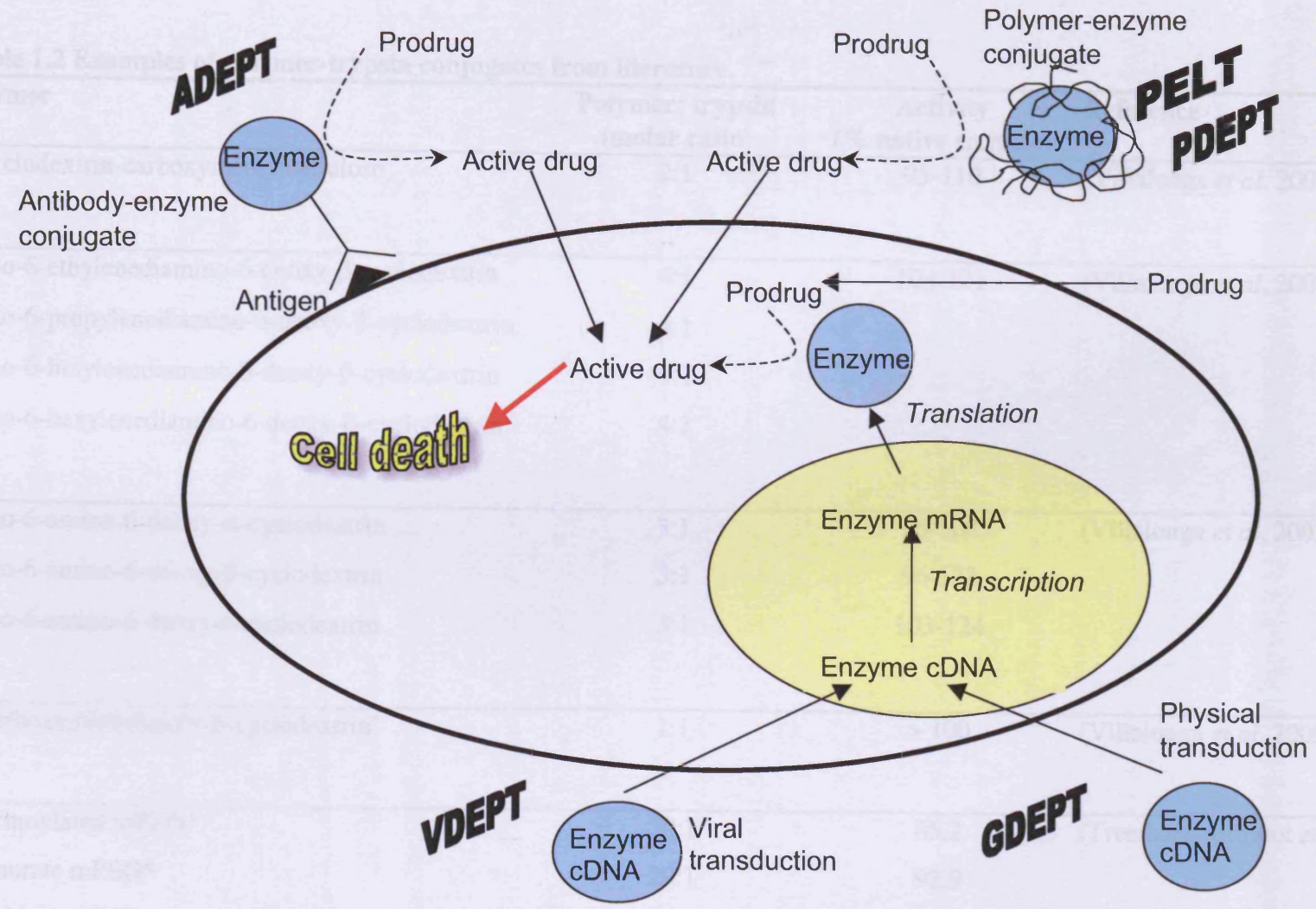

Figure 1.7 General schematic of enzyme-prodrug cancer therapy approaches.

Table 1.2 Examples of polymer-trypsin conjugates from literature.

Polymer	Polymer: trypsin (molar ratio)	Activity (% native enzyme)	Reference
β-cyclodextrin-carboxymethylcellulose	2:1	95-110	(Villalonga *et al*, 2003a)
mono-6-ethylenediamino-6-deoxy-β-cyclodextrin	4:1	104-121	(Villalonga *et al*, 2003c)
mono-6-propylenediamino-6-deoxy-β-cyclodextrin	4:1		
mono-6-butylenediamino-6-deoxy-β-cyclodextrin	4:1		
mono-6-hexylenediamino-6-deoxy-β-cyclodextrin	4:1		
mono-6-amino-6-deoxy-α-cyclodextrin	3:1	96-108	(Villalonga *et al*, 2003b)
mono-6-amino-6-deoxy-β-cyclodextrin	3:1	96-128	
mono-6-amino-6-deoxy-γ-cyclodextrin	3:1	103-124	
O-carboxymethyl-poly-β-cyclodextrin[+]	1:1	> 100	(Villalonga *et al*, 2005)
Succinoylated mPEG*	20:1	65.2	(Treetharnmathurot *et al*, 2008)
Cyanurate mPEG*	20:1	92.9	
Tosylate-mPEG*	20:1	67.6	

[+] = MW was 13,000 g/mol; * = MW was 5,000 g/mol (remaining MW not stated)

normally slowly degrade PK1 intracellularly. This release of free doxorubicin can be considerably accelerated by the PDEPT concept (Satchi-Fainaro *et al*, 2003). Experiments have confirmed the viability of the PDEPT concept, by demonstrating that the bound enzyme retains ~ 20-25 % of its activity *in vitro*, as well as a significantly prolonged plasma half-life and a 4.2 fold increase in tumour accumulation than the free enzyme. Furthermore, it was also shown that when PK1 was administered IV to C57 mice bearing palpable B16F10 tumours, followed 5 h later by administration of HPMA copolymer-cathepsin B, there was a marked increase in doxorubicin release at the tumour site, compared to PK1 alone (Satchi *et al*, 2001). It is also of interest to note that Satchi reported a relatively high yield from polymer-enzyme conjugation (30-35 % protein conjugation), compared to other conjugates. This was attributed to the semi-random aminolysis reaction used to conjugate the two starting materials.

Following from the success of the HPMA copolymer-cathepsin B/ PK1 combination, the group moved on to develop a combination containing HPMA copolymer-methacryloyl-cephalosporin-doxorubicin (5.85 %) (HPMA-*co*-MA-Gly-Gly-C-dox) and HPMA copolymer-β-lactamase (HPMA-*co*-MA-Gly-Gly-β-L) (Satchi-Fainaro *et al*, 2003). Cephalosporin cytotoxic drug derivatives have previously been used successfully in the antibody-directed enzyme prodrug (ADEPT) approach (Grant and Smyth, 2004). These derivatives are advantageous as they do not contain a mammalian enzyme, and should, therefore, not interfere with other mammalian systems. In Satchi-Fainaro's PDEPT studies, the HPMA-*co*-MA-Gly-Gly-β-L conjugate retained 70-80 % of its activity; depending on whether it was acting on free cephalosporin C or HPMA-*co*-MA-Gly-Gly-C-dox. *In vivo* experiments showed prolonged plasma half-life and accumulation of the conjugates in tumours, compared to free β-lactamase. Moreover, the group established a substantial decrease in tumour growth (treatment/control ratio (T/C) 132 %), with no measurable toxicity at the doses used in the study (Satchi-Fainaro *et al*, 2003).

1.5.2 PELT: Polymer Enzyme Liposome Therapy

Following on from the development of PDEPT, a similar concept was then considered as a means of enhancing drug release from liposomes as a method of

overcoming toxicity and enhancing tumour targeting.

Liposomes were first described by Bangham in 1965 (Bangham *et al*, 1965). They are microscopic spherical vesicles (0.03 – 10 μm diameter) that are formed when phospholipids are dispersed in excess water. They are characterised by the presence of a lipid bilayer (able to incorporate lipophilic drugs) surrounding an aqueous core (able to incorporate hydrophilic drugs) (Kirby and Gregoriadis, 1999; Talsma, 1991; Van Winden, 1996). Liposomes have the capacity to carry a high drug loading, and the incorporation of cholesterol and PEGylation can improve their stability and reduce immunogenicity (Andresen *et al*, 2005). There are four key features that are responsible for the behaviour of liposomes; vesicle size, morphology and number of bilayers, fluidity of bilayers, and surface characteristics, such as charge and hydrophobicity (Van Winden, 1996).

Two liposomal anti-cancer formulations are already approved in the UK for routine clinical use for the treatment of breast cancer: Caelyx® and Myocet®. Caelyx® is an 85-100 nm liposome formulation consisting of doxorubicin hydrochloride (2 mg/mL) encapsulated in fully hydrogenated soy phosphatidylcholine: cholesterol: PEG-distearoylphosphatidylethanolamine (molar ratio 1.5:1:0.15) liposomes. Inclusion of PEG chains at the liposome surface (known as PEGylation) protects liposomes from detection by the RES thus increasing blood circulation time. Conversely, Myocet® is a 180 nm in diameter liposome composed of egg distearoylphosphatidylcholine: cholesterol (molar ratio 1:1), containing doxorubicin hydrochloride.

Although these formulations contain the same active drug, they have significantly different lipid composition, size and loading method, which results in dramatically different plasma pharmacokinetics and tissue distribution profiles. Consequently, the side effects seen with the two drug formulations vary too. The main dose limiting toxicity associated with Myocet® is myelosuppression, in particular, neutropenia, while, due to its altered lipid composition, Caelyx® has the propensity to cause mucositis, stomatitis and palmar-plantar erythrodysesthesia (commonly known as hand-foot syndrome). Liposomal formulations of anti-cancer drugs have numerous advantages over their parent drugs, including reduced toxicity

and side effects resulting from improved tumour targeting. In particular, liposomal formulations of doxorubicin have successfully reduced the cardiomyopathy commonly associated with doxorubicin therapy.

Unfortunately however, liposomes are not without their disadvantages, including an inability to control drug release rate, insufficient drug loading, difficulty in overcoming biological barriers (such as skin, blood-brain barrier), and problems of active targeting within the body. Consequently, while liposomes significantly reduce the toxicity of otherwise cytotoxic drugs by containing them inside the liposome, they are not able to rapidly release the drugload into the tumour interstitium. This obstacle led to the PELT concept. Following the development of PDEPT, Satchi-Fainaro and Duncan (unpublished) examined the feasibility of designing a polymer-enzyme/ liposome combination as a means to rapidly release drug payload from liposomes after accumulation in the tumour interstitium by the EPR effect. PELT utilises a polymer-bound enzyme to trigger the release of drug encapsulated within a liposome (Figure 1.9). Satchi-Fainaro and Duncan (unpublished) used HPMA copolymer-Gly-Gly-phospholipase C (PLC) (60 wt. % PLC, MW = 75-150,000 g/mol) to trigger doxorubicin or daunorubicin release from Doxil® or DaunoXome®, respectively. Incubation of HPMA copolymer-Gly-Gly-PLC with Doxil® resulted in partial release of doxorubicin, while complete daunorubicin release was seen from DaunoXome®. In both cases, polymer-conjugated PLC retained the enzyme activity of the free PLC.

The advantages of PELT include the ability to modulate the release of drugs from the liposomes, and cause them to burst locally in the tumour interstitium. It is hoped that PELT will reduce systemic toxicity of the drug by delivery of the liposome to the tumour, thereby protecting normal tissue by limiting exposure of normal tissue to the cytotoxic drug.

1.6 Aims of project

The overall aims of this project were to investigate the potentials of polymer-PLA_2 conjugates as anti-cancer agents; both acting as therapeutic entities themselves, and as a means of triggering the release of liposome-encapsulated drug, in the

Table 1.3 Examples of enzyme-prodrug combinations undergoing investigations.

Application	Enzyme	Prodrug	Viral vector/ antibody/ Polymer	Reference
GDEPT	Thymidine phosphorylase	5'-fluorouracil	-	(Evrard *et al*, 1999)
	E. Coli β-galactosidase	Anthracycline	-	(Bakina and Farquhar, 1999)
VDEPT	Yeast cytosine reductase	5-fluorocytosine	Retrovirus	(Weedon *et al*, 2000)
	E. coli nitroreductase	CB1954 (5-(aziridin-1-yl)-2,4-dinitrobenzamide)	Adenovirus	(Hamstra *et al*, 1999)
ADEPT	β-glucosidase	Amygdalin	Bladder cancer-associated monoclonal antibody	(Syrigos *et al*, 1998)
	Human β-glucoronidase	Doxorubicin	Single chain anti-CD20 antibody	(Syrigos *et al*, 1998)
PDEPT	Cathepsin B	Doxorubicin	HPMA copolymer	(Satchi *et al*, 2001)
	β-lactamase	Doxorubicin	HPMA copolymer	(Satchi-Fainaro *et al*, 2003)
PELT	Phospholipase C	Doxorubicin	Liposome	(Satchi-Fainaro and Duncan, Unpublished)

context of PELT.

Specifically, the focus of the work initially centred on the synthesis of dextrin-trypsin and HPMA copolymer-trypsin conjugates (Chapter 3). The conjugation method was optimised to produce the best reaction efficiency while retaining maximum enzyme activity. Activity of free and bound trypsin was tested using L-BAPNA a colourless chromogenic substance.

Once dextrin had been selected as the most suitable polymer, bee venom PLA_2 was chosen to synthesise dextrin-PLA_2 conjugates using the previously optimised reaction method (Chapter 4). A library of dextrin-PLA_2 conjugates was prepared and the PLA_2 activity was tested using an egg yolk emulsion. This assay was subsequently used to test the PUMPT hypothesis. Finally, to assess whether the conjugate would cause non-specific toxicity following IV administration, haemolysis of red blood cells by free and conjugated PLA_2 was measured. α-Amylase was used to unmask dextrin-PLA_2 conjugates for haemolysis testing.

Given the success in these primary studies, the next studies were intended to determine the ability of the conjugate to kill various cancer cell lines (Chapter 5). In order to better understand the mechanism by which PLA_2 exerts its cytotoxic activity, three different cancer cell lines were studied (HT29, MCF-7, B16F10), each expressing varying levels of EGFR. Cytotoxicity to these cells with dextrin-PLA_2, co-incubated with EGF and a tyrosine kinase inhibitor, was measured using the MTT assay. Further studies investigating the potential of using dextrin-PLA_2 in combination with conventional chemotherapeutics (doxorubicin and daunorubicin) were also performed.

Having established the involvement of the EGFR in PLA_2 cytotoxicity, it was considered important to perform preliminary studies using Oregon Green-labelled conjugates to follow the cellular uptake of native and dextrin-conjugated PLA_2 (Chapter 6). Analysis of the cellular uptake of free and dextrin-conjugated PLA_2 was measured using flow cytometry and confocal microscopy.

It was also intended that this work would examine the feasibility of the PELT concept using a well-characterised dextrin-PLA_2 conjugate as a model polymer-enzyme combination (Chapter 7). The overall objectives of the study were to provide proof of concept data. This was achieved by monitoring the ability of dextrin-PLA_2 conjugates to rupture liposomal daunorubicin (DaunoXome®), thus enhancing the release of drug.

Chapter Two

General Methods

2.1 Chemicals

2.1.1 General chemicals

HPMA copolymer-Gly-Gly-ONp (5 mol %) was supplied by Polymer Laboratories (Church Stretton, UK). Type 1 dextrin from corn was supplied by ML laboratories (Keele, UK). Gefitinib was provided by AstraZeneca (Macclesfield, UK). Trypsin from porcine pancreas, PLA_2 from honey bee venom, PLA_2 from porcine pancreas, anhydrous dimethyl sulfoxide (DMSO), calcium chloride, sodium tetraborate ($Na_2B_4O_7$), lithium acetate dihydrate, 98 % sodium hydroxide (NaOH), 1-Ethyl-3-(3-dimethylaminopropyl carbodiimide hydrochloride) (EDC), copper (II) sulphate pentahydrate 4 % w/v solution, bovine serum albumin (BSA), bicinchoninic acid solution (BCA), TRIZMA base, sodium dodecyl sulfate (SDS), TRIZMA hydrochloride (Tris HCl), triton X-100, glycerol, ammonium persulfate, acrylamide/bis-acrylamide, hydrindantin, ninhydrin, 2,4,6-trinitrobenzene 1-sulphonic acid (TNBS) boric acid (H_3BO_3) and L-BAPNA were all from Sigma-Aldrich (Poole, UK). Sodium acid phosphate, sodium phosphate, sodium chloride, 5 M HCl, anhydrous N,N-dimethylformamide (DMF), ethanol, diethyl ether, methanol, acetone, acetic acid, paraformaldehyde (PFA) and sucrose were all purchased from Fisher Scientific (Loughborough, UK). N,N,N,N-Tetramethyl-Ethylenediamine (TEMED) was from Bio-Rad (Perth, UK). Glycine was purchased from ICN Biomedicals, Inc.. DL-amino-2-propanol was from Acros (Loughborough, UK). Sulfo-NHS was from Fluka (Gillingham, UK). Bromophenol blue was from BDH (Poole, UK). Oregon Green 488 cadaverine *5-isomer (OG) was from Invitrogen Molecular Probes (Paisley, UK). EGF was from Prospec-Tany Technogene Ltd (Rehovot, Israel). Unless otherwise stated, all chemicals were of analytical grade.

2.1.2 Chemicals for cell culture and tissue culture media

Tissue culture grade dimethyl sulfoxide (DMSO, 3-(4,5-dimethylthiazol-2yl)-2,5-diphenyl tetrazolium bromide (MTT), trypan blue and optical grade DMSO were from Sigma-Aldrich (Dorset, UK).

2.2 Cells and tissue culture media

The cell line MCF-7 (human breast carcinoma) was provided by Tenovus Centre

for Cancer Research (Cardiff, UK), HT29 cells (human colon cancer) were obtained from the European Collection of Cell Cultures, Centre for Applied Biology, Microbiology and Research (ECACC) (Salisbury, UK) and B16F10 murine melanoma were from American Type Culture Collection (ATCC) (Manassas, USA). All cell lines were screened and found to be free of mycoplasma contamination. Foetal calf serum (FCS) (untreated and heat-inactivated (HI FCS)), 0.05 % w/v trypsin-0.53 mM EDTA, RPMI 1640 with L-glutamine (with and without phenol red as pH indicator), RPMI 1640 with GlutaMAX and McCoy's 5A were obtained from Invitrogen Life Technologies (Paisley, UK). PBS was prepared using the chemicals listed above, and autoclaved.

2.3 Equipment

2.3.1 Equipment for cell culture

With the exception of the centrifugation steps, all cell work was performed in Bioair (Siziano, Italy) and Bioquell Microflow (Andover, UK) class II laminar flow cabinets. For general cell culture a Leica inverted bright-field microscope was used (Wetzlar, Germany). Bright-field images of cell morphology were taken using an inverted Leica DM IRB microscope (Wetzlar, Germany) with 12-bit cooled monochrome Retiga 1300 camera (Surrey, Canada). For routine cell counting, a Marienfield silver stained Neubauer haemocytometer (Lauda-Königshofen, Germany) was used. Tissue culture flasks (25, 75 and 150 cm^3) and tissue culture sterile plates (6-well, 96-well) were from Corning Inc. (New York, USA). Sterile pipettes (5, 10 and 25 mL), sterile cell scrapers, kwills, 7 mL bijoux, universal containers and 60 mL pots were from Elkay (Birmingham, UK).

2.3.2 Analytical equipment

Ultraviolet (UV): The UV plate reader (Sunrise Touchscreen) was from Tecan (Reading, UK). UV-visible spectrophotometer (Cary 1G) was from Varian Inc. (Walton-on-Thames, UK), with software version 2.0.

Fluorescence: A Fluostar Optima fluorescence plate reader from BMG Lab Technologies (Offenburg, Germany) and an Amnico-Bowman Series 2 luminescence

spectrophotometer from Spectronic Instruments (Leeds, UK) were used for fluorescence measurements.

Infrared (IR): The FT-IR spectrophotometer (Avatar 360) was from Nicolet Instrument Corp. (Newington, USA), fitted with a Nicolet Smart Arc diffuse reflectance accessory. Nicolet E-Z Omnic ESP 5.2 software was used for data collection.

Sodium dodecyl sulphate polyacrylamide gel electrophoresis (SDS PAGE): All electrophoresis equipment, including a Power Pac 300 and GelAir Drying Frame were from Bio-Rad (Perth, UK).

Gel permeation chromatography (GPC): The aqueous GPC was equipped with a JASCO HPLC pump and two TSK-gel columns in series (4000 PW followed by 3000 PW) and a guard column (progel PWXL) from Polymer Laboratories (Church Stretton, UK). The eluate was monitored using a differential refractometer (Gilson 153) and a UV-visible spectrophotometer at 279 nm (UV Severn Analytical SA6504) in series. PL Caliber Instrument software, version 7.0.4, from Polymer laboratories (Church Stretton, UK) was used for data analysis.

Fast performance liquid chromatography (FPLC): An ÄKTA FPLC from Amersham Pharmacia Biotech (Little Chalfont, UK) system was used. The unit was connected to a pre-packed Superdex 75 HR 10/30 column and a Frac-950 fraction collector from Amersham Pharmacia Biotech (Little Chalfont, UK). The UV detector data was collected using Unicorn 3.20 software and analysed using FPLC director® version 1.10 software.

Flow cytometry: Uptake studies were performed using a Becton Dickinson FACSCalibur cytometer (Franklin Lakes, USA) equipped with an argon laser (488 nm) and emission filter for 550 nm. Data were acquired in 1024 channels with band pass filters (FL-1 530 nm ± 30 nm; FL-2 585 ± 42 nm; FL-3 670 nm long pass filter). Data were processed using CELLQuest™ version 3.3 software.

Miscellaneous: The pH meter (3150 pH meter) was from Jenway (Leeds, UK). Freeze-dryer (Flexi Dry FD-1.540 freezer-dryer) was from FTS Systems (Stone Ridge, USA), connected to a high vacuum pump (DD75 double stage) from Javac (Middlesbrough, UK). Dialysis membranes Spectra/POR® CE (Cellulose Ester) were from Pierce & Warriner (Chester, UK) MW cut-off 10,000 g/mol, 25,000 g/mol and 50,000 g/mol. Vivaspin 6 tubes were from Sartorius Vivascience (Goettingen, Germany) MW cut-off 30,000 g/mol. Thin-layer chromatography (TLC) was performed using Sigma-Aldrich silica gel TLC plates (200 μm thick; 25 μm particle size; on an aluminium support) (Dorset, UK).

2.4 Methods

This section gives a detailed description of the general methods used in these studies. Those specific methods used in each chapter are described in full there.

Methods used for conjugate synthesis and purification are described in detail in Chapter 3 (section 3.2). However, the methods used for conjugate characterisation are described in this chapter, as they apply to all methods explored for polymer-protein conjugation.

2.4.1 Ninhydrin Assay

Prior to conjugation of polymer to protein, it was first important to determine the number of available amine groups for conjugation. Two methods were investigated for this purpose, namely the ninhydrin assay and the TNBS assay (next section, 2.4.2). Ninhydrin is a powerful oxidising agent, with the ability to react with all primary amino acids between pH 4 and 8 resulting in a purple colour, which forms the basis of the quantitative measurement of amine content. (Plummer, 1978).

First, a 4 M lithium acetate buffer solution was prepared by dissolving lithium acetate dihydrate (102.02 g) in 150 mL ddH_2O. Sufficient acetic acid (glacial) was added until pH 5.2 was reached. The volume was made up to a final volume of 250 mL with ddH_2O. Next, ninhydrin (0.8 g) and hydrindantin (0.12 g) were dissolved in 30 mL DMSO and 10 mL lithium acetate buffer. Buffered ninhydrin reagent (2 mL) was added to an equal quantity of sample/ standard solution and heated in a water

bath at 100 °C for 15 min. The mixture was subsequently cooled to room temperature and 3 mL of 50 % v/v ethanol was added, before spectrophotometric analysis at 570 nm. A typical calibration curve is shown in Figure 2.1a.

2.4.2 TNBS Assay

The TNBS assay works by the delocalisation of the π-electrons of the benzene ring of TNBS, and the subsequent absorption of UV light as the ring binds to primary amines (Mokrasch, 1967).

Samples were prepared by first making a 1 mg/mL solution of enzyme in ddH_2O and allowing it to fully dissolve. Next, 100 μL of this solution was diluted to 10 mL in ddH_2O to produce a 0.01 mg/mL solution of enzyme. This stock solution was used to make up the final solutions of enzyme. Standard samples were prepared in ddH_2O by diluting 10 μL DL-amino-2-propanol in 10 mL ddH_2O. Next, 100 μL of this solution was made up to 10 mL with ddH_2O. This stock solution was used to make up the final solutions of amino acid standards with concentrations in the range of $1.29 - 9.04 \times 10^{-5}$ mol/L.

An aliquot of each enzyme solution (0.08 mL) was added to a well in a 96 well plate. The same was done for the standards. To each well containing either sample or calibration solution, TNBS (0.01 mL, 0.017 M) and borate buffer (0.2 mL, pH 9.3) were added. For blanks, borate buffer (0.28 mL, pH 9.3) and TNBS (0.01 mL, 0.017 M) were used.

Every well was replicated six times. The plate was then covered in aluminium foil and placed on a rocker for 30 min. The plate was read at 430 nm. A typical calibration curve is shown in Figure 2.1b.

2.4.3 Purification of polymer-enzyme conjugates

Several methods were used to purify polymer-protein conjugates to remove salts, unreacted protein and linking agents (see Chapter 3). FPLC was later chosen as the method of choice (see below).

Purification of polymer-protein conjugates by FPLC

FPLC was used for purification of HPMA copolymer-protein and dextrin-

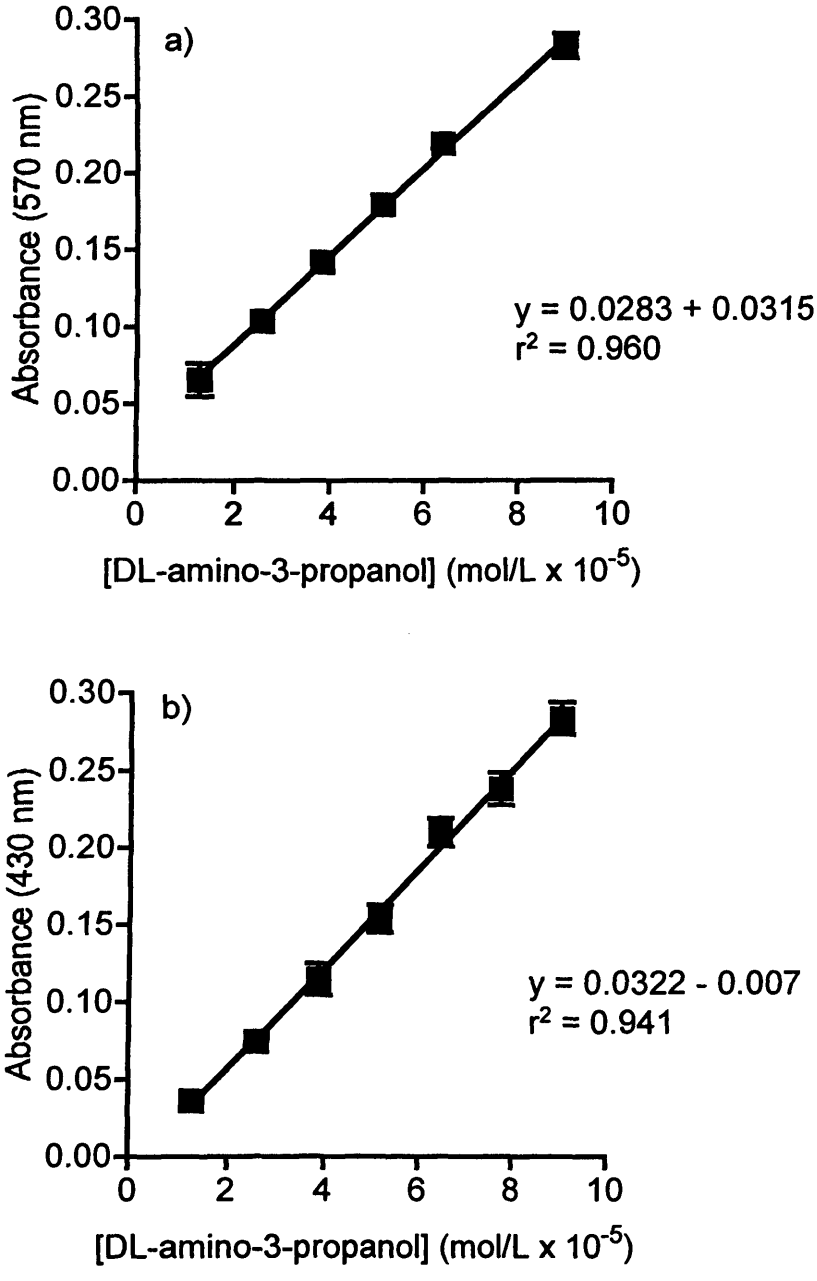

Figure 2.1 Ninhydrin and TNBS assays to quantify the number of primary amines available for conjugation. Panel (a) represents a typical calibration curve for the ninhydrin assay using DL-amino-2-propanol standards. Panel (b) represents a typical calibration curve for the TNBS assay using DL-amino-2-propanol standard. Data represents mean ± SEM (6). Where error bars are invisible they are within size of data points.

protein conjugates. An ÄKTA FPLC (Amersham Pharmacia Biotech, UK) system was used to separate free protein and conjugated protein according to their molecular weight.

A pre-packed Superdex 75 HR/10/30 column was washed with 2 column volumes (~ 48 mL) of filtered (0.2 μm; Millipore) and sonicated ddH_2O. Next, the column was equilibrated with 3 column volumes (~ 72 mL) of filtered and sonicated mobile phase (PBS buffer, pH 7.4) prior to use. First, the column was calibrated (0.5 mL/min flow rate) using standardised proteins of various molecular weight: aprotinin from bovine lung 6,500 g/mol; cytochrome c from bovine heart 12,400 g/mol; carbonic anhydrase from bovine erythrocytes 29,000 g/mol; albumin from bovine serum 66,000 g/mol; and alcohol dehydrogenase 150,000 g/mol. The calibration curve can be seen in Figure 2.2. Then samples (1 mL) were injected into a 2 mL loop (partial fill method) and allowed to run at a flow rate of 0.5 mL/min. When conjugates were being purified, fractions (1 mL) were collected and assayed for protein content (section 2.4.4.3) before pooling the appropriate fractions containing conjugate.

After use, the column was thoroughly washed with eluant, followed by ddH_2O and finally was stored in 20 % v/v ethanol.

2.4.4 Characterisation of polymer-enzyme conjugates

Once the conjugates were made, it was necessary to characterise the products in respect of protein content, free protein, molecular weight and polydispersity.

2.4.4.1 Size Exclusion Chromatography (SEC) for characterisation of conjugates

Polymer-protein conjugates are notoriously difficult to characterise as they are neither protein nor polymer. Therefore, while it was not possible to accurately assign the molecular weight of the conjugate, GPC and FPLC were used in combination with SDS PAGE to quantitatively define the molecular weight of the conjugate and its purity in respect of free enzyme. The BCA assay was used to quantify the total protein content of the conjugate.

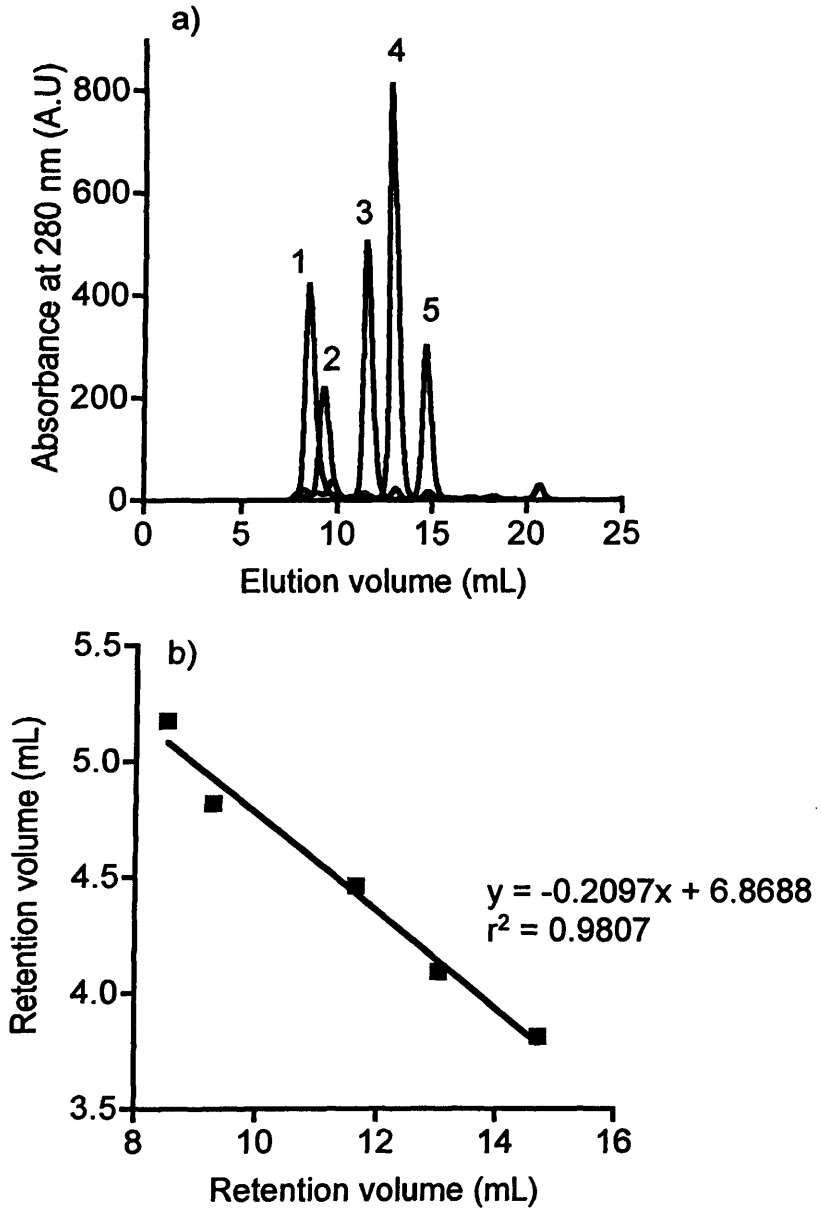

Figure 2.2 FPLC analysis of protein molecular weight standards using a Superdex HR 10/30 size exclusion column. Panel (a) shows the chromatogram of the protein standards: (1) aprotinin (6,500 g/mol); (2) cytochrome c (12,400 g/mol); (3) carbonic anhydrase (29,000 g/mol); (4) albumin (66,000 g/mol); and (5) alcohol dehydrogenase (150,000 g/mol). V_0 and V_b represents the void and bed volume, respectively. Panel (b) represents the calibration curve for estimation of sample molecular weight.

Characterisation by FPLC

FPLC (as described previously) was also used to estimate the conjugate's molecular weight in comparison to standardised proteins of various molecular weights (detailed in section 2.4.3) and measure the ratio of free and bound protein. The same FPLC system as was used for purification was used for characterisation. After appropriate equilibration and calibration, samples of purified conjugate (200 μL) were injected into a 100 μL loop then allowed to run at a flow rate of 0.5 mL/min. Output from the UV detector was analysed using Unicorn 3.20 software from Amersham Pharmacia (Little Chalfont, UK).

Characterisation by GPC

HPMA copolymer-trypsin and dextrin-trypsin conjugates were analysed using aqueous phase GPC. GPC is commonly used to separate polymers according to their size and shape (hydrodynamic radius). Polysaccharide (pullulan) standards (MW from 11,800 to 210,000 g/mol) were used to produce a calibration curve (Figure 2.3). All samples were prepared in PBS (3 mg/mL). Of these solutions, approximately 60 μL was injected (injection loop 20 μL). PBS (filtered and sonicated for 30 min) was used as the mobile phase (flow rate 1.0 mL/min). Both RI and UV detection ($\lambda = 279$ nm) were used and data were analysed using PL Caliber Instrument software.

2.4.4.2 SDS PAGE

The method used for the electrophoresis was adapted from one described by Laemmli (1970). First, the following reagents were prepared: 10 % w/v SDS (stored at room temperature), 10 % w/v ammonium persulfate (made up fresh daily), running buffer gel and stacking gel buffer (see Table 2.1 for composition). The two glass plates, side spacers and clamps were rinsed in ddH_2O and assembled. The assembly was then stood upright, using the clamps as supports, and filled with ethanol to test for leaks.

Next, the separating gel was prepared according to Table 2.1, adding TEMED last. This solution was gently inverted to mix, without introducing air bubbles. This solution was immediately pipetted into the spaces between the glass plates, up to a level of 3 cm from the top. A thin layer of isopropanol was applied to form an even

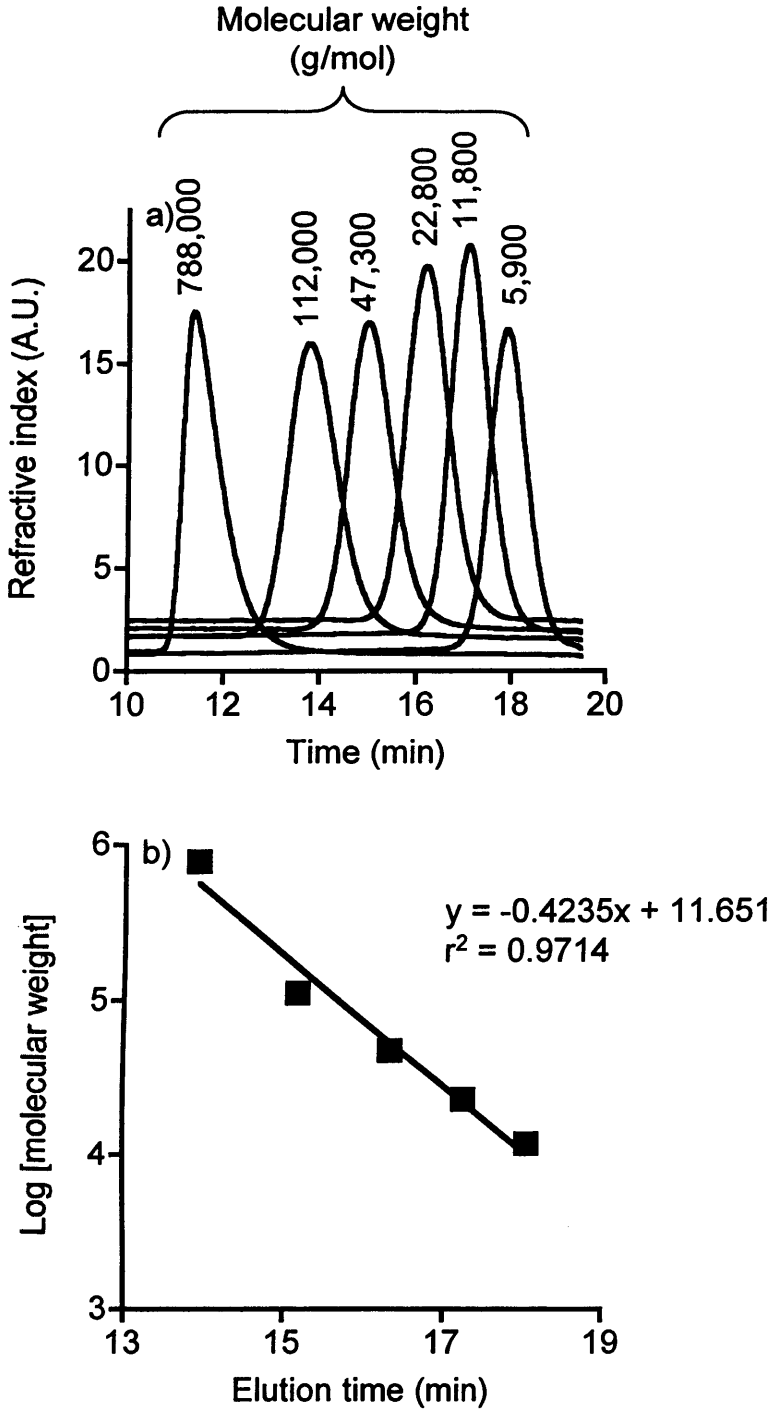

Figure 2.3 GPC analysis of pullulan molecular weight standards using TSK-gel columns G4000 PWXL and G3000 PWXL in series. Panel (a) shows the chromatogram of the pullulan standards (5,900 - 788,000 g/mol). V_0 and V_b represents the void and bed volume, respectively. Panel (b) represents the calibration curve for estimation of sample molecular weight.

Table 2.1 Summary of the composition of buffers and solutions used for SDS PAGE.

Lower (separating) gel	Upper (stacking) gel	Running buffer
8.44 mL ddH_2O	5.85 mL ddH_2O	3 g Tris HCl
5 mL separating buffer (Tris base, pH 6.8, 1.5 M)	2.5 mL stacking buffer (Tris base, pH 6.8, 0.5 M)	14.4 g glycine
200 μL 10 % w/v SDS solution	100 μL 10 % w/v SDS solution	10 mL 10 % w/v SDS solution
6.25 mL 40 % w/v acrylamide/bis-acrylamide	1 mL 40 % w/v acrylamide/bis-acrylamide	ddH_2O up to 1 L pH 8.3
100 μL 10 % w/v ammonium persulfate solution	50 μL 10 % w/v ammonium persulfate solution	
10 μL TEMED	5 μL TEMED	

surface on the gel and prevent oxidation, which inhibits polymerisation. The separating gel was then left to polymerise for 30-60 min, during which time the stacking gel was prepared as detailed in Table 2.1, adding TEMED last. Again, this mixture was gently inverted to mix, taking care not to introduce bubbles. The isopropanol was poured out of the assembly, and the stacking gel was pipetted onto the separating gel. The 10-well comb was inserted, the glass plate assemblies topped up with stacking gel and this construction was left to polymerise for 30-45 min.

Meanwhile, the samples were prepared by adding 1 volume of 2x denaturing buffer (ddH_2O (3.8 mL), Tris HCl (pH 6.8, 0.5 M, 5 mL), Glycerol (4 mL), 10 % w/v SDS (8 mL), 2-mercaptoethanol (2 mL), and bromophenol blue 1 % w/v (0.4 mL)) to 1 volume of each sample and protein markers. The eppendorf tubes were capped and heated for 5 min at 100 °C, then immediately chilled on ice for a further 5 min. These samples were finally centrifuged for approximately 5 s. Once the stacking gel had polymerised, the comb was removed and the plates were loaded onto the frame. The assembly was subsequently lowered into the tank, which was filled up with running buffer (see Table 2.1).

Each well was filled with 10 μL sample, while the first well of every gel was filled with 10 μL molecular weight markers (1 mg/mL). The lid was put on the tank, and connected to a power supply. The gel was then run at 200 V for 1 h, or until dye reached the bottom of the gel.

The gels were then removed and the plates separated. The gels were removed from the glass plates, transferred into plastic trays containing 100-200 mL coomassie blue stain and gently agitated for 1 h. Next, this solution was poured off and replaced with a strong destain solution (35 % v/v methanol, 5 % v/v acetic acid) and left for 1 h. Finally, this solution was poured off and replaced with weak destain solution (7 % v/v methanol, 5 % v/v acetic acid), until the background became clear. The gels were then placed between two water-prewetted thin films, air bubbles removed and left to dry at room temperature for two days.

The ratio of the distance travelled by the protein band to that of the solvent front (Rf value) was used to determine the molecular weight distribution of the conjugate. Molecular weight standards (myosin 194,239 g/mol; β-galactosidase 115,660 g/mol;

bovine serum albumin 97,316 g/mol; ovalbumin 53,533 g/mol; carbonic anhydrase (37,248 g/mol; soybean trypsin inhibitor 29,385 g/mol; lysozyme 20,415 g/mol; and aprotinin 6,919 g/mol) were used to prepare a calibration curve of Rf values (Figure 2.4). This was then used to estimate the molecular weight of polymer-protein conjugates in relation to the standardised proteins.

2.4.4.3 BCA protein assay

The BCA assay was used to determine the total protein content of the polymer-protein conjugates (Smith *et al*, 1985). The assay consists of two steps. First, the protein reduces the Cu^{2+} to Cu^{1+} by the biuret reaction. The resulting Cu^{1+} forms a coloured coordination complex with four to six nearby peptide bonds. Next, the BCA forms complexes with the remaining Cu^{2+}, which produces a purple coloured solution and is detectable at 562 nm. The intensity of the colour is directly proportional to the number of peptide bonds participating in the reaction (Figure 2.5).

A 96-well microtitre plate was used. Each well was prepared to contain 20 μL of polymer-conjugate sample (1 mg/mL; n = 6), or standard (0-1 mg/mL; n = 3), and 200 μL of BCA reagent (1 mL BCA: 20 μL Cu (II) sulfate). The plate was gently agitated and left in the dark, at 37 °C, for 20 min, and then read on the spectrophotometer at 550 nm. Typical calibration curves for BSA, trypsin and PLA_2 are shown in Figure 2.6 and were used to determine the protein content of polymer conjugate.

2.4.5 Biological characterisation of enzymes and polymer-enzyme conjugates

Detailed methods for these enzyme activity assays are described in Chapters 3 and 4 (sections 3.2 and 4.2).

2.4.6 Cell Culture

Cell culture was performed according to the United Kingdom Co-ordinating Committee on Cancer Research (UKCCCR) guidelines. In order to ensure sterility of the incubator the safety cabinets and equipment were sprayed with 70 % v/v ethanol in water. Those items not supplied pre-sterilised were sterilised by (a) autoclaving (120 °C, 15 lb/m^2, 15 min) for glassware, certain plastics, PBS and ddH_2O; (b)

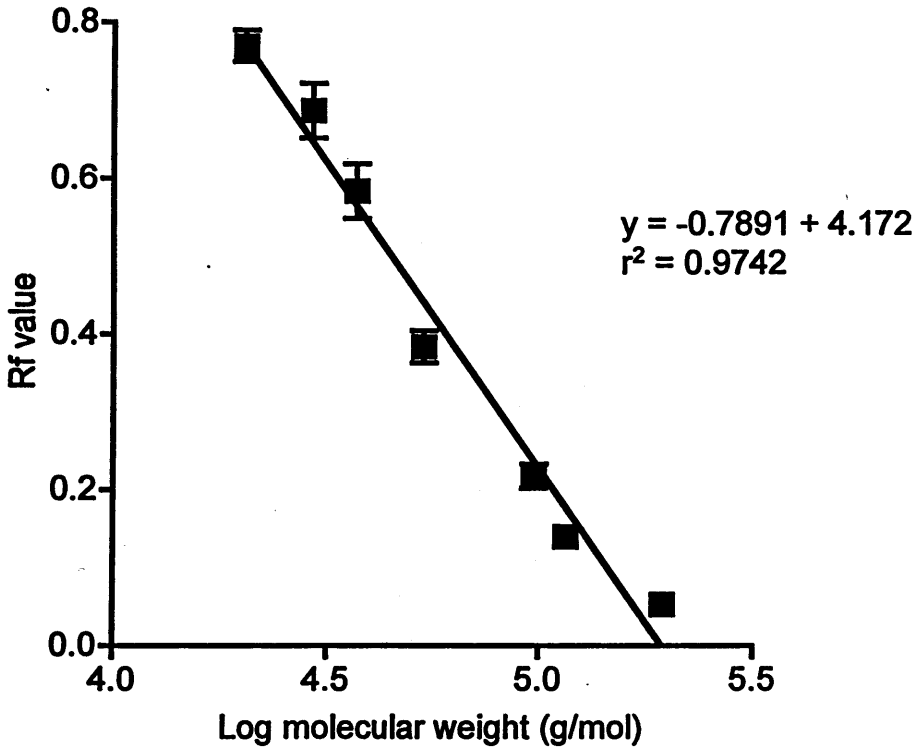

Figure 2.4 Calibration curve for SDS PAGE using protein molecular weight standards. Data shown represents mean ± SD (n = 3). Where error bars are invisible they are within size of data points.

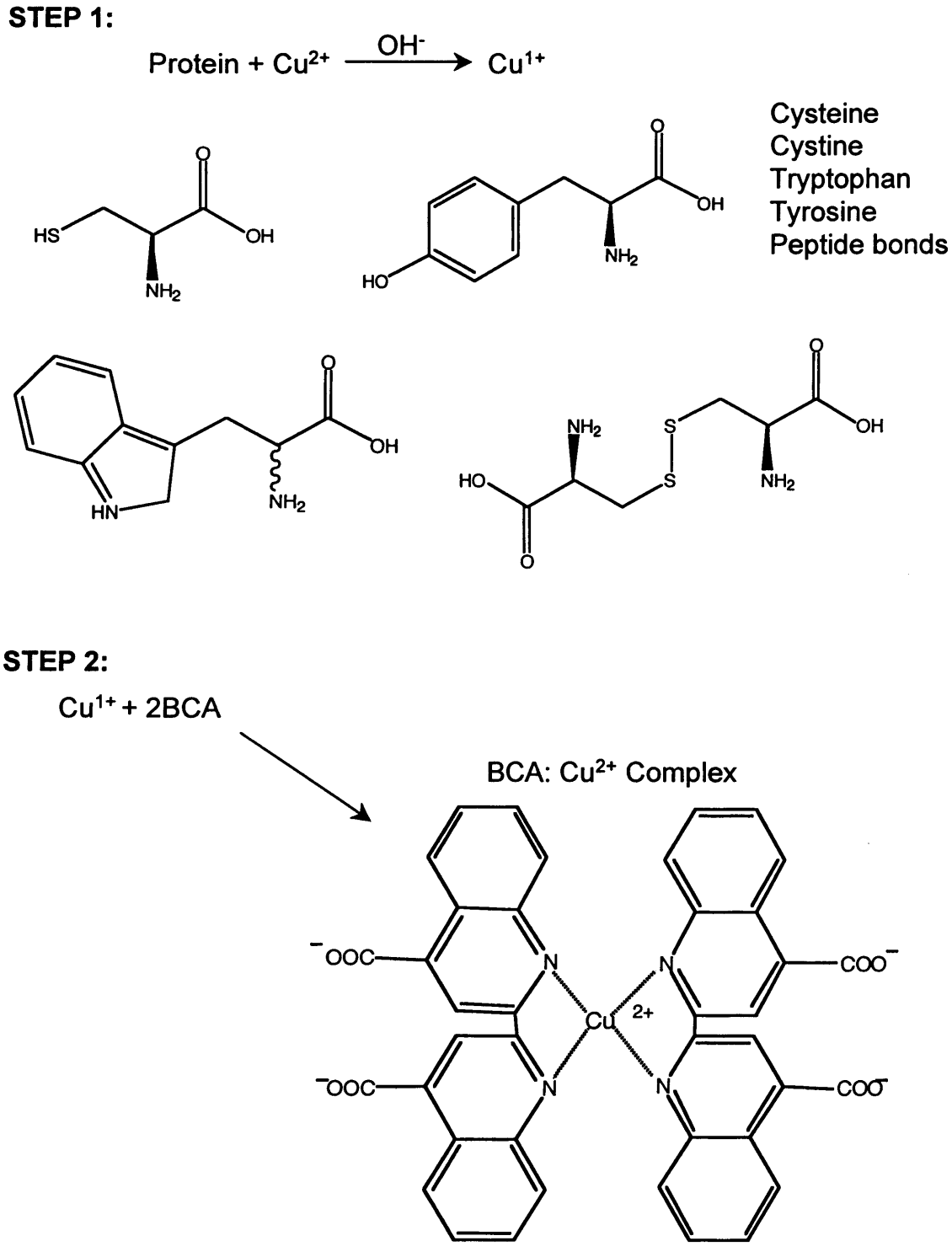

Figure 2.5 BCA assay for protein quantification: mechanism (adapted from Pierce Chemical Technical Library, 2002).

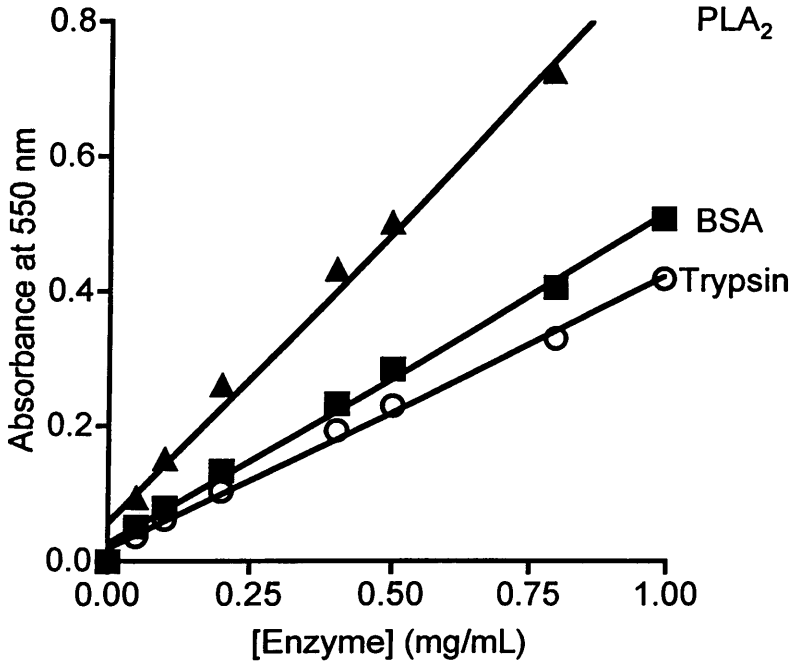

Figure 2.6 Typical BCA assay calibration curves obtained using PLA_2, BSA and trypsin as protein standards. Data shown represents mean ± SD (n = 3). Where error bars are invisible they are within size of data points.

microfiltration (0.2 μm) for solutions; or (c) UV irradiation (30 min).

2.4.6.1 Defrosting cells

Cells were grown from frozen stock (vials containing 1 mL of cell suspension). First, cells were thawed rapidly in a water bath at 37 °C, then transferred to a universal container containing 9 mL of cell-specific medium (Table 2.2) with 20 % FCS. Cells were centrifuged at 20 °C for 5 min at 1000 rpm, and the supernatant removed by aspiration. The cells were then resuspended in 5 mL of the appropriate complete medium. Next, the cell suspension was transferred to a 25 cm^3 flask and stored in the incubator at 37 °C. After 24 h, the medium was replaced with fresh medium and the cells allowed to grow until they reach ~ 80 % confluency and can be passaged.

2.4.6.2 Cell maintenance and passaging

Cells were grown in vented 75 cm^2 tissue culture flasks in their cell-specific complete medium (see Table 2.2) at 37 °C, in humidified atmosphere with 5 % CO_2. Once ~ 80 % confluence was reached, the cells were passaged as described below. First, the old media was removed by aspiration with a kwill and the cells were washed with 10 mL sterile PBS to remove residual media and any dead cells. Trypsin-EDTA solution (1.5 mL) was added and cells were incubated for approximately 3 min or until detached. Fresh medium (8.5 mL) was added and the cell suspension was collected in a universal container and centrifuged for 5 min at 1000 rpm, at 20 °C. The supernatant was removed by aspiration and the cells were resuspended in fresh medium. This suspension was used to prepare new flasks after appropriate dilution. MCF-7 cells to be used in experiments were grown in RPMI 1640 without the pH indicator (WRPMI 1640), as it has been shown that phenol red has mitogenic activity towards this cell line (Devleeschouwer *et al*, 1992), and might therefore interfere with the oestrogen pathway.

2.4.6.3 Counting cells and seeding cells

Cells were washed with PBS, trypsinised and resuspended as described previously. Cells were subsequently passed though a needle (23 G), to ensure a

Table 2.2 Cell lines and culture conditions.

Tumour origin	Cell line	Culture media	Split	Supplier
Human breast carcinoma	MCF-7	5 % v/v FCS, RPMI 1640, 5 mM L-glutamine *(5 % v/v FCS, RPMI 1640 (without phenol red), 5 mM L-glutamine)	1:10	Tenovus
Human colon cancer	HT29	10 % v/v FCS, McCoy's 5A, 5 mM L-glutamine	1:10	ECCAC
Murine melanoma	B16F10	10 % v/v FCS, RPMI 1640, glutaMAX	1:10	ATCC

* = culture media used for performing experiments

homogenous suspension of cells. An aliquot of the suspension (100 μL) was removed and diluted with an equal volume of trypan blue (0.2 % trypan blue in PBS). After 1 min, some of this cell suspension was placed in a haemocytometer. Cells from ten 0.1 mm^3 squares (five taken from the top chamber, and five taken from the bottom chamber of the haemocytometer) were counted. Non-viable cells (stained with trypan blue) were not included in the count.

The following formula was used to determine the cell concentrations:

$$\text{Cells/mL} = \text{mean cell count} \times 2 \times 10^4$$

Where: mean is the arithmetic mean of the 10 values

2 takes into account the trypan blue dilution

10^4 accounts for the conversion from 0.1 mm^3 to mL

Subsequently, the cell suspension was diluted with medium to obtain the appropriate seeding density for the experiment.

2.4.6.4 MTT assay as a means to assess cell viability: growth curve

The MTT assay is a method of assessing cell viability. A redox reaction of the yellow substrate solution (MTT 5 mg/mL in PBS) with mitochondrial respiration products NADH and NADPH, results in the formation of insoluble blue crystals (Mosmann, 1983).

Cells were seeded into 96-well plates (MCF-7 and HT29: 4 x 10^4; B16F10: 1 x 10^4 cells/ mL) and allowed to adhere for 24 h. A sterile filtered solution of MTT (20 μL) was added to each well and the reaction allowed to proceed for 5 h at 37 °C. The solution containing MTT and medium was carefully removed, ensuring not to remove the precipitated crystals. Next, the crystals were dissolved in 100 μL of sterile DMSO and incubated for a further 30 min at 37 °C. The absorbance of the solution was read in a UV absorbance plate reader (λ = 550 nm). This measurement was performed on a daily basis. After reading absorbance, the DMSO solution was removed and replaced with sterile PBS, to maintain moist conditions for the remaining cells in the plate. Growth curves were produced by plotting absorbance against time and used to calculate cell doubling times.

2.4.6.5 MTT assay as a means to assess cell viability: treatment effects

Cell viability in the presence of PLA_2, dextrin, dextrin-PLA_2, EGF, gefitinib, doxorubicin, daunorubicin and DaunoXome® was evaluated using the MTT assay (72 h incubation) (Sgouras and Duncan, 1990), with the human breast cancer cell line, MCF-7, murine melanoma cell line, B16F10, and human colon carcinoma cell line, HT29. Cell viability was always measured while cells were in exponential growth phase, as determined using the methods described in section 2.4.6.4.

Cells were seeded into sterile 96-well microtitre plates (MCF-7 and HT29: 4 x 10^4 cells/ mL, B16F10: 1 x 10^4 cells/mL) in 0.1 mL/well of media (WRPMI 1640/ McCoy's 5A/ RPMI 1640, respectively) with FCS (5-10 % v/v) and allowed to adhere for 24 h. After 24 h, the medium was removed and test compounds (0.2 μm filter-sterilised) were added to the cells. After a further 67 h incubation, MTT (20 μL of a 5 mg/mL solution in PBS) was added to each well and the cells were incubated for 5 h. The medium was then removed and the precipitated formazan crystals were solubilised for 30 min with the addition of optical grade DMSO (100 μL). Absorbance, which was proportional to cell viability, was measured at 550 nm. Cell viability was expressed as a percentage of the viability of untreated control cells. The IC_{50} values were expressed as concentration of test compound (± SEM).

2.4.6.6 Determination of cellular uptake of polymer conjugates by flow cytometry

Flow cytometry was used to study the uptake of OG-labelled dextrin, PLA_2 and dextrin-PLA_2 by MCF-7 cells. Cells were seeded in 6-well plates (1 x 10^6 cells/mL) in their respective media, supplemented with FCS, and allowed to adhere for 24 h. In order to account for external binding, the experiment was performed at 37 °C and 4 °C. Solutions for treatment were prepared in medium and equilibrated to 37 °C or 4 °C. For experiments performed at 37 °C, cells were kept under normal cell culture conditions throughout the incubation period, while cells used in experiments at 4 °C were incubated at 4 °C for 30 min prior to the addition of treatment media. OG-labelled dextrin, PLA_2 or dextrin-PLA_2 (synthesis and characterisation described in Chapter 6) was added at a concentration of 1.5 μg/mL in medium. Cells were then incubated for 60 min at 37 °C or 4 °C.

At the end of the incubation period, the plates were placed on ice to prevent further uptake and kept at 4 °C. The cells were washed three times with ice-cold PBS (3 x 1 mL). Next, PBS (1 mL) was added and the cells scraped from the plates, collected in falcon tubes and centrifuged at 4 °C, 1000 x g for 5 min. Finally, cells were re-suspended in ice-chilled PBS (200 μL) and analysed using a Becton Dickinson FACSCalibur cytometer equipped with an argon laser (488 nm) and emission filter for 550 nm.

Data were collected with 10,000 total cell counts per sample and processed using CELLQuest™ version 3.3 software. Control cells (incubated with medium only) were used in all cases to account for background fluorescence output (M1). Data was acquired in 1024 channels with band pass filter FL-1 (530 nm ± 15 nm). Results were expressed as (geometric mean x % positive cells)/ 100 (See Chapter 6 for details).

Several methods were used to interpret the flow cytometry data. An increase in fluorescence of the cell population can be estimated using two methods. Firstly, by measuring the increase in average fluorescence of the population using the mean, geometric mean or median. The second method involves analysis of the number of cells that have taken up the fluorescently labelled compound. In this instance control cells were compared to cells exposed to OG-labelled probe to account for background fluorescence. From this data, two regions were arbitrarily set (Figure 2.7). Region M1 corresponds to a region covering 98 % of the control population events, while M2 relates to any area with higher fluorescence than M1. As cell-associated fluorescence increases, so too does the number of events in the M2 region.

2.5 Statistical Analysis

Data were expressed as mean ± the error, calculated as either standard deviation (SD) or standard error of the mean (SEM), where appropriate. Statistical significance was set at $p < 0.05$ (indicated by *). Where only two groups were compared, student's t-test for a small sample size was used. In situations where more than two groups were compared evaluation of significance was achieved using a one-way analysis of variance (ANOVA) followed by bonferroni *post hoc* tests that correct for

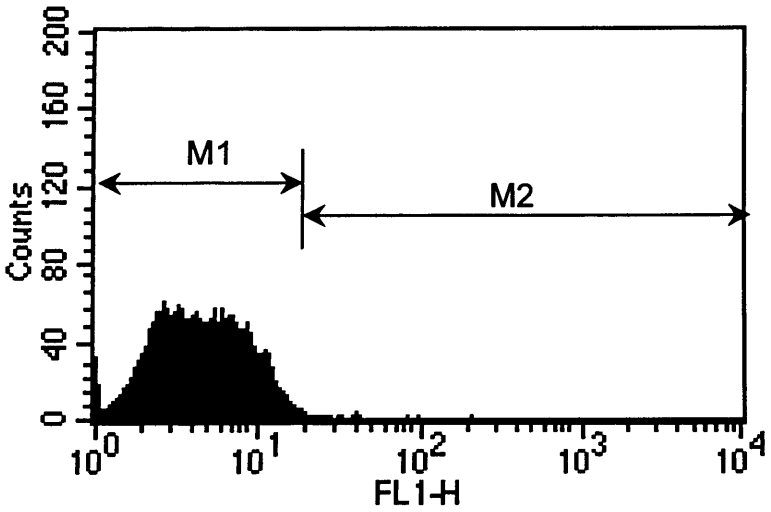

Figure 2.7 Typical flow cytometry distribution. Region M1 corresponds to a region covering 98 % of the control population events, while M2 relates to any area with higher fluorescence than M1.

multiple comparisons. All statistical calculations were performed using GraphPad Prism, version 4.0c for Macintosh, 2005.

Chapter Three

Synthesis and Characterisation of HPMA Copolymer- and Dextrin-Trypsin Conjugates

3.1 Introduction

To develop the concepts of polymer-PLA_2 conjugates as (i) anti-cancer therapeutics, and (ii) triggers for PELT (see section 1.5.2) it was first necessary to optimise the methods to be used for polymer-protein conjugation. It was important to choose both an appropriate polymer and a conjugation chemistry that would be reproducible, and give the best yield. From the biological point of view, it was important to generate a stable conjugate that would retain enzymatic activity.

Furthermore, it is well known that conjugation of a polymer to a protein (particularly enzymes) can significantly improve biological efficacy *in vivo* by reducing proteolytic degradation, extension of plasma circulation time and by reducing protein immunogenicity (reviewed in Harris and Chess, 2003; reviewed in Roberts *et al*, 2002; reviewed in Sato, 2002; Werle and Bernkop-Schnurch, 2006). Many methods have been previously described for conjugation of proteins to polymers. Numerous polymers have been used to prepare such conjugates, and Table 1.1 summarises some polymer-enzyme conjugates described in the literature.

3.1.1 Choice of polymer

In these studies it was first necessary to consider which polymer would be best for PLA_2 conjugation. Any polymer used must be non-toxic and non-immunogenic, contain suitable functionality for conjugation (using either a polymer with a single reactive group (e.g. mPEG (reviewed in Pasut *et al*, 2008)) or a multi-functional polymer (e.g. HPMA copolymer (Satchi-Fainaro *et al*, 2002) or dextrin (Hreczuk-Hirst *et al*, 2001b)). To design a polymer conjugate that would have the required stability, pharmacokinetic profile and pharmacological activity, features such as the polymer molecular weight, the linking chemistry, and the number of reactive groups on the polymer were considered.

The main polymers used clinically to synthesise polymer therapeutics have been introduced in Chapter 1 (sections 1.2.1 and 1.3) and they include PEG, dextran, PGA, HPMA copolymers and dextrin. Of these, dextrin and HPMA copolymers were selected for conjugation and they are described in more detail below.

HPMA Copolymers

HPMA copolymers were chosen because they have already been used to prepare polymer therapeutics including polymer-anticancer drug conjugates, polymer-protein conjugates (reviewed in Duncan, 2005; reviewed in Duncan, 2006) and gene delivery systems (Oupicky *et al*, 2000). HPMA copolymers have already proven to be non-toxic, non-immunogenic in patients (Vasey *et al*, 1999), and they can be synthesised to be either semi-telichelic (one functional group), or multi-functional. Many different linker chemistries have been used in HPMA copolymer conjugates (reviewed in Duncan, 2005; Kopecek, 1984). Peptide linkers have been most widely used to bind anticancer agents, e.g. -Gly-Phe-Leu-Gly-, which is degraded by the lysosomal thiol-dependent proteases following uptake of the conjugate by endocytosis (Vasey *et al*, 1999). Typically, -Gly-Gly- linkers have been used to prepare HPMA copolymer-protein conjugates (Satchi-Fainaro *et al*, 2003). As PLA_2 is probably not required to enter the cell to exert its therapeutic effect, it was decided that lysosomal degradation of the linker was not important, and so -Gly-Gly- was a more appropriate linker group.

A frequently encountered problem with protein conjugation is the potential loss of biological activity; therefore, it is also of particular interest to consider the site of conjugation. This will be affected by the availability and reactivity of functional groups in the protein as well as the nature of reactive groups on the polymer. Reduced biological activity is often due to steric hindrance of the protein by the polymer chain, often as a result of covalent binding of the polymer in or close to the active site of the enzyme. It has been suggested that a 1:1 polymer-protein ratio may minimise loss of biological activity (Satchi, 1999) especially when non-degradable polymers (e.g. PEG, HPMA copolymers) are used. Use of biodegradable polymers (Duncan *et al*, 2008) or polymer-protein linkers (Pan *et al*, 2006) can circumvent this problem, for example dextrin, where degradation by α-amylase results in an unmasking effect. In the case of HPMA copolymer, however, a conjugation ratio of 1:1 was aimed for, to also reduce the risk of cross-linking.

It is possible to conjugate a polymer to a protein using hydroxyl and thioether

reactive groups, however these derivatised bonds tend to produce weaker linkages and the stability of the conjugate would be questionable. Therefore in these studies, HPMA copolymers containing a carboxylic acid were reacted with amine groups within the structure of trypsin, leading to the formation of a stable amide bond. Primarily, primary NH_2 groups of lysine (pKa = 10.53) residues found on the surface of enzymes, arginine (pKa = 12.48), histidine (pKa = 6.10), as well as terminal NH_2 groups (pKa = ~ 9) are also able to react in this way.

Several approaches for HPMA copolymer-trypsin conjugation were explored in these studies using methods adapted from previous techniques described in the literature (see Figure 3.1 for reaction schemes). Conjugation typically involves a polymer analogous reaction using a polymer precursor containing a reactive leaving group that can be displaced by the protein (e.g. HPMA copolymer –ONp). Initially, non-specific aminolysis was investigated as this method had successfully been used previously to synthesise HPMA copolymer-cathepsin B and HPMA copolymer-β-lactamase conjugates (Satchi *et al*, 2001; Satchi-Fainaro *et al*, 2003) producing conjugates with a yield of 30-35 wt. %. However, as this method was not successful here, two further conjugation methods were investigated. These methods also used HPMA copolymer-ONp, but employed different reaction conditions that had been described for the synthesis of anti-O antibody- and transferrin-polymer conjugates (Kopececk *et al*, 1985b).

A final conjugation method was explored for HPMA copolymer-trypsin conjugation. This utilised the crosslinking agents EDC and sulfo-NHS. EDC reacts with the carboxyl groups of an HPMA copolymer-COOH intermediate, forming an amine-reactive O-acylisourea intermediate. This can then react with the amine of lysine residues in a protein, to give a conjugate joined by a stable amide bond. However, EDC alone is not particularly efficient. Failure to react quickly with an amine results in hydrolysis and regeneration of the carboxyl, making it unstable and short-lived in aqueous solution. The addition of sulfo-NHS stabilises the amine-reactive intermediate by converting it to an amine-reactive sulfo-NHS ester, thus increasing the efficiency of EDC-mediated coupling reactions. The amine-reactive

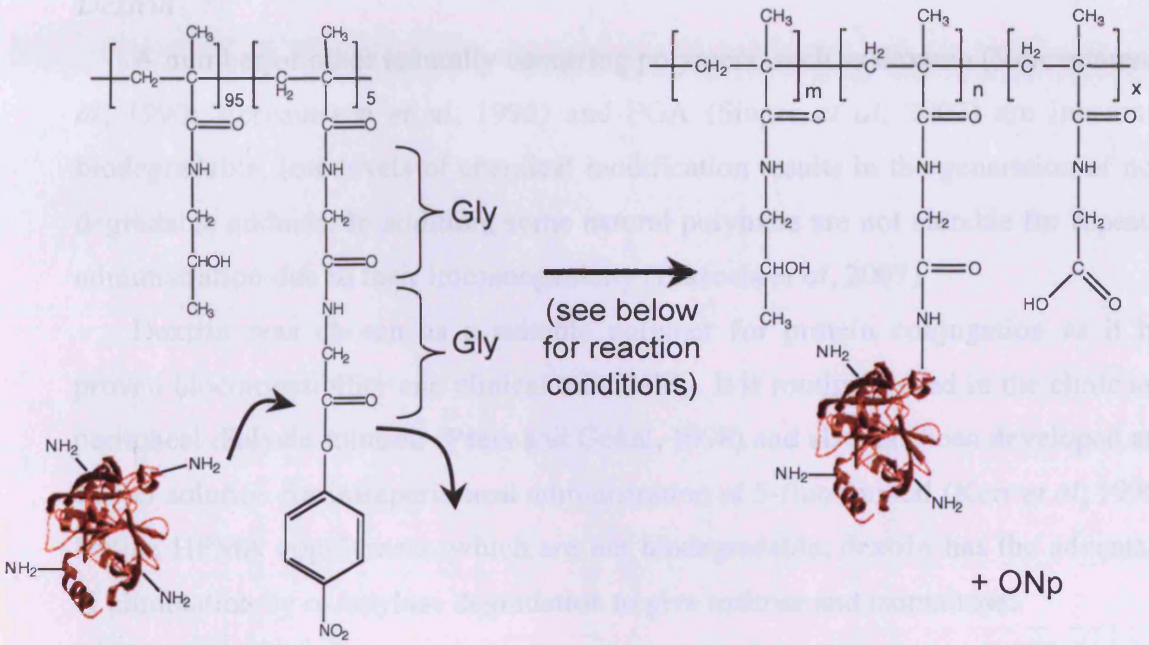

Reaction Conditions

a) 4 °C, dark (8 h)
pH 7.2 – 8.5, by addition of tetraborate buffer (30 min)

b) 0.5 mL HCl (pH 3.0)
0.6 mL Sorensen's buffer (pH 8.0, 0.15 M NaCl)

c) 20 ° C (75 min)
0.25 mL HCl (pH 3.0)
1.25 mL Sorensen's buffer (pH 8.0, 0.1 M NaCl)

d) *Hydrolysis of HPMA copolymer-Gly-Gly-ONp:*
NaOH (0.1 M, 10 eq.), ddH_2O, 4-5 h
Conjugation of trypsin:
20 °C, EDC (10 min), sulfo-NHS (45 min)
18 h, pH 8

Figure 3.1 Schematic of reaction to conjugate trypsin to HPMA copolymer-Gly-Gly-ONp. Reaction conditions tested in these studies are given. Where m and n are reaction products, x is a side product that occurs by hydrolysis of HPMA copolymer-Gly-Gly-COOH.

sulfo-NHS ester intermediate has sufficient stability to permit two-step crosslinking procedures, which allows the carboxyl groups on the protein to remain unaltered.

Dextrin

A number of other naturally occurring polymers, such as dextran (Vercauteren *et al*, 1990; Vercauteren *et al*, 1992) and PGA (Singer *et al*, 2003) are inherently biodegradable, low levels of chemical modification results in the generation of non-degradable adducts. In addition, some natural polymers are not suitable for repeated administration due to their immunogenicity (Bisaccia *et al*, 2007).

Dextrin was chosen as a suitable polymer for protein conjugation as it has proven biocompatibility and clinical tolerability. It is routinely used in the clinic as a peritoneal dialysis solution (Peers and Gokal, 1998) and also has been developed as a carrier solution for intraperitoneal administration of 5-fluorouracil (Kerr *et al*, 1996). Unlike HPMA copolymers, which are not biodegradable, dextrin has the advantage of elimination by α-amylase degradation to give maltose and isomaltose.

The PUMPT concept has recently been coined by Duncan *et al* (2008) using dextrin as the model polymer. The hypothesis was that conjugation of a biodegradable polymer to a biologically active protein can mask activity and enhance stability in the bloodstream, while subsequent regeneration of activity can be achieved by triggered degradation of the polymer at the target site. A detailed description of this concept is given in Chapter 4.

Since dextrin doesn't contain a convenient amine or carboxy group for protein conjugation, functionalisation has, in the past, been achieved using several methods. For example, cyanogen bromide activation (Costa and Reis, 2004), chloroformate activation (Bruneel and Schacht, 1993b), periodate oxidation (Bruneel and Schacht, 1993a) and succinoylation (Bruneel and Schacht, 1994). These activation techniques are summarised in Table 3.1. However, since the reagents for succinoylation are relatively non-toxic, the synthesis of dextrin-protein conjugates has typically used activation of the polymer by incorporation of functional groups by succinoylation, which can react directly with the trypsin (Hreczuk-Hirst *et al*, 2001a; Hreczuk-Hirst *et al*, 2001b).

Table 3.1 Methods of polysaccharide activation by introducing pendant groups.

Activation method	Method overview	Disadvantages	Example polysaccharides
Cyanogen bromide activation	Primary amine groups are introduced directly into reactive intermediate, under aqueous conditions at room temperature	Reactive intermediates produced during activation of hydroxyl group can disrupt polymer backbone Hydrogen cyanide is toxic and must be carefully removed Linkage is not stable, resulting in slow release of pendant group	*Hyaluronate* (Mlcochova *et al*, 2006) *Starch* (Costa and Reis, 2004)
Chloroformate activation	Introduces hydroxyl groups within the polymer	Possibility of formation of intra- or inter-chain carbonate esters Formation of five-member rings can interfere with polymer backbone	*Cellulose* (Rupprich *et al*, 1990) *Dextran* (Chiu *et al*, 1999)
Periodate oxidation	Formation of an aldehyde group by oxidation of 1,2-diol groups	Aldehyde groups canlead to toxicity if not completely neutralised	*Dextran* (Devakumar and Mookambeswaran, 2007) *Mannan* (Ramirez *et al*, 2006)
Succinoylation	Uses succinic anhydride to introduce a carboxyl group without disrupting polymer backbone		*Starch* (Lawal, 2004), *Chitosan* (Kato *et al*, 2004)

Succinoylation has been used to modify pullulan (Bruneel and Schacht, 1994) and pullulan was reacted with succinic anhydride in DMSO, using DMAP as a catalyst. Hreczuk-Hirst *et al* (2001a) optimised dextrin succinoylation with respect to temperature and reaction time. They concluded 50 °C with a minimum of 8 h reaction time to be optimal for dextrin succinoylation. Using these conditions it was possible to reproducibly succinoylate dextrin with a coefficient of variation of < 10 % and a yield of ~ 50 %. Further, it was demonstrated that different degrees of dextrin succinoylation (0.5 - 30 mol %) could be achieved by variation of the reactant ratios, and that the rate of α-amylase degradation of succinoylated dextrins could be prolonged by increasing the degree of modification to the polymer (Hreczuk-Hirst *et al*, 2001a). As dextrin is normally degraded in the body very quickly by α-amylase ($t_{1/2}$ < 10 min) this fundamental study suggested the potential of controlling the rate of dextrin degradation by tailoring backbone modification. This approach made dextrin a more practical polymer for use in targeted drug delivery and also for use in protein modification in the context of PUMPT.

Hreczuk-Hirst *et al* (2001b) also developed the conjugation chemistry techniques for coupling drugs and other amino-group containing compounds. Gilbert *et al* (2005) subsequently applied this methodology to the preparation of dextrin-trypsin conjugates. EDC and sulfo-NHS were used as linking agents and first studies investigated the effect of dextrin molecular weight (comparing 7,700 and 47,200 g/mol) and degree of succinoylation on enzyme activity and ability to regenerate enzyme activity in the presence of α-amylase (Gilbert *et al*, 2005). It was concluded that the higher molecular weight dextrin (47,200 g/mol) with ~ 25 mol % succinoylation achieved the optimal trypsin masking and then allowed unmasking. The same reaction conditions were therefore chosen for these studies.

In summary, HPMA copolymer was selected for conjugation because it has the advantages of a narrow polydispersity (usually 1.3 – 1.5), it has been previously used for protein modification, and the loading of protein can be controlled.

On the other hand, dextrin was chosen because, while it has a higher polydispersity index than HPMA copolymers (> 2.0), its α-amylase-triggered degradation lends it to masking protein activity and subsequent reinstatement of

activity by unmasking (PUMPT concept described in detail in Chapter 4). However, unlike HPMA copolymer, dextrin requires chemical modification to introduce reactive groups for protein conjugation.

3.1.2 Selection of trypsin and analysis of enzyme kinetics

Trypsin was chosen as a model enzyme for the first conjugate studies since it is a well-characterised enzyme (Johnson *et al*, 2002) and many polymer-trypsin conjugates had been described in the literature (Table 1.2) so it was easy to make comparisons. Additionally, as outlined in Chapter 1 trypsin has a similar molecular weight, number of lysine residues and pI to PLA_2, making it a good choice for optimisation of the conjugation reaction. Trypsin preferentially cleaves peptides on the c-terminal side of arginine and lysine amino acid residues. Its activity can also be reproducibly assayed using synthetic derivatives of amino acids such as BAEE, p-toluenesulfonyl-L-arginine methyl ester (TAME), L-BAPNA (Buck *et al*, 1962; Kell, 1971) so comparisons can be easily made between the activity free and conjugated trypsin.

In order to quantify the activity of free and polymer-bound trypsin and allow comparisons between experimental conditions, a direct continuous assay was used. L-BAPNA was chosen as a chromogenic substrate. Incubation of L-BAPNA with trypsin results in the release of NAp, which is not coloured when bound but yields a yellow-coloured product when released that can be measured spectrophotometrically. Mathematical analysis of the initial rate of release can be used to establish classical enzyme kinetics parameters, namely V_{max}, K_m and K_{cat}.

- V_{max} represents the maximum rate for the reaction.
- K_m corresponds to the affinity of the enzyme for the substrate and denotes the substrate concentration required for effective catalysis.
- K_{cat}, also known as the turnover number, is a measure of the number of substrate molecules turned over by each enzyme, per second.

These parameters are based on the Michaelis-Menten equation:

$$V \text{ (velocity)} = \frac{K_2[E]_t[S]}{(K_m\,[S])} = K_2[ES]$$

$$\text{Where } E + S \underset{K_{-1}}{\overset{K_1}{\rightleftarrows}} ES \xrightarrow{K_2} E + P$$

$[E]_t$ = total enzyme, [E] = free enzyme, [ES] = complexed enzyme

This equation assumes that the reverse reaction is negligible, resulting in a simple, first-order reaction, whose rate is determined by [ES] and K_2. Briggs and Haldane (1925) noted that [ES] increases rapidly after initiation of the reaction by mixing of enzyme and substrate. However, after a short while, steady state is reached and maintained until almost all the substrate is consumed (Eisenthal and Danson, 1998). Steady state occurs when [ES] is almost constant.

Enzyme kinetic data may be analysed by several mathematical models. The first of these is the Lineweaver-Burk plot (Figure 3.2a) which is derived from the inverse of the Michaelis-Menten equation. For a reaction obeying Michaelis-Menten kinetics, the fit should yield a straight line. The advantage of this model is that it doesn't require a direct measurement of V_{max}. However, it requires a long extrapolation for the determination of K_m, which gives rise to inaccuracies if there are significant experimental errors. Hence, this equation is not normally recommended for the determination of kinetic parameters.

The Eadie Hofstee plot is shown in Figure 3.2b. However, this model is also poorly able to handle data containing significant experimental error. The inaccuracy of the Eadie Hofstee plot is not as severe as for the Lineweaver-Burk plot, and is considered to be a more reliable method (Cornish-Bowden, 2004). Furthermore, in this case the horizontal axis is not truly independent of the vertical axis as the values contain an element of the reaction rate. Therefore, any error in the experiment will affect both axes.

A third model for analysing kinetic data utilises the Hanes-Woolfe plot. This is shown in Figure 3.2c. This plot has less scatter as the two axes are completely independent of each other. For this reason, the Hanes-Woolfe plot was selected here to estimate trypsin kinetic constants.

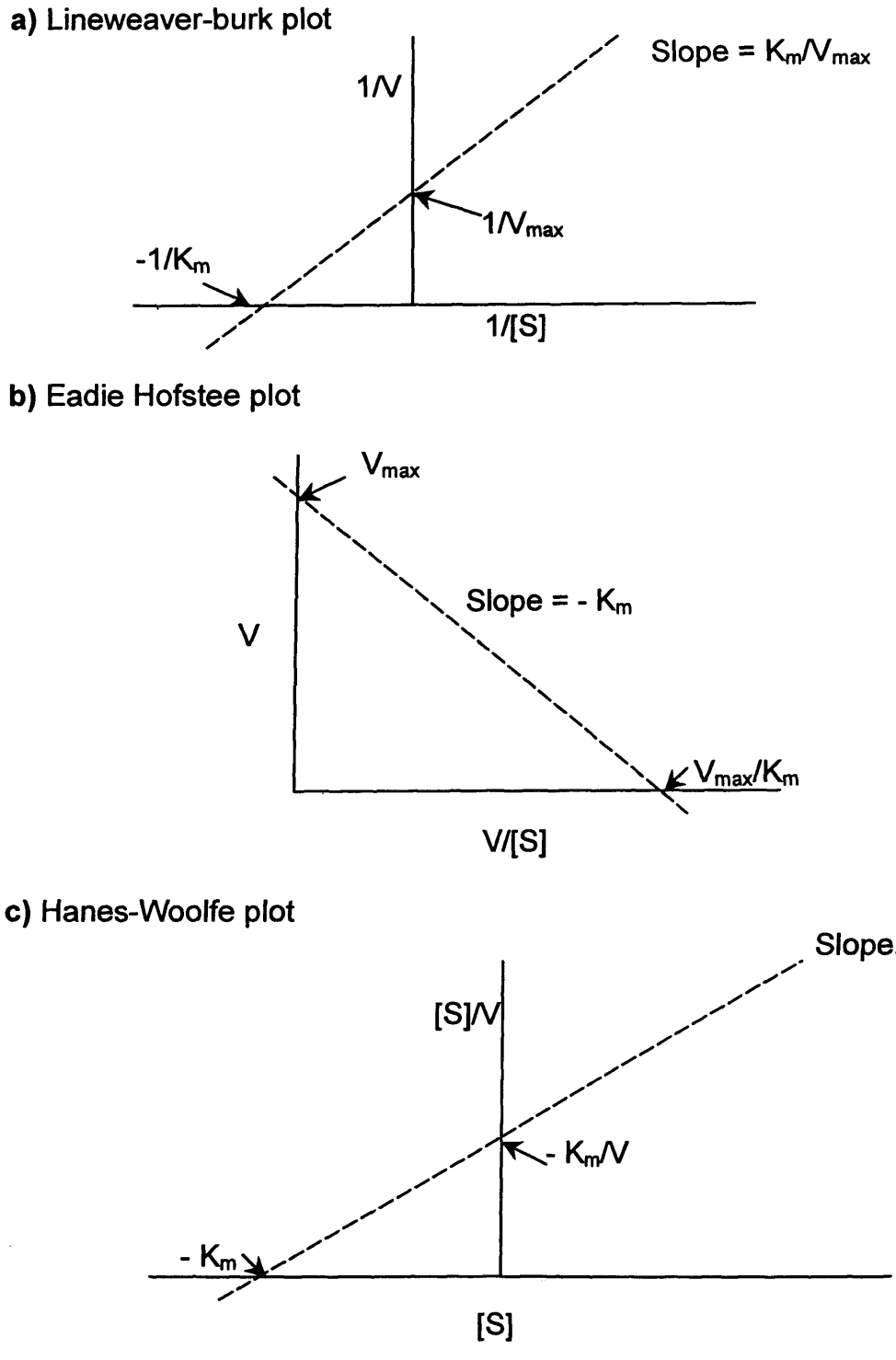

Figure 3.2 Enzyme kinetics models for data interpretation, based on the Michaelis-Menten equation. Panel (a) Lineweaver-Burk plot, (b) Eadie-Hofstee plot, and (c) Hanes-Woolfe plot.

3.1.3 Experimental aims

The aims of this study were to:

- Try to optimise methods for conjugation of
  - HPMA copolymer-Gly-Gly (5 mol %) –ONp,
  - HPMA copolymer-Gly-Gly (5 mol %) –COOH, and
  - succinoylated dextrin to trypsin
- Establish methods for characterising the polymer-protein conjugates proposed, with respect to:
  - total protein content (BCA assay)
  - free protein content (FPLC, SDS PAGE)
  - molecular weight and molecular weight distribution (GPC, FPLC and SDS PAGE)
- Set up a biological assay to investigate the retention of trypsin activity following polymer conjugation

3.2 Methods

A number of general methods (Chapter 2) were used for characterisation of the polymer-trypsin conjugates synthesised; BCA assay (section 2.4.4.3), SDS PAGE (section 2.4.4.2), FPLC and GPC (section 2.4.4.1). In addition, the trypsin NH_2 groups were quantified using the ninhydrin (section 2.4.1) and TNBS assays (section 2.4.2) as described in Chapter 2.

3.2.1 Synthesis of HPMA copolymer-trypsin conjugates

First, the extinction coefficient (ε) of ONp was calculated in all the solvents used to explore the aminolysis reaction; ddH_2O, DMSO and DMF. Samples of ONp (5-30 μg/mL) were prepared in each solvent (1 mL) and added to a quartz cuvette. A UV scan was made between 200 nm and 500 nm. The value of ε was derived from the gradient of a calibration curve of ONp concentration vs. maximum absorbance at ~ 320 nm.

In addition, it was necessary to determine the stability of HPMA copolymer-Gly-Gly-ONp in the different solvents that would be used for the aminolysis reaction

(ddH_2O, PBS buffer, DMSO and DMF). Solutions of HPMA copolymer-Gly-Gly-ONp (1 mL, 1 mg/mL) were made up in each solvent and ONp release was monitored spectrophotometrically at 400 nm over 30 min.

To synthesise HPMA copolymer-trypsin conjugates four different conjugation methods were explored. These are described in detail below.

a) Synthesis of HPMA copolymer-Gly-Gly-trypsin using aminolysis

Initially, a non-specific aminolysis reaction was investigated using the method described earlier for cathepsin B and β-lactamase conjugation to HPMA copolymer-Gly-Gly-ONp (Satchi *et al*, 2001; Satchi-Fainaro *et al*, 2003) (Figure 3.1a).

Briefly, HPMA copolymer-Gly-Gly-ONp (40 mg) was dissolved in ddH_2O (20 mL) in a 100 mL round-bottomed flask and trypsin (81 mg) in 0.05 M phosphate buffer (pH 7.2, 40.5 mL) was added at 4 °C, under stirring. This mixture was stirred for 30 min in the dark at pH 7.2. Then the pH was increased over 4 h by the addition of saturated sodium tetraborate buffer to obtain a pH of 8.5. This helped to prevent enzyme denaturation. The mixture was then stirred for a further 4 h and the reaction was terminated by addition of D,L-amino-2-propanol (0.5 eq. of ONp groups). Next, the solution was acidified to pH 7.2 with 0.1 M HCl, and was dialysed (molecular weight cut-off 25,000 g/mol) against 5 L of ddH_2O with ~ 8 water changes, with 1-2 h between each. The contents of the dialysis sac were then collected and freeze-dried for 2 days.

Reaction of HPMA copolymer-Gly-Gly-ONp copolymer with trypsin by aminolysis was initially followed by UV to monitor ONp release. This was possible as there is a difference in UV maximum absorption of bound (270 nm) and free (400 nm) ONp. After termination of the reaction, the crude reaction products were analysed by SDS PAGE and GPC to determine the reaction yield.

b) Conjugation of HPMA copolymer-Gly-Gly-ONp to trypsin according to anti-O antibody-polymer method (Kopecek *et al*, 1985b)

The procedure is summarised in Figure 3.1b. Briefly, HPMA copolymer-Gly-Gly-ONp (77 mg) was dissolved at 5 °C in diluted hydrochloric acid (0.5 mL, pH

3.0). Sorensen's buffer (0.6 mL, pH 8.0) containing 0.15 M NaCl was then added followed by the dropwise addition of trypsin solution (0.67 mL, containing 39.5 mg trypsin) in the same buffer. The reaction was allowed to proceed for 30 min at 5 °C. During the following 30 min the temperature was gradually increased to 20 °C. (At the beginning of the reaction the molar ratio of reactive groups ONp: NH_2 = 1:1 and the concentration of macromolecules was 6.6 % wt.). After 1 h a solution of D-L-amino-2-propanol in 0.2 mL Sorensen's buffer (10 % v/v, 0.2 mL, pH 8.0) containing NaCl (0.15 M) was added. After 10 min the reaction mixture was transferred into a visking dialysis tubing and dialysed against phosphate buffered saline (pH 7.2).

c) Conjugation of HPMA copolymer-Gly-Gly-ONp to trypsin according to transferrin-polymer method (Kopecek *et al*, 1985b)

The method is summarised in Figure 3.1c. HPMA copolymer-Gly-Gly-ONp (27.4 mg) was dissolved in diluted hydrochloric acid (0.25 mL, pH 3.0). Sorensen's buffer (1.25 mL, pH 8.0) containing NaCl (0.1 M) was then added followed by a solution of trypsin (0.5 mL, 28.4 mg/mL) of the same buffer. After 45 min, D-L-amino-2-propanol dissolved in Sorensen's buffer (200 μL, 50 μL/mL) was added to the mixture. After 30 min the reaction was stopped and transferred to visking dialysis tubing and dialysed against phosphate buffered saline (pH 7.2).

d) Conjugation of HPMA copolymer-Gly-Gly-COOH to trypsin with EDC/ sulfo-NHS

First, HPMA copolymer-Gly-Gly-ONp was hydrolysed to HPMA copolymer-Gly-Gly-COOH. HPMA copolymer-Gly-Gly-ONp (~ 100 mg) was dissolved in ddH_2O and 10 molar eq. of a solution of NaOH (0.1 M) was added and stirred for 4-5 h at room temperature. The resultant product was then dialysed (molecular weight cut-off 2,000 g/mol) to remove free ONp in 5 L of ddH_2O for ~ 8 water changes, allowing 1-2 h between water changes. The product was then isolated and freeze-dried for 2 days.

This procedure is summarised in Figure 3.1d. Next, the HPMA copolymer-Gly-

Gly-COOH (~ 10 mg) was dissolved in ddH_2O (1 mL) in a 25 mL round-bottomed flask. EDC (range between 10-30 eq.) was added to the reaction mixture under stirring, and the mixture was left to stir for 10 min. Then sulfo-NHS was added (concentration range between 10-30 eq.) and the mixture was stirred for 40 min. Next, trypsin was added as an aqueous solution (1 trypsin: 2 COOH groups). The pH was adjusted to ~ 8 by dropwise addition of NaOH (0.1 M) solution, and the mixture left stirring for 18 h at room temperature. After 18 h, the mixture was dialysed (molecular weight cut-off 25,000 g/mol) in ddH_2O for ~ 8 water changes. The contents of the dialysis sac were then freeze-dried for 2 days.

3.2.2 Synthesis of dextrin-trypsin conjugates

First, succinoylated dextrin was synthesised according to the method of Hreczuk-Hirst *et al* (2001b) as summarised in Figure 3.3a.

Briefly, dextrin (100 mg) was dissolved in anhydrous DMF (10 mL) in a 50 mL round bottom flask. Succinic anhydride (37 mg) and DMAP (16 mg) were subsequently added to the flask. The reaction mixture was then purged with nitrogen, sealed and left to stir at 50 °C for 18 h. Next, the reaction mixture was poured into vigorously stirring diethyl ether (250 mL) and stirred overnight. The ether was removed by filtration under vacuum and the residual solid was dissolved in minimal ddH_2O, poured into a dialysis membrane (molecular weight cut-off 10,000 g/mol) and dialysed against 4 x 5 L ddH_2O. The resultant solution was freeze-dried to yield succinoylated dextrin.

The degree of succinoylation was quantified by titration against a standard solution of NaOH (4.925×10^{-5} M) with bromophenol blue as indicator. The product was further characterised by FT-IR, ^{1}H-NMR and ^{13}C-NMR.

To conjugate succinoylated dextrin to trypsin (Figure 3.3b), succinoylated dextrin (117 mg, 1.50×10^{-2} mol COOH) and EDC (16 mg) were dissolved in ddH_2O (2 mL). After 10 min, sulfo-NHS (17 mg) was added under stirring and allowed to react for 40 min at room temperature. Trypsin (30 mg, 1.25×10^{-4} mol) was added and sufficient NaOH (0.1 M) was added to bring the reaction mixture to pH 8.0 (this

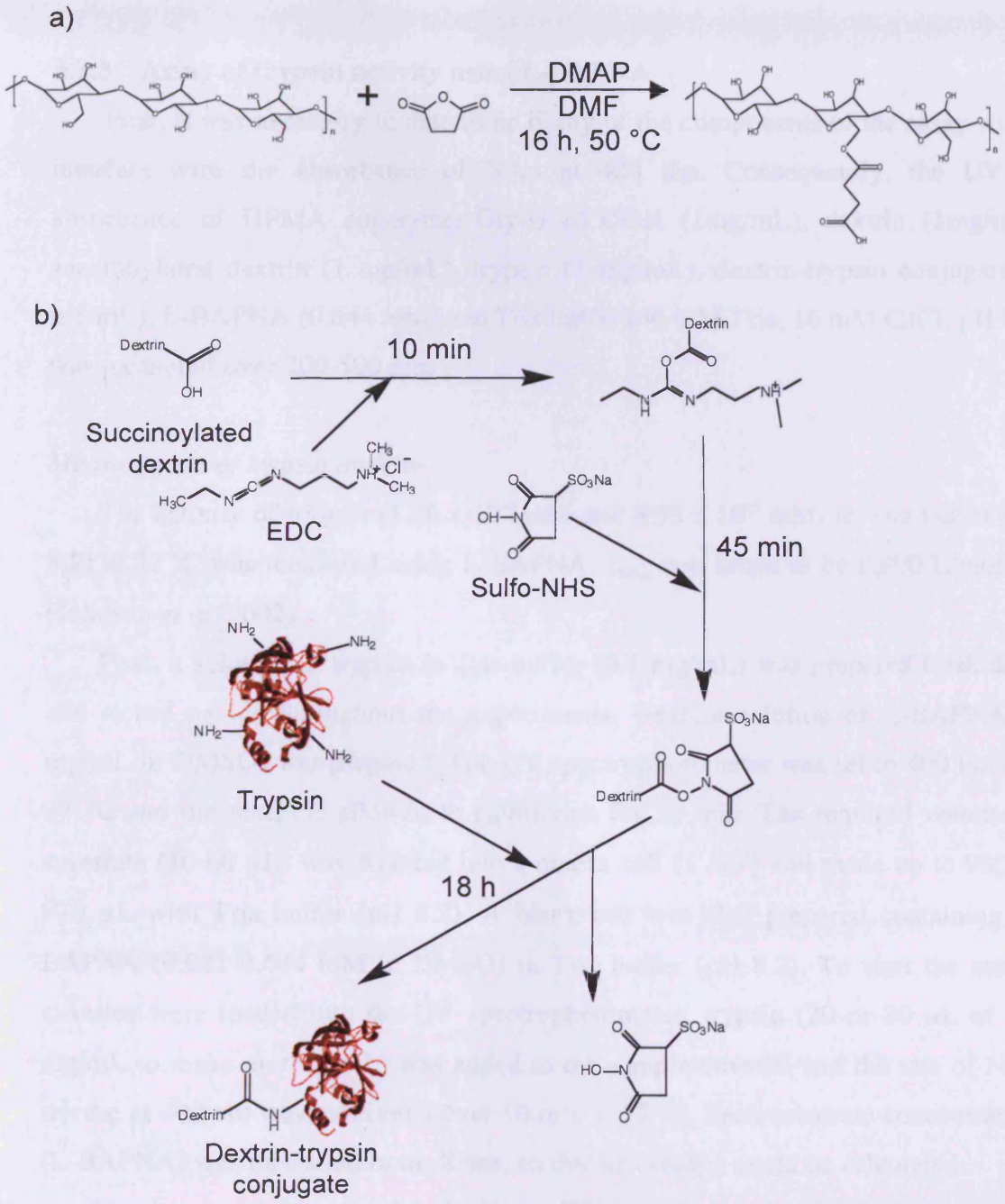

Figure 3.3 Reaction scheme for (a) succinoylation of dextrin, and (b) conjugation of succinoylated dextrin to trypsin.

helps reduce risk of enzyme denaturation). This mixture was subsequently allowed to stir overnight at room temperature. Free enzyme was removed by dialysis (molecular weight cut-off 50,000 g/mol) against 8 x 5 L ddH_2O. The product was freeze-dried.

3.2.3 Assay of trypsin activity using L-BAPNA

First, it was necessary to determine if any of the components of the assay would interfere with the absorbance of NAp at 400 nm. Consequently, the UV-vis absorbance of HPMA copolymer-Gly-Gly-COOH (1mg/mL), dextrin (1mg/mL), succinoylated dextrin (1 mg/mL), trypsin (1 mg/mL), dextrin-trypsin conjugate (1 mg/mL), L-BAPNA (0.644 mM) and Tris buffer (40 mM Tris, 16 mM CaCl, pH 8.2) was measured over 200-500 nm.

Measurement of trypsin activity

The activity of trypsin (1.28 x 10^{-4} mM and 8.55 x 10^{-5} mM) in Tris buffer (pH 8.2) at 37 °C was measured using L-BAPNA. ε_{NAp} was taken to be 8,800 L/mol/cm (Johnson *et al*, 2002).

First, a solution of trypsin in Tris buffer (0.1 mg/mL) was prepared fresh daily and stored on ice throughout the experiments. Next, a solution of L-BAPNA (7 mg/mL in DMSO) was prepared. The UV spectrophotometer was set to 400 nm and 37 °C and the machine allowed to equilibrate for 30 min. The required volume of substrate (10-60 μL) was pipetted into a quartz cell (1 cm^3) and made up to 980 or 970 μL with Tris buffer (pH 8.2). A blank cell was also prepared containing L-BAPNA (0.081-0.644 mM in DMSO) in Tris buffer (pH 8.2). To start the assay, cuvettes were loaded into the UV spectrophotometer, trypsin (20 or 30 μL of 0.1 mg/mL to make up to 1 mL) was added to the sample cuvette, and the rate of NAp release at 400 nm was monitored over 10 min at 37 °C. Each substrate concentration (L-BAPNA) was measured in triplicate, so that an average could be calculated.

The data was analysed using the Hanes-Woolfe plot (section 3.1.2).

Measurement of polymer-trypsin conjugate activity

In order to assess the retention of trypsin activity following polymer

conjugation, the conjugates were also analysed using the L-BAPNA assay described here. Using the trypsin content of the conjugate, determined by the BCA assay, solutions of polymer-trypsin conjugate were prepared to contain 1.28 x 10^{-4} mM trypsin eq.. The activity of the conjugate was then assessed against the substrate L-BAPNA (0.081-0.644 mM in DMSO) as above. Conjugate activity was expressed as a percentage of the activity of free trypsin. The kinetics rate constants were also assessed using the Hanes-Woolfe plot (section 3.1.2).

3.3 Results

The extinction coefficients estimated for ONp in ddH_2O, DMSO and DMF were calculated using the Beer-Lambert law, the values obtained were: ddH_2O $\varepsilon_{318\ nm}$ = 10,307 L/mol/cm, DMSO $\varepsilon_{323\ nm}$ = 9,501 L/mol/cm, and DMF $\varepsilon_{318\ nm}$ = 11,675 L/mol/cm (Figure 3.4).

The release of ONp from HPMA copolymer-Gly-Gly-ONp precurser in aqueous (ddH_2O, PBS buffer) and organic (DMSO, DMF) solvents was monitored by UV spectroscopy (Figure 3.5). There was little release observed in ddH_2O, DMF, and DMSO, but there was a rapid release of ONp by hydrolysis in PBS buffer.

3.3.1 Synthesis and characterisation of HPMA copolymer-Gly-Gly-trypsin conjugates

The ninhydrin assay indicated that trypsin had 12.1 ± 3.7 (SD) NH_2 groups per molecule. This figure (12), which also includes terminal amine groups and several other NH-containing amino acids (arginine, histidine), was used to calculate molar ratio of trypsin to succinoylated dextrin (NH_2 : COOH) for all conjugation reactions and not the total number of lysine groups in trypsin (10).

HPMA copolymer-Gly-Gly-trypsin conjugate: Cathepsin B method

Initially, when the methods of Satchi *et al* (2001) (section 3.2.1a) were used to react HPMA copolymer-Gly-Gly-ONp with trypsin in aqueous medium, conjugation was not achieved. Later, this was repeated with varying reaction conditions and ratio of trypsin: polymer in an attempt to improve the conjugation. However, still SDS PAGE showed only a band for free trypsin (MW ~ 20,000 g/mol), suggesting that no

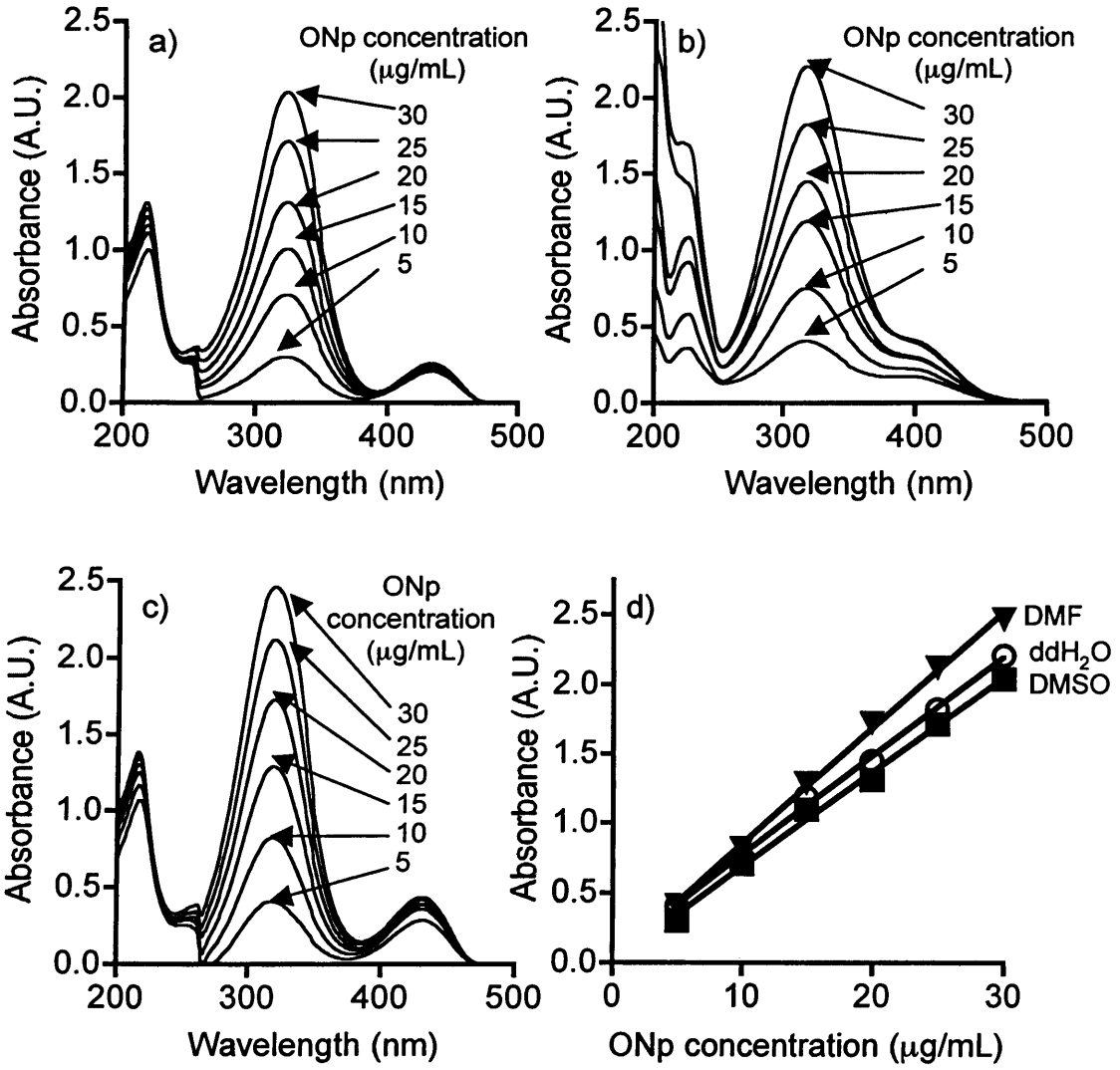

Figure 3.4 UV absorption spectra of ONp. Panel (a) in DMSO (λ_{max} = 323 nm), panel (b) in ddH_2O (λ_{max} = 318 nm),and (c) in DMF (λ_{max} = 318 nm). Panel (d) shows a calibration curve for ONp in ddH_2O, DMSO, and DMF. Data shown represents n=1.

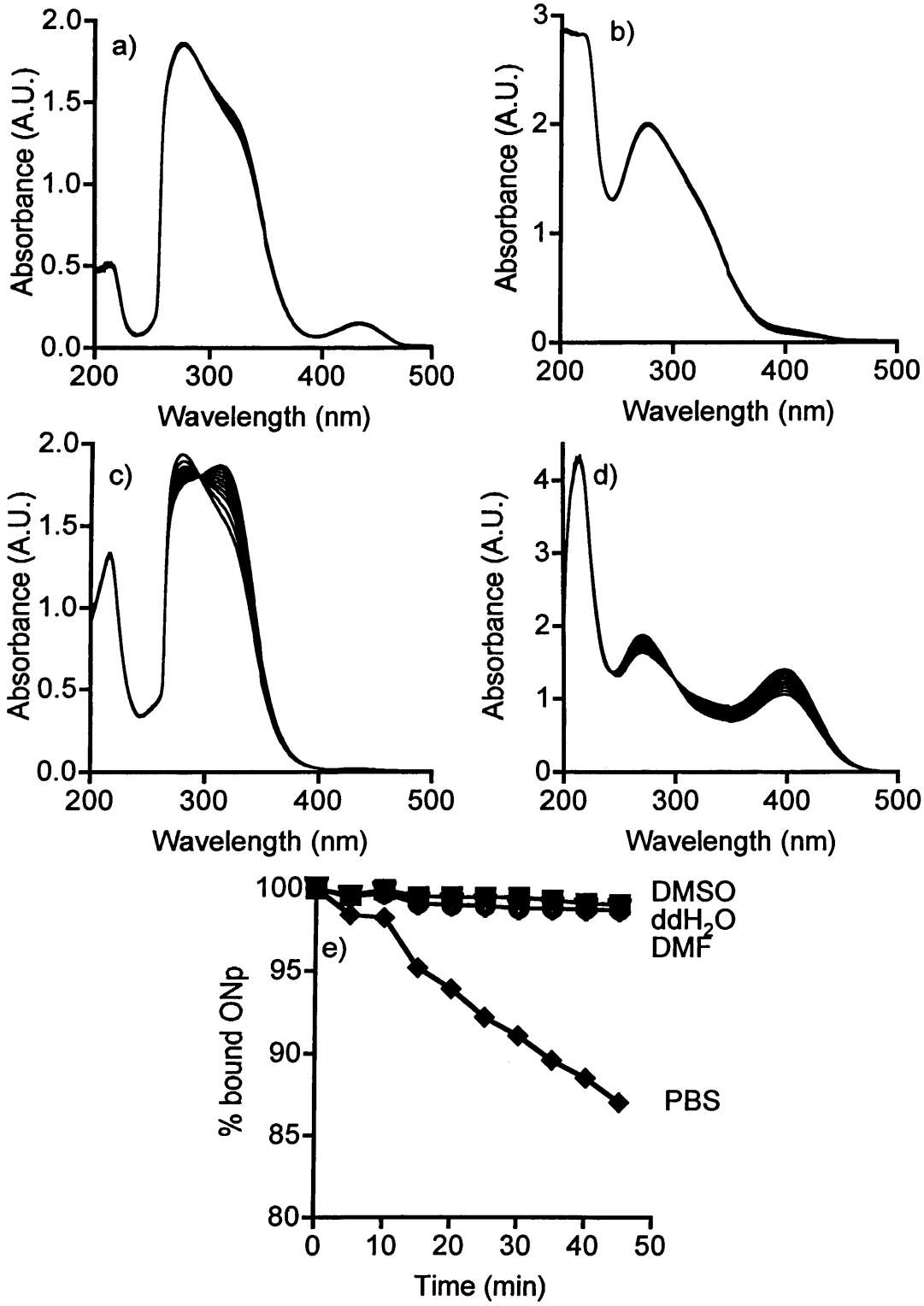

Figure 3.5 Stability of HPMA copolymer-Gly-Gly-ONp during incubation in different solvents. Panel (a) DMSO, panel (b) ddH_2O, panel (c) DMF, and panel (d) PBS buffer. Panel (e) shows release of ONp over time. All at 1 mg/mL, recorded every 5 min for 40 min. % bound ONp calculated from peak absorbance at 280 nm. Data shown represents n=1.

conjugation was achieved (Figure 3.6, lanes 3-12). Even altering the rate of addition of saturated borate buffer did not improve reaction efficiency. The reaction conditions explored are summarised in Table 3.2.

FPLC was used to better characterise these reactions. First, the FPLC was first calibrated using protein standards (Figure 2.2). Then samples of reaction mixtures were analysed. It was noted that the elution profile for unconjugated trypsin was complicated by some contamination with smaller molecular weight peptides (Figure 3.7). This was also observed in the SDS PAGE gels (Figure 3.6, lane 2). However, there was a pronounced peak at ~ 12 mL, corresponding to trypsin and, even after purification of the trypsin by PD-10 column (results not shown), there was no noticeable polymer conjugation and the reaction mixtures showed only a peak appearing at the same elution volume as free trypsin (~ 12 mL) (data not shown).

HPMA copolymer-Gly-Gly-trypsin conjugate: Anti-O antibody and transferrin methods

When conjugation was attempted using the methods described by Kopecek *et al* (1985b) (section 3.2.1b and 3.2.1c), SDS PAGE began to show a faint smearing indicative of a HPMA copolymer-Gly-Gly-trypsin conjugate. However, there was also a strong band corresponding to free trypsin (Figure 3.8, lanes 3-6). GPC also showed some evidence of conjugation (Figure 3.9) but there remained a very large amount of free trypsin present in conjugates synthesised using both of these methods. Further purification by dialysis resulted in a very low yield of conjugate (Figure 3.8 and 3.9). Therefore, conjugates synthesised using this method were not progressed to biological testing.

HPMA copolymer-Gly-Gly-COOH: Use of EDC and sulfo-NHS

When EDC and sulfo-NHS were used to conjugate trypsin to HPMA copolymer-Gly-Gly-COOH (section 3.2.1.d) SDS PAGE (Figures 3.10 (lane 3)) of the reaction mixtures showed a dark smearing down the sample lane indicating that a polymer-protein conjugate had been successfully synthesised. However, there was also a clear band of free trypsin. FPLC confirmed conjugate synthesis (peak at ~ 8 mL) but there

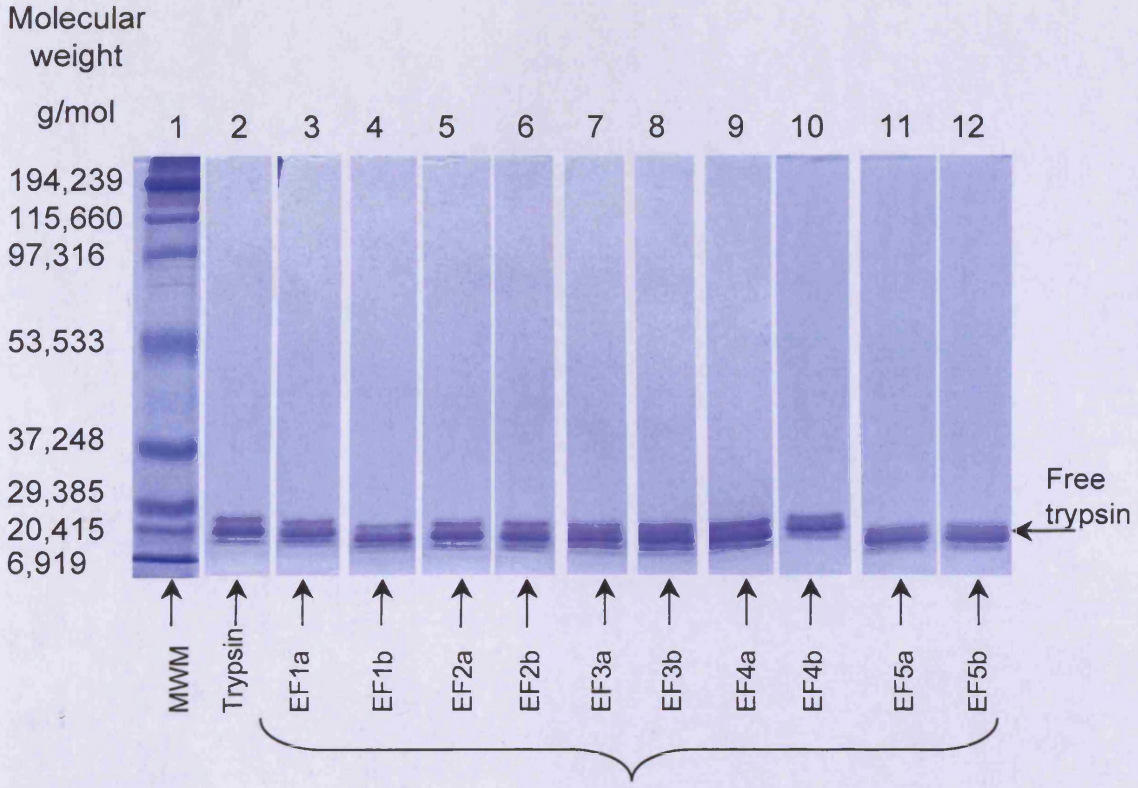

Figure 3.6 SDS PAGE of HPMA copolymer-Gly-Gly-trypsin conjugates prepared according to method described in 3.2.1a. Where MWM = molecular weight marker and EF## = attempts to synthesise HPMA copolymer-trypsin under different reaction conditions (detailed in Table 3.2).

Table 3.2 Examples of variables examined in the synthesis of HPMA copolymer-Gly-Gly-trypsin conjugates.

Batch no.	HPMA: trypsin (weight ratio)	HPMA copolymer solution (2 mg/mL)	Trypsin solution (2 mg/mL)	Reaction conditions
EF1a	1:1	1 mL	1 mL	Increase pH to 8.5 (borate buffer) over 4 h. Reaction time = 4 h at 4 °C
EF1b	1:1	1 mL	1 mL	Increase pH to 8.5 (borate buffer) at start of reaction. Reaction time = 4 h at 4 °C
EF2a	1:2	1 mL	2 mL	Increase pH to 8.5 (borate buffer) over 4 h. Reaction time = 4 h at 4 °C
EF2b	1:2	1 mL	2 mL	Increase pH to 8.5 (borate buffer) at start of reaction. Reaction time = 4 h at 4 °C
EF3a	1:3	1 mL	3 mL	Increase pH to 8.5 (borate buffer) over 4 h. Reaction time = 4 h at 4 °C
EF3b	1:3	1 mL	3 mL	Increase pH to 8.5 (borate buffer) at start of reaction. Reaction time = 4 h at 4 °C
EF4a	2:1	2 mL	1 mL	Increase pH to 8.5 (borate buffer) over 4 h. Reaction time = 4 h at 4 °C
EF4b	2:1	2 mL	1 mL	Increase pH to 8.5 (borate buffer) at start of reaction. Reaction time = 4 h at 4 °C
EF5a	3:1	3 mL	1 mL	Increase pH to 8.5 (borate buffer) over 4 h. Reaction time = 4 h at 4 °C
EF5b	3:1	3 mL	1 mL	Increase pH to 8.5 (borate buffer) at start of reaction. Reaction time = 4 h at 4 °C

50 μL taken at t=0 min, 0.1 min, 15 min, 30 min, 1 h, 2 h, 3 h, 4 h (frozen immediately for SDS PAGE analysis)
5 μL taken at t=0 min, 0.1 min, 15 min, 30 min, 1 h, 2 h, 3 h, 4 h (analysed in UV spectrophotometer)

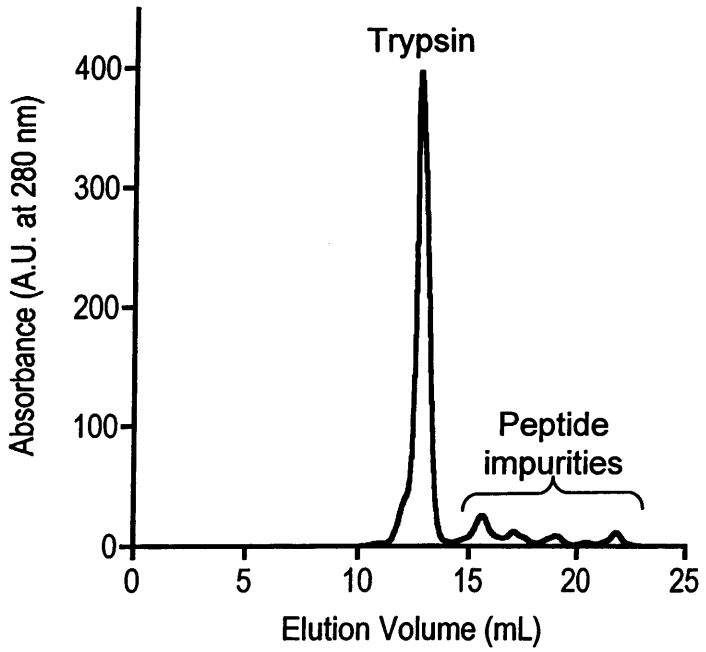

Figure 3.7 FPLC analysis of free trypsin. Where a) trypsin. V_0 = void volume (7.7 mL), and V_b = bed volume (24 mL). UV absorbance taken at 280 nm.

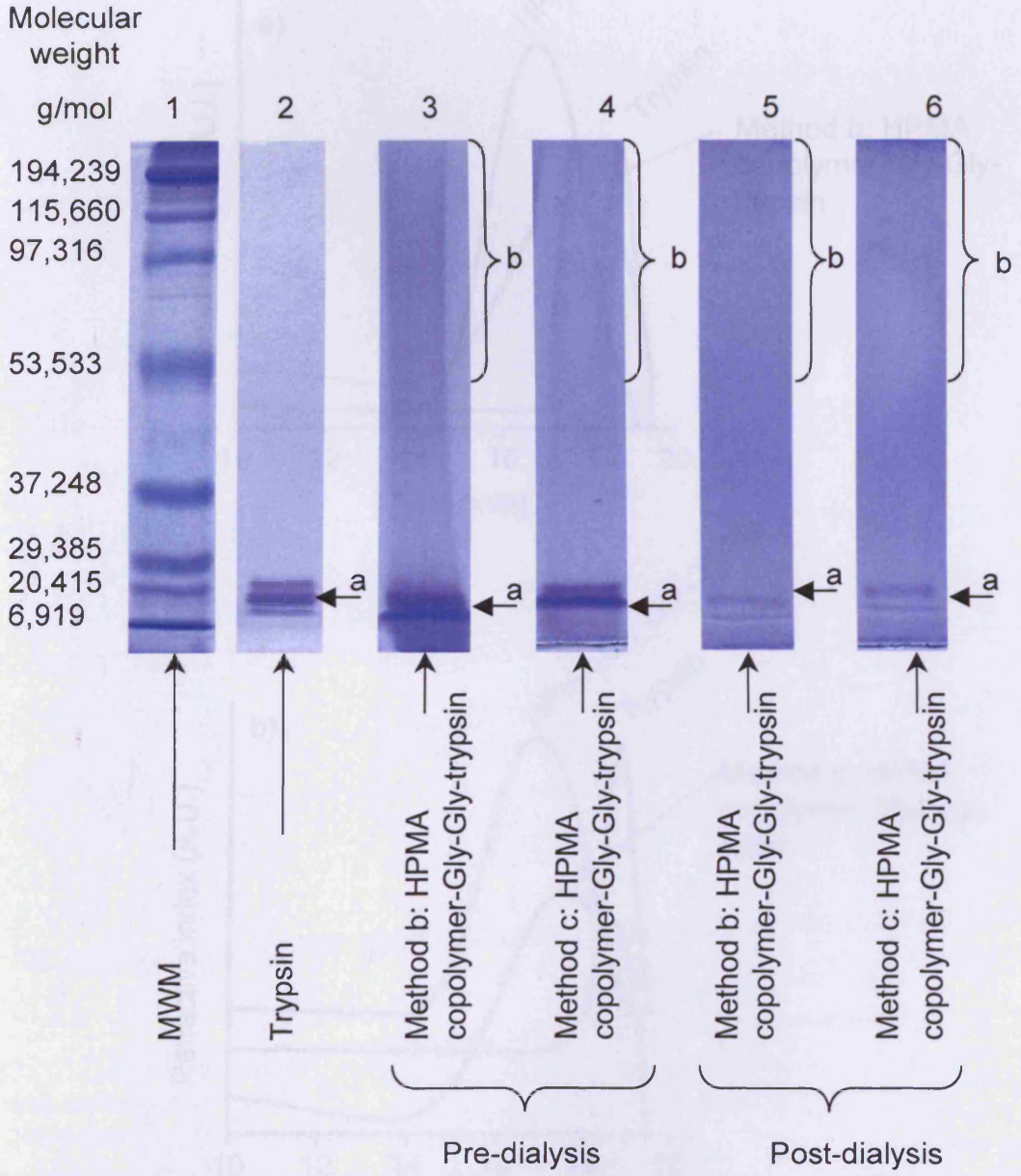

Figure 3.8 SDS PAGE analysis of free and bound trypsin, purified by dialysis. Method b = anti-O antibody method (described in 3.2.1b), method c = transferrin method (described in 3.2.1c). Where a) trypsin, and b) HPMA copolymer-Gly-Gly-trypsin. MWM = molecular weight marker.

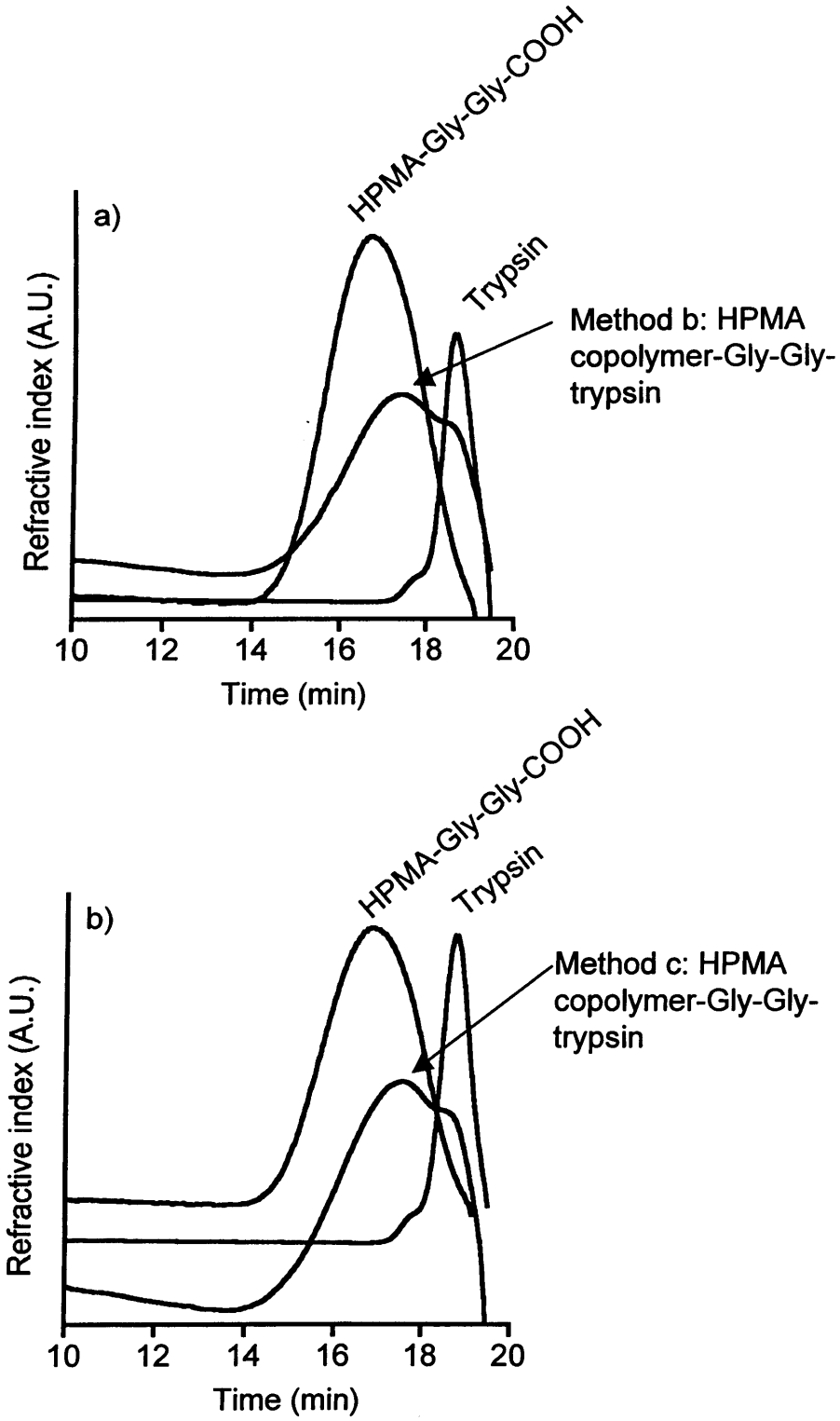

Figure 3.9 Characterisation by GPC of HPMA copolymer-Gly-Gly-trypsin conjugates. Panel (a) shows the GPC trace of HPMA copolymer-Gly-Gly-trypsin conjugates prepared using method b = anti-O antibody method (described in 3.2.1b), and panel (b) shows conjugates synthesised using method c = transferrin method (described in 3.2.1c). Molecular weight given is relative to pullulan standards. V_0 = void volume (13 mL), and V_b = bed volume (20 mL).

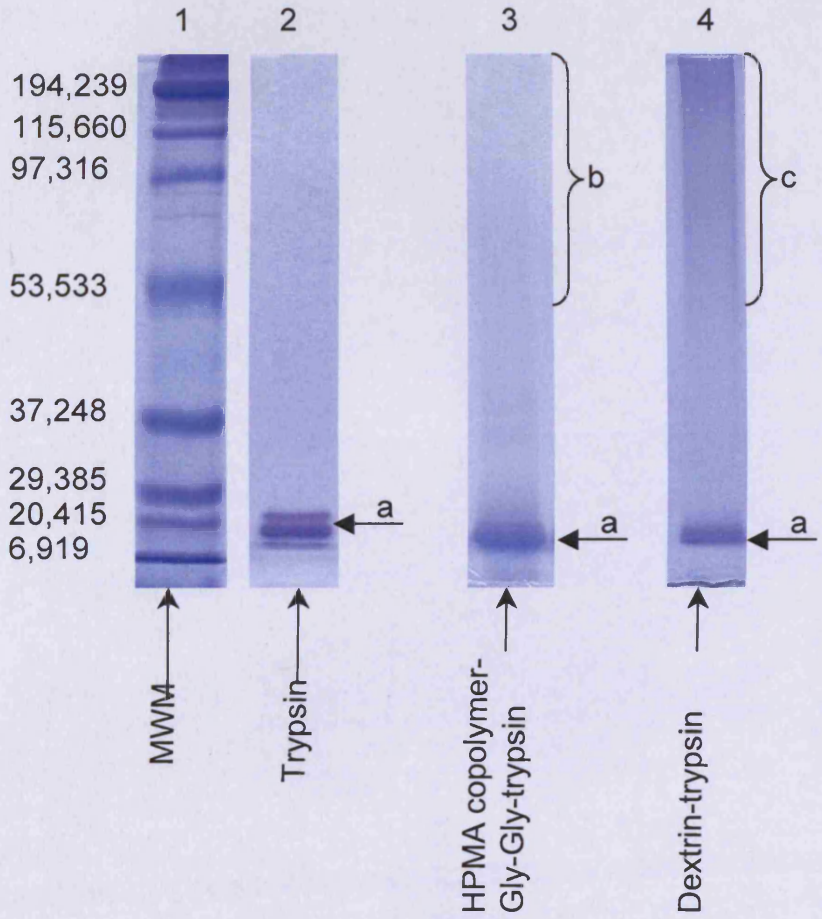

Figure 3.10 SDS PAGE analysis of free and bound trypsin. Polymer-trypsin conjugates were prepared using EDC and sulfo-NHS as linking agents. Where a) trypsin, b) HPMA copolymer-Gly-Gly-trypsin, and c) dextrin-trypsin. MWM = molecular weight marker.

was also a large amount of free trypsin (peak at ~ 12 mL) (Figure 3.11a).

Even when experiments were performed to try and optimise the ratios of coupling agents to get a better conjugate yield, analysis by SDS PAGE and GPC also revealed no improvement in conjugation efficiency (Figure 3.12a).

The HPMA copolymer-Gly-Gly-trypsin conjugates synthesised in this way had a total trypsin content of 59 - 84 % w/w (HPMA copolymer-Gly-Gly-COOH showed minimal interference with the BCA assay) and in the final purified batch there was < 2 % w/w free trypsin.

The characteristics of the HPMA copolymer-trypsin conjugates synthesised here are summarised in Table 3.3. However, after removal of unreacted trypsin, the yield was so low that HPMA copolymer conjugates were not progressed further.

3.3.2 Synthesis and characterisation of dextrin-trypsin conjugates

When dextrin (51,000 g/mol) was succinoylated, the degree of modification was confirmed by titration to be 17 - 23 mol %. Typically, the reaction conversion efficiency for succinoylation was ~ 30 - 40 % of the theoretical maximum. A summary of the batches of succinoylated dextrins produced for these studies is shown in Table 3.4.

GPC using pullulan standards suggested an increase in dextrin molecular weight following succinoylation (MW increase from 60,455 to 73,802 g/mol) with little change in polydispersity. Characterisation of succinoylated dextrins by FT-IR (Figure 3.13a) showed characteristic peaks at 3,350 (OH), 1,723 (ester), 1,630 (carboxyl) and 1,020 cm^{-1} ($O\text{-}CH_2$). After succinoylation, the ester peak at 1,723 cm^{-1} was seen to increase in signal strength in relation to degree of modification. When NMR was used to analyse succinoylated dextrin, ^{1}H-NMR demonstrated peaks at 2.8 ppm, which can be assigned to aliphatic carbons that are not present in unreacted dextrin (Figure 3.13b). ^{13}C-NMR also showed the presence of two aliphatic carbons (30 ppm) (Figure 3.13c).

When the succinoylated dextrin intermediate was conjugated to trypsin using

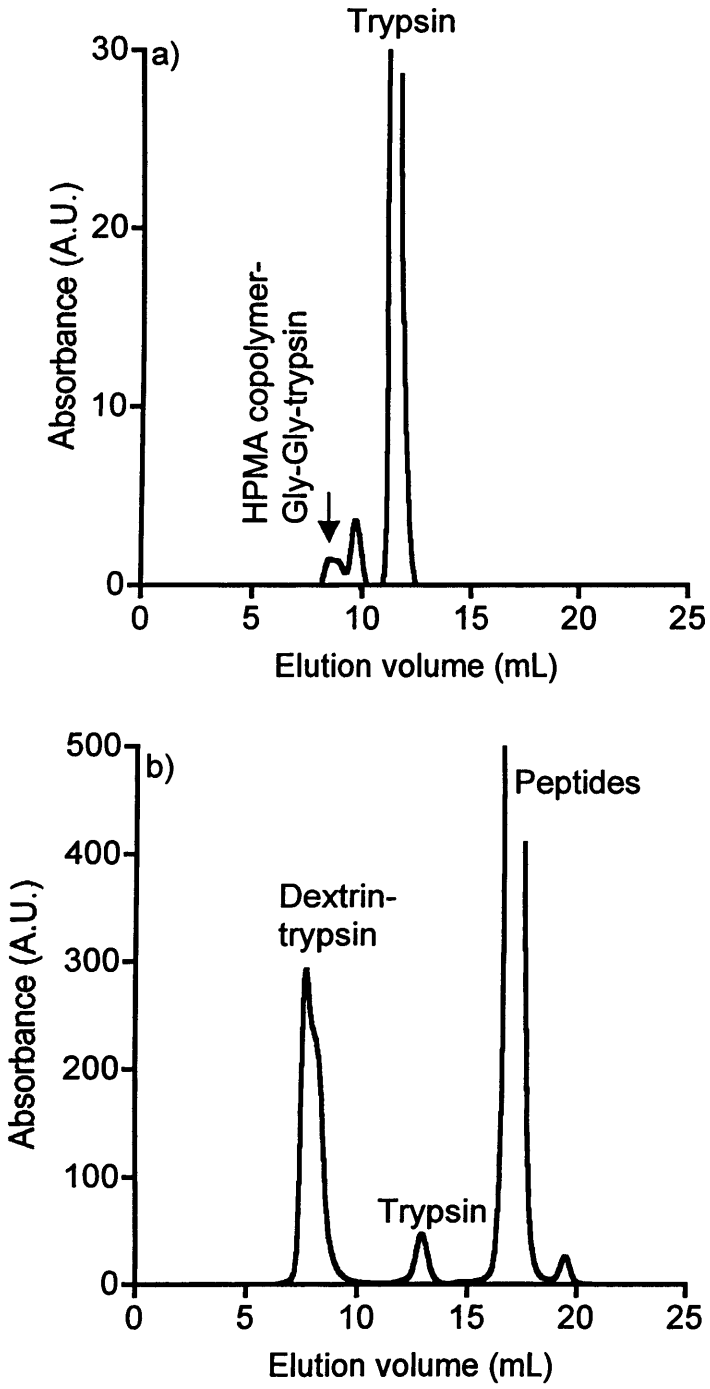

Figure 3.11 FPLC analysis of free and conjugated trypsin. Panel (a) shows characterisation of HPMA copolymer-Gly-Gly-trypsin conjugates, and panel (b) shows dextrin-trypsin conjugates. Polymer-trypsin conjugates were prepared using EDC and sulfo-NHS as linking agents. V_0 = void volume (7.7 mL), and V_b = bed volume (24 mL). UV absorbance taken at 280 nm.

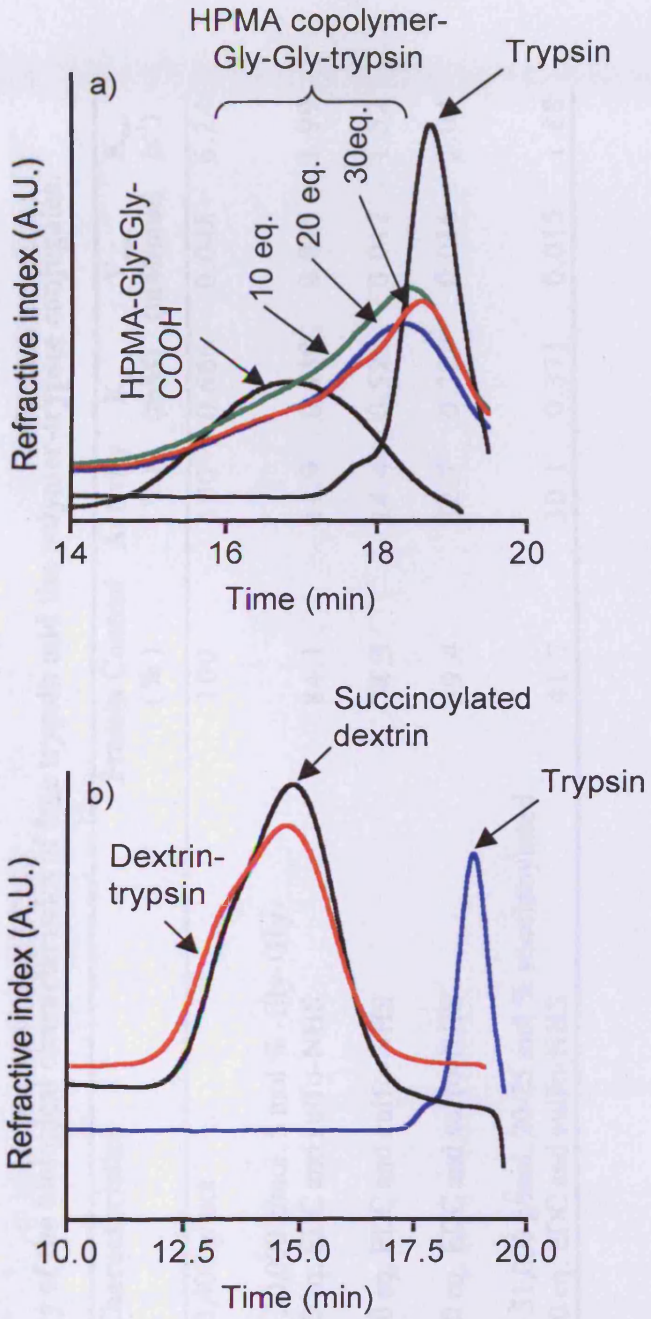

Figure 3.12 Characterisation by GPC of polymer-trypsin conjugates. Panel (a) shows the GPC trace of HPMA copolymer-Gly-Gly-trypsin conjugates prepared using different ratios of EDC and sulfo-NHS, and panel (b) shows dextrin-trypsin conjugates. Molecular weight given is relative to pullulan standards. Unless otherwise stated, response measured is refractive index. V_0 = void volume (13 mL), and V_b = bed volume (20 mL).

Table 3.3 Summary of the biological characteristics of free trypsin and the polymer-trypsin conjugates.

Polymer	Characteristics	Protein Content (%)	Activity (%)	K_m (mM)	V_{max} (mM/min)	K_{cat} (s^{-1})
Trypsin	23,400 g/mol	100	100	0.666	0.048	6.24
HPMA copolymer	~ 30,000 g/mol, 5 mol % -Gly-Gly- 10 eq. EDC and sulfo-NHS	84.1	31.9	0.430	0.015	1.99
	20 eq. EDC and sulfo-NHS	74.5	24.4	0.523	0.012	1.52
	30 eq. EDC and sulfo-NHS	59.4	32.7	0.329	0.016	2.04
Dextrin	~ 51,000 g/mol, 20-25 mol % succinoylated 10 eq. EDC and sulfo-NHS	41.7	30.1	0.371	0.015	1.88

Table 3.4 Characteristics of batches of succinoylated dextrin, and their uses.

Name	Batch size (mg)	Theoretical (mol %)	Actual (mol %)	Conversion (%)	Uses
Efdex1	200	60	16.8	27.9	Dextrin-trypsin
Efdex2	1000	60	23.2	38.7	Dextrin-PLA_2 (batches DexPLA1, DexPLA2)
Efdex3	1000	60	23.3	37.1	Dextrin-PLA_2 (batches DexPLA3, DexPLA4)
EFdex4	1000	60	19.4	33.3	MTT of S.dextrin, haemolysis of S.dextrin
EFdex5	1000	60	20.9	34.8	Dextrin-PLA_2 (batches DexPLA5, DexPLA7)
EFdex6	1000	60	22.3	37.2	Dextrin-OG, dextrin-PLA_2 (DexPLA6)

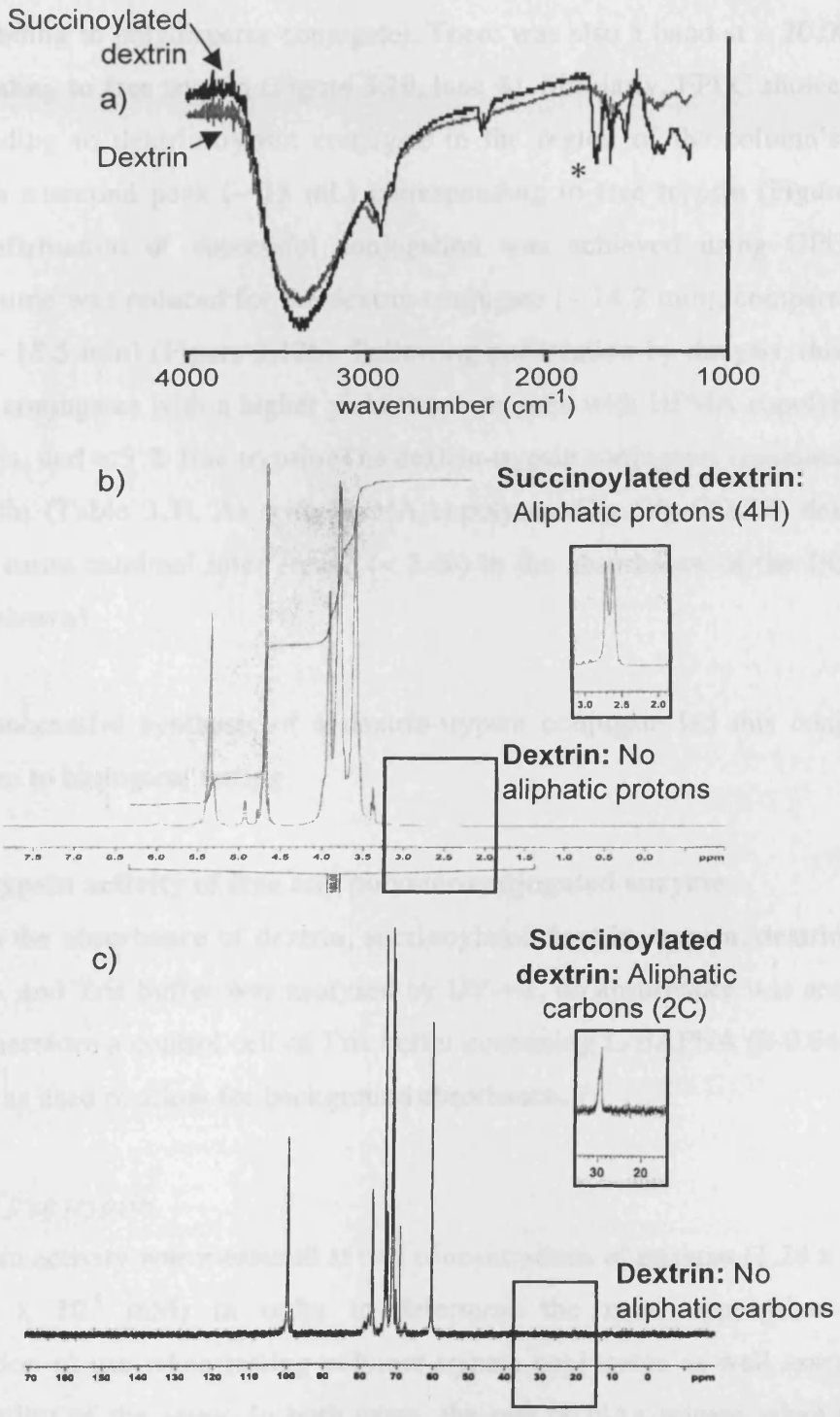

Figure 3.13 Characterisation by FT-IR and NMR of succinoylated dextrin. Panel (a) shows an FT-IR spectra illustrating the increase in peak intensity at 1720 cm^{-1}(*) when succinoyl ester groups are incorporated into dextrin. Also shown are (b) ^{1}H and (c) ^{13}C NMR spectra of dextrin and succinoylated dextrin (inserted panel).

EDC and sulfo-NHS, SDS PAGE confirmed the presence of a high molecular weight conjugate with dark smearing appearing between ~ 50,000 - 194,000 g/mol (corresponding to polydisperse conjugate). There was also a band at ~ 20,000 g/mol corresponding to free trypsin (Figure 3.10, lane 4). Similarly, FPLC showed a peak corresponding to dextrin-trypsin conjugate in the region of the column's V_o (7.7 mL), with a second peak (~ 13 mL) corresponding to free trypsin (Figure 3.11b). Final confirmation of successful conjugation was achieved using GPC, where retention time was reduced for the dextrin-conjugate (~ 14.2 min), compared to free trypsin (~ 18.5 min) (Figure 3.12b). Following purification by dialysis, this method produced conjugates with a higher yield than was seen with HPMA copolymer-Gly-Gly-trypsin, and < 5 % free trypsin. The dextrin-trypsin conjugates contained ~ 42 % w/w trypsin (Table 3.3). As with HPMA copolymer-Gly-Gly-COOH, dextrin was shown to cause minimal interference (< 2 %) in the absorbance of the BCA assay (data not shown).

The successful synthesis of a dextrin-trypsin conjugate led this conjugate to progression to biological testing.

3.3.3 Trypsin activity of free and polymer-conjugated enzyme

When the absorbance of dextrin, succinoylated dextrin, trypsin, dextrin-trypsin, L-BAPNA and Tris buffer was analysed by UV-vis, no absorbance was seen at 400 nm, and therefore a control cell of Tris buffer containing L-BAPNA (0-0.644 mM in DMSO) was used to allow for background absorbance.

Activity of free trypsin

Trypsin activity was measured at two concentrations of enzyme (1.28×10^{-4} mM and 8.55×10^{-5} mM) in order to determine the most appropriate enzyme concentration to use when testing polymer-trypsin conjugates as well assessing the reproducibility of the assay. In both cases, the rate of NAp release when substrate was incubated with native trypsin increased as L-BAPNA concentration was increased (Figures 3.14 and 3.15). In addition, an initial linear rate of NAp release was observed using both concentrations. When investigating the effect of pH,

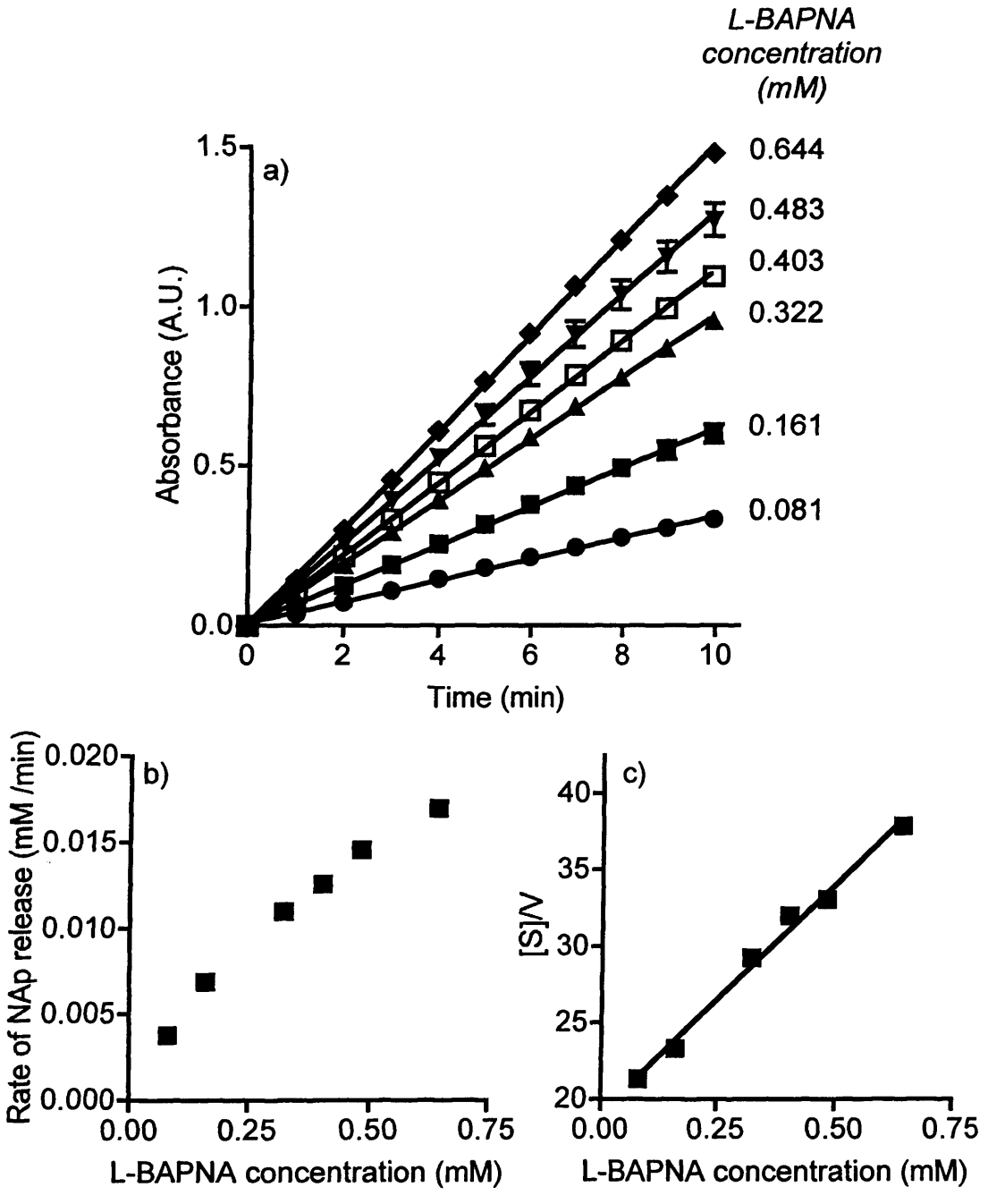

Figure 3.14 Activity of trypsin (8.55 x 10^{-5} mM) against the substrate L-BAPNA. Progress curves in panel (a) show the UV absorbance (400 nm) of NAp release from L-BAPNA by trypsin (8.55 x 10^{-5} mM) over 10 min. Panel (b) shows concentration-dependent rate of NAp release, and panel (c) shows a Hanes-Woolfe plot to determine kinetics rate constants from the data. Data shown represents the mean ± SD (n=3). Where error bars are not visible, error is within the data point.

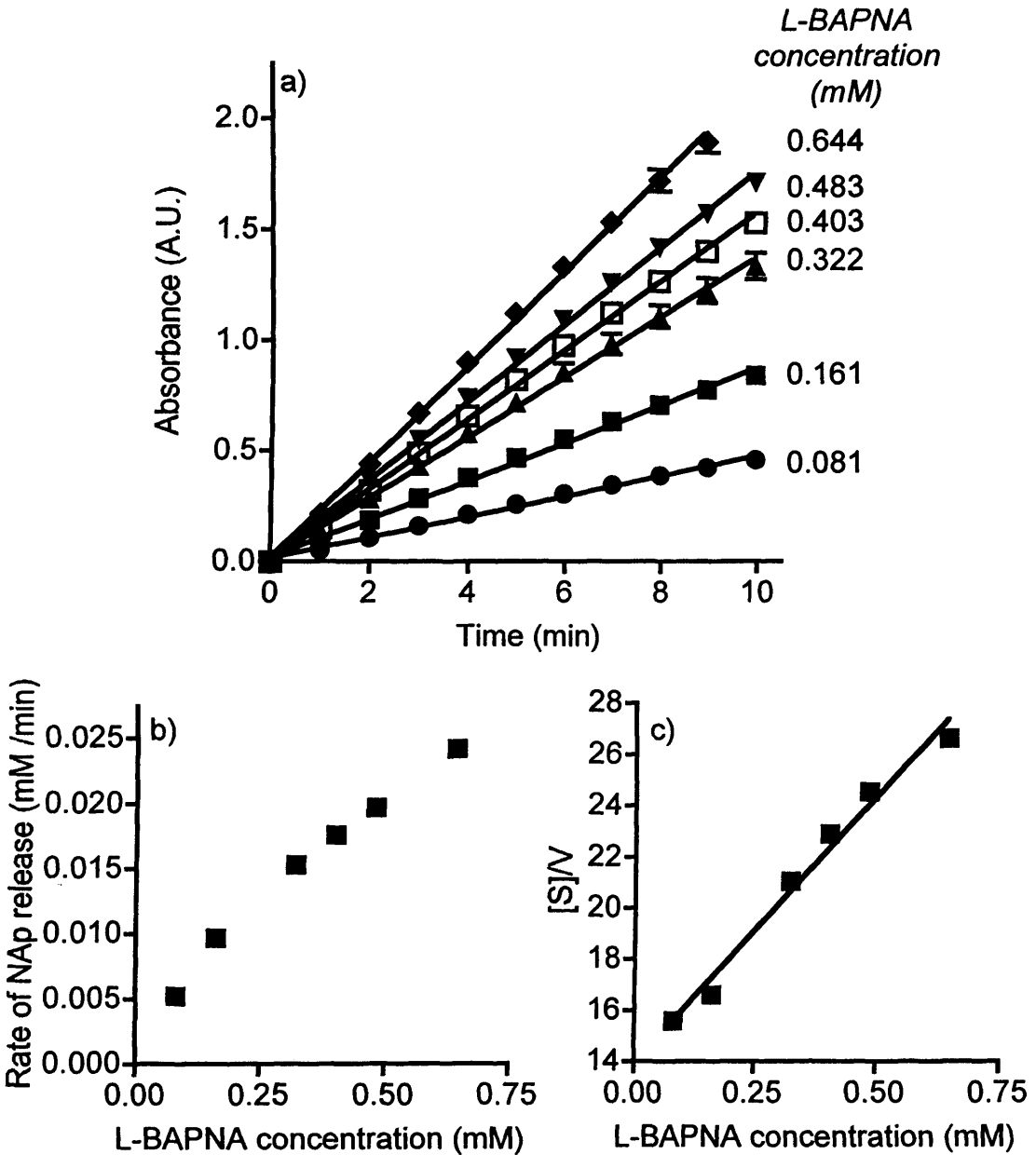

Figure 3.15 Activity of trypsin (1.28 x 10^{-4} mM) against the substrate L-BAPNA. Progress curves in panel (a) show the UV absorbance (400 nm) of NAp release from L-BAPNA by trypsin (1.28 x 10^{-4} mM) over 10 min. Panel (b) shows concentration-dependent rate of NAp release, and panel (c) shows a Hanes-Woolfe plot to determine kinetics rate constants from the data. Data shown represents the mean ± SD (n=3). Where error bars are not visible, error is within the data point.

maximum enzyme activity was seen at pH 8.2, while activity was most markedly reduced at pH 5.39 (Figure 3.16).

Activity of polymer-trypsin conjugates

When enzyme activity was measured following conjugation, 1.28 x 10^{-4} mM trypsin eq. was used at pH 8.2. Since HPMA copolymer-Gly-Gly-trypsin conjugates synthesised using EDC and sulfo-NHS were the most successful in terms of yield, only these conjugates were assessed for activity retention. When compared to the activity of free trypsin, enzyme activity was reduced for both dextrin (to ~ 30 %) and HPMA copolymer conjugates (to 24-33 %) (Figure 3.17, Table 3.3).

For HPMA copolymer-Gly-Gly-trypsin conjugates synthesised using different concentrations of EDC and sulfo-NHS, 10 eq. and 30 eq. produced conjugates with ~ 32 % native trypsin activity, while conjugates produced using 20 eq. EDC and sulfo-NHS had just ~ 24 % activity of the native enzyme.

The rate constants K_m, V_{max} and K_{cat} derived from the Hanes-Woolfe plot are summarised in Table 3.3. All the Hanes-Woolfe plots had a correlation coefficient of > 0.98 (2 s.f.). Free trypsin typically had a K_{cat} of ~ 6 s^{-1}, and this value was unaffected by changing enzyme concentration. K_m also remained similar at both concentrations of enzyme (~ 0.6 mM), but V_{max} was increased at higher trypsin concentration (0.0335-0.0480 mM/min).

After polymer conjugation, K_m remained similar to that of free trypsin, while V_{max} decreased (0.048 to 0.012-0.016 mM/min). Similarly, K_{cat} of trypsin also decreased following polymer conjugation (6.24 to 1.52-2.04 s^{-1}). K_{cat} correlated well with the trypsin activity, such that the slowest turnover rates were seen in HPMA copolymer-Gly-Gly-trypsin conjugate (30 eq. EDC and sulfo-NHS) having maximal enzyme masking (32.7 % activity remaining). Varying the amount of EDC and sulfo-NHS used in the reaction resulted in slightly different kinetic constants, as summarised in Table 3.3.

3.4 Discussion

The overall aim of these studies was to synthesise HPMA copolymer-Gly-Gly-

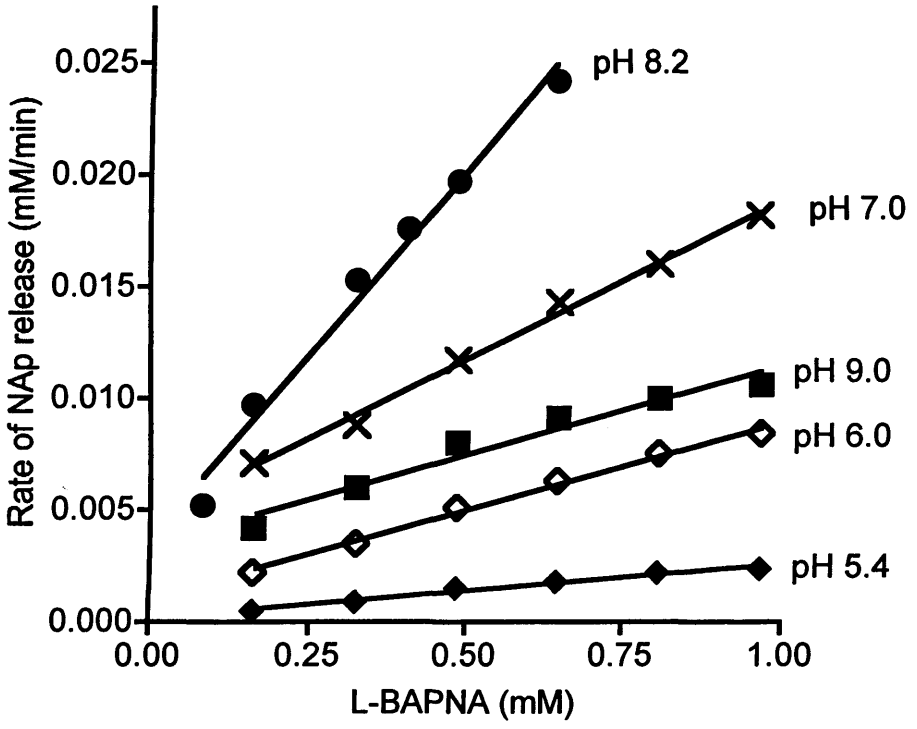

Figure 3.16 Effect of pH on the cleavage rate of L-BAPNA by trypsin. Absorbance (400 nm) of NAp measured over 5 min. Trypsin concentration = 1.28 x 10^{-4} mM using different substrate concentrations. Data shown represents n=1.

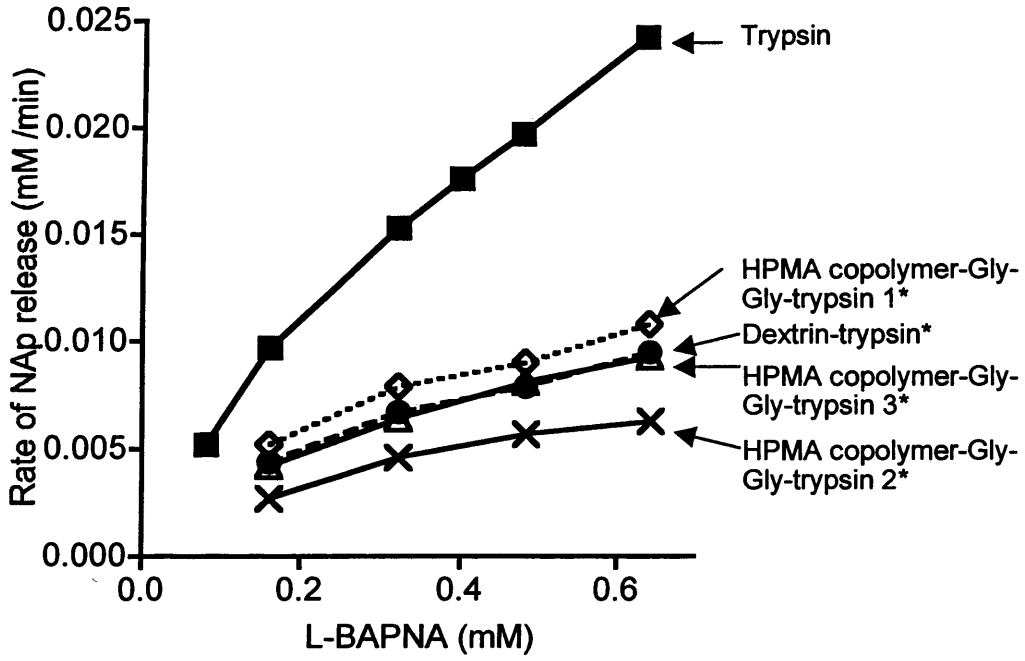

Figure 3.17 Effect of polymer conjugation on the rate of NAp release from L-BAPNA by trypsin. Where HPMA copolymer-Gly-Gly-trypsin 1 = 10 eq. EDC and sulfo-NHS, HPMA copolymer-Gly-Gly-trypsin 2 = 20 eq. EDC and sulfo-NHS, and HPMA copolymer-Gly-Gly-trypsin 3 = 30 eq. EDC and sulfo-NHS. Absorbance (400 nm) of NAp measured over 10 min. Trypsin concentration = 1.28 x 10^{-4} mM trypsin eq. using different substrate concentrations. Data shown represents the mean ± SD (n=3). Where error bars are not visible, error is within the data point. * indicates significance compared to free trypsin control, where $p<0.05$ (ANOVA and Bonferroni *post hoc* test).

trypsin and dextrin-trypsin conjugates in order to (i) select the best polymer, and (ii) optimise the conjugation chemistry for future synthesis of polymer-PLA_2 conjugates.

When quantifying the NH_2 groups available for polymer conjugation, the ninhydrin assay estimated a different number (12) from the actual value (10) (ExPASy, 2004). The discrepancy between the actual and calculated NH_2 groups could result from impurities in the trypsin purchased from Sigma, leading to a slight overestimation of amine groups. In fact, the TNBS assay was also explored for amine quantification, however it gave markedly different values (6.6 ± 1.5 SD). Due to the mechanism of action of the TNBS assay, it is important to have a standard which is either the same as the sample, or at least with the same chemical influence on the TNBS ring structure. As there is no such standard available for trypsin, the TNBS assay is liable to giving a false estimate of NH_2 numbers. This problem is not so pronounced with the ninhydrin assay, and so this amine quantification method was used for these studies.

3.4.1 Polymer-trypsin conjugation

It was possible to synthesise reproducibly HPMA copolymer-Gly-Gly-trypsin and dextrin-trypsin conjugates with protein content of 41-84 wt. %.

HPMA copolymer-trypsin conjugates

Several methods of protein conjugation were studied. Initially the methods used previously for the synthesis of HPMA copolymer-Gly-Gly-β-lactamase and HPMA copolymer-Gly-Gly-cathepsin B conjugates were used (Satchi *et al*, 2001; Satchi-Fainaro *et al*, 2003). A buffered enzyme solution was initially used in an attempt to maintain enzyme activity. However, when conjugating HPMA copolymer to any protein it is also important to minimise the hydrolysis of the ONp groups, while maximising aminolysis due to protein conjugation. These studies showed clear release of ONp when HPMA copolymer was dissolved in PBS buffer, so it is likely that the competition between hydrolysis and aminolysis was responsible for compromising the protein conjugation efficiency. After trying a variety of solvents, reaction conditions and reactant ratios, SDS PAGE still showed no sign of

conjugation. It soon became apparent that this method was not suitable for synthesis of the HPMA copolymer-trypsin conjugates, despite the fact that it had successfully been used to prepare many polymer-protein conjugates in the past (see Table 3.5). The precise reasons for failure of this method was unclear and even passage of the trypsin solution through a PD-10 desalting column prior to adding it to the reaction mixture did not improve conjugation efficiency. However, as trypsin has a pI of 10.2 - 10.8 (Malamud and Drysdale, 1978), this may explain the problems encountered when trying to conjugate trypsin to HPMA copolymer-Gly-Gly-ONp by aminolysis.

For this reason, it was decided to try conjugation of HPMA copolymer-Gly-Gly-COOH to trypsin using EDC and sulfo-NHS as coupling agents. Trypsin was thought to be a good model, as PLA_2 has a similar pI (10.5 ± 1.0) (Malamud and Drysdale, 1978). However, although this approach improved conjugation efficiency the yield was still very low.

Dextrin-trypsin conjugates

Synthesis of dextrin-trypsin conjugates following the methods of Duncan *et al* (2008) was much more successful. Succinoylation of dextrin was reproducible, with an overall reaction efficiency of 30 - 40 % (determined by titration). As reported previously by Hreczuk-Hirst *et al* (2001b), the reaction yield was lower than the theoretical value: ~ 40 - 50 % conversion was achieved.

GPC analysis of dextrin and the succinoylated intermediates demonstrated a decreased retention time following modification, which represented a greater increase in molecular weight than would be expected. This is likely to be due to conformational changes associated with incorporation of COOH groups resulting in an increased hydrodynamic radius. This observation is consistent with the studies of Hreczuk-Hirst *et al* (2001b) where they also reported a higher than expected increase in dextrin molecular weight following succinoylation.

Synthesis of a dextrin-trypsin conjugate using the methods described by Duncan and Gilbert (Duncan *et al*, 2008; Gilbert *et al*, 2005) was successful, with a higher yield than HPMA copolymer-trypsin conjugates.

Table 3.5 Examples of HPMA copolymer-protein conjugates prepared to date.

	Reaction time (h)	Conditions	Yield	Reference
Chymotrypsin	5	0.15 M NaCl, 0.01 M $CaCl_2$ 5 °C	Not stated	(Oupicky and Ulbrich, 1999)
Bovine seminal ribonuclease	5	0.15 M NaCl, 0.01 M $CaCl_2$ 5 °C	Not stated	(Oupicky and Ulbrich, 1999)
Cathepsin B	8.5	0.05 M phosphate buffer, pH 7.2 4 °C	30-35	(Satchi *et al*, 2001)
β-lactamase	0.33	DMSO room temperature	30-35	(Satchi-Fainaro *et al*, 2003)
Intraglobin F (human immunoglobulin)	19	ddH_2O pH 7.8 20 °C	16-18 wt. %	(Sirova *et al*, 2007)
Prostaglandin E	6	THF DMAP 0.1 mmol, 0 °C DCC 0.97 mmol, 6 h 4 °C	3.7 mol %	(Pan *et al*, 2006)
RGD4C: $\alpha v\beta_3$ integrin-targeting peptide	22	DMF Pyridine (1:1 ONp) N_2, 20 °C	0.377 mmol/g polymer	(Mitra *et al*, 2006)
RGE4C: non-active peptide	22	DMF Pyridine (1:1 ONp) N_2, 20 °C	0.5089 mmol/g polymer	(Line *et al*, 2005)

Challenges for characterisation of polymer-trypsin conjugates

Characterisation of a polymer-protein conjugate is difficult, as it doesn't behave like either component. This is especially significant when using GPC to determine molecular weight. In these studies, pullulan molecular weight standards were used to calibrate the GPC since the use of protein standards greatly underestimated the molecular weight of conjugates (results not shown). Pullulan, like dextrin, is a polysaccharide that would be expected to take on a random coil structure in solution, and therefore is expected to behave similarly to dextrin. However, due to the globular structure of proteins, protein standards, and not pullulan, would be the most appropriate standard for analysing trypsin. For these studies, pullulan was deemed the most appropriate choice of molecular weight standard, however, it was recognised that estimation of polymer-trypsin conjugate molecular weight is likely to be difficult.

Similarly, it remains impossible to obtain an absolute molecular weight of conjugate using FPLC because of the properties of the conjugate as compared to the protein standards. Proteins have a unique tertiary structure that is, not only, dependent on their molecular weight, but also on their charge, thus making accurate calibration of the FPLC column difficult. Also, a polymer-protein conjugate doesn't have the same properties as a native enzyme, due to the influence of the polymer on the shape and conformation of the protein and the steric effects of the polymer.

SDS PAGE was used to confirm an increase in the molecular weight of the protein, suggestive of successful conjugation of dextrin and trypsin. Free enzyme was compared to the purified reaction product, and both were evaluated in relation to a series of molecular weight markers. The smearing seen for polymer-protein conjugates indicates that polydisperse HPMA copolymer-Gly-Gly- and dextrin-trypsin conjugates were produced due to the random coil nature of dextrin and HPMA copolymer, uneven protein distribution along the polymer chain, as well as between different chains, could occur. There are numerous conformations that a dextrin-trypsin conjugate could take, as a result of the multiple binding sites on succinoylated dextrin which have the potential to bind one or more amine residues

on the trypsin, resulting in a variety of conjugate conformations (summarised in Figure 3.18). The potential of cross-linking was reduced by using an excess of NH_2 residues. Knowing the protein content of the conjugates (BCA assay) it is possible to estimate the number of polymer molecules to protein molecules. The trypsin conjugates synthesised here are estimated to contain polymer : protein ratios of: 1:3.5 (HPMA copolymer-Gly-Gly-COOH, 10 eq. EDC and sulfo-NHS), 1:3 (HPMA copolymer-Gly-Gly-COOH, 20 eq. EDC and sulfo-NHS), 1:2.5 (HPMA copolymer-Gly-Gly-COOH, 30 eq. EDC and sulfo-NHS), and 1:1.5 (dextrin-trypsin).

Protein content of dextrin-trypsin conjugates (42 %) was lower than HPMA coplymer conjugates (59-84 %). However, this variation did not appear to affect enzyme activity of the conjugate, which is understandable considering the difference in molecular weight of HPMA copolymer and dextrin. Since HPMA copolymer has a molecular weight of ~ 30,000 g/mol and dextrin's molecular weight is ~ 50,000 g/mol, the molar protein loading is similar for the conjugates and explains the similar trypsin activity observed for the conjugates.

3.4.2 Retention of enzymatic activity

Trypsin-conjugates activity

As expected, trypsin activity was reduced by polymer conjugation ($p < 0.05$, ANOVA and Bonferroni *post hoc* test). Activity masking was similar for all conjugates tested here and did not seem to vary greatly between polymers or ratio of linking agents (EDC and sulfo-NHS), in the case of HPMA copolymer. Polymer conjugation of enzymes has been widely studied in the literature (summarised in Table 3.6), demonstrating a wide range of yields and retention of activity after conjugation. The conjugates synthesised in these studies showed better activity masking than the PEG conjugates in the literature, and similar activity retention to dextran. While PEG-protein conjugation aims to retain protein activity by limiting binding to one reactive group, the conjugates synthesised in these studies used multivalent polymers to intentionally mask activity of the enzyme. The reduction in trypsin activity following conjugation to multivalent HPMA copolymer and dextrin is, therefore, likely to be due to the polymer sterically hindering access of substrate

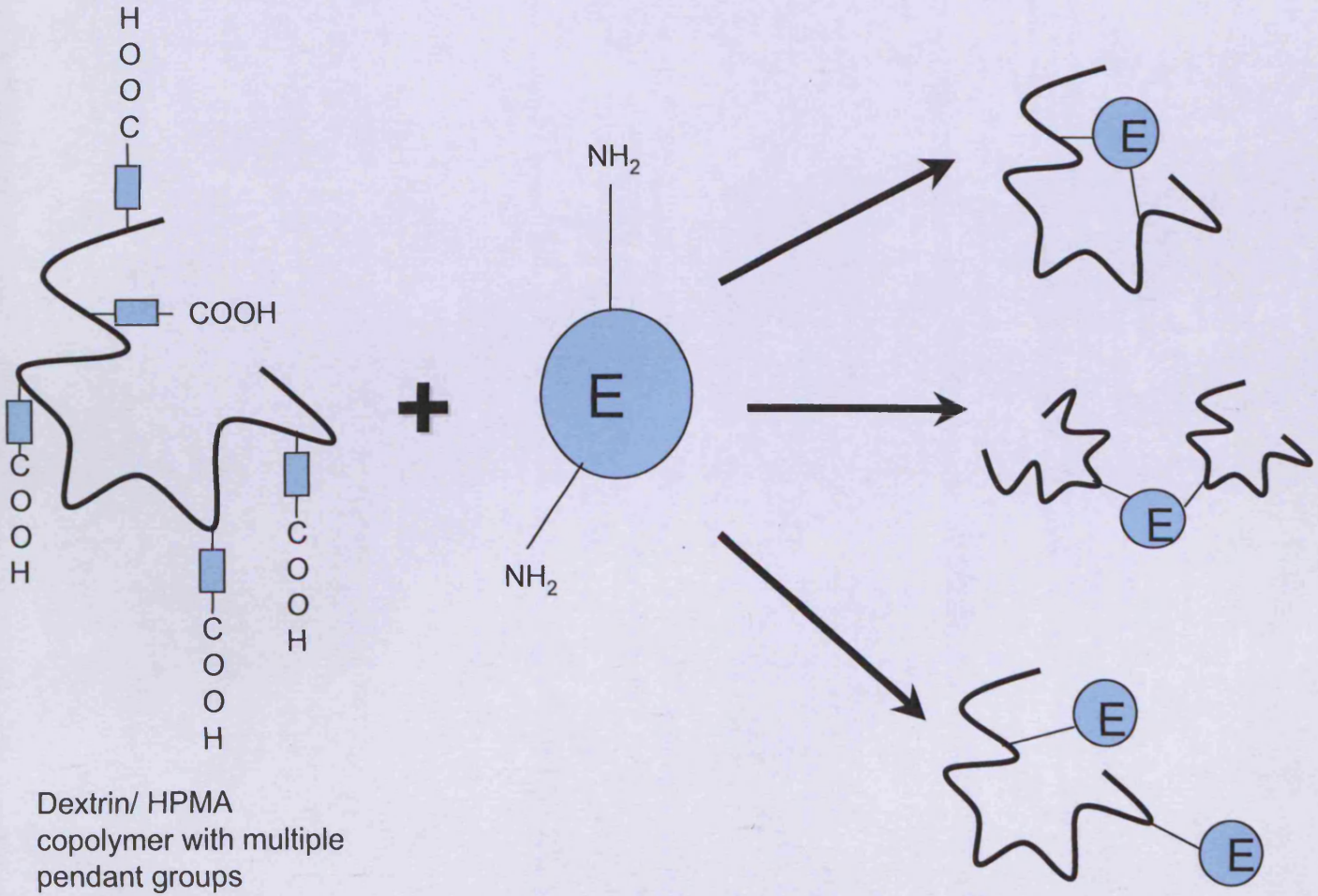

Figure 3.18 Theoretical products that could be formed during conjugation of dextrin and/or HPMA copolymer to trypsin. Where E = functionalised enzyme.

Table 3.6 Examples from the literature showing the effect of polymer modification on protein activity retention.

Polymer (g/mol)	Protein	NH_2/sulfone : polymer (molar ratio)	Modification (%)	Remaining activity (%)	Reference
PEG (5,000)	Trypsin	2:1	47	40	(Mero *et al*, 2008)
PEG (5,000)	Trypsin	1:1	22	70	(Mero *et al*, 2008)
POZ* (5,300)	Trypsin	2:1	57	40	(Mero *et al*, 2008)
POZ* (5,300)	Trypsin	2:1	26	80	(Mero *et al*, 2008)
PEG (12,000)	IFN-alpha2b (Intron A)	1:1	50	28	(Grace *et al*, 2001)
PEG (40,000)	IFN-alpha2b (Intron A)	1:1	30-55	5-10	(Ramon *et al*, 2005)
PEG (5,000)	Asparaginase	1:1.3	91	99	(Balan *et al*, 2007)
PEG (10,000)	Asparaginase	1:1.3	91	99	(Balan *et al*, 2007)
PEG (20,000)	Asparaginase	1:1.3	91	98	(Balan *et al*, 2007)

POZ = Poly(2-ethyl-2-oxazoline)

to the active site of the enzyme.

When attempting to produce HPMA copolymer-trypsin conjugates, varying the molar ratio of EDC and sulfo-NHS showed no obvious relationship with activity retention of the conjugates. However, the protein content was reduced as the amount of linking agents was increased (84 – 59 %). This could also be caused by steric hindrance blocking access of the substrate to trypsin's active site, which is unaffected by the degree of polymer conjugation. Each lysine residue on trypsin's structure will vary in its susceptibility to polymer conjugation, so it is likely that one of the most susceptible residues is located near the active site and further conjugation does not enhance protein masking to a great extent.

Previous studies with dextrin showed that the most effective protein masking was achieved when 51,000 g/mol dextrin was modified to ~ 26 % succinoylation (Duncan *et al*, 2008), and the reported activity remaining (34 %) was similar to the results from these studies (30 %). Ideally, the enzyme's activity would be 100 % masked, however it has not been possible in these or many other previous studies to reduce activity to such an extent. Given that L-BAPNA has a low molecular weight, it is unlikely to be fully obstructed by the polymer as it diffuses into the active site. Also, conjugating the hydrophilic polymers to trypsin's surface would be expected to influence the conformation of the enzyme and alter trypsin's microenvironment.

An exciting advantage of using dextrin for protein conjugation is its application in the recently coined concept of PUMPT. Since the unmasking capabilities of α-amylase-triggered degradation of dextrin have been shown to unmask the conjugated enzyme and enable reinstatement of activity (Duncan *et al*, 2008), this concept was investigated when dextrin-PLA_2 conjugates were synthesised (concept described in detail in Chapter 4).

Michaelis-Menten kinetics

As might have been expected, significant masking of activity was achieved after HPMA copolymer and dextrin conjugation. In order to assess the influence of polymer conjugation and compare HPMA copolymer-trypsin and dextrin-trypsin conjugates, it was considered necessary to establish kinetic parameters using a

derivative of the Michaelis-Menten equation. As described in section 3.1.2, kinetic data are commonly analysed using the Lineweaver-Burk, Eadie-Hofstee and Hanes-Woolfe plots (Cornish-Bowden, 2004). Despite the initial acceptance of the Lineweaver-Burke and Eadie-Hofstee plots, they rely on subjective, and sometimes inaccurate, estimations of initial velocities and have failed to produce reliable kinetic constants. Therefore, the Hanes-Woolfe plot was used in these studies. This method of calculating kinetic parameters is not without faults, but these were minimised by ensuring that a suitably large range of substrate concentrations were studied. Also, since experimental conditions, such as temperature and pH can influence the K_m (Cornish-Bowden, 2004) and enzyme purity and concentration can affect the V_{max} values (Cornish-Bowden, 2004; Samoshina and Samoshin, 2005), these variables were kept constant unless being specifically studied (i.e. when effect of pH and trypsin concentration were measured). K_{cat}, however, should not be greatly affected by experimental conditions. Therefore, it was possible to compare the trypsin K_{cat} values obtained in these studies to those obtained by Johnson *et al* (2002). The results obtained in these studies calculated a K_{cat} value of 6.24 and 6.53 s^{-1}, while Johnson *et al* (2002) reported K_{cat} values of 2.89 s^{-1}. This value was calculated using the least squares fit of the Michaelis–Menten equation to the reciprocal data using LUCENZIII, a computer software programme. Additionally, Johnson *et al* (2002) performed these experiments at 35 °C, using 0.1-1.5 mM L-BAPNA in 0.1 M Tris-HCl and 10 mM $CaCl_2$, while the studies performed in these investigations were undertaken at 37 °C, using 0.081-0.644 mM L-BAPNA in 40 mM Tris-HCl and 16 mM $CaCl_2$. These variations could explain the disparity between the values calculated here and those in the literature. Following polymer conjugation, the K_{cat} of HPMA copolymer bound trypsin decreased to 1.52-2.05 s^{-1} and, for dextrin-trypsin conjugates, a K_{cat} value of 1.88 s^{-1} was calculated. No obvious relationship was seen between K_{cat} values for trypsin conjugates of HPMA copolymer and dextrin.

Enzyme kinetics revealed a decrease in the apparent K_m of trypsin upon attachment to both HPMA copolymer and dextrin, suggesting that apparent affinity is increased by polymer conjugation. However, since K_{cat} was lower following polymer conjugation, overall enzyme efficiency was lower. This is in agreement with the observed reduction in conjugate activity and is likely to be due to steric hindrance

restricting access of the substrate to the active site.

It is desirable for the ideal conjugate to be able to hydrolyse its substrate rapidly (high K_{cat}) and be able to work efficiently at low substrate concentrations (low K_m). These results indicate that both trypsin conjugates retained sufficient activity to fulfil these requirements and provide encouraging evidence for implementing this method with PLA_2.

3.5 Conclusions

From these pilot studies dextrin was selected as the best polymer for future synthesis of PLA_2 conjugates. The main advantage of this polymer is its proven ability to 'unmask' the enzyme by degradation of dextrin by α-amylase, which would be a valuable property for a PLA_2-conjugate. Although it was apparent that trypsin conjugates with similar activity retention could be prepared with HPMA copolymer-Gly-Gly-COOH, as well as dextrin, reaction yield for HPMA copolymer-trypsin conjugates was extremely. It was also evident that it would be easier to purify the dextrin conjugate using FPLC, and this conjugate also has the added potential of masking the activity of PLA_2 after administration. Investigations into masking/unmasking of dextrin-PLA_2 will be described in the following chapter. This work showed that it is possible to synthesise trypsin conjugates containing dextrin with an approximate trypsin content of 42 % w/w and retention of 30 % enzyme activity.

Therefore, the next studies were intended to use the chemistry optimised here to synthesise dextrin-PLA_2 conjugates. After characterisation of the conjugates, the applicability of PUMPT was assessed and non-specific toxicity was measured.

Chapter Four

Synthesis of Dextrin-PLA_2 Conjugates and Characterisation of PLA_2 Activity

4.1 Introduction

Before synthesis of dextrin-PLA_2 conjugates, it was first necessary to select the most appropriate source of the enzyme. As mentioned in Chapter 1 (section 1.1), PLA_2 has been investigated previously as a potential anticancer agent. In fact, it is not only crotoxin that has shown anticancer activity though. PLA_2 extracted from *crotalus terrificus* venom (Cura *et al*, 2002), *Naja nigricollis* venom (Chwetzoff *et al*, 1989) and Russell's viper venom (Maity *et al*, 2007) have also shown activity. It was therefore very important to select the best source of enzyme for these studies. Ideally, the PLA_2 would be commercially available, be selective for cancer cells, and exert minimal toxic side effects. Initially studies were undertaken to evaluate the potential of PLA_2 derived from bee venom and bovine pancreas.

4.1.1 Introduction to PLA_2s chosen for these studies

PLA_2s have been previously described in section 1.4. Briefly, they are small secreted proteins (~ 14,500 g/mol) with between 5-8 disulfide bonds (summarised in Table 4.1). This group of enzymes require Ca^{2+} (mM concentrations) for catalysis and contain a histidine residue at their active site. To date, 19 distinct groups of enzyme have been identified, and classified according to their primary structure and the location of disulfide bonds in the protein (Dennis, 1997; Murakami and Kudo, 2004; Six and Dennis, 2000). PLA_2 isoforms have been assigned to one of five distinct types; namely the secreted PLA_2s ($sPLA_2$), the cytosolic PLA_2s ($cPLA_2$), the Ca^{2+}-independent PLA_2s ($iPLA_2$), the platelet-activating factor acetylhydrolases (PAF-AH), and the lysosomal PLA_2s. They represent a very diverse range of catalytically active and inactive forms of PLA_2, that display a range of biological activities, including neurotoxicity, myotoxicity, cardiotoxicity, necrotoxicity, haemolysis, hypotensivity, and haemorrhagic and oedema-inducing activities (Kini, 2003). The secreted form of PLA_2 was selected for this work since a number of studies have shown anti-tumour activity of these isoforms (Chwetzoff *et al*, 1989; Cura *et al*, 2002; Lee *et al*, 2006). The abbreviation "PLA_2" is used throughout the rest of this thesis to describe these secreted PLA_2s.

Table 4.1 Sub-groups of PLA_2 and their characteristics.

GROUP	IA*	IB*	IIA*	IIB	IIC	III*	V	X
Source	Cobras, Kraits	Mammalian pancreas, spleen	Rattlesnakes, vipers, human synovial fluid/ platelets	Vipers	Rat/ Mouse testis	Insects, Lizards, Mammals	Human/Rat/Mouse macrophages,lung	Human leucocytes, spleen, thymus, lung, colon, pancreas
No. of amino acids	119	130	124	122	117	134	118	123
Molecular weight (g/mol)	13-15,000	13-15,000	13-15,000	13-15,000	15,000	16-18,000	14,000	14,000
Co-factor	mM Ca^{2+}	mM Ca^{2+}	mM Ca^{2+}	mM Ca^{2+}	mM Ca^{2+}	mM Ca^{2+}	mM Ca^{2+}	mM Ca^{2+}
Disulfides	7	7	7	6	8	5	6	8
Molecular characteristics	His-Asp pair	His-Asp pair, elapid loop	His-Asp pair, carboxyl extension	His-Asp pair, , carboxyl extension	His-Asp pair, , carboxyl extension	His-Asp pair	His-Asp pair	Carboxyl extension, propeptide at NH_2 terminal
N-type receptor affinity	115	2,000,000	9	N/S	N/S	80	N/S	N/S
M-type receptor affinity	>300,000	30,000	36,000	N/S	N/S	>>300,000	N/S	N/S

$K_{0.5}$ = values of inhibition, expressed in pM; * = commercially available from Sigma-Aldrich; N/S = not stated

Honeybee venom PLA_2 was largely used in this thesis. It is a group III PLA_2 (MW = 15,800 g/mol) that is secreted by cells and is composed of 123 amino acids twelve of which are lysine residues. It also contains five disulphide bonds (Shipolini *et al*, 1974). The protein structure is shown in Figure 4.1. Bee venom PLA_2 requires millimolar concentrations of Ca^{2+} as cofactor, and consequently, addition of EDTA inhibits enzyme activity (Scott *et al*, 1990). Bee venom-derived PLA_2 has been shown to have an optimum pH for hydrolytic activity of 8.0 (Shipolini *et al*, 1971). Interestingly Op den Kamp *et al* (1974) found that while bee venom PLA_2 is active against liposomes containing dilauroyl-, dimyristoyl-, and dipalmitoylphosphatidylcholine at temperatures other than the transition temperature (0, 23 and 41 °C respectively, liquid crystalline to gel phase), the pancreatic enzyme is active only at or near the transition temperature. This could be useful therapeutically since the enzyme would be required to act at 37 °C inside the body.

For comparison to the bee venom PLA_2 bovine pancreatic PLA_2 was also studied, but only as the native enzyme and it was subsequently not used to prepare polymer conjugates. Pancreatic PLA_2 is a group IB secretory enzyme. It is composed of 133 amino acids (~14,500 g/mol) and it contains 7 disulfide bonds. The protein structure is shown in Figure 4.2. Like all $sPLA_2$s, this enzyme also has a requirement for millimolar concentrations of Ca^{2+} as a cofactor. While there appears to be little sequence homology between the bee venom- and pancreatic-derived PLA_2s (Puijk *et al*, 1977), the Thr-His-Asp residues found in pancreatic PLA_2 also appear in the bee venom sequence and these are thought to be essential for the catalytic activity (Drenth *et al*, 1976). Mammalian forms of PLA_2 show little selectivity for the particular fatty acids they hydrolyse, however, they do show higher activity towards phospholipids containing anionic headgroups (Diez *et al*, 1994; Diez *et al*, 1992).

Mechanism of action of PLA_2

A description of the mechanism of action of PLA_2 has already been given in Chapter 1 (section 1.4). Briefly, these enzymes catalyse the hydrolysis of fatty acids at the sn-2 position to release free fatty acids such as arachidonic acid, and lysophospholipids (Murakami and Kudo, 2002). These products are precursors to a

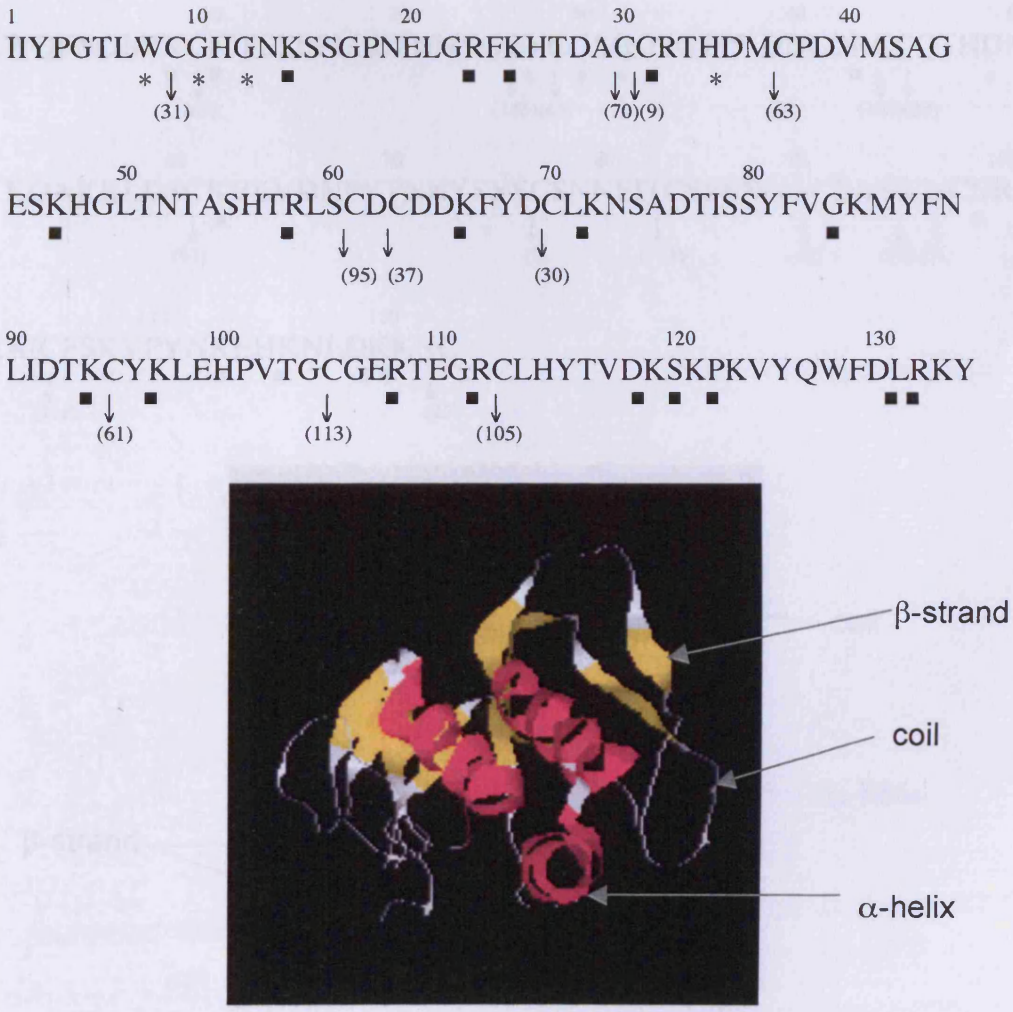

Figure 4.1 Protein structure of bee venom PLA_2. Panel (a) shows the Amino acid sequence of bee venom PLA_2. Numbers in parentheses indicate the positions of cysteines involved in disulfide bonds. *, residues involved involved in the coordination of Ca^{2+} co-factor; ■, amino acids containing NH_2 groups as potential conjugation sites for succinoylated dextrin. Panel (b) represents the 3-D image of bee venom PLA_2 structure. Image taken from Expasy (2004).

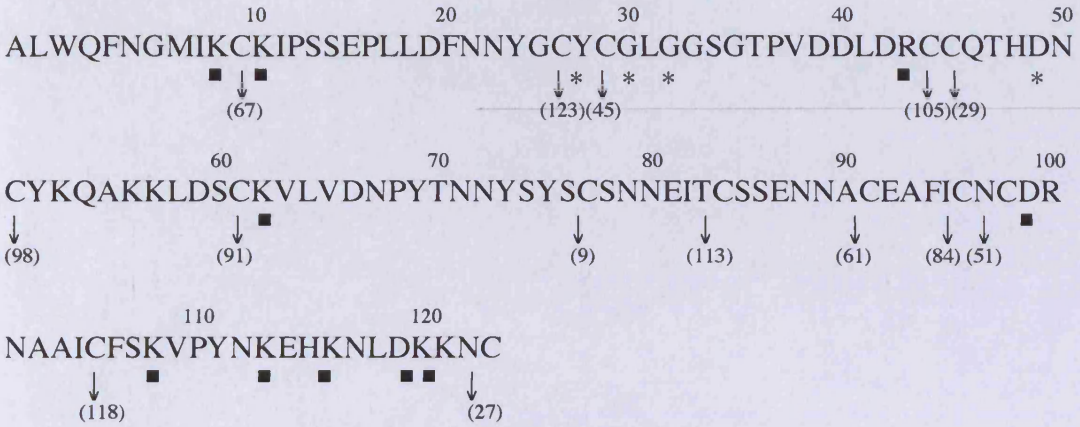

Figure 4.2 Protein structure of bovine pancreas PLA_2. Panel (a) shows the amino acid sequence of bovine PLA_2. Numbers in parentheses indicate the positions of cysteines involved in disulfide bonds. *, residues involved involved in the coordination of Ca^{2+} co-factor; ■, amino acids containing NH_2 groups as potential conjugation sites for succinoylated dextrin Panel (b) represents the 3-D image of bovine pancreas PLA_2 structure. Image taken from Expasy (2005).

number of signalling molecules with numerous biological functions. However, PLA_2 doesn't only exert an effect through its enzymatic activity mediated by the hydrolysis of phospholipids (Lambeau and Lazdunski, 1999). It also interacts with at least two other membrane receptors, and these have been called N-type and M-type receptors (Lambeau *et al*, 1995; Lambeau and Lazdunski, 1999; Valentin and Lambeau, 2000). The N-type receptor is composed of at least two classes of binding site and it is most abundant in the brain. Binding of PLA_2 to N-type receptors is very sensitive to the presence of Ca^{2+} ions, and this is responsible for the neurotoxic effects of PLA_2 (Nicolas *et al,* 1997). Conversely, the M-type receptor consists of only one type of binding site and it is found abundantly in the skeletal muscle of rabbits. Binding of $sPLA_2$ to these receptors is independent of Ca^{2+}, and the receptor is believed to behave as a physiological PLA_2 inhibitor in humans. That is, interaction with the M-type receptor can lead to internalisation, and subsequent removal of PLA_2. Different types of PLA_2 have different affinities for the M-type receptor. While the honeybee venom PLA_2 has very low M-type affinity, crotoxin and bovine pancreas display a relatively higher affinity for the receptor (Valentin and Lambeau, 2000), resulting in an apparent reduced bovine PLA_2 activity.

4.1.2 Rationale for synthesis of dextrin-PLA_2 conjugates

PLA_2 was selected as the active enzyme in these studies after crotoxin showed promising results as an anticancer agent in Phase I clinical trials (Cura *et al*, 2002) (details of trials discussed in section 1.1). However, despite noting 2 partial responses and 1 complete response in the 23 patients involved in the trial, neurotoxic side effects were observed in 13 patients. Since PLA_2 is also notoriously cytotoxic and haemolytic, the proposal to synthesise dextrin-PLA_2 conjugates hoped to minimise this adverse effect on normal cells while still allowing full enzyme activity at the site of action within the tumour.

Dextrin was chosen for conjugation after previous studies using trypsin as a model enzyme showed good conjugation efficiency, successful masking of activity and straightforward characterisation (Chapter 3). Dextrin is also an appealing polymer since it can be used to inactivate a protein during transit (masking), but

triggered degradation of the polymer can reinstate protein activity at a tailored rate (PUMPT) (Duncan *et al*, 2008). As mentioned earlier, preliminary studies by Duncan *et al* (2008) investigated the effect of molecular weight (7,700 and 47,200 g/mol) and degree of succinoylation (9, 32 mol %) on the ability of dextrin to mask/unmask trypsin activity. They found that the higher molecular weight polymer succinoylated to 26 mol % gave optimum masking/unmasking for PUMPT. This combination led to masking of activity to 34-69 % of free trypsin, with subsequent regeneration of activity to a maximum of 92-115 %. Similarly, these studies also confirmed the applicability of dextrin in PUMPT when conjugated to melanocyte stimulating factor (MSH), a receptor-binding ligand. In this case, activity was reduced to 11 % of free activity. However, in this case, it was only possible to reinstate 33 % of the control value, possibly due to MSH degradation during incubation and/or irreversible inactivation of MSH by dextrin conjugation.

The method used in Chapter 3 for dextrin-trypsin conjugation was used here for the conjugation of succinoylated dextrin to PLA_2 using EDC and sulfo-NHS (Figure 4.3). It was reasonable to assume that dextrin-PLA_2 could be prepared using the linking agent method implemented for trypsin, as they are a similar size (16,000 compared to 23,000 g/mol) and have a similar number of NH_2 groups available for conjugation (12 compared to 10).

4.1.3 Choice of PLA_2 activity assay

A number of assays have been described to measure the activity of PLA_2 (summarised in Table 4.2). The egg yolk assay was chosen for these studies because it is a rapid, simple and inexpensive technique that has been used before to assay PLA_2 activity (Reynolds *et al*, 1991). It is based on the concept that PLA_2 can hydrolyse the phospholipids in an egg yolk suspension, resulting in a decrease in turbidity of the solution (Marinetti, 1965). This solution 'clearing' can be followed spectrophotometrically in a continuous assay to measure PLA_2 activity. However, the assay does have some disadvantages; the most significant being its low sensitivity. It is also not capable of producing quantitative results, and instead provides only relative activities rather than moles of phospholipids hydrolysed.

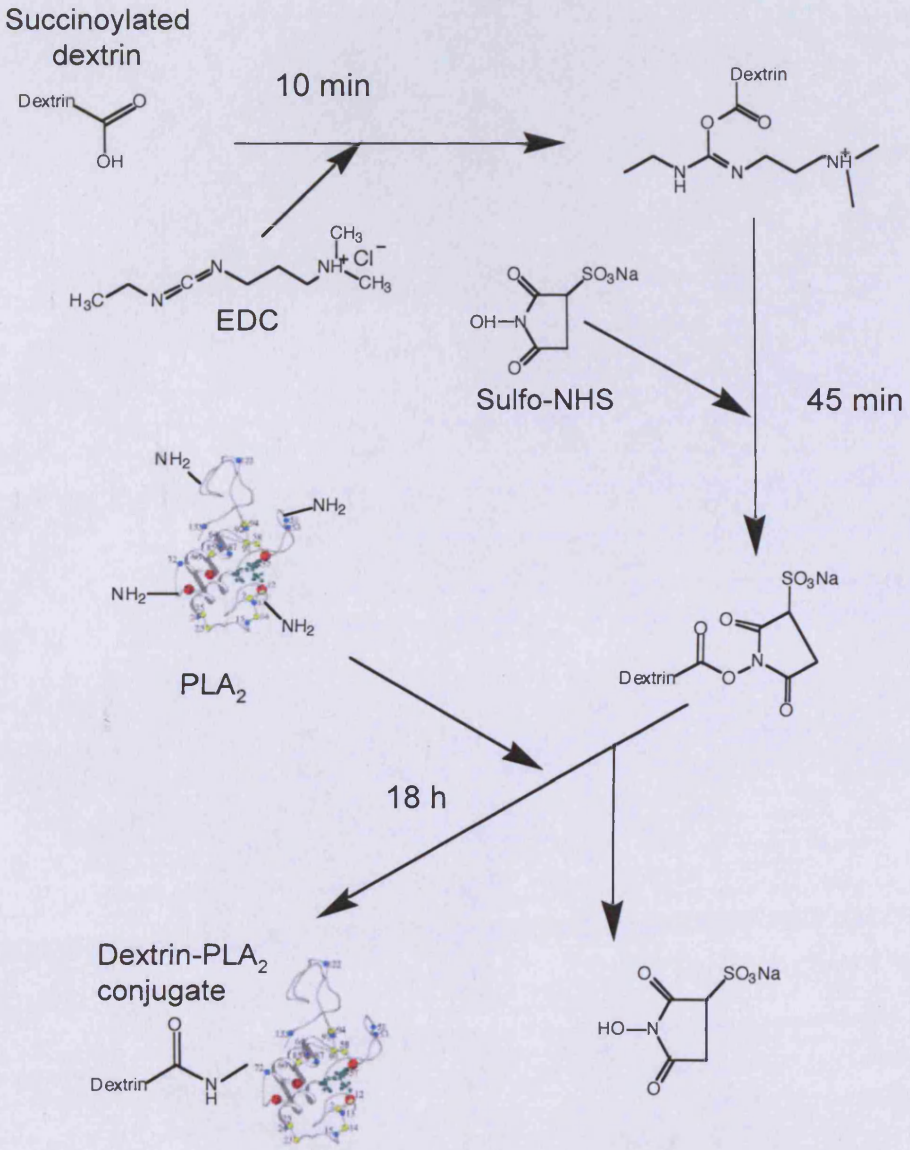

Figure 4.3 Reaction scheme for conjugation of succinoylated dextrin to PLA_2.

Table 4.2 Advantages and disadvantages of different methods of PLA_2 activity measurement. Summarised from (Reynolds *et al*, 1991).

Method name	Brief description	Advantages	Disadvantages
Titrametric (pH stat)	One of most commonly used PLA_2 assay. pH is held constant by titration of liberated fatty acids, and PLA_2 activity is quantitated continuously according to amount of base consumed. Detection limit: 20 nmol	Straightforward & requires relatively inexpensive equipment Continuous assay	Not sensitive enough to detect intracellular PLA_2 before purification Does not detect reaction product, but proton release
Acidametric	Detects protons released from fatty acid liberation by monitoring pH change over time. Detection limit: 100 nmol	Continuous and simple detection possible	pH of assay varies throughout assay Change in pH is highly dependent on presence of buffers, including substrate/enzyme Sensitivity is determined by starting pH & therefore varies over time course
Radiometric	Follows hydrolysis of synthetic, radio-labelled phospholipids by direct measurement of hydrolysis products. Detection limit: 1 fmol-1 pmol	Most sensitive and widely used assay	Commercially available radio-labelled substrates can be expensive Sensitivity depends on specific radioactivity of labelled substrate Discontinuous assay Requires time-consuming separation radioactive substrate from products (e.g. TLC, HPLC, solvent extraction)

Table 4.2 Advantages and disadvantages of different methods of PLA_2 activity measurement. Summarised from (Reynolds *et al*, 1991) (cont.)

Method name	Brief description	Advantages	Disadvantages
NMR	Commonly involves ^{31}P and ^{13}C. Detection limit: 20 μmol	Natural abundance levels of ^{31}P means natural substrates can be used- no need for synthetic substrates	Very low sensitivity (>10 mM substrate, 10 % hydrolysis required for quantitation) Natural abundance and sensitivity of C is low, so levels must be enhanced
Monolayer	Phospholipid monolayers are formed in monolayer troughs. PLA_2 activity is determined by measuring the decrease in surface area required to maintain a constant surface pressure	Extremely sensitive and utilises natural substrates	Difficult to study $PLA_2 \geq$ Km since very low concentrations of substrate are used Requires specialised, often expensive, equipment
Spectrophotometric	Often involve generation of a chromophore following hydrolysis of synthetic phospholipids substrates	Rapid, convenient, continuous, and can be adapted for large sample numbers	
Turbidometric	Follows decrease in turbidity of phospholipid solution (e.g. egg yolk suspension) during hydrolysis	Continuous, rapid, simple and cheap Can also be performed with a multibilayer liposome substrate	Low sensitivity Difficult to quantitate amount of phospholipids hydrolysed- only gives relative activity, not moles of lipid hydrolysed Turbidity is dependent on assay conditions (pH and metal ions can affect substrate solubility)

4.1.4 Assessment of non-specific toxicity

If the dextrin-PLA_2 conjugate was to be tested *in vivo*, or to be used clinically as an anticancer agent, it would be administered by IV injection. Therefore, it was essential to assess potential non-specific toxicity of the dextrin-PLA_2 conjugates. PLA_2 is believed to exert its cytotoxic effects by hydrolysis of phospholipids, resulting in membrane permeabilisation and rupture. Since RBCs are composed of phospholipids and dextrin-PLA_2 would encounter these cells following IV administration, it was important to test haemolytic activity. A well-established RBC lysis model was used that has been applied to test the membrane activity of polymers (Duncan *et al*, 1994; Lavignac *et al*, 2005), and PLA_2 (Lin *et al*, 1987; Watala and Kowalczyk, 1990).

Native PLA_2 is known to cause haemolysis of RBCs (Best *et al*, 2002; Watala and Kowalczyk, 1990). Studies by Watala and Kowalczyk (1990) showed RBCs were rapidly lysed in a time- and concentration dependent manner by bee venom PLA_2 (Hb_{50} = 5.73 μg/mL after 60 min incubation). However, they also noted that incubation of RBCs with purified bee venom PLA_2 in concentrations of up to 10 μg/mL (60 min, 37 °C) was not accompanied by haemolysis. Supplementation with melittin (0.6 μg/mL), however, significantly increased RBC lysis.

4.1.5 Experimental aims

In summary, the aims of this study were to:

- Assess suitability of PLA_2s derived from bovine pancreas and bee venom for dextrin-conjugation, by testing its purity, enzyme activity and *in vitro* cytotoxicity against MCF-7 cells to select the best one for dextrin conjugation.
- Synthesis of dextrin-PLA_2 conjugates and optimise the conditions with respect to reaction yield and free protein content (FPLC).
- Characterisation of conjugates with respect to purity, molecular weight and size distribution (FPLC, SDS PAGE), total protein content (BCA assay), free protein content (FPLC).
- Compare enzyme activity of free PLA_2 and dextrin-PLA_2 conjugate,
- Assess feasibility of unmasking dextrin-PLA_2 conjugates by incubation

with amylase in the context of PUMPT.

- Measure RBC haemolysis by PLA_2, dextrin-PLA_2 conjugate and unmasked dextrin-PLA_2 conjugate +/- Ca^{2+}.

4.2 Methods

The method used for synthesis of dextrin-trypsin conjugates (optimised in Chapter 3) was initially tested here using a small batch of dextrin-PLA_2 (5 mg PLA_2) to see if the same procedure could be used to synthesise dextrin-PLA_2 conjugates. As the method was transferable it was subsequently scaled up to 25 mg PLA_2 batch sizes (as described below).

The methods used for the characterisation of dextrin-PLA_2 conjugates were essentially the same as those described to characterise dextrin-trypsin conjugates (Chapter 3). They are described in detail in sections 2.4.1, 2.4.4.1, 2.4.4.2, 2.4.4.3 and 2.4.6.5 (ninhydrin assay, FPLC, SDS PAGE, BCA assay, MTT assay respectively).

4.2.1 Synthesis of dextrin-PLA_2 conjugates

Succinoylated dextrin (51,000 g/mol; 19-23 mol % succinoylation) was prepared and characterised using methods outlined in Chapter 3 (section 3.2.2). It was then conjugated to PLA_2 using EDC and sulfo-NHS as coupling agents as described in Chapter 3. Briefly, succinoylated dextrin (154 mg, 3.02 x 10^{-6} mol) was dissolved under stirring in ddH_2O (2 mL) in a 10 mL round-bottomed flask. To this, EDC (21.1 mg, 0.1 mol) was added, and the mixture allowed to dissolve for 10 min. Next, sulfo-NHS (22.4 mg, 0.1 mol) was added and the mixture left stirring for 40 min. Subsequently, PLA_2 (25 mg, 1.58 x 10^{-6} mol) dissolved in ddH_2O (1 mL) was added, followed by NaOH (0.5 M) dropwise to raise the pH to 8.0. The reaction mixture was left stirring overnight (18 h).

The conjugate was then purified from the reaction mixture by FPLC. Fractions (1 mL) were collected and desalted using Vivaspin tubes (10,000 g/mol cut-off) before pooling the appropriate fractions containing conjugate for activity testing (Figure 4.4). The final conjugate was lyophilised and stored at -20 °C.

Dextrin-PLA_2 conjugates were characterised in respect of free PLA_2 by SDS PAGE (section 2.4.4.2) and using the same FPLC system as was used for purification (section 2.4.4.1). The total protein content of the conjugate was determined by the BCA assay (section 2.4.4.3).

4.2.2 PLA_2 activity measured using the egg yolk assay

The enzyme activity of PLA_2 and the dextrin-PLA_2 conjugate was measured using an egg yolk suspension assay according to Marinetti (1965). Native PLA_2 or dextrin-PLA_2 conjugate was dissolved in Tris buffer (equivalent to 0.5 mg/mL PLA_2, pH 8.2). All samples were prepared fresh before use and placed on ice throughout the experiments. The egg yolk solution (0.9 mL of a 0.05 - 0.25 % v/v solution in Tris buffer at pH 8.2) was added to a 1 cm^3 quartz cell. To start the assay, free enzyme or conjugate (0.1 mL) was added to the cuvette.

Degradation of phospholipids was monitored by measuring the increase in absorbance at 400 nm for 30 min. Tris buffer (0.1 mL) was added to the blank sample in the place of the PLA_2 or dextrin-PLA_2 conjugate solution. Results were expressed as absorbance change (% ± SD, n = 3) over time (30 min). This data was subsequently interpreted to produce a graph showing rate of absorbance change against egg yolk emulsion concentration. Significance of the data was assessed using ANOVA and Bonferroni *post hoc* test.

4.2.3 Degradation of dextrin and succinoylated dextrin by α-amylase

In order to compare the rate of α-amylase degradation of dextrin and succinoylated dextrin, solutions (2 mL, 4 mg/mL in PBS, pH 7.4) of each polymer was prepared. Then α-amylase (2 mg/mL) was added. These solutions were incubated at 37 °C for 0 – 1440 min. At time points samples (100 μL) were taken, immediately snap frozen in liquid N_2 to stop the reaction and then stored at –20 °C until analysis by GPC.

Prior to GPC analysis, samples were placed in a water bath (100 °C) for 5 min to denature the enzyme activity of the α-amylase and stop polymer degradation. The

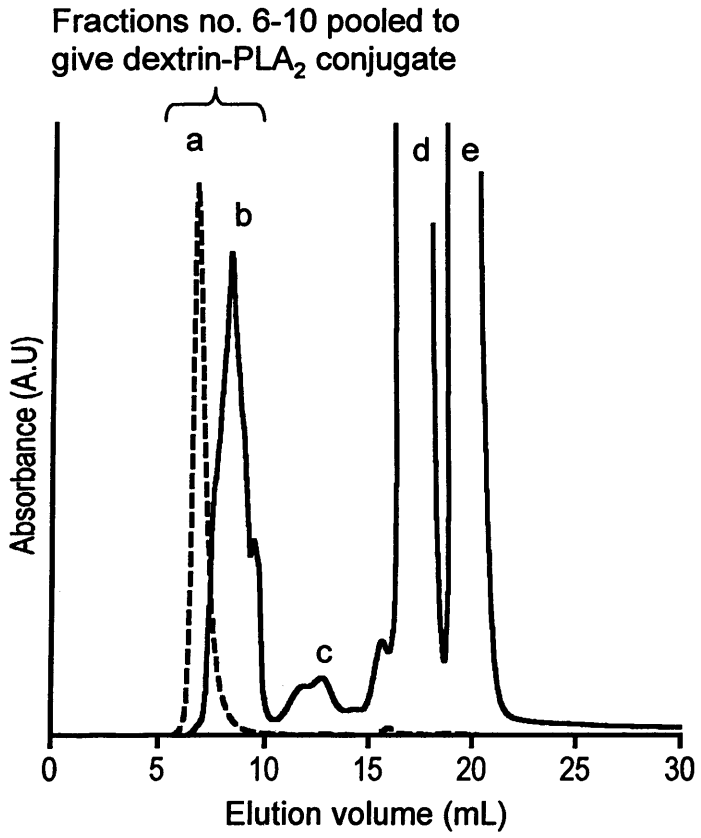

Figure 4.4 FPLC of dextrin-PLA_2 conjugation reaction mixture (UV absorbance at 280 nm). Where the peaks represent a) purified dextrin-PLA_2, b) dextrin-PLA_2, c) free PLA_2, d) and e) peptides

supernatant was then analysed by GPC (section 2.4.4.1) to determine the change in molecular weight over time.

4.2.4 Unmasking of dextrin-PLA_2 conjugates by incubation with α-amylase

To study the effects of α-amylase on the activity of dextrin-PLA_2 conjugates, dextrin-PLA_2 conjugates (0.5 mg/mL PLA_2 eq.) were first incubated with α-amylase (2 mg/mL, 200 Sigma units (SU)/mL) for 16 h at 37 °C in Tris buffer (1.5 mL, pH 8.2). The enzyme activity assay using an egg yolk emulsion in Tris buffer (see section 4.2.2 for method) was then followed.

4.2.5 Assessment of haemolytic activity

Rat RBCs were prepared as previously described by Duncan *et al* (1994). Briefly, blood was obtained from a male Wistar rat (~ 250 g body weight) by cardiac puncture and collected in a heparin/lithium blood tube, in PBS (pH 7.4). The tubes were centrifuged at 1500 g for 10 min at 4 °C. The supernatant was removed and the RBC pellet was resuspended in PBS at 4 °C and transferred to a pre-weighed, clean disposable centrifuge tube. The centrifugation step was repeated twice, followed by the removal of the supernatant, and resuspension of the pellet in PBS. After the final removal of the supernatant, the pellet (of known weight) was resuspended in PBS to produce a 2 % w/v RBC suspension. Erythrocyte suspension was stored at 4 °C and always made fresh on the day of the experiment.

Subsequently, this RBC suspension (100 μL) was added to a 96-well plate containing the PLA_2 test compound solutions to be tested.

PBS was used as a negative control, and triton X-100 (1 % v/v) was used to achieve 100 % haemolysis. The plate was then incubated for 1 h at 37 °C, then the plate was centrifuged at 1500 g for 10 min at 4 °C. The supernatant (100 μL) of each well was then carefully removed and placed into a clean 96-well plate. The absorbance at 550 nm was read, using a microtitre plate reader, to assess the degree of RBC lysis. The background values from incubation of the RBCs with PBS was subtracted from the sample values and the results were expressed as haemoglobin released (% ± SEM) relative to the triton X-100 control. The significance of the data was assessed using ANOVA and Bonferroni *post hoc* test.

Since calcium is an essential cofactor for PLA_2 activity, these experiments were also performed in the absence and presence of Ca^{2+} by supplementing the buffer with calcium carbonate to produce a final Ca^{2+} concentration of 8 mM.

4.3 Results

4.3.1 Comparison of PLA_2 sources: purity and enzyme activity

Before conjugating dextrin to PLA_2, the properties of PLA_2s derived from bovine pancreatic and bee venom were compared. The bee venom-derived PLA_2 contained 76 wt. % protein, while bovine pancreatic PLA_2 had an apparent protein content of just 13 wt. %. However, the bovine PLA_2 was relatively free from protein contaminants (Figure 4.5, lane 2 and 4.6a), whereas the bee venom PLA_2 displayed several peaks on the FPLC trace- at ~ 10.5, ~ 12.5 and ~ 18 mL (Figure 4.6b), and multiple bands on SDS PAGE analysis (Figure 4.5, lane 3). FPLC and SDS PAGE of melittin, a common contaminant of bee venom PLA_2, revealed a peak at ~ 18.5 mL (Figure 4.6c) and a band coincident with a band in the PLA_2 lane (Figure 4.5, lane 4).

The *in vitro* cytotoxicity of bovine pancreatic and bee venom PLA_2s (all conjugate MTT results are described in the next chapter) showed that bovine pancreatic PLA_2 was non-toxic to MCF-7 cells up to 1 mg/mL, while bee venom PLA_2 had an IC_{50} of 308.6 ± 6.9 μg/mL (Figure 4.7).

Consequently, bee venom PLA_2 was selected for conjugation to dextrin.

4.3.2 Synthesis and purification of dextrin-PLA_2 conjugates

The ninhydrin assay indicated that PLA_2 has 9.8 ± 1.1 (SD) NH_2 groups per molecule, and this value (10) was used to calculate molar ratios of PLA_2 to succinoylated dextrin (NH_2:COOH) for all conjugation reactions, and not the total number of NH_2 groups in PLA_2 (12).

When conjugation of dextrin-PLA_2 was initially attempted, the method optimised for the synthesis of dextrin-trypsin was used. First, a small batch of dextrin-PLA_2 was synthesised to confirm the method and to investigate an

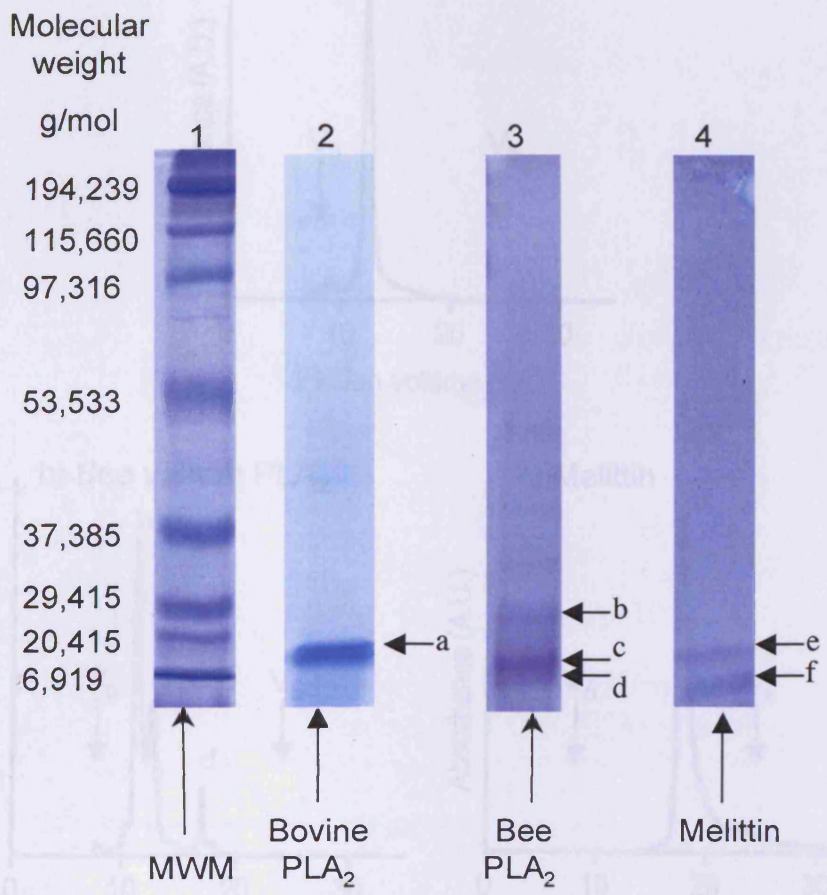

Figure 4.5 SDS PAGE analysis of bovine pancreatic PLA_2, bee venom PLA_2, and melittin. Key: a) PLA_2 monomer, b) PLA_2 dimer, c) PLA_2 monomer, d) melittin contaminant, e) PLA_2 contaminant, and f) melittin. MWM = molecular weight marker.

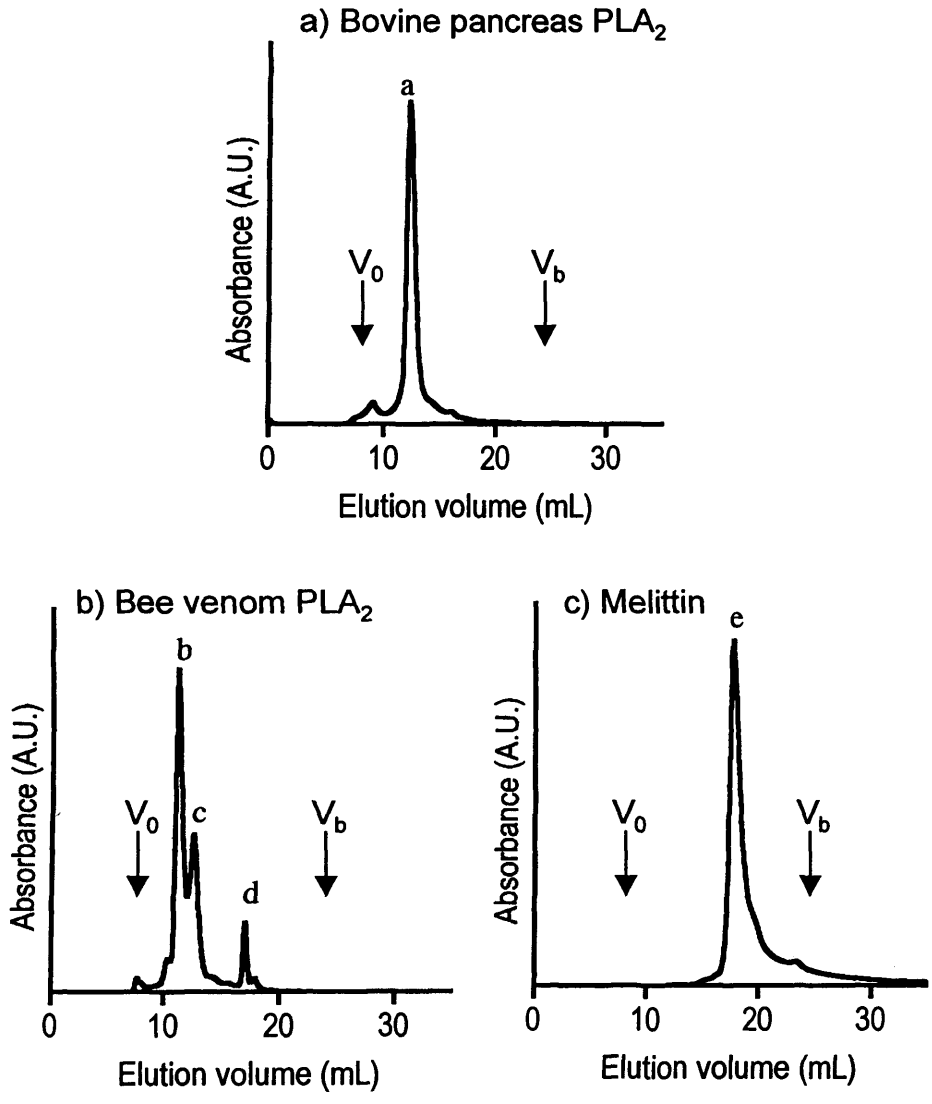

Figure 4.6 FPLC analysis of bovine pancreatic PLA_2, bee venom PLA_2, and melittin. Key: a) PLA_2, b) PLA_2 dimer, c) PLA_2 monomer, d) melittin contaminant (9.4 %), e) melittin. V_0 = void volume (7.7 mL), and V_b = bed volume (24 mL). UV absorbance taken at 280 nm.

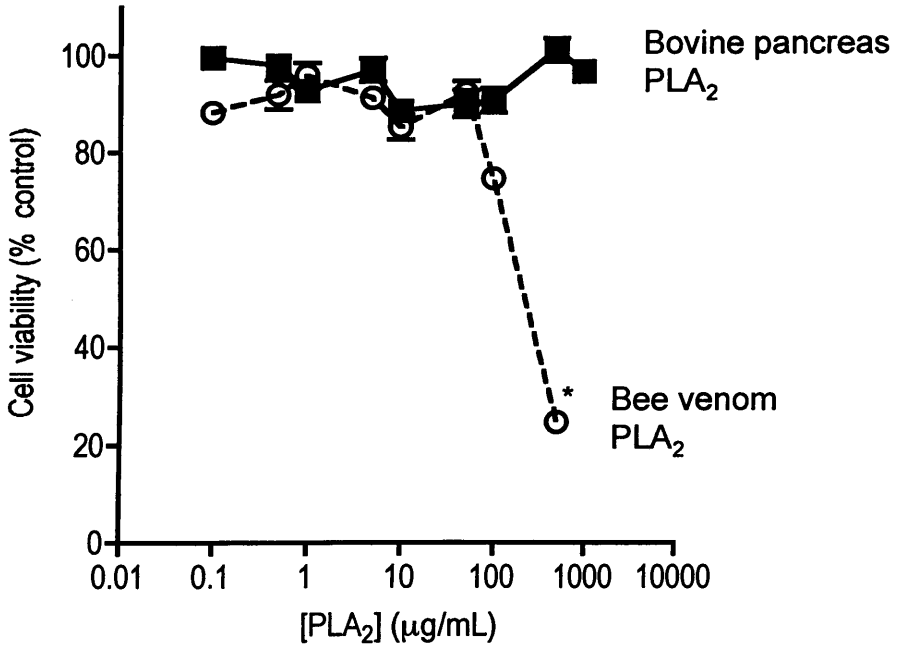

Figure 4.7 Effect of bovine pancreatic and bee venom PLA_2 on MCF-7 cell viability. Data represents % control cell growth ± SEM (n = 18). Where error bars are invisible they are within size of data points. * indicates significance compared to bovine pancreas PLA_2, where $p<0.05$ (student's t-test).

appropriate conjugate purification method. Initial studies using dialysis showed incomplete removal of free enzyme and reaction by-products when reanalysed by SDS PAGE (Figure 4.8, lane 4). However, no free PLA_2 band was detectable in the dextrin-PLA_2 conjugate after FPLC with Vivaspin purification (Figure 4.8, lane 5). Consequently, FPLC with Vivaspin was selected to separate the conjugate from the reaction mixture.

4.3.3 Characterisation of dextrin-PLA_2 conjugates

Typical FPLC elution profiles of the crude reaction mixture (Figure 4.4) and free PLA_2 and purified conjugate are shown (Figure 4.9). There was a good separation between bound and free PLA_2, with the conjugate eluting at the void volume (V_o) of the column (~ 7.7 mL), thus enabling the separation of free and bound PLA_2 using this method. FPLC showed a peak corresponding to dextrin-PLA_2 conjugate in the region of the column's V_o.

SDS PAGE of the conjugates confirmed the presence of a high molecular weight conjugate (~ 200,000 g/mol), with dark smearing appearing between ~ 50,000 g/mol and the top of the gel (suggestive of a polydisperse conjugate) (Figure 4.8, lane 5).

Dextrin-PLA_2 conjugation showed good batch-to-batch reproducibility and a reaction yield of 93-100 % (see Table 4.3). The conjugates contained 3-9 % w/w protein using a BCA assay calibrated with free PLA_2 (see Figure 2.6). Control studies showed that succinoylated dextrin had minimal interference with the assay, with a relative contribution of absorbance of 0-1.8 %. The pilot scale batch (5 mg PLA_2) synthesised initially had PLA_2 content of 3.7 wt. %, but scaled-up conjugate batches (25 mg PLA_2) had a PLA_2 content of 7-9 wt. %.

To determine the amount of free PLA_2 in the batches, SDS PAGE was calibrated by running different concentrations of free PLA_2 to determine the lowest detectable concentration (data not shown). Further control experiments showed that unreacted dextrin gave no band, while free PLA_2 showed two prominent bands where the monomeric and dimeric forms of the enzyme would be expected to appear (~ 15,000 and 30,000 g/mol, respectively) (Figure 4.8, lane 2). FPLC was also used to

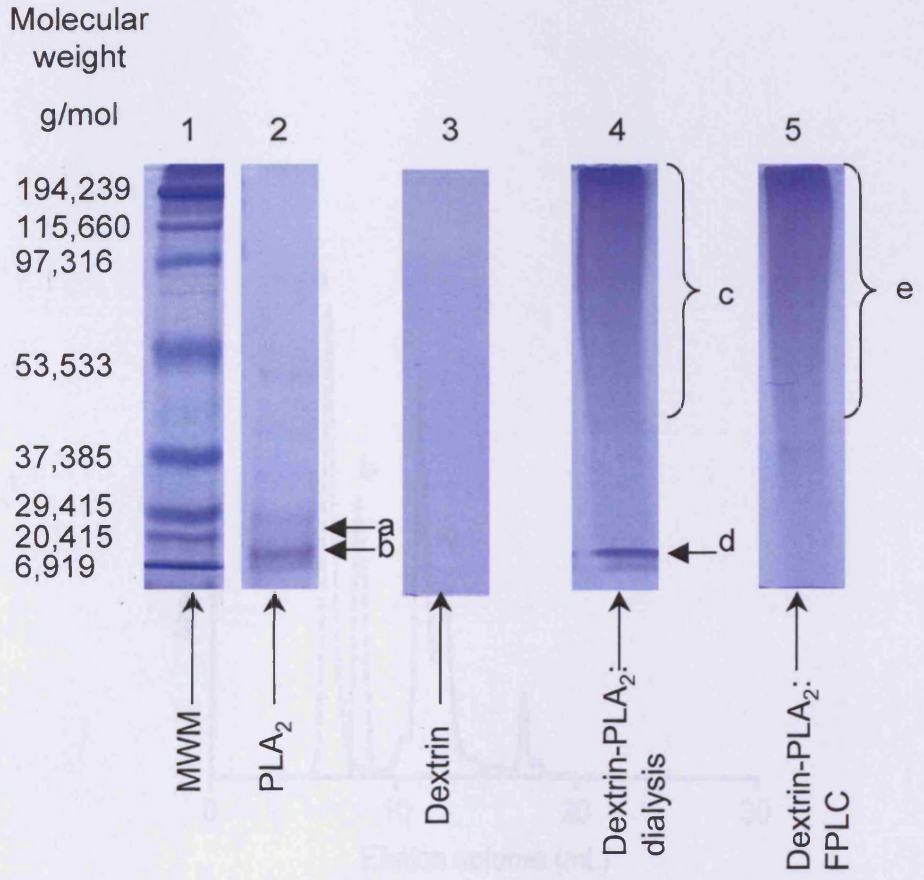

Figure 4.8 SDS PAGE analysis of dextrin-PLA_2 (purified by dialysis), dextrin-PLA_2 (purified by FPLC with Vivaspin), and bee venom PLA_2 and dextrin controls. Key: a) PLA_2 dimer, b) PLA_2 monomer, c) dextrin-PLA_2 conjugate, d) free PLA_2, and e) dextrin-PLA_2 conjugate. MWM = molecular weight marker.

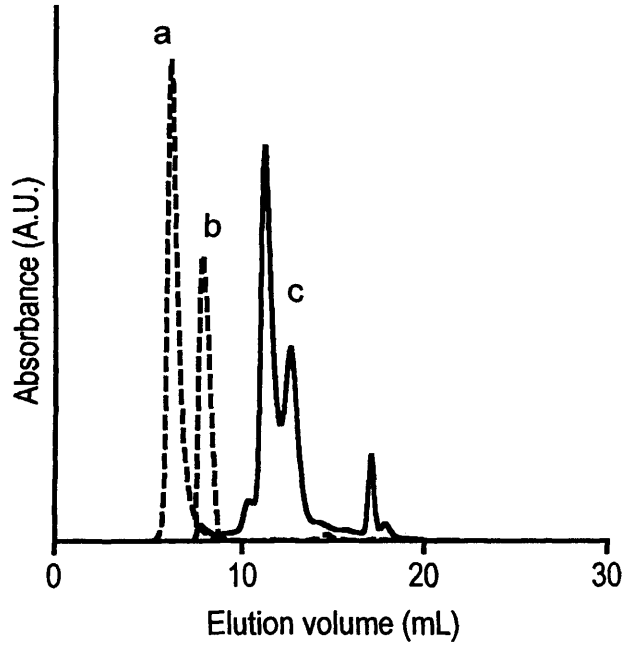

Figure 4.9 FPLC analysis of free and conjugated PLA_2. Key: a) dextrin-PLA_2 (DexPLA5), b) dextrin-PLA_2 (DexPLA1) and c) PLA_2. V_0 = void volume (7.7 mL), and V_b = bed volume (24 mL). UV absorbance taken at 280 nm.

Table 4.3 Characterisation of dextrin-PLA_2 conjugates.

Conjugate[c]	Batch size (mg)	Protein content[a] (wt. % ± SD)	Molecular weight[b] (g/mol)	Uses
DexPLA1	5 mg	3.7 ± 0.014	160,000	Purification and characterisation optimisation
DexPLA2	25 mg	7.2 ± 0.014	185,000	Egg yolk activity assays
DexPLA3	15 mg	5.0 ± 0.010	180,000	Unmasking studies
DexPLA4	25 mg	7.0 ± 0.006	210,000	Haemolysis
DexPLA5	25 mg	7.3 ± 0.013	215,000	MTT
DexPLA6	5 mg	6.1 ± 0.011	190,000	OG-labelled for uptake studies
DexPLA7	25 mg	9.4 ± 0.014	195,000	PELT

[a] relative to native PLA_2 (BCA assay)
[b] FPLC, relative to protein standards (see text for details)
[c] Free PLA_2 was always < 1 % w/w

quantitatively detect the presence of free PLA_2 in the purified dextrin-PLA_2. The conjugates always contained < 1 % free protein.

4.3.4 PLA_2 activity of free and dextrin-conjugated PLA_2

Degradation of egg yolk in the presence of PLA_2 is shown in Figure 4.10a. There was a short lag phase followed by a linear rate of degradation. This linear part of the data was used to calculate the concentration-dependence of degradation (Figure 4.10b). The activity of the dextrin-PLA_2 conjugates was reduced (35.8 % ± 4.5 (SD)) compared to free PLA_2 (Figure 4.10b).

Enzyme activity measured following incubation of the dextrin-PLA_2 conjugate with α-amylase was increased (Figure 4.10b) to 114.6 % ± 2.6 (SD) that of free PLA_2.

4.3.5 Degradation of dextrin and succinoylated dextrin by incubation with α-amylase

When α-amylase was added to dextrin there was a rapid decrease in apparent molecular weight (seen using GPC (Figure 4.11)) with a $t_{1/2}$ of 0.5 min. Succinoylated dextrin was degraded more slowly, such that its $t_{1/2}$ was 30 min, and a plateau in molecular weight was seen.

4.3.6 Haemolysis of RBCs

Free PLA_2 was very haemolytic at concentrations > 100 μg/mL native PLA_2, while no lytic activity was seen with dextrin-PLA_2 up to 500 μg/mL (Figure 4.12a). Furthermore, it was shown that, even following unmasking by α-amylase, dextrin-PLA_2 did not induce red blood cell haemolysis at concentrations at which haemolysis is seen for the native enzyme. Addition of calcium to the incubation buffer enhanced the haemolytic potency of native PLA_2 (Figure 4.12b), such that 56 % RBC lysis was seen at 50 μg/mL, compared to 6 % haemolysis in the absence of calcium. This effect was not observed with the dextrin-PLA_2 conjugate. Control experiments with α-amylase and dextrin showed < 10 % haemolysis (data not shown).

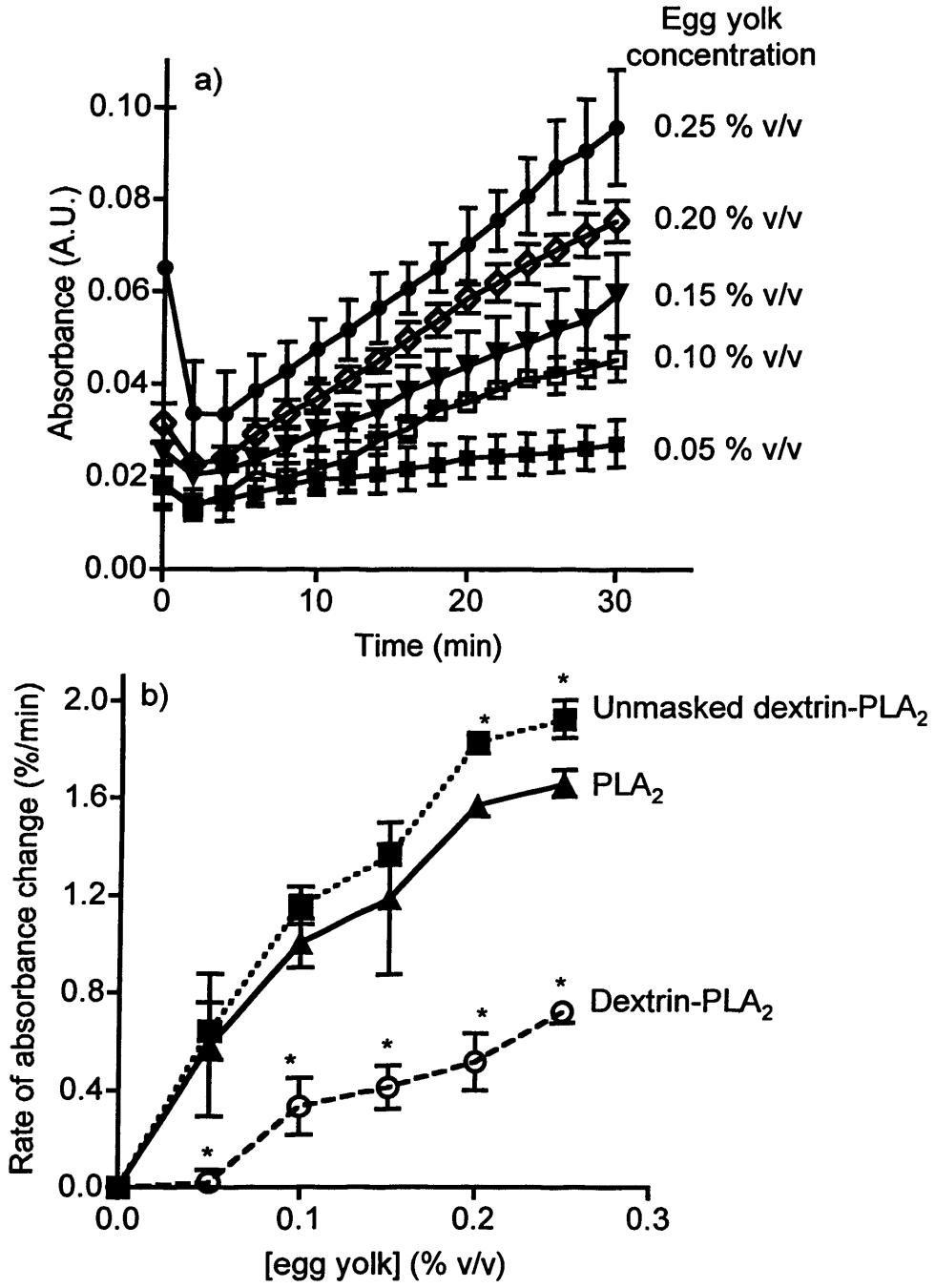

Figure 4.10 PLA_2 activity measured using an egg yolk emulsion. Progress curves in panel (a) show the UV absorbance (540 nm) of egg yolk clearing in increasing concentrations of egg yolk emulsion by PLA_2 (0.5 mg/mL) over 30 min. Panel (b) shows concentration-dependent rate of clearing of egg yolk solutions. Data shown represents the mean ± SD (n=3). Where error bars are not visible, error is within the data point. * indicates significance compared to free PLA_2 control, where $p<0.05$ (ANOVA and Bonferroni *post hoc* test).

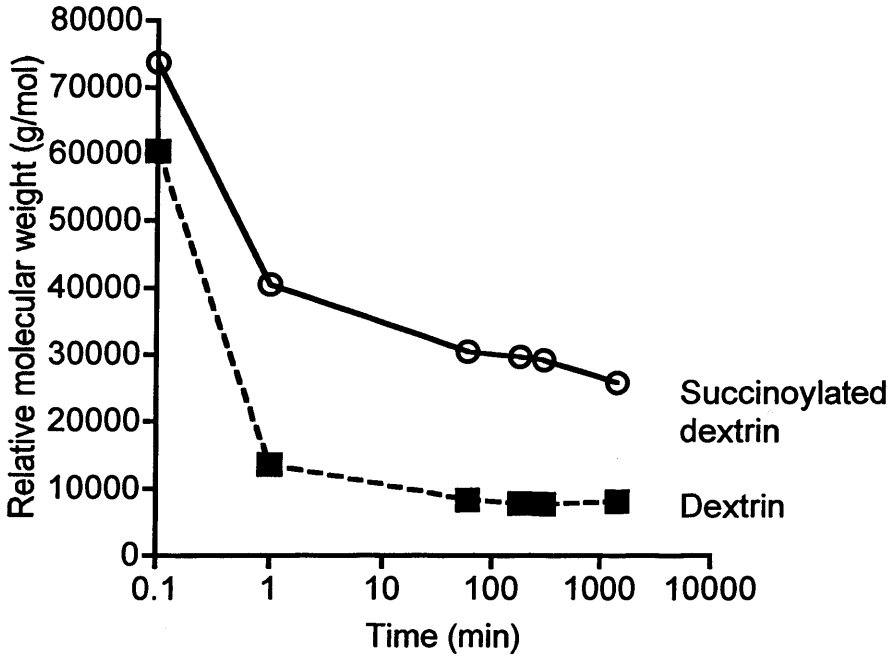

Figure 4.11 Degradation of dextrin and succinoylated dextrin over time, when incubated with the dextrin degrading enzyme α-amylase. This graph shows the change in molecular weight of the main peak fraction over time for dextrin and its succinoylated intermediate. Data shown represents n=1. Molecular weight given is relative to pullulan standards.

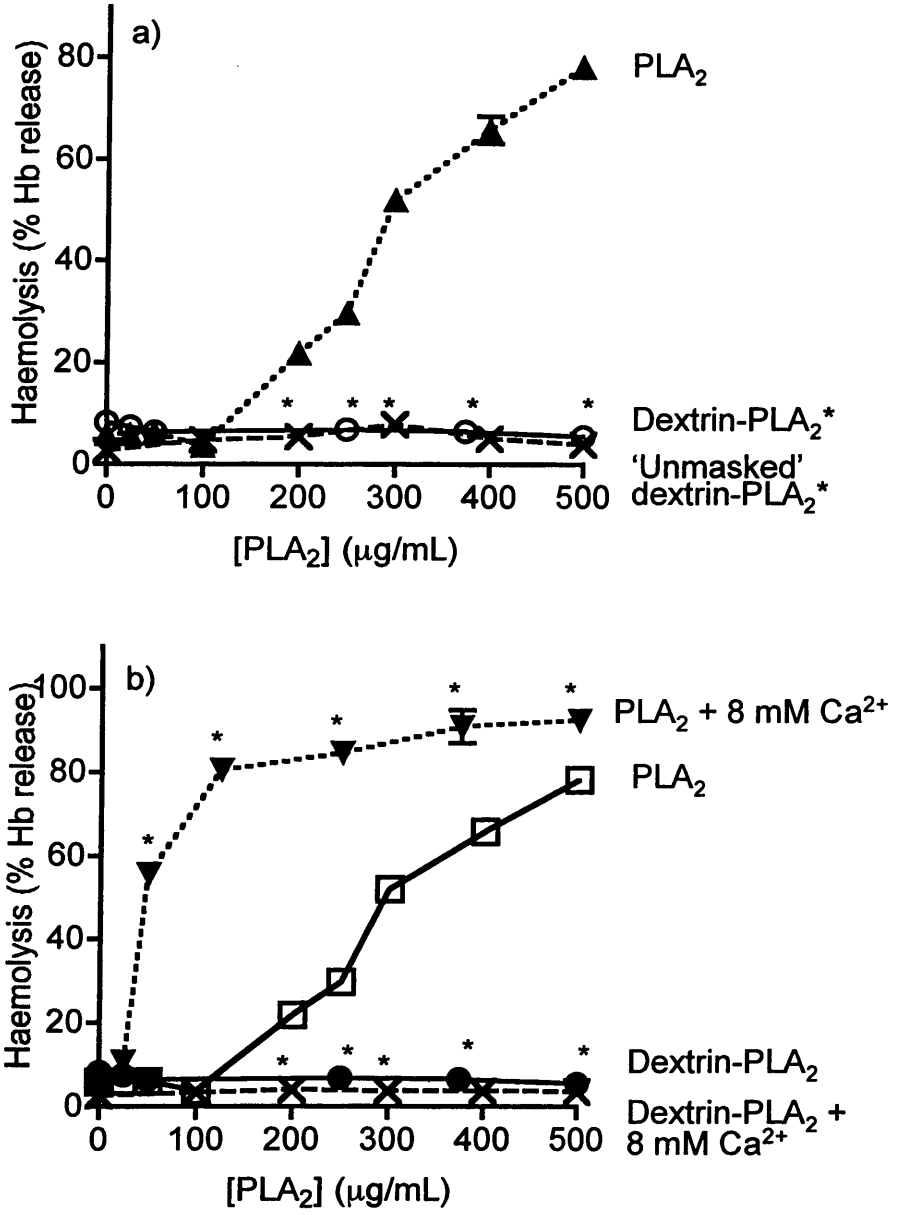

Figure 4.12 Haemolysis of RBCs by PLA_2 and dextrin-PLA_2 (masked and unmasked). Panel (a) shows haemoglobin release from RBCs after 60 min incubation with PLA_2, dextrin-PLA_2 and 'unmasked' dextrin-PLA_2. Panel (b) demonstrates the effect of Ca^{2+} on haemolytic activity of PLA_2 and dextrin-PLA_2. Data represents % RBC lysis relative to triton-X100 solution ± SEM, (n=9). Where error bars are not visible, error is within the data point. * indicates significance compared to free trypsin control, where $p<0.05$ (ANOVA and Bonferroni *post hoc* test).

4.4 Discussion

Although bovine pancreatic and bee venom PLA_2 were considered for conjugation to dextrin the bovine PLA_2 was found to be non-toxic up to 1 mg/mL when incubated with the breast cancer cell line MCF-7. In contrast the bee venom PLA_2 had an IC_{50} of 308.6 μg/mL (discussed in more detail in Chapter 5). These results were not surprising, given the affinity constants of these enzymes to the M- and M-type receptors (Table 4.1) and the likelihood that bovine PLA_2 is susceptible to N-type receptor mediated internalisation, while bee venom PLA_2 is not. It has been shown that melittin can enhance and stimulate the lipolytic activity of PLA_2, so it is possible that the contamination seen in bee venom PLA_2 could be attributed to this effect, and not to PLA_2 alone. However, it is unlikely that melittin alone is responsible for the enhanced cytotoxicity since it only accounts for < 10 % bee venom PLA_2 and would be removed during the conjugate purification steps.

Given the greater cytotoxicity of bee venom PLA_2, this was chosen for conjugation to dextrin.

The method used to synthesise the library of dextrin-PLA_2 conjugates (Table 4.3) was reproducible and gave a protein content of 5-9 wt. % with < 1 % free PLA_2. This protein loading was less than was seen for the dextrin-trypsin conjugates synthesised in Chapter 3 (41-84 % w/w), despite having similar polymer: enzyme (and NH_2: COOH) ratios in the reaction mixture. This could be due to bee venom PLA_2's tendency to form dimers which can conceal some Lys residues, reducing the number available for conjugation. It was also noted, however, that the protein loading achieved was greater for larger batch sizes and similar to yields described in the literature for polymer-protein conjugation (~ 10 %) (reviewed in Harris and Chess, 2003) but still lower than other dextrin-protein conjugates described in the literature (Table 4.4).

Although this method of conjugation is not site-specific, the polymer is likely to react preferentially with certain NH_2 groups, depending on their pKa and their protein conformation. The ninhydrin assay predicted that there were ~ 10 accessible NH_2 groups PLA_2, while the literature suggests there are 12 lysine residues, as well

Table 4.4 Summary of the activity of various dextrin-protein conjugates before and after addition of α-amylase.

	Protein content (wt. %)	Masked activity (%)	Unmasked activity (%)	Reference
Trypsin	50-80	34	58	(Duncan *et al*, 2008)
MSH	37	11	33	(Duncan *et al*, 2008)
EGF	16	6.5	101	(Hardwicke *et al*, submitted)
RNase	48.4	13.7	-	(Treetharnmathurot *et al*, unpublished)
PLA_2	7.2	36	116	(Ferguson *et al*, 2006)

as a terminal amine group and several other NH-containing amino acids (arginine, histidine) (Scott et al, 1990; Shipolini et al, 1971). Interestingly, Bianco *et al* (2002) reported that PEGylation of PLA_2 could be enhanced by isolating the conjugate fraction from the high MW PEG-PLA_2 complexes. They suggest that access of the reactive polymer to some of the Lys of the remaining PLA_2 was impaired in highly PEGylated proteins and that some of the reactive Lys residues were not initially available for conjugation due to dimerisation of the enzyme.

FPLC was found to be the only reliable method of conjugate purification. It should, however, be born in mind that it is that it is not possible to distinguish between dextrin-PLA_2 conjugate and free dextrin using FPLC as they both elute at the same point. Duncan *et al* (2008) used two-dimensional diffusion-ordered NMR spectroscopy (DOSY) to show that there was free dextrin remaining in dextrin-trypsin conjugates. Although it is not ideal to include free dextrin in the product, dextrin is known to be non-immunogenic and is already used clinically so it's presence would not be a concern at this stage. This is however an issue that would need addressing in the future before clinical use.

As with dextrin-trypsin conjugates, accurate characterisation of the molecular weight of dextrin-PLA_2 conjugates proved problematic due to difficulties selecting appropriate calibration standards (discussed in Chapter 3). However, both SDS PAGE and FPLC were useful indicators that a conjugate had been synthesised, and for the detection of the presence of free PLA_2. These methods also showed that the conjugates were a polydisperse mixture of species. This is not surprising and can be attributed to the multivalency of both dextrin and PLA_2, which would, in theory, lead to a variety of conjugated species. It can be estimated from the protein assay that, on average, the dextrin-PLA_2 conjugates synthesised contained between 1 protein: 3-9 dextrin.

4.4.1 Enzyme activity

As has been observed with other dextrin conjugates (Gilbert *et al*, 2005) PLA_2 activity was retained following conjugation. Incomplete inactivation suggests that

dextrin does not always bind to a region which would block access to the enzyme's active site. There is no clear trend in protein content of polymer-protein conjugates and activity retention. In these studies, dextrin-PLA_2 conjugates retained slightly higher activity than dextrin-trypsin conjugates (36 % compared to 24-32 %) and had a lower protein content (5-9 % compared to 41-84 %). However, the conjugates in Table 4.4 do not all follow this trend and it is likely that site of polymer conjugation relative to the enzyme's active site influences activity masking the most.

Degradation and reinstatement of activity of dextrin-PLA_2 conjugates

Full reinstatement of activity was seen following α-amylase incubation (16 h) with dextrin-PLA_2. Previous α-amylase 'unmasking studies' using dextrin conjugates showed differences in the ability of α-amylase to reinstate protein activity (summarised in Table 4.4). While only partial reinstatement of activity was seen for dextrin-trypsin (34 % (masked) to 58 % (unmasked)), and dextrin-MSH conjugates (11 % (masked) to 33 % (unmasked)) (Duncan *et al*, 2008), full unmasking was achieved for dextrin-EGF conjugates (6.5 % (masked) to 101 % (unmasked)) (Hardwicke *et al*, submitted). The differences in masking could be due to the different protein sizes. MSH (2,644 g/mol and EGF (6,666 g/mol) are substantially smaller than trypsin and PLA_2, and would therefore be more susceptible to activity masking by polymer conjugation.

It is also possible that irreversible inactivation of trypsin and MSH occurs following dextrin binding in the active site region of the enzyme. In fact, MSH has just one Lys residue, which is located one amino acid away from the active site sequence, and a terminal amine. Therefore, steric hindrance of the active site by remaining maltose residues could hinder full reinstatement of activity. PLA_2, on the other hand, has many more NH_2-containing amino acids. While it is reported that K14, R23, R58, K85 and K133 are found in the collar of the active site and are involved in the enzyme's interaction with phospholipids, there remains a further 5-7 NH_2 groups available for dextrin conjugation, located away from the active site (Bollinger *et al*, 2004; Ghomashchi *et al*, 1998).

Since these unmasking experiments were performed in Tris buffer (pH 8.4), it is

worth noting that the optimal pH for α-amylase is actually 7.0 (Sky-Peck and Thuvasethakul, 1977). This buffer was selected to provide the optimum conditions for the activity of PLA_2 in the egg yolk assay, but it is important to note that full α-amylase activity may not be achievable under these conditions. In fact, studies show that α-amylase is stable between pH 5-10.5 (Sky-Peck and Thuvasethakul, 1977), and since the unmasking is performed at its optimal temperature (37 °C) for a long duration (16 h), it is reasonable to assume that complete unmasking is achieved.

When GPC was used to compare the degradation rates of dextrin and succinoylated dextrin before conjugation, a reduction in molecular weight of ~ 80 % and ~ 50 %, respectively, was seen. After 24 h incubation, dextrin's apparent molecular weight was ~ 10 % of the initial molecular weight, while succinoylated dextrin had only degraded to ~ 35 % of its original weight. Succinoylation has previously been shown to control the degradation rate of dextrin by α-amylase (Hreczuk-Hirst *et al*, 2001a). However, the concentration of α-amylase (200 SU/mL) and degree of succinoylation (~ 23 mol %) used here was markedly different to Hreczuk-Hirst *et al* (2001a)'s method (2.5 SU/mL and 34 mol %, respectively), so it is not surprising that the $t_{1/2}$ was also different (30 min compared to > 180 min, respectively). Still, there was a distinct difference between degradation rates of dextrin and succinoylated dextrin (0.5 min compared to 30 min, respectively).

Although the concentration of α-amylase used in these experiments (200,000 SU/L) is much higher than those found in human plasma (40-125 IU/L) it is also worth remembering that some breast cancers have shown elevated levels of α-amylase (up to 85-fold normal) (Inaji *et al*, 1991; Weitzel *et al*, 1988), which may help reduce toxicity to normal tissues. Previous studies have shown a correlation between Sigma units (SU) and international units (IU) used clinically to describe amylase concentrations (1 SU = 0.466 IU) (Hardwicke *et al*, submitted).

Having confirmed that dextrin-PLA_2 conjugates could retain biological activity in a physiological setting it was important to consider their possible toxicological profile. Haemocompatibility of dextrin-PLA_2 conjugates would be essential for safe

systemic administration by IV injection that would be needed to benefit from the EPR effect. PLA_2 is extremely haemolytic. This occurs due to hydrolysis of RBC phospholipids and/or generation of lysophospholipids and free fatty acids, which are also lytic and can cause further membrane damage. In this study, it was found that PLA_2 showed concentration-dependent RBC lysis after 1 h (Hb_{50} = 300 μg/mL (- Ca^{2+}); 50 μg/mL (+ Ca^{2+})).

The fact that dextrin-PLA_2 conjugates had no haemolytic activity suggests an improved safety profile for IV administration. It is possible that dextrin-conjugation enhances enzyme activity by modifying the surface charge of PLA_2. It has been postulated that a conformational change in PLA_2 upon binding is required for interfacial activation (Peters *et al,* 1992; van den Berg *et al,* 1995), and the presence of dextrin, or even maltose, following α-amylase degradation of dextrin, could interfere with this.

Effect of Ca^{2+} on haemolysis

The addition of 8 mM Ca^{2+} enhanced the haemolytic potency of native PLA_2, however it did not influence the toxicity of dextrin-PLA_2 conjugates towards RBCs. The results seen for native PLA_2 were as predicted since it has been shown previously that the enzymatic activity of PLA_2 is Ca^{2+}-dependent, with optimum activity seen in the presence of 10 mM Ca^{2+} (Kingma *et al*, 2002).

Physiological Ca^{2+} levels are normally in the range of 1.9-2.7 mM (Alscher *et al*, 2001), while metastatic breast cancer cells are reportedly exposed to levels as high as 40 mM (Journe *et al*, 2004). This is a particularly interesting finding since it means that PLA_2 may show enhanced enzyme activity in metastases. It is proposed that dextrin conjugation blocks calcium coordination with the calcium binding loop of PLA_2 by steric hindrance. It is possible that dextrin binds to Lys 14, which is situated very close to 3 residues involved in the coordination of Ca^{2+} cofactor (Figure 4.1).

4.5 Conclusions

Here a method was developed for the synthesis and purification of dextrin-PLA_2 conjugates. Dextrin-PLA_2 conjugates containing 5-9 wt. % PLA_2 and a molecular weight of ~ 200,000 g/mol were reproducibly synthesised. It was shown that

conjugation reduces enzyme activity (36 %), but addition of α-amylase restores activity by degradation of dextrin. Haemolytic activity of PLA_2 was also reduced by dextrin conjugation.

Therefore, these preliminary studies confirmed the potential of polymer-PLA_2 conjugates for further evaluation as an anti-cancer therapy. The following studies (Chapter 5) examined in more detail the mechanism of action of dextrin-PLA_2.

Chapter Five

Investigating the In Vitro Cytotoxicity and Mechanism of Action of Dextrin-PLA_2 Conjugates

5.1 Introduction

As described in Chapter 1 (section 1.4), PLA_2 is a potent membrane active agent. Since dextrin-PLA_2 has already shown greatly reduced haematoxicity (Chapter 4), it was important to demonstrate that the conjugate still retained cytotoxicity towards cancer cells. Therefore, in these studies, the cytotoxicity of dextrin-PLA_2, and dextrin and free PLA_2 (as reference controls) was evaluated using the human breast cancer cell line, MCF-7, murine melanoma cell line, B16F10, and human colon carcinoma cell line, HT29.

In addition this study was designed to investigate the role of EGFR in the cytotoxicity of dextrin-PLA_2 since this receptor has been implicated in the cytotoxic mechanism of PLA_2 (Donato *et al*, 1996). Thus, it was felt that elucidating any link between PLA_2 activity and EGF receptor status would be of fundamental importance in defining the potential tumour specificity for dextrin-PLA_2 activity. Many studies have been undertaken to quantify the number of EGFR expressed by different cell types (examples given in Table 5.1). MCF-7 cells have been reported to have between 800-2,800 EGFR per cell (Fitzpatrick *et al*, 1984b; Imai *et al*, 1982). This is significantly lower than other breast cancer cell lines, such as MDA-MB-231 (700,000 per cell) and BT-474 (68,000 per cell). HT29 cells, on the other hand, have been reported to have 44,000 EGF binding sites per cell (Heimbrook *et al*, 1990), which is 15-55 times more receptors than the MCF-7 cell line. Given that B16F10 cells are of mouse origin, they would not express human EGFR so they were chosen as controls.

Finally, since combination therapy is showing the greatest efficacy in cancer treatment (Early Breast Cancer Trialists' Collaborative Group, 1998), it was considered interesting to assess whether the dextrin-PLA_2 conjugate could be used to enhance the cytotoxicity of the commonly-used anticancer agent, doxorubicin.

5.1.1 EGFR: epidermal growth factor receptor

The EGFR is a 170 kDa transmembrane glycoprotein and a member of the ErbB, or type I, receptor tyrosine kinase (TK) receptor family. It is present on a number of

Table 5.1 Comparison of EGFR expression described in the literature using various methods of quantification.

Cell line	Origin	EGFR (sites/cell)	EGFR (fmol/mg protein)	Method of quantification	Reference
MCF-7	Human mammary epithelial carcinoma from pleural effusion	800	12	^{125}I-EGF binding assay	(Fitzpatrick *et al*, 1984b)
		2,800	-	^{125}I-EGF binding assay	(Imai *et al*, 1982)
		-	≤ 20	EGFR mAb immunoassay	(Bier *et al*, 1998)
HT29	Human colon carcinoma metastatic lesions	-	3430	^{125}I-EGF binding assay	(Magne *et al*, 2002)
		44,000	-		(Heimbrook *et al*, 1990)
RT4	Recurrent papillary bladder carcinoma	44,000	-	Flow cytometry	(Brockhoff *et al*, 1994)
J82	Invasive urothelial bladder carcinoma	42,500	-	Flow cytometry	(Brockhoff *et al*, 1994)
A431	Human epidermoid carcinoma	1,600,000	-	^{125}I-EGF binding assay	(Good *et al*, 1992)
DU4475	Human mammary epithelial carcinoma (suspension)	Non detectable	Non detectable	^{125}I-EGF binding assay	(Imai *et al*, 1982)
		Non detectable	Non detectable	^{125}I-EGF binding assay	(Fitzpatrick *et al*, 1984a)
COS	Simian fibroblasts	40,000		^{125}I-EGF binding assay	(Livneh *et al*, 1986)

normal and cancerous cells (see Table 5.1). It is comprised of an extracellular binding domain (621 amino acids) and an intracellular tyrosine kinase domain (542 amino acids), linked by a small lipophilic transmembrane segment (23 amino acids). These receptors are most commonly found on the cell surface (Cohen, 1987), although further intracellular receptors have been described (Wiegant *et al*, 1986).

The signalling pathway of EGFR is illustrated in Figure 5.1. Activation of EGFR occurs when one of its ligands, such as EGF, transforming growth factor (TGF)-α, amphiregulin, betacellulin, heparin-binding EGF or epiregulin (Yarden, 2001), binds to the receptor in its open conformation. Ligand binding causes oligomerisation of two or more receptor-ligand complexes, which are subsequently internalised by clathrin-coated pits; although high concentrations of ligand can stimulate internalisation by non-clathrin-mediated pathways (Sigismund *et al*, 2005). Phosphorylation of tyrosine residues in the carboxyl tail domain initiates a number of cascades leading the signal towards the nucleus. EGFR in A431 cells was shown to have a half life of 13 h, although addition of EGF caused this to drop markedly to less than 6 h (Goldkorn *et al*, 1997). Following internalisation, receptor-ligand complexes are either degraded in the lysosome or recycled to the cell surface.

Activation of EGFR triggers a variety of cellular events, resulting in cellular proliferation, differentiation, protection from apoptosis, cell migration and adhesion, and stimulation of angiogenesis. While these processes are essential for normal cell survival, they also have a great impact on the behaviour of cancer cells.

EGFR has been widely implicated in malignant disease and is regarded as one of the most important growth regulatory signal transduction proteins. Research has revealed that levels of this receptor are amplified in several human tumours, including breast, gliomas, lung bladder and colon cancer, and is therefore considered to be a clinical marker of poor prognosis and correlates with poor response to treatment, rapid disease progression and poor survival (reviewed in Oliveira *et al*, 2006). Previous investigations have shown that EGFR can be detected in approximately half of all breast cancer biopsies (Fitzpatrick *et al*, 1984a), which led to EGFR becoming a key target for novel anti-cancer therapies.

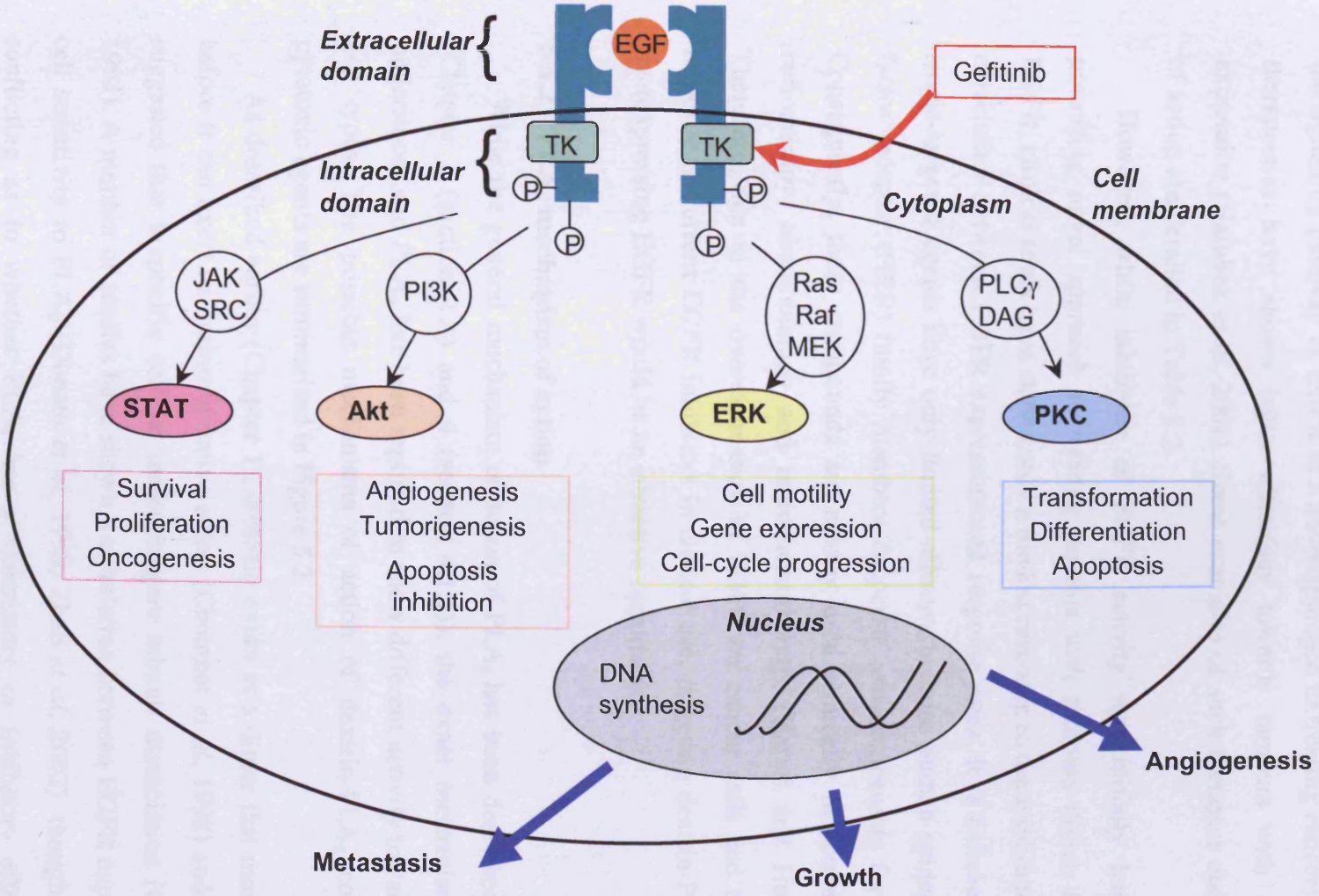

Figure 5.1 Schematic illustration of the EGFR signalling pathway, involving EGF-activated protein kinase to the nucleus and stimulation of cell cycle machinery. Adapted from: Nyati, MK *et al* (2006) and Harari and Huang (2004).

Following initial studies showing that mAbs were able to inhibit growth of cancer cells through their interaction with EGFR (Gill *et al*, 1984; Sato *et al*, 1983), a number of strategies have been developed over the past 20 years which interfere with the signalling pathway of EGFR as a novel approach to treating cancers. These new therapeutics have shown better efficiency towards tumours with high EGFR expression (Hambek *et al*, 2001). Some examples of such therapies and their mode of action are detailed in Table 5.2.

However, while inhibition of EGFR activity was initially heralded as a promising novel approach to treating patients with tumours driven by activated EGFR, clinical trials have shown only a modest response to these inhibitors and poor correlation between EGFR expression and response rates. It is believed that these single-targeted agents have only limited efficacy because human epidermal growth factor receptor (HER) family members cooperate and compensate for each other. Consequently, these compounds are usually used clinically in combination with radiotherapy, chemotherapy and radiochemotherapy (Harari and Huang, 2004). Therefore, due to the overexpression of EGFR on cancer cells and their modest response to current EGFR inhibitors in clinical use, targeting dextrin-PLA_2 to cells overexpressing EGFR would be an attractive opportunity.

5.1.2 PLA_2 mechanism of action

While the general mechanism of action of PLA_2 has been described previously (Chapter 1 (section 1.4) and 4 (section 4.1.1)), the exact mechanism is poorly understood, and PLA_2 has been reported to show different activity towards different cell types. The possible mechanisms of action of dextrin-PLA_2 conjugates as cytotoxic agents are summarised in Figure 5.2.

As described earlier (Chapter 1), crotoxin exists as a dimer that must dissociate before it can exert its antiproliferative effect (Choumet *et al*, 1998) and it has been suggested that a specific cellular target triggers subunit dissociation (Corin *et al*, 1993). A number of studies have shown a correlation between EGFR expression and cell sensitivity to PLA_2 (Donato *et al*, 1996; Zhao *et al*, 2002), though results are conflicting as to whether PLA_2 has a stimulatory or inhibitory effect on cell proliferation and/or EGFR activation. Zhao *et al* (2002) reported inhibition of EGF-

Table 5.2 Examples of some EGFR inhibitors in clinical use.

Agent and manufacturer	Molecule	Target site	Comments	Reference
Cetuximab (IMC-C225, Erbitux®); ImClone Systems/BMS)	Mouse-human chimeric mAb	Extracellular domain	FDA approved for CRC with irinotecan, and with radiotherapy for SCSHN. Also as single agent for recurrent or metastatic SCSHN after platimum-based treatment failure (Apr 2004).	(Astsaturov *et al*, 2006)
Panitumumab (ABX-EGF, rHuMAb-EGFR); Amgen	Fully human mAb	Extracellular domain	Phase I/II trials for NSCLC, CRC, renal and oesophageal cancer.	(Rowinsky *et al*, 2004)
Matuzumab (EMD72000); EMD Pharma	Mouse-human chimeric mAb	Extracellular domain of EGFR	Phase II trials for NSCLC, gynaecological, pancreatic and oesophageal cancers.	(Kollmannsberger *et al*, 2006)
Erlotinib (OSI774, Tarceva®); Genentech Inc.	Anilinoquinazoline; reversible binding	Intracellular domain (TKI) of EGFR	FDA approved for locally advanced or metastatic NSCLC after failure of ≥ chemotherapy regimen (Nov 2004). FDA approved in combination with gemcitabine for locally advanced, unresectable or metastatic pancreatic carcinoma (Nov 2005).	(Smith, 2005)
Lapatinib (GW572016, Tykerb®); GlaxoSmithKline	Thiazolylquinazoline; reversible binding	Intracellular domain (TKI) of EGFR and ErbB1/2	FDA approved, combined with capecitabine for advanced or metastatic breast cancer overexpressing HER2 (ErbB2) after previous therapy including an anthracycline, a taxane, and trastuzumab (March 2007).	(Mukherjee *et al*, 2007)

SCCHN, squamour cell carcinoma of the head and neck; CRC, colorectal cancer; NSCLC, non-small cell lung cancer

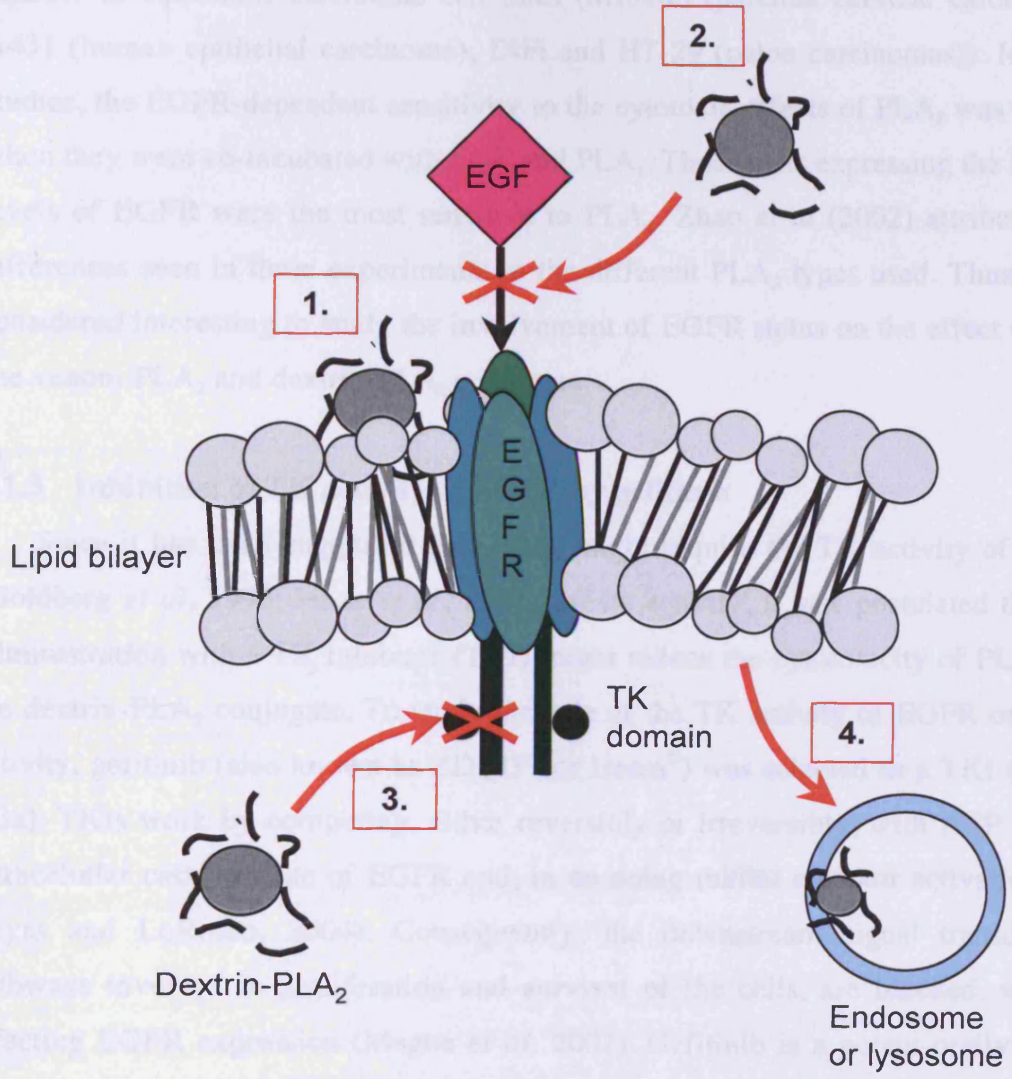

Figure 5.2 Proposed mechanisms of action of dextrin-PLA_2 conjugate. Where 1. PLA_2 degrades cancer cell membrane phospholipids (Rosenberg, 1990); 2. PLA_2 blocks access of EGF to receptor (Hack *et al*, 1991); 3. PLA_2 blocks TK activity of EGFR (Goldberg *et al*, 1990); 4. PLA_2 degrades endosomal membrane phospholipids.

induced receptor activation by PLA_2 from *Agkistrodon halys pallas*. Addition of PLA_2 to A431 (human epithelial carcinoma) cells caused a rise in intracellular ceramide formation leading to the release of arachidonic acid. It was therefore suggested that PLA_2 downregulates EGFR-mediated intracellular signal transduction. Conversely, Donato *et al* (1996) noted a crotoxin-mediated activation of EGFR in a number of squamous carcinoma cell lines (ME-180 (parental cervical carcinoma), A431 (human epithelial carcinoma), DiFi and HT-29 (colon carcinomas)). In these studies, the EGFR-dependent sensitivity to the cytotoxic effects of PLA_2 was altered when they were co-incubated with EGF and PLA_2. Those cells expressing the highest levels of EGFR were the most sensitive to PLA_2. Zhao *et al* (2002) attributed the differences seen in these experiments to the different PLA_2 types used. Thus it was considered interesting to study the involvement of EGFR status on the effect of both bee venom PLA_2 and dextrin-PLA_2 conjugate.

5.1.3 Inhibition of TK activity of EGFR by gefitinib

Since it has been suggested that PLA_2 might require the TK activity of EGFR (Goldberg *et al*, 1990; Hack *et al*, 1991) for its activity, it was postulated that co-administration with a TK inhibitor (TKI) might reduce the cytotoxicity of PLA_2 and the dextrin-PLA_2 conjugate. To study the role of the TK activity of EGFR on PLA_2 activity, gefitinib (also known as ZD1839 or Iressa®) was selected as a TKI (Figure 5.3a). TKIs work by competing, either reversibly or irreversibly, with ATP for the intracellular catalytic site of EGFR and, in so doing inhibit receptor activation (El-Rayes and LoRusso, 2004). Consequently, the downstream signal transduction pathways involved in proliferation and survival of the cells, are blocked, without affecting EGFR expression (Magne *et al*, 2002). Gefitinib is a potent orally active reversible inhibitor of the intracellular domain of the EGFR TK that was approved by the FDA in 2003 for patients with refractory advanced NSCLC. However, in 2005 the FDA announced that gefitinib should be limited to patients who, in their physician's opinion, are currently benefiting, or have previously benefited from gefitinib treatment, after a large study revealed that gefitinib did not, in fact, prolong life.

It was considered important to study the dextrin-PLA_2/ gefitinib combination to

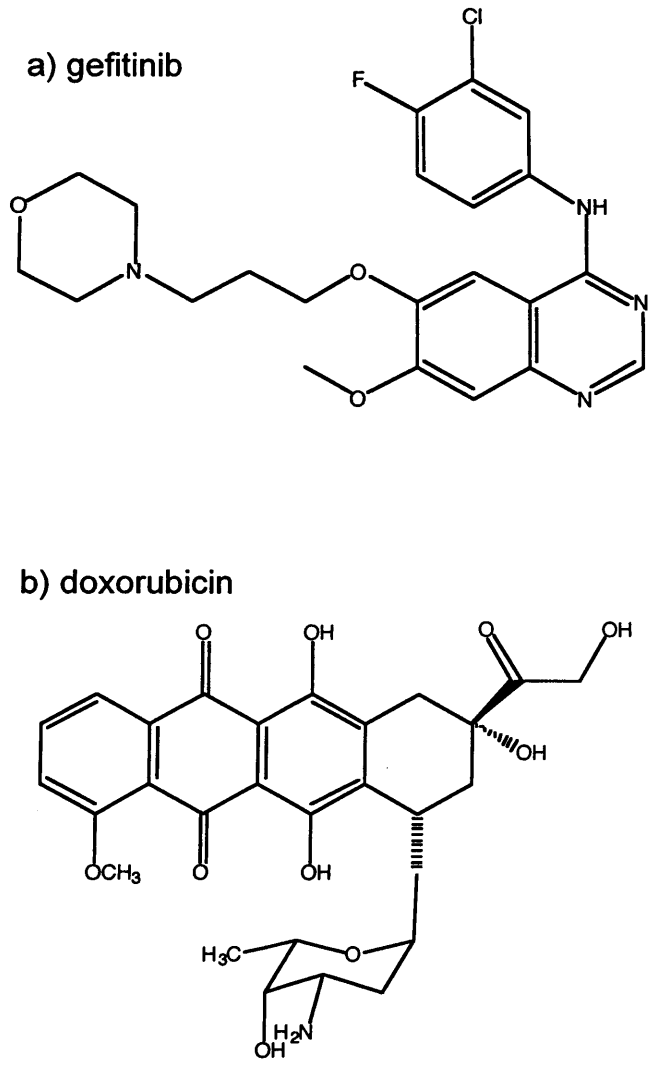

Figure 5.3 Chemical structure of a) gefitinib (4-(3-chloro-4-fluoroanilino)-7-methoxy-6(3-morpholinopropoxy)quinazoline, RMM = 446.9 and b) doxorubicin, RMM = 543.52. RMM = Relative molecular mass.

(i) investigate whether TK activity was important for PLA_2 activity, and (ii) to define the potential clinical impact of using this combination of drugs clinically.

5.1.4 Combination chemotherapy

As a separate study, it was considered interesting to study dextrin-PLA_2 in combination with a conventional chemotherapeutic. Due to the molecular complexity of cancer, adjuvant chemotherapy with classical combinations of two or more drugs including alkylating agents, antimetabolites, taxanes and anthracyclines has shown the best 10-year survival rate in women with metastatic breast cancer (Early Breast Cancer Trialists' Collaborative Group, 1998). Addition of tamoxifen, a selective oestrogen-receptor modulator, to these regimens has improved survival rates among oestrogen-receptor positive women by 31 % (Early Breast Cancer Trialists' Collaborative Group, 2005), while trastuzumab, a mAb against HER type 2 (HER2) has improved disease-free survival by ~ 50 % among HER2-positive patients (Romond *et al*, 2005).

More recently, studies have been investigating the potential of polymer-based combinations (reviewed in Duncan, 2006). PGA-paclitaxel with carboplatin has been tested in phase III trials on performance status level 2 (PS2) patients with advanced NSCLC (Nemunaitis *et al*, 2005). Although the trials did not show a difference in overall survival compared to free paclitaxel and carboplatin combination, a clear gender difference was noted, such that women receiving PGA-paclitexel demonstrated an improved survival at 1 year. Current opinion suggests that a correlation between oestrogen levels and conjugate activity exist, and oestrogen has been shown to increase the expression of cathepsin B, the lysosomal enzyme responsible for degradation of PGA (Kremer *et al*, 1995).

It was therefore considered interesting to investigate whether dextrin-PLA_2 would show enhanced activity when used in combination with a conventional low-molecular weight chemotherapeutic agent. Doxorubicin (Figure 5.3b), an anthracycline, was selected as a model since it is widely used as a first line treatment for breast cancer.

5.1.5 Methods used for *in vitro* cell viability assessment

Cell viability is routinely assessed using a number of different methods, including i) measuring the incorporation of radiolabelled DNA precursors, such as [^{3}H]-thymidine (Amirghofran *et al*, 2007), ii) measuring the uptake of dyes, such as trypan blue (Campbell *et al*, 2007), as an indication of membrane integrity and iii) the MTT assay. Despite the high sensitivity of the radiolabelled DNA precursors, this assay is highly hazardous due to the radioelements and can be expensive. The trypan blue exclusion assay is a cheaper alternative, however it is time consuming and is more suitable to suspension cells than monolayers since dead cells could detach from monolayers and would be lost from the assay.

For these studies, the MTT assay was chosen to measure the effect of free and dextrin-conjugated PLA_2 on cell viability. This assay has been routinely used to screen anticancer agents and polymer-anticancer agents (Alley *et al*, 1988) and was selected due to its simplicity, reproducibility and lack of requirement for radioisotopes.

5.1.6 Experimental aims

In summary, the aims of this study were to:

- Determine *in vitro* the cytotoxicity of the dextrin-PLA_2 conjugate towards high and low EGFR expressing cells (HT29, MCF-7 and B16F10) using the MTT assay (72 h). The cytotoxicity of dextrin and PLA_2 was determined as reference controls.

- Investigate the mechanism of action of PLA_2 and dextrin-PLA_2, by:
  - Studying the influence of EGF co-incubation on the cytotoxicity of PLA_2 and dextrin-PLA_2 in HT29, MCF-7 and B16F10 cells
  - Studying the effect of gefitinib on the activity of PLA_2 and dextrin-PLA_2 in HT29, MCF-7 and B16F10 cells

- Investigate the cytotoxicity of dextrin-PLA_2 in the presence of doxorubicin in MCF-7 cells as a possible combination therapy.

5.2 Methods

Succinoylated dextrin was prepared as described in section 3.2.2. EFdex4 (19.4 mol % succinoylation) was used as a control for succinoylated dextrin in the cytotoxicity assays. EFdex5 (20.9 mol % succinoylation) was used to synthesise dextrin-PLA_2 conjugates in these studies. Dextrin-PLA_2 conjugates were synthesised and characterised according to methods described in Chapter 4. DexPLA5 (MW ~ 215,000 g/mol; PLA_2 content 7.3 wt. %) was used for all the cell viability assays described here.

The general method for obtaining cell growth curves is described in section 2.4.6.4.

5.2.1 Imaging of cell lines

The morphology of the cells was observed whilst *in situ* in sterile glass-bottomed culture dishes. Cells were passaged and counted as described in section 2.4.6.3. Cells were subsequently seeded in sterile glass-bottomed culture dishes and allowed to adhere for 24 h. Bright-field images of cell morphology were taken using an inverted Leica DM IRB microscope with 12-bit cooled monochrome Retiga 1300 camera.

5.2.2 Use of the MTT assay to assess cell viability

For determination of cytotoxicity against MCF-7, HT29 and B16F10 cells, treatments were tested by MTT assay (section 2.4.6.5) using media supplemented as detailed in Table 5.3.

To study the effect of dextrin-PLA_2 conjugate, PLA_2 and dextrin on cell viability complete media was supplemented with a range of concentrations of each.

The influence of EGF on cell viability was assessed using complete media, including heat-inactivated FCS, and was supplemented with a range of EGF concentrations. (Heat-inactivated FCS was used to ensure denaturation of the growth hormones found naturally in FCS.)

To examine the effect of EGF on PLA_2 and dextrin-PLA_2 conjugate activity, complete media was used including heat-inactivated FCS, supplemented with EGF

Table 5.3 Conditions and concentration ranges used for MTT assays.

Study	HI FCS?*	PLA_2 (μg/mL eq.)	EGF (ng/mL)	Gefitinib (μM)	Doxorubicin (μg/mL)	Dextrin (mg/mL)
PLA_2	x	0.1-500				
Doxorubicin	x				0.001-0.5	
EGF	yes		1-500			
Gefitinib	yes			0.01-100		
PLA_2 + dox	x	50			0.0025-0.5	
PLA_2 + EGF	yes	0.1-500	10			
PLA_2 + gefitinib	yes	0.1-500		1		
Dextrin	x					0.1-1000
Dextrin- PLA_2	x	0.1-500				
Dextrin- PLA_2 + dox	x	50			0.0025-0.5	
Dextrin-PLA_2 + EGF	yes	0.1-500	10			
Dextrin-PLA_2 + gefitinib	yes	0.1-500		1		

* HI FCS = heat-inactivated FCS

(10 ng/mL).

To study the effect of gefitinib on cell viability, complete media including heat-inactivated FCS was used and was supplemented with a range of gefitinib concentrations.

When investigating the effect of gefitinib on cytotoxicity of PLA_2 and dextrin-PLA_2 conjugate, complete media including heat-inactivated FCS was also used but in this case was supplemented with gefitinib (1 μM) and the concentration of PLA_2 or dextrin-PLA_2 conjugate was varied.

When investigating the cytotoxicity of doxorubicin, complete medium was used and the doxorubicin concentration varied.

To study the effect of the dextrin-PLA_2 conjugate or PLA_2 combination with doxorubicin, complete medium was used. A PLA_2 or dextrin-PLA_2 conjugate concentration of 50 μg/mL was used and the doxorubicin concentration varied.

5.3 Results

First, the cell morphology and growth of HT29, MCF-7 and B16F10 cells was assessed (Figure 5.4). During the exponential phase of growth of HT29, MCF-7 and B16F10 cells, cell doubling times during the exponential growth phase were 1.2 days, 1.5 days and 1 day, respectively.

Having established the exponential growth phase of the cells, all cell viability experiments were carried out during this growth phase.

5.3.1 Cytotoxicity of free and dextrin-bound PLA_2

The concentration-dependent cytotoxicity of free PLA_2, dextrin and dextrin-PLA_2 in HT29, MCF-7 and B16F10 cells is shown in Figure 5.5. Table 5.4 summarises the IC_{50} values derived from these plots.

As expected, dextrin was not toxic towards any of the cell lines (up to 1 mg/mL). Free PLA_2 was cytotoxic in all cell lines, and toxicity was most marked in HT29 cells (IC_{50} = 40.0 μg/mL (HT29), 308.6 μg/mL (MCF-7), 108.3 μg/mL (B16F10)). Dextrin-PLA_2 was also cytotoxic in a dose-dependent manner in all cell lines and there was a tendency towards increased cytotoxicity compared to free PLA_2 (IC_{50} = 16.3 μg/mL (HT29), 62.9 μg/mL (MCF-7), 133.3 μg/mL (B16F10)). Both

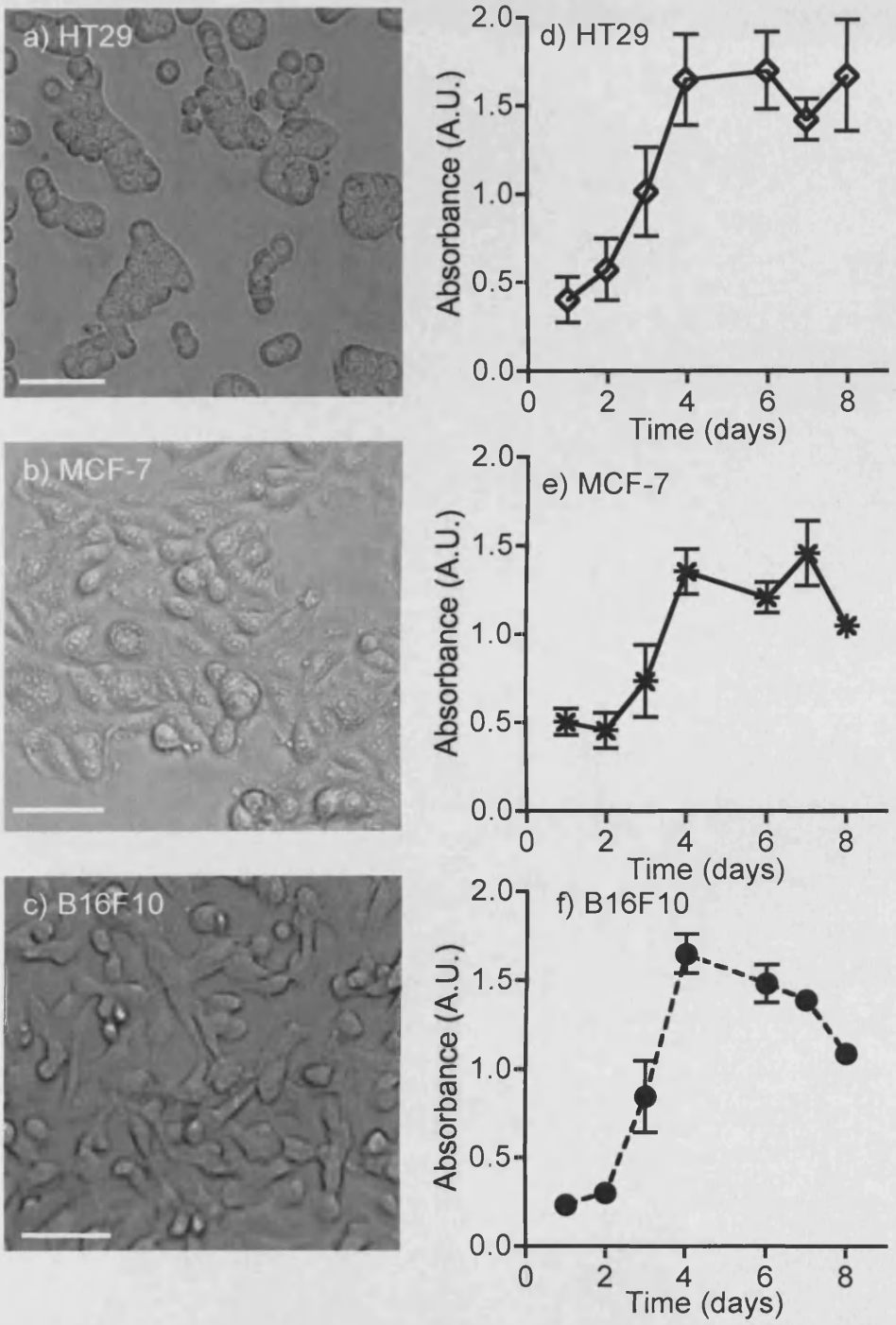

Figure 5.4 Morphology and growth curves for HT29, MCF-7 and B16F10 cells. Panel (a) HT29, panel (b) MCF-7, and panel (c) B16F10 cells. Panels d, e and f) show typical growth curve for the cell lines over 8 days. Pictures taken by bright field microscopy. Size bar = 10 μm. Cells were seeded at a density of 4 x 10^4 cells/mL (HT29 and B16F10) and 1 x 10^4 cells/mL (B16F10). Data shown represents the mean (n=6) ± SD.

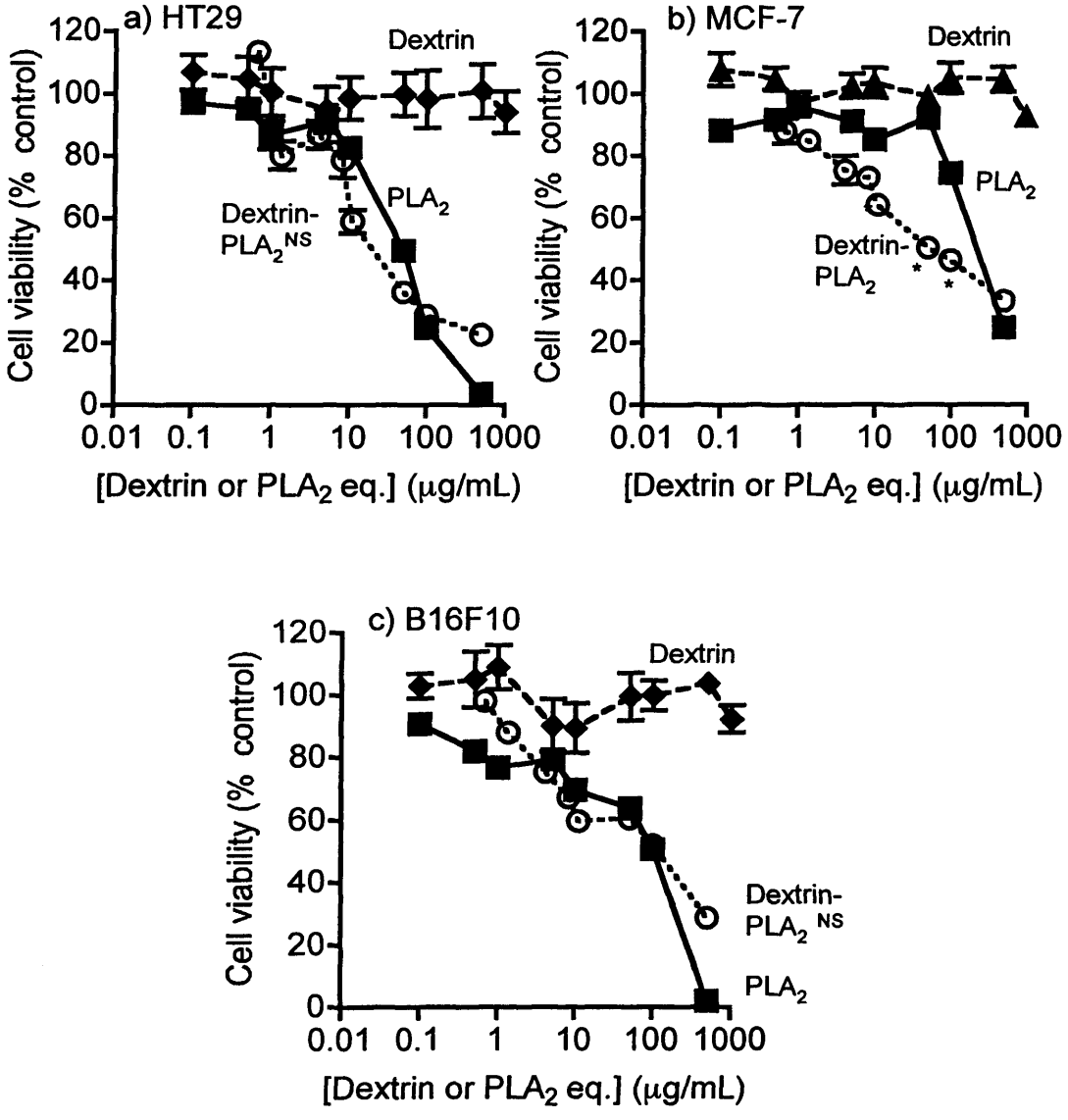

Figure 5.5 Cell viability of HT29, MCF-7 and B16F10 cells incubated with native PLA_2, dextrin and dextrin-PLA_2 conjugate. Data represents % normal growth of control cells ± SEM, (n = 18). Where error bars are invisible they are within size of data points. * indicates significance compared to free PLA_2 control, where $p<0.05$ (ANOVA and Bonferroni *post hoc* test). NS defines no significant difference, where $p>0.05$, (calculated using ANOVA).

Table 5.4 IC_{50} values for PLA_2, dextrin and dextrin-PLA_2 in HT29, MCF-7 and B16F10 cells.

Cell line	Tumour origin	IC_{50} (μg/mL) PLA_2	Dextrin	Dextrin-PLA_2	*% change*
HT29	Human colon cancer	40.0 ± 2.0	> 1000	16.3 ± 2.3	*↓ 59*
MCF7	Human breast cancer	308.6 ± 6.9	> 1000	62.9 ± 5.7	*↓ 80*
B16F10	Murine melanoma	108.3 ± 13.8	> 1000	133.3 ± 21.1	*↑ 23*

Data represents IC_{50} ± SEM, (n = 18).

free and dextrin-conjugated PLA_2 were most toxic in HT29 cells, having the highest level of EGFR expression.

5.3.2 Effect of EGF on viability of cells treated with PLA_2 and dextrin-PLA_2 conjugate

When cells were incubated with EGF alone (up to 500 ng/mL), there was no significant effect on cell viability/ growth (Figure 5.6).

When cells were incubated with EGF and PLA_2 or dextrin-PLA_2, the IC_{50} values were derived from data represented in Figure 5.7 and are summarised in Table 5.5. Addition of EGF (10 ng/mL) and PLA_2 to HT29, MCF-7 and B16F10 cells led to an increase in PLA_2 toxicity. The IC_{50} values seen decreased for all cell lines (26.5 μg/mL, 192.5 μg/mL and 194.0 μg/mL for HT29, MCF-7 and B16F10 cells, respectively).

In contrast, when dextrin-PLA_2 was added together with EGF there was a marked decrease in toxicity. The IC_{50} values increased in all cell lines tested (91.2 μg/mL, 463.6 μg/mL and 339.4 μg/mL for HT29, MCF-7 and B16F10 cells, respectively). There was a significant difference between cytoxicity of the treatment combinations in the different cell types (where $p<0.05$ (ANOVA and Bonferroni *post hoc* test)).

5.3.3 Effect of gefitinib on viability of cells treated with PLA_2 and dextrin-PLA_2 conjugate

Addition of gefitinib to HT29, MCF-7 and B16F10 cells caused concentration-dependent toxicity in all cases (Figure 5.8). The IC_{50} values were in the micromolar range for all cell types, namely 9 μM, 55 μM and 2.5 μM for HT29, MCF-7 and B16 F10 cells, respectively.

Addition of gefitinib (1 μM) together with PLA_2 during incubation of HT29, MCF-7 and B16F10 cells led to decreased cytotoxicity (Figure 5.9 and IC_{50} values are summarised in Table 5.6). An increase in the IC_{50} values was seen for all cell lines tested (254.5 μg/mL, > 500 μg/mL and > 500 μg/mL for HT29, MCF-7 and B16F10 cells, respectively).

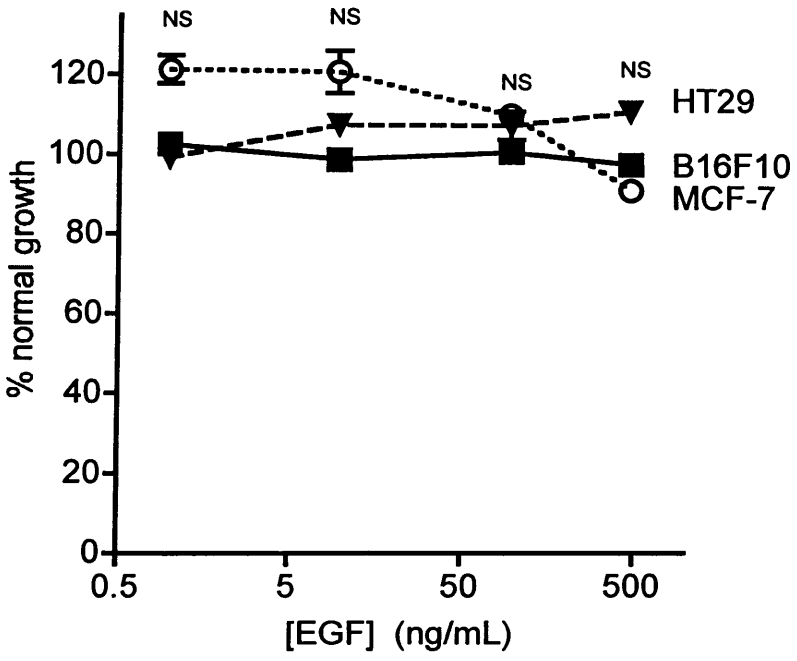

Figure 5.6 Cell viability of MCF-7, HT29 and B16F10 cells after 72 h incubation with EGF. Data represents % normal growth of control cells ± SEM, (n = 18). Where error bars are invisible they are within size of data points. NS defines no significant difference ($p>0.05$), calculated using ANOVA.

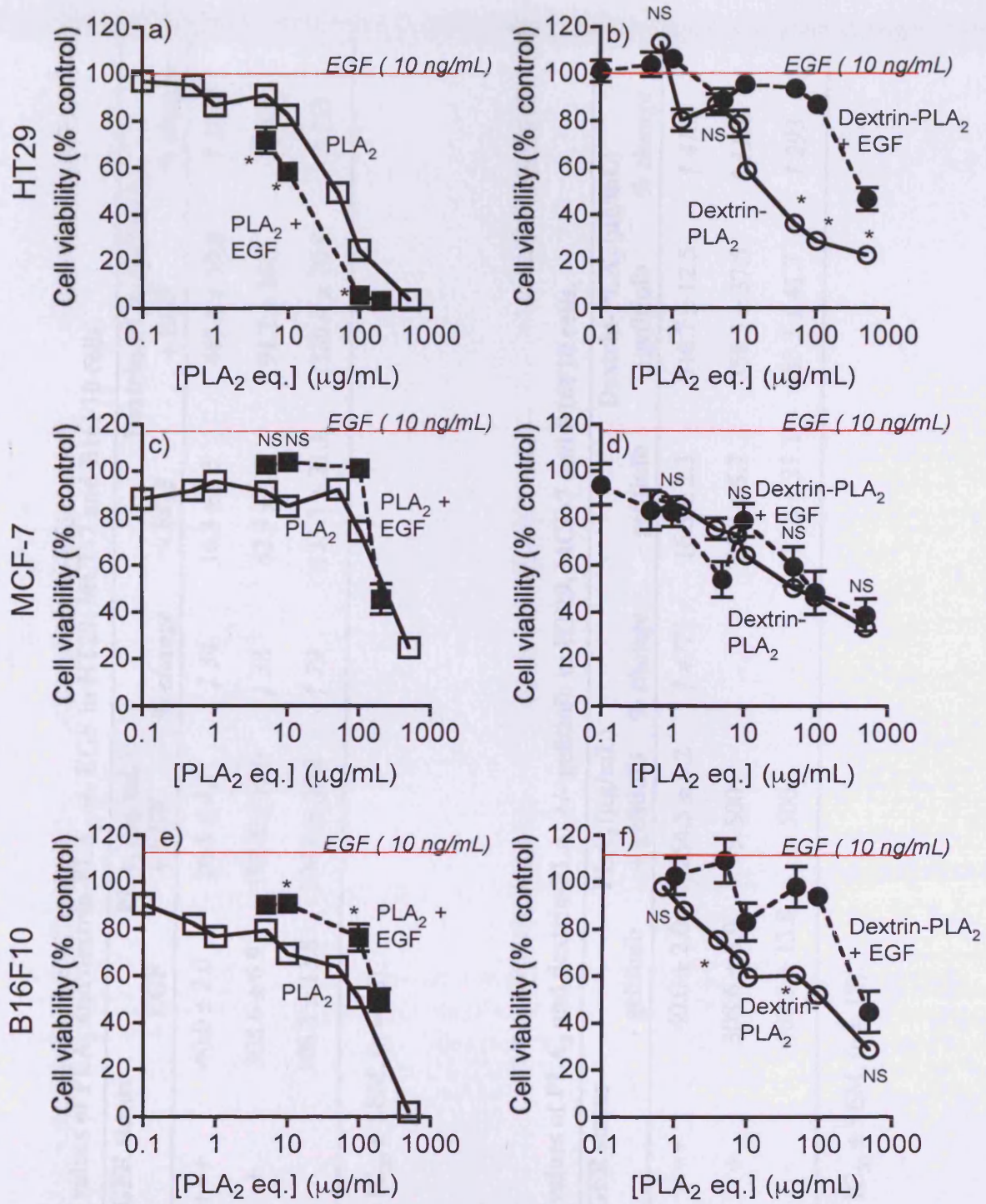

Figure 5.7 Cytotoxicity of PLA_2, PLA_2 + EGF, dextrin-PLA_2 conjugate and dextrin-PLA_2 conjugate + EGF against HT29 (panels a, b), MCF-7 (panels c, d) and B16F10 (panels e, f) cells after 72 h incubation. Data represents mean ± SEM (n = 18). Where error bars are invisible they are within size of data points. * indicates significance compared to PLA_2 or dextrin-PLA_2 control, where $p<0.05$ (calculated using student's t-test). NS defines no significant difference, where $p>0.05$.

Table 5.5 IC_{50} values of PLA_2 and dextrin-PLA_2 +/- EGF in HT29, MCF-7 and B16F10 cells.

Cell line	EGFR status	PLA_2 (μg/mL)			Dextrin-PLA_2 (μg/mL)		
		- EGF	+ EGF	*% change*	- EGF	+ EGF	*% change*
HT29	+++	40.0 ± 2.0	26.5 ± 4.5	*↓ 34*	16.3 ± 2.3	463.6 ± 50.0	*↑ 2744*
MCF7	+	308.6 ± 6.9	192.5 ± 12.0	*↓ 38*	62.9 ± 5.7	91.2 ± 36.7	*↑ 45*
B16F10	-	108.3 ± 13.8	194.0 ± 20.8	*↑ 79*	133.3 ± 21.1	339.4 ± 70.8	*↑ 155*

Data represents IC_{50} ± SEM, (n = 18).

Table 5.6 IC_{50} values of PLA_2 and dextrin-PLA_2 +/- gefitinib in HT29, MCF-7 and B16F10 cells.

Cell line	EGFR status	PLA_2 (μg/mL)			Dextrin-PLA_2 (μg/mL)		
		- gefitinib	+ gefitinib	*% change*	- gefitinib	+gefitinib	*% change*
HT29	+++	40.0 ± 2.0	254.5 ± 5.2	*↑ 477*	16.3 ± 2.3	516.7 ± 12.5	*↑ 4135*
MCF7	+	308.6 ± 6.9	> 500	-	62.9 ± 5.7	358.3 ± 37.5	*↑ 1170*
B16F10	-	108.3 ± 13.8	> 500	-	133.3 ± 21.1	383.3 ± 41.7	*↑ 293*

Data represents IC_{50} ± SEM, (n = 18).

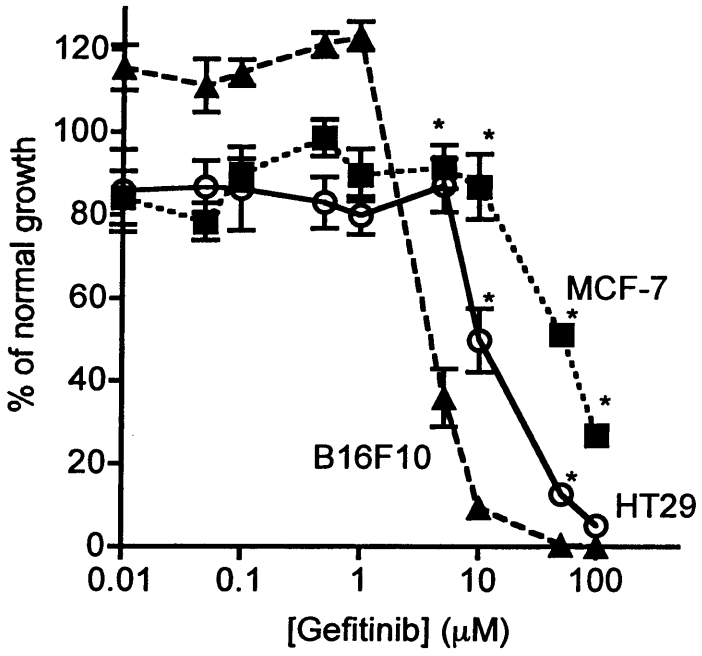

Figure 5.8 Cell viability of HT29, MCF-7 and B16F10 cells incubated with gefitinib for 72 h. Data represents % normal growth of control cells ± SEM, (n = 18). Where error bars are invisible they are within size of data points. * indicates significance compared to B16F10 control, where $p<0.05$ (ANOVA and Bonferroni *post hoc* test).

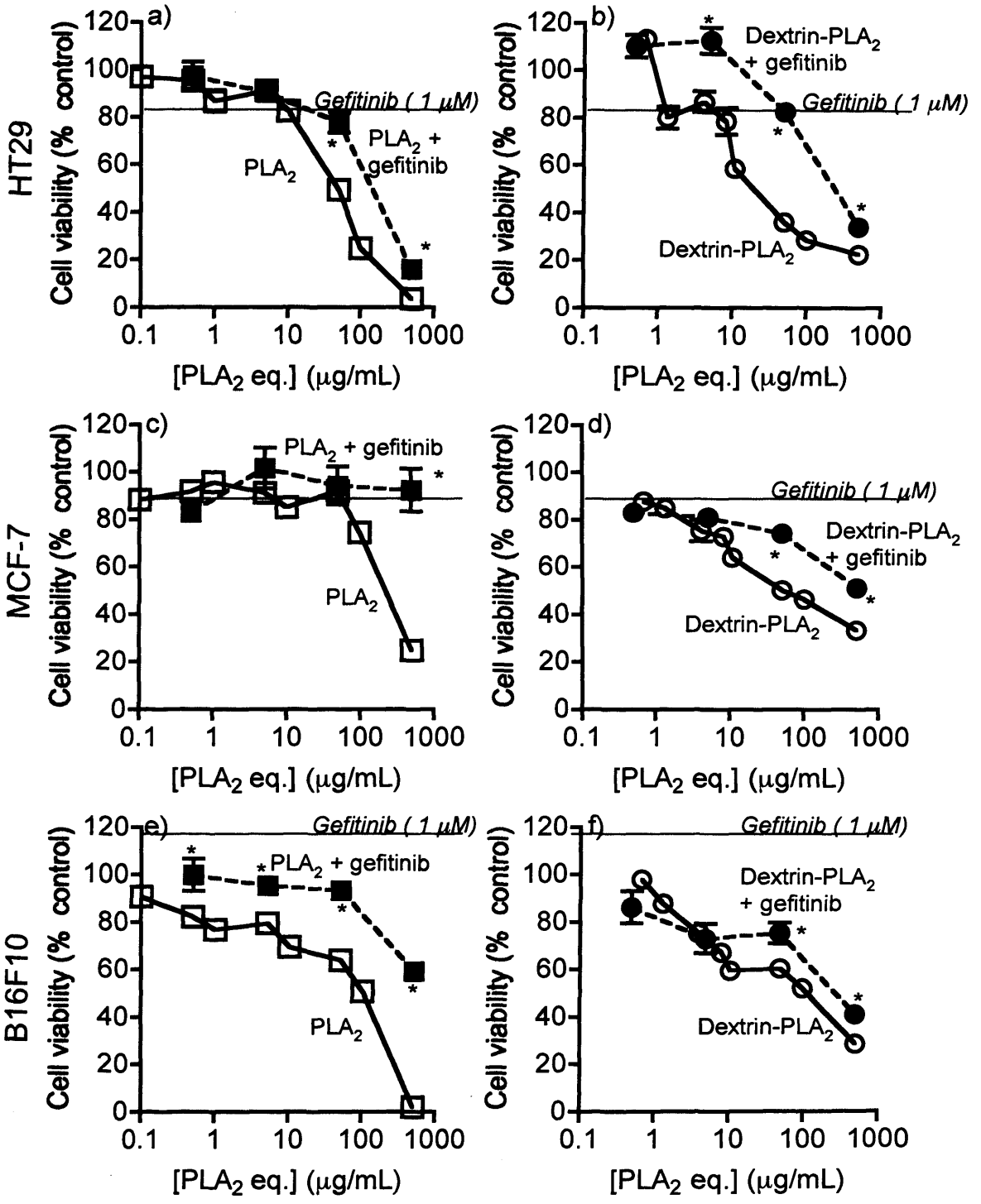

Figure 5.9 Cytotoxicity of PLA_2, PLA_2 + gefitinib, dextrin-PLA_2 conjugate and dextrin-PLA_2 conjugate + gefitinib against HT29 (panels a, b), MCF-7 (panels bc, d and B16F10 (panels e, f) cells after 72 h incubation. Data represents % normal growth of control cells ± SEM, (n = 18). Where error bars are invisible they are within size of data points. * indicates significance compared to PLA_2 or dextrin-PLA_2 control, where $p<0.05$ (calculated using student's t-test). NS defines no significant difference, where $p>0.05$.

Similarly, when gefitinib (1 μM) was added together with dextrin-PLA_2 conjugate, toxicity was also decreased for all cell types (IC_{50} values = 516.7 μg/mL, 358.3 μg/mL and 383.3 μg/mL for HT29, MCF-7 and B16F10 cells, respectively). This effect was most marked for HT29 cells and was least noticeable in B16F10 cells. There was a statistically significant difference between cytotoxicity of the treatment combinations in the different cell types (where $p<0.05$ (ANOVA and Bonferroni *post hoc* test).

5.3.4 Combination of doxorubicin with PLA_2 or dextrin-PLA_2 conjugate

When MCF-7 cells were incubated with doxorubicin and PLA_2 or dextrin-PLA_2, cytotoxicity was significantly increased compared to the doxorubicin control, where $p<0.05$ (ANOVA and Bonferroni *post hoc* test) (Figure 5.10). Doxorubicin alone had an IC_{50} value of 173.3 ng/mL, whereas addition of PLA_2 or dextrin-PLA_2 conjugate (50 μg/mL PLA_2-equiv.) decreased the IC_{50} values to 36.7 ng/mL and 8.3 ng/mL, respectively (summarised in Table 5.7).

5.4 Discussion

5.4.1 Cytotoxicity of PLA_2

Previous studies reported the IC_{50} values of the PLA_2, crotoxin, to be in the range of 50-100 μg/mL and 42 μg/mL in MCF-7 and HT29 cells, respectively (Donato *et al*, 1996; Yan *et al*, 2007). These values are similar to those obtained here with the bee venom PLA_2. Interestingly, Martikainen *et al* (1993) found no toxic effects when incubating MCF-7 cells with bee venom PLA_2. However they only investigated PLA_2 concentrations up to 4.5 U/mL (1.25 μg/mL) for 72 h, and since these studies showed that bee venom PLA_2 had an IC_{50} of 308.6 μg/mL over a 72 h incubation, this lack of toxicity is not surprising.

5.4.2 Cytotoxicity of dextrin-PLA_2 conjugate

The cell viability studies conducted here (Figure 5.5, Table 5.4) showed that the dextrin-PLA_2 conjugate retained the cytotoxicity of native enzyme against all three cell lines studied. In fact, the IC_{50}values observed for the dextrin-PLA_2 conjugate were lower, suggesting that the conjugate may be more active against these cells

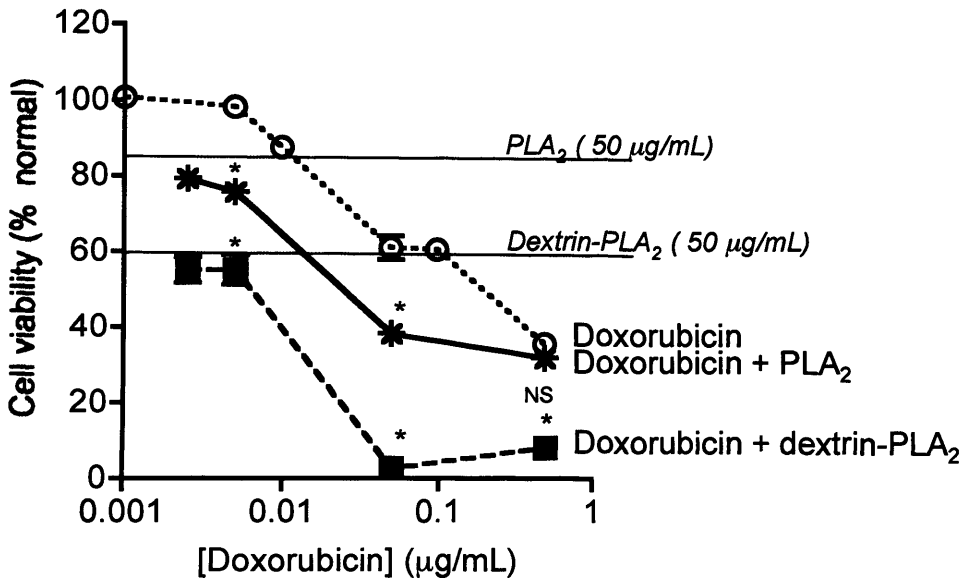

Figure 5.10 Cell viability of MCF-7 cells incubated with doxorubicin +/- PLA_2 and dextrin-PLA_2 conjugate (50 µg/mL PLA_2 eq.) for 72 h. Panel (a) shows effect of doxorubicin concentration on cell viability. Data represents % normal growth of control cells ± SEM, (n = 18). Where error bars are invisible they are within size of data points. * indicates significance compared to doxorubicin control, where $p<0.05$ (ANOVA and Bonferroni *post hoc* test). NS defines no significant difference, where $p>0.05$ (calculated using ANOVA).

Table 5.7 IC_{50} values estimated from MTT assay (72 h) of MCF-7 cells incubated with doxorubicin +/- PLA_2 or dextrin-PLA_2 conjugate.

	IC_{50} (ng/mL)	
Doxorubicin	**Doxorubicin + PLA_2**	**Doxorubicin + dextrin-PLA_2**
173.3 ± 45	36.7 ± 3.3*	8.3 ± 3.3*

Data represents % normal growth of control cells ± SEM, (n = 18).
* $p<0.05$, vs. doxorubicin

lines than crotoxin. This was surprising given the potential masking of PLA_2 activity observed in Chapter 4.

It is postulated that while native PLA_2 hydrolyses phospholipids rapidly (turnover rate (K_{cat}) = 130 s^{-1} (derived from native bee venom hydrolysis of 1,2-dimyristoyl-*sn*-glycero-3-phosphomethanol (DMPM) vesicles in the scooting mode at pH 8)) (Annand *et al*, 1996), the dextrin-PLA_2 conjugate is likely to have a slower turnover rate. Therefore, cytotoxicity after 72 h is the same for both free and conjugated PLA_2. In addition, the FCS present in the cell culture media contains proteins, including α-amylase. Over 72 h incubation this would be expected to slowly unmask the conjugated PLA_2. It was previously shown in Chapter 4 that succinoylated dextrin is degraded by α-amylase within 16 h ($t_{1/2}$ = 30 min).

5.4.3 Mechanism of action of PLA_2 and conjugate cytotoxicity

Interestingly, dextrin-PLA_2 appeared to be more toxic towards HT29 (IC_{50} = 16.3 μg/mL) than MCF-7 (IC_{50} = 62.9 μg/mL) and B16F10 (IC_{50} = 133.3 μg/mL) cells. This might be due to (i) co-localisation of PLA_2 to the EGFR (differences in expression reviewed in section 5.1.2), or (ii) differences in membrane composition of the various cell types.

Donato *et al* (1996) also noticed that crotoxin caused the most effective growth suppression in cells expressing high intrinsic levels of EGFR. Here, DiFi rectal carcinoma cells, having ~ 100 fold greater EGFR expression than HT29 cells, demonstrated ~ 20 fold greater sensitivity to crotoxin than HT29 cells (IC_{50} = 2.2 μg/mL (DiFi), 42 μg/mL (HT29)).

While the addition of EGF (10 ng/mL) to PLA_2 enhanced the cytotoxicity seen in HT29 and MCF-7 cells (Figure 5.7, Table 5.5), the reverse was true when EGF was added to dextrin-PLA_2. It is interesting to consider why.

Activation of EGFR induces very rapid trafficking of the internalised receptor pool to the cell surface resulting in initial upregulation of EGFR numbers (Mathur *et al*, 2000). This is followed by significantly accelerated endocytosis of EGFR-ligand complexes by clathrin-coated pits. After internalisation, the receptors are directed via endosomes to the lysosomal compartment for proteolytic degradation. This leads to

EGFR downregulation and an associated reduction of growth factor signalling (Sorkina *et al*, 2002).

Perhaps when cells are treated with PLA_2 in the presence of EGF they both interact with the cell surface immediately and can therefore take advantage of the high number of EGFR on the cell surface. However, since dextrin-PLA_2 must first be unmasked, it may be that the EGFR are downregulated during the lag phase for PLA_2 release. Consequently, there would be less EGFR available on the cell surface for the dextrin-PLA_2 conjugate to interact with. This hypothesis would explain the observed differences in cytotoxicity but the literature is confused in this respect.

Donato *et al* (1996) showed that pre-treatment of cells with 2 nM EGF (4 h) prior to crotoxin exposure partially suppressed its anti-proliferative activity in A431 cells. They concluded that this was as a result of downregulation of EGFR since no direct binding of crotoxin to the receptor was observed. In another study, Goldberg *et al* (1990) studied the effect of EGF on PLA_2 activity in HER14 cells. They showed that pre-incubation of cells with 16 nM EGF (20 min) increased PLA_2 activity by 226 ± 30 %.

Another plausible explanation for the relationship between PLA_2 and EGFR stems from research showing that stimulation of epidermoid cells with EGF triggers immediate membrane ruffling and macropinocytosis (Araki *et al*, 2007; Hewlett *et al*, 1994). Since membrane ruffling requires actin, which in turn relies on TK-activated effectors such as Ras, SRC and PI 3-kinase found downstream in the EGFR signalling pathway (Figure 5.1), it follows that these two processes are connected. In fact, Jones (2007) reviewed a number of studies showing that activation of SRC oncogene, a non-receptor kinase, leads to macropinocytosis. Since it has been previously shown that PLA_2 is most active towards unstable membranes (Burack and Biltonen, 1994; Jorgensen *et al*, 2002), it is feasible that EGF-induced membrane ruffling could disturb the cell's membrane integrity and make it more prone to PLA_2. Moreover, cells expressing higher levels of EGFR would be expected to display more extensive membrane ruffling.

The PLA_2 and dextrin-PLA_2 conjugate cytotoxicity showed partial correlation with the EGFR expression. They were more cytotoxic towards HT29 than MCF-7 and B16F10 cells. However, melanoma cells have been reported to constitutively express multiple growth factors (Rodeck *et al*, 1991) and it is possible that there are some non-specific effects of EGF occurring in B16F10 cells. For this reason, it is not surprising that B16F10 results did not always correlate with the predicted behaviour.

5.4.3.1 Evidence for a role of the TK domain of EGFR in the mechanism of dextrin-PLA_2 cytotoxicity

Since there is evidence that TK activity is required for membrane ruffling and macropinocytosis, it is postulated that co-incubation of PLA_2 and dextrin-PLA_2 conjugate with gefitinib, a TKI, inhibits these processes and its associated membrane destabilising effects. This theory would provide an explanation for the decreased sensitivity of cells exposed to PLA_2 and dextrin-PLA_2 in the presence of gefitinib.

An inverse correlation has been reported between the IC_{50} value of gefitinib and the cell's EGFR expression (Magne *et al*, 2002). This was also true in part here as gefitinib showed greater activity towards HT29 than MCF-7 cells. Interestingly, here B16F10 cells showed the greatest sensitivity to gefitinib. This is difficult to explain but could be due to non-specific effects of murine growth factor receptor inhibition.

The IC_{50} values obtained in these studies were comparable to those described by Magne *et al* (2002b) who reported IC_{50} values of 6.1 μM and 31.2 μM for CAL33 and Hep-2 cells, respectively. Since gefitinib selectively inhibits TK activity only at concentrations up to 1 μM (AstraZeneca, 2003) it is unlikely that these results are purely related to the effects on the EGFR signalling pathway. It is thought that at concentrations above 1 μM, the effects on cell viability cannot be solely attributed to inhibition of the EGFR pathway.

Addition of gefitinib (1 μM) to cells incubated with PLA_2 or dextrin-PLA_2 conjugate led to diminished cytotoxicity of PLA_2 and dextrin-PLA_2 conjugate in all cases. This is consisitent with previous suggestions that PLA_2 requires TK activity of the EGFR for its cytotoxic effects (Goldberg *et al*, 1990). Furthermore, crotoxin has been shown to stimulate tyrosine phosphorylation of the EGFR in A431 cells *in*

vitro, but with no apparent binding to the receptor itself (Donato *et al*, 1996).

These results with gefitinib confirm that the EGFR TK domain is indirectly involved in the cytotoxicity of dextrin-PLA_2 and suggest that it would not be clinically beneficial to administer dextrin-PLA_2 conjugate with gefitinib as a combination therapy.

5.4.3.2 Alternative explanation

As briefly mentioned in section 5.4.3, there is a second possible explanation for the different cytotoxicities seen in the cell lines tested. Cancer cells are known to have a different membrane composition to normal cells (Monteggia *et al*, 2000; Punnonen *et al*, 1989). A PLA_2 demonstrates preference towards certain phospholipids (PC, PE and SM). Therefore, it is possible that HT29 (and MCF-7, to a lesser extent) have a higher proportion of these phospholipids in their cell membranes.

Differences between the lipid composition of the cell membrane and the endosome membrane have also been described. However, while some research suggests that SM and PS are more enriched in endosomes than plasma membranes (Urade *et al*, 1988), others have reported a high SM and low PS content in both endosomes and the plasma membrane (Evans and Hardison, 1985). If endosomes and lysosomes contain high levels of PC, PE and SM, it is possible that PLA_2 (or the dextrin-PLA_2 conjugate) which has been endocytosed preferentially hydrolyses the endosomal membrane, rather than the cell membrane. This could result in cell death by the release of acidic contents and/or lysosomal enzymes.

These findings led us to investigate whether PLA_2 is internalised by the cell, and if conjugation to dextrin alters this process (Chapter 6).

5.4.4 Potential for combination therapy with doxorubicin

The use of doxorubicin continues to be limited by its cumulative dose-related cardiotoxicity and the related resistance mechanisms (reviewed in Hortobagyi, 1997). Therefore, administering this drug in combination with dextrin-PLA_2 might

lead to improved activity.

In fact, the cytotoxicity of doxorubicin towards MCF-7 cells was enhanced by the addition of both PLA_2 and dextrin-PLA_2. Addition of doxorubicin to PLA_2 did not enhance cytotoxicity as much as seen for dextrin-PLA_2 conjugate. However, since dextrin-PLA_2 conjugate alone was more toxic than free PLA_2 in MCF-7 cells (Figure 5.5), the effects seen here appear to be just additive (i.e. A + B = C), and not synergistic (A + B = C^{++}).

These findings are interesting considering that low, yet clinically relevant concentrations of doxorubicin, have been reported to inhibit $iPLA_2$ activity *in vitro* and *in vivo* (Swift *et al*, 2003; Swift *et al*, 2007). Anthracycline-induced inhibition of porcine pancreatic $sPLA_2$ has also been described, suggesting that it is not just $iPLA_2$ that is susceptible to inhibition (Mustonen and Kinnunen, 1991).

5.5 Conclusions

These studies demonstrated that dextrin-PLA_2 was equal to or better than free PLA_2 as a cytotoxic agent towards HT29, MCF-7 and B16F10 cells *in vitro*. There was generally a correlation between EGFR expression and PLA_2-mediated cytotoxicity, with cells expressing higher levels of EGFR being more susceptible to the anti-proliferative activity of PLA_2.

Whereas the activity of free PLA_2 was enhanced by the addition of EGF, the activity of the conjugate was reduced. This was presumably due to the altered kinetics of PLA_2 bioavailability.

It has been shown that inhibition of the TK domain of EGFR reduces cytotoxicity of PLA_2 and dextrin-PLA_2, implying that PLA_2 requires TK activity of the EGFR for its activity.

Finally, addition of doxorubicin to MCF-7 cells incubated with PLA_2 or dextrin-PLA_2 resulted in additive, but not synergistic cytotoxic activity.

To investigate further the cellular fate of the dextrin-PLA_2 conjugates flow cytometry and confocal microscopy were used to examine cell uptake and intracellular trafficking (Chapter 6).

Chapter Six

Cellular Uptake and Intracellular Localisation of OG-labelled Dextrin-PLA_2 Conjugates

6.1 Introduction

It has been shown that dextrin-PLA_2 conjugates retained the cytotoxicity of free PLA_2 (Chapter 5). However, it remained unclear whether PLA_2 was acting at the cell surface, or on endosomal membranes following internalisation (Figure 6.1). Therefore, the aim of this study was to investigate to what extent dextrin-PLA_2 conjugates are taken up by cells and to compare uptake to that of unconjugated PLA_2 and dextrin. It was hoped that this might clarify whether PLA_2 exerts its lipolytic activity at the cell surface, or inside endosomes after internalisation.

Flow cytometry was used to quantitate cell uptake at 37 °C, and cell binding at 4 °C. In parallel, confocal microscopy was used to visualise the intracellular fate of fluorescently labelled dextrin, dextrin-PLA_2 conjugate and PLA_2.

6.1.1 Need to study endocytosis and trafficking of dextrin-PLA_2 conjugates

Although interfacial catalysis by PLA_2 has been widely studied in terms of enzyme kinetics and EGFR involvement (Scott *et al*, 1990; van den Berg *et al*, 1995), its endocytic pathway has not been as well characterised. While most research assumes that PLA_2 acts at the cell surface, there are a number of factors that suggest that PLA_2 could preferentially act on endosomal or other intracellular membranes following endocytosis. These include: (i) PLA_2's preference for curved membranes (Best *et al*, 2002), and (ii) the potentially higher endosomal content of phospholipids that are preferentially hydrolysed by PLA_2 (PC, PE and SM) (Diez *et al*, 1994; Monteggia *et al*, 2000). Moreover, previous studies have shown that crotoxin induces upregulation of lysosomal enzymes, and an increased formation of autophagosomes and autophagic vacuoles (Yan *et al*, 2007).

Polymer conjugation has been widely used as a means of improving drug delivery (reviewed in Duncan, 2007; reviewed in Haag and Kratz, 2006). However, while polymer-protein conjugation has shown particular success for the delivery of proteins to extracellular targets, intracellular delivery has proved to be more challenging (Brown *et al*, 2001). Therefore, it was important to establish whether conjugation of PLA_2 to dextrin would alter its endocytic properties.

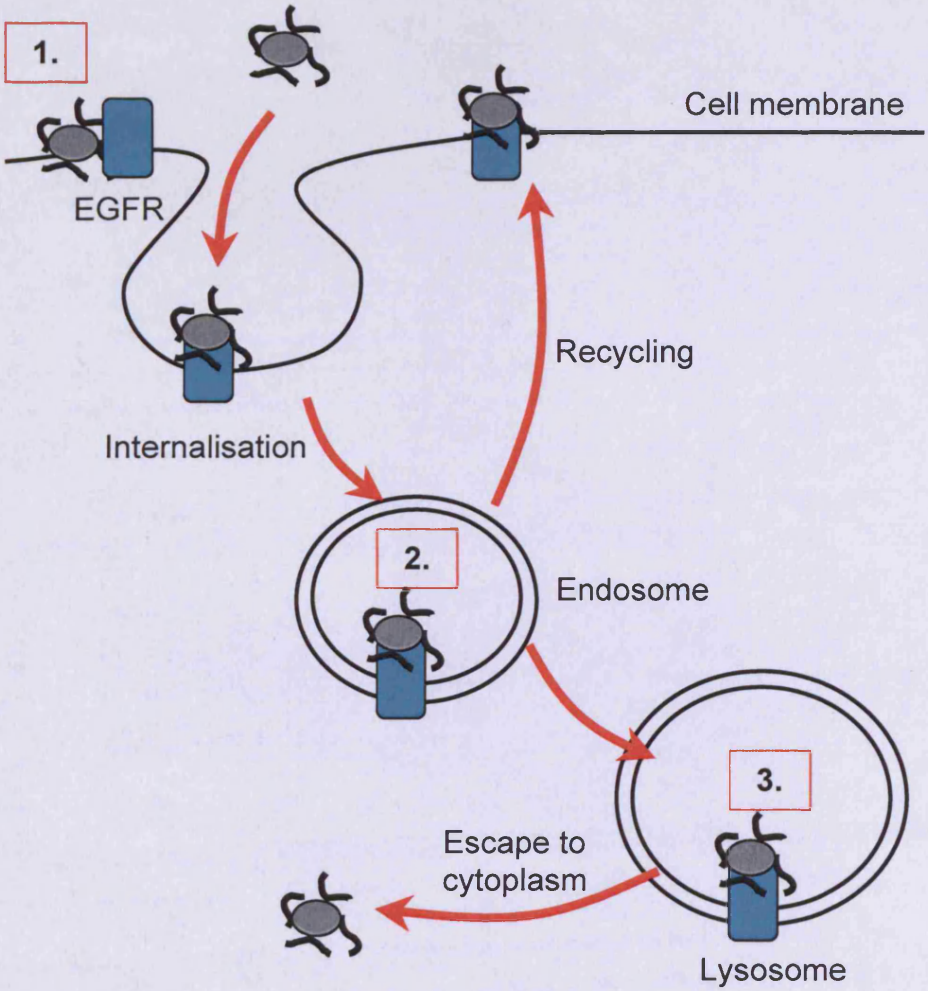

Figure 6.1 Schematic of the possible sites of PLA_2 activity. Where (1) co-localisation to EGFR triggers hydrolysis of phospholipids in cell membrane, (2) hydrolysis of endosomal membrane phospholipids, and (3) hydrolysis of lysosomal membrane phospholipids.

6.1.2 Mechanism of uptake

Given that polymer-protein conjugates typically have a diameter of ~ 20 nm (reviewed in Duncan, 2003) they are potentially liable to internalisation by a number of different endocytic pathways, as shown schematically in Figure 6.2.

These are briefly described here in more detail:

1. Clathrin-mediated endocytosis: Clathrin-coated pits have a diameter of ~ 120 nm. Typically, the assembly of a clathrin coated basket-like structure results in membrane invagination and eventual internalisation of a variety of ligand-receptor complexes into clathrin-coated vesicles (reviewed in Johannes and Lamaze, 2002). Since it has been suggested that PLA_2 interacts with EGFR and/or its ligand (Donato *et al*, 1996; Hack *et al*, 1991; Margolis *et al*, 1988; Zhao *et al*, 2002) and EGF is known to be internalised by clathrin-mediated endocytosis (Sorkina *et al*, 2002), it is plausible that PLA_2 could be internalised by this mechanism. Some studies have suggested that while negatively-charged nanoparticles do not utilise the clathrin-mediated endocytic pathway for endocytosis, positively charged nanoparticles are rapidly internalised by this mechanism (Harush-Frenkel *et al*, 2007). Consequently, given that succinoylated dextrin has a net negative charge as a result of the unreacted carboxylic acid groups, dextrin-conjugation may influence uptake of PLA_2 by this route.

2. Caveolae-mediated endocytosis: Caveolae are flask-shaped invaginations of the cell membrane with a diameter of 50-90 nm (reviewed in Nichols, 2003), meaning that a typical polymer-protein conjugate could be taken up by the cell by this route. Studies of cationic polymers have shown that they use the caveolae-mediated route of endocytosis for cellular uptake (van der Aa *et al*, 2007), which could imply that dextrin-PLA_2 conjugates may be precluded from this route since dextrin would mask the enzyme's charge.

3. Macropinocytosis: Macropinosomes occur as a result of membrane ruffling and subsequent formation of big vesicles called macropinosomes (1-5 μm). Macropinocytosis occurs constitutively in some tumour cells (reviewed in Johannes

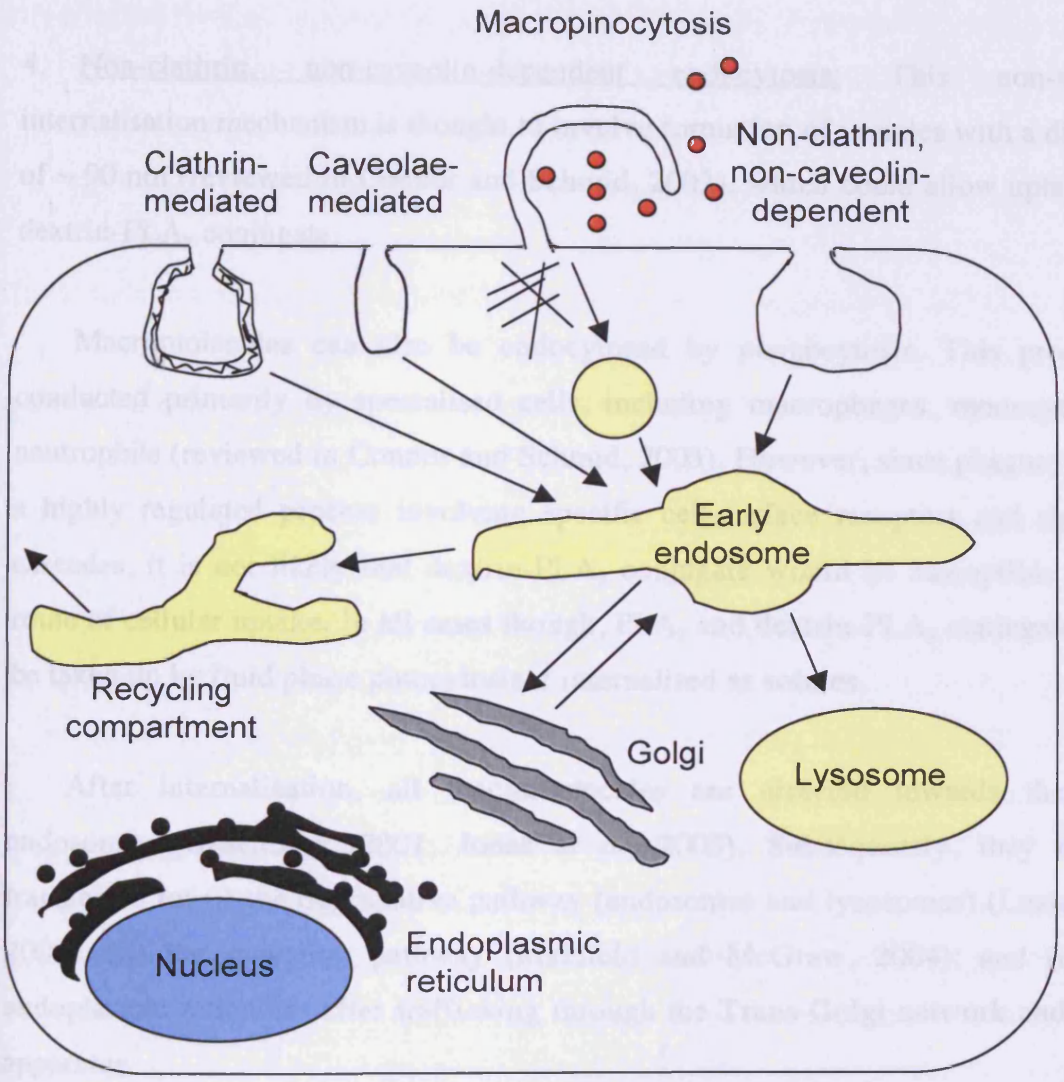

Figure 6.2 Simplified schematic of the possible routes of uptake of dextrin-PLA_2 conjugates. Adapted from Connor and Schmid (2003); Sorkin (2000).

and Lamaze, 2002), although it is more commonly a triggered event, most notably following stimulation by EGF (West *et al*, 1989). Since there is evidence that PLA_2 activity is associated with EGFR (Chapter 5), PLA_2 may itself stimulate macropinocytosis by this mechanism. Furthermore, the large size of macropinosomes permits the inclusion of dextrin-PLA_2 conjugates, which are ~ 20 nm.

4. Non-clathrin, non-caveolin-dependent endocytosis: This non-specific internalisation mechanism is thought to involve formation of vesicles with a diameter of ~ 90 nm (reviewed in Connor and Schmid, 2003), which could allow uptake of a dextrin-PLA_2 conjugate.

Macromolecules can also be endocytosed by phagocytosis. This process is conducted primarily by specialised cells, including macrophages, monocytes and neutrophils (reviewed in Connor and Schmid, 2003). However, since phagocytosis is a highly regulated process involving specific cell-surface receptors and signaling cascades, it is not likely that dextrin-PLA_2 conjugate would be susceptible to this route of cellular uptake. In all cases though, PLA_2 and dextrin-PLA_2 conjugate could be taken up by fluid phase pinocytosis if internalised as solutes.

After internalisation, all macromolecules are directed towards the early endosomes (Gruenberg, 2001; Jones *et al*, 2003). Subsequently, they can be transferred to: (i) the degradative pathway (endosomes and lysosomes) (Luzio *et al*, 2001); (ii) the recycling pathway (Maxfield and McGraw, 2004); and (iii) the endoplasmic reticulum after trafficking through the Trans-Golgi network and Golgi apparatus.

Although no correlation has been found between 'entry route' of polymer therapeutics and their subsequent trafficking, it is important to determine the cellular fate of dextrin-PLA_2 conjugates, since this may affect the cytotoxicity of PLA_2. For example, it was previously suggested that polymeric vectors for protein delivery do not promote cytosolic access if they are rapidly trafficked to the lysosomes (reviewed in Duncan, 2003).

6.1.3 Selection of a fluorescent probe

In order to follow the intracellular fate of dextrin, PLA_2 and dextrin-PLA_2 by flow cytometry and confocal microscopy it was first necessary to label them with a fluorescent probe. Before conjugation, it was essential to select an appropriate probe. A hydrophobic probe would promote non-specific cell binding or alter the conformation of the polymer or protein, thus altering its intracellular trafficking.

OG was selected as the fluorescent probe of choice here since it has previously been conjugated to cationic PAMAM dendrimers and linear and branched PEI (Seib *et al*, 2007) as well as HPMA copolymer conjugates (Wallom, 2008). The fluorescence excitation and absorption wavelengths (λ_{ex} = 488 nm and λ_{em} = 520 nm) and molar extinction coefficient of OG are similar to those of FITC, a popular fluorescent probe, however, FITC has the disadvantage of being susceptible to photobleaching and fluorescence quenching at pH < 7 and following protein conjugation (Lanz *et al*, 1997). OG, on the other hand, has demonstrated better photostability and the fluorescence of OG is less susceptible to quenching upon protein conjugation (Invitrogen Molecular Technologies, 2006).

Intracellular trafficking can expose polymer conjugates to markedly different environments within the cell, so it was important for the fluorescent probe to be unaffected by the changing pH through the endocytic pathway. pH-dependent quenching of fluorescent probes leads to inaccurate quantification of cell-associated fluorescence, because equal quantities of fluorescent probe would lead to altered fluorescent outputs, depending on its cellular localisation. OG has demonstrated less pH dependent quenching between pH 5.5-7.4 than FITC (where pH 5.4, 6.4 and 7.4 correspond to the pH found in the extracellular environment, endosomes and lysosomes, respectively) (Seib *et al*, 2007).

6.1.4 Flow cytometry

Flow cytometry was used to monitor cell uptake and binding. It allows rapid analysis of a large number of cells for the individual measurements of cell fluorescence and light scattering (Melamed *et al*, 1990). Further categorisation and cell sorting of cell populations by parallel staining of other cellular parameters, including DNA, is also possible using this system (Lostumbo *et al*, 2006). This

technique has been used to assess accumulation of fluorescent drugs, such as doxorubicin (Dordal *et al*, 1995; Greco *et al*, 2007) and fluorescently labelled polymers (Seib *et al*, 2007; Shukla *et al*, 2006) in cells. Flow cytometry was chosen because it is more sensitive than simple measurement of cell-associated fluorescence and does not require fixation or digestion prior to measurement (Ramanathan, 1997).

6.1.5 Confocal microscopy

Confocal microscopy allows visualisation of several co-incubated fluorescent probes to enable comparison of their cellular localisation relative to specific intracellular organelles and it has been widely used to visualise the cellular fate of fluorescently-labelled polymer conjugates (Nan *et al*, 2005; Seib *et al*, 2007). It has the advantage that live cell imaging avoids fixation artefacts.

However, fixation of cells brings the advantage of enabling immunostaining of specific markers and definitive subcellular localisation of fluorescently-labelled components. Unfortunately, traditional fixation methods, such as aldehyde cross-linking followed by detergent extraction or cold solvent precipitation/extraction are inappropriate, since they permeabilise intracellular membranes, allowing non-fixed materials, including water-soluble polymers, to diffuse out of their subcellular compartments. The main challenge associated with fixation of polymers for fluorescence microscopy is ensuring their containment within the vesicular compartments they occupy in living cells.

We recently developed a new method of cell fixation to circumvent these fixation problems and ensure retention of OG-labelled dextrin within specific intracellular vesicles (Richardson *et al*, 2008). In these studies, the early endocytic compartments of MCF-7 cells were identified using an antibody to early endosomal antigen 1 (EEA1) (Mills *et al*, 1999), and late endocytic structures (including late endosomes and lysosomes (LE/L)) were characterised using an antibody to lysosome-associated membrane protein 1 (LAMP-1) (Luzio *et al*, 2001). Here these techniques were used to follow the intracellular fate of OG-labelled dextrin.

6.1.6 Aims of this study

In summary, the aims of these studies were to:

- Synthesise, purify and characterise OG-labelled dextrin, PLA_2 and dextrin-PLA_2. Also, it was important to investigate the effect of conjugation on the fluorescence properties of OG.

- Measure the intracellular uptake (37 °C) and extracellular binding (4 °C) of OG-labelled conjugates by MCF-7 cells over 1 h using flow cytometry.

- In parallel, fluorescence microscopy (confocal microscopy) was used to visualise the cellular localisation of the OG-labelled conjugates in MCF-7 cells using EEA1 to mark early endosomes and LAMP-1 to label late endosomes.

6.2 Methods

Succinoylated dextrin was prepared as described in section 3.2.2. EFdex6 (22.3 mol % succinoylation) was used for these studies. Dextrin-PLA_2 conjugates were synthesised and characterised according to methods described in Chapter 4. DexPLA6 (MW ~ 190,000 g/mol; PLA_2 content 6.1 wt. %) was used in these studies.

The general methods used in these studies for conjugate characterisation included the BCA assay (section 2.4.4.3), SDS PAGE (section 2.4.4.2) and FPLC (section 2.4.4.1).

6.2.1 OG-labelling of dextrin, PLA_2 and dextrin-PLA_2, and conjugate characterisation

The methods used are summarised in Figure 6.3.

First, OG cadaverine was conjugated to dextrin and PLA_2. Succinoylated dextrin (150 mg) and PLA_2 (5 mg) were each dissolved under stirring in 1 mL PBS buffer (pH 7.4) in a 10 mL round-bottomed flask. To this, EDC (20 molar eq.) was added, and the mixture allowed to dissolve for 10 min. Next, sulfo-NHS (20 molar eq.) was added to the mixture and left stirring for 40 min. Subsequently, OG (dissolved in ddH_2O (5 mg/mL) and stored at -20 °C until use; 2 molar eq.) was added. NaOH (0.5

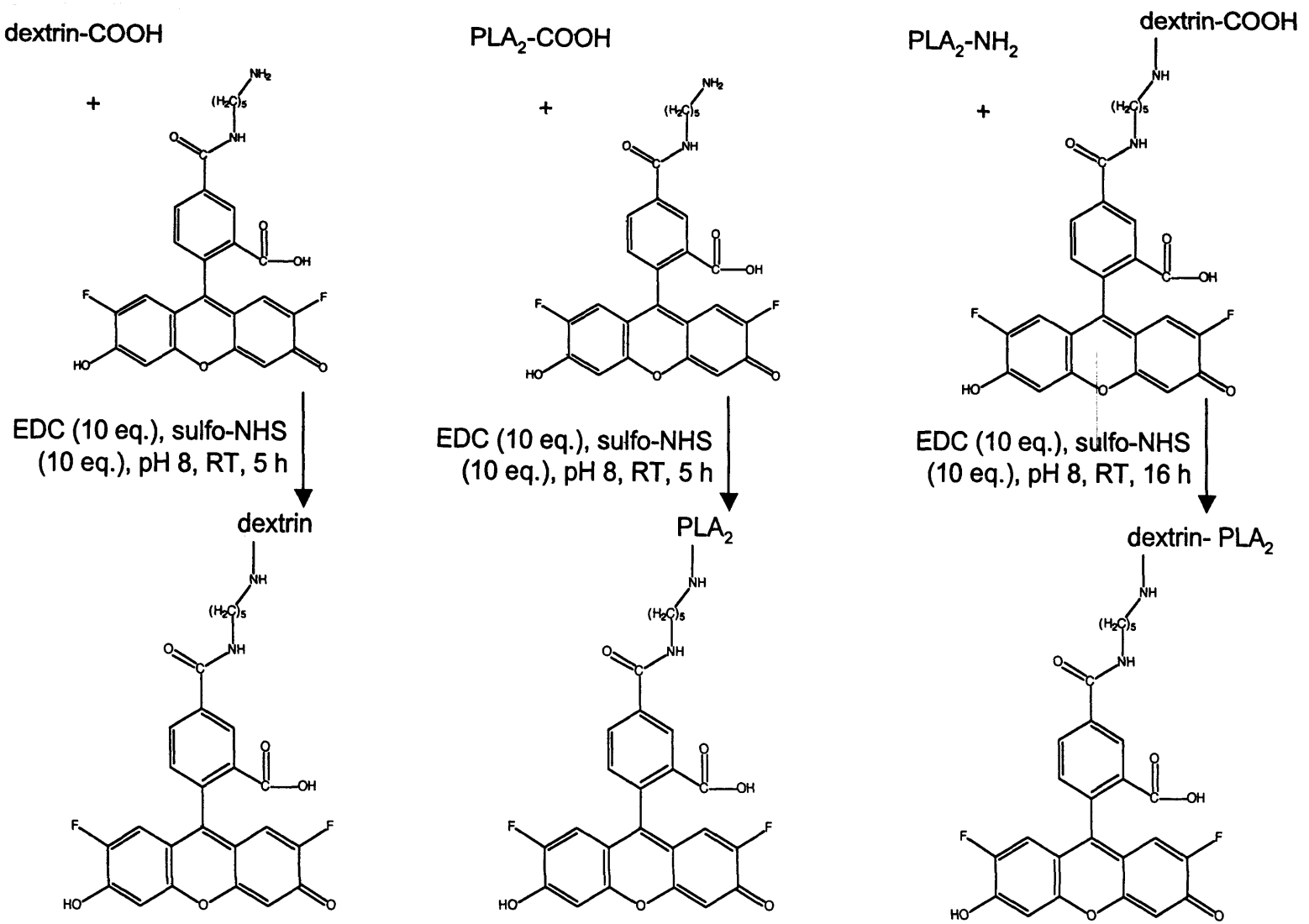

Figure 6.3 Summary of synthetic routes for OG conjugation. Methods described in section 6.2.1.

M) was added dropwise to raise the pH to 8.0 and the reaction mixture was left stirring in the dark (5 h) and monitored by TLC.

Free OG solution and a crude reaction mixture were spotted onto a silica gel TLC plate (on aluminium support). It was placed in a tank containing the methanol solvent and allowed to run until the solvent front was 1 cm from the top. The spots were visualised under a UV light.

The conjugate was purified by SEC using a disposable PD-10 desalting column containing Sephadex G25 equilibrated with PBS (25 mL added in total). The entire reaction mixture was added to the column and 7 mL of the eluted PBS was collected, lyophilised and stored at -20 °C. UV spectroscopy was used to determine the total OG content. The OG-loading was determined by analysing a 1 mg/mL solution in PBS and relating this to a previously derived extinction coefficient for OG in PBS (pH 7.4) (75,000 L/mol/cm). Free OG content was always < 2 % of total OG content.

Specific activity (μg OG per mg OG-labelled conjugate) was calculated using the following equation:

$$\text{Specific activity (μg OG/ mg OG conjugate)} = \frac{\text{(μg OG from UV) x \% OG bound}}{\text{100 x mg OG-labelled conjugate}}$$

The reaction mixture was characterised by SEC prior to and after purification by analysis of SEC fractions for fluorescence (free: bound OG). Fractions (0.5 mL) were collected in 0.5 mL eppendorf tubes (total 45 fractions). A sample of each fraction (100 μL) was placed in duplicate into a black 96-well microtitre plate and measured using a fluorescent plate reader (λ_{ex} = 485 nm, λ_{em} = 520 nm, gain 1000).

To estimate how much bound and free OG was present in each conjugate, a sample (50 μL) of the crude reaction mixture and final product were diluted to 0.5 mL with PBS and subjected to PD-10 elution with PBS. The values were then plotted against fraction volume and bound OG was expressed as percentage of total fluorescence measure for all fractions.

Dextrin-PLA_2 conjugate was prepared using OG-labelled dextrin synthesised as

described above, and unlabelled PLA_2, according to the methods described in section 4.2.

6.2.2 Effect of OG-conjugation to dextrin, PLA_2 and dextrin-PLA_2 on fluorescence output

First, the fluorescence emission spectrum for OG and the OG-labelled conjugates was determined in ddH_2O. OG and OG-labelled conjugates were dissolved in ddH_2O (100 ng/mL OG-eq.) and their emission spectra measured using excitation and emission filters selected from the λ_{ex} and λ_{em} wavelengths of OG (λ_{ex} = 488 nm and λ_{em} = 520 nm).

6.2.3 Measurement of MCF-7 uptake and binding by flow cytometry

The general methods used for flow cytometry and the data analysis were described in section 2.4.6.6. In these experiments all probes were used at an OG-eq. concentration of 1.5 μg/mL OG-eq. in all cases. An incubation of MCF-7 cells without probe was used to account for cell autofluorescence. The cytotoxicity studies involving PLA_2 were performed after an incubation period of 72 h, so it is important to note that all uptake studies were undertaken for a maximum of 1 h, to ensure no cell toxicity. Throughout results are expressed as the cell-fluorescence association (geometric mean) of the viable cell population, corrected for cell auto-fluorescence.

6.2.4 Detection of free OG after incubation of OG-labelled conjugates with cells

Since liberation of free OG in the culture medium or after cell uptake could potentially cause artefacts in the cell fluorescence seen (due to more rapid uptake compared to macromolecular conjugates), the cell culture medium was subjected to analysis by PD-10 chromatography in specific experiments to measure the levels of free OG at the end of the incubation period.

First, a disposable PD-10 desalting column containing Sephadex G25 was equilibrated with PBS (25 mL added in total). A sample of the culture media was added to the PD-10 column (0.5 mL). Fractions (0.5 mL in PBS) were then collected in 0.5 mL eppendorf tubes (total 45 fractions). Then, 100 μL of each fraction was

placed (in duplicate) into a black 96-well microtitre plate and the fluorescence measured using a fluorescent plate reader (λ_{ex} = 485 nm, λ_{em} = 520 nm, gain 1000). The values obtained were then plotted against fraction volume and free OG content was expressed as percentage of total fluorescence measured in all fractions.

FPLC was also used to evaluate the stability of OG-labelled dextrin-PLA_2 conjugates after incubation with MCF-7 cells. Cell culture media containing OG-labelled conjugate was removed from the 6-well plate using a pipette and immediately added to the PD-10 column (200 μL). The method for FPLC is described in section 2.4.4.1.

6.2.5 Confocal microscopy

Figure 6.4 shows a schematic summary of the protocols used for the fluorescence microscopy experiments conducted using MCF-7 cells.

MCF-7 cells were seeded in 12-well plates containing a sterile glass coverslip in each well (1 x 10^6 cells/mL) in WRPMI + 5 % FCS and allowed to adhere for 24 h. The medium was then replaced with either fresh medium containing:

- BSA-Texas Red (BSA-TR) (TR eq. at 50 μg/mL),
- OG-labelled dextrin and BSA-TR (OG eq. at 50 μg/mL, TR eq. at 50 μg/mL),
- OG-labelled dextrin-PLA_2 or OG-labelled PLA_2 (OG eq. at 50 μg/mL).

The cells were incubated for either 4 h (BSA-TR, OG-labelled dextrin) or 1 h (OG-labelled dextrin-PLA_2 or OG-labelled PLA_2) in the presence of 200 μM leupeptin (to minimise lysosomal degradation by proteases). Then the medium was removed and the cells were washed with PBS (37 °C, 3 x 0.5 mL). After the final wash, fresh medium (0.5 mL) containing 200 mM leupeptin was added for the prescribed chase time (16 h for BSA-TR, OG-labelled dextrin and BSA-TR; 4 h for OG-labelled dextrin-PLA_2 or OG-labelled PLA_2). At the end of the chase, the medium was removed and the cells were washed with PBS (37 °C, 3 x 0.5 mL) prior to cell fixation. Control cells (not incubated with a probe) were also prepared for analysis to account for the cell autofluorescence. Cells were fixed in either cold methanol (pre-chilled to -20 °C) and incubated for 5 min at -20 °C or placed in

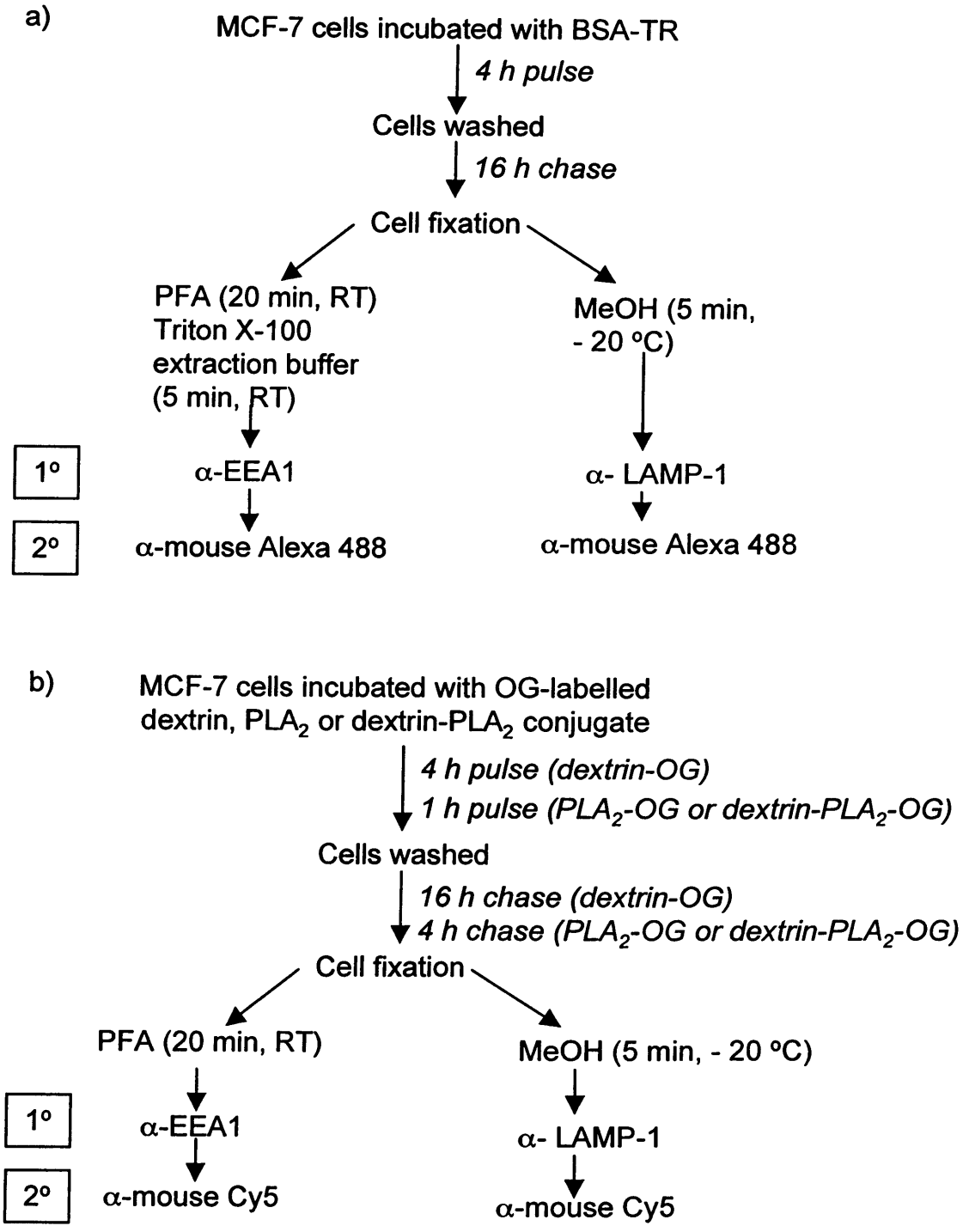

Figure 6.4 Schematic describing the protocols used for confocal microscopy experiments. Panel (a) shows the methods used to generate data in Figures 6.12b and 6.12c, and panel (b) shows the methods used to generate data in Figures 6.12a, 6.13 and 6.14.

freshly prepared 2 % w/v PFA (20 min, at 25 °C).

Those cells to be immunolabelled after aldehyde fixation were subjected to detergent extraction with PBS containing 50 mM glycine and 0.2 % v/v Triton-X 100 (5 min, 25 °C), however, this step was omitted when imaging OG-labelled dextrin in order to maintain the integrity of the limiting membrane of intracellular vesicles and prevent leaking of OG-labelled dextrin from vesicles. Before immunolabelling, non-specific binding sites were blocked by incubating the cells in 2 % v/v goat serum in PBS (60 min, 25 °C). The following dilutions were used for the primary hybridisation (60 min at 25 °C): anti-EEA1 (1:300), anti-LAMP-1 (1:10). The secondary hybridisation was performed using anti-mouse antibodies labelled with either Alexafluor 488 or Cy5 for 60 min at 25 °C (1:500).

Confocal microscopy was performed on a Leica SP5 system. Standard procedures were followed to minimise bleed from one channel to another (giving rise to false positives) and sample photobleaching. All images were collected using monochromatic CCD cameras and data was collected using dedicated software supplied by the manufacturers. At least three representative images were obtained for each sample and exported as tagged image files (TIF); typical results are shown. Merged image were generated using Photoshop. Examples of co-localisation between the endocytic probe (i.e. BSA-TR) and the compartment marker (i.e. antibody) are indicated using arrows.

6.3 Results

6.3.1 Synthesis and characterisation of OG-labelled conjugates

TLC performed after a 5 h reaction at 20 °C in the dark showed a fluorescent spot on the baseline for OG-labelled conjugates while free OG moved up the plate with the solvent front. These reaction conditions were ample for efficient OG conjugation and all subsequent batches of OG-labelled conjugates were synthesised using this method.

Free OG eluted from the PD-10 column after 6.5 - 20 mL whereas the OG

conjugates eluted in the void volume (0.5 - 4 mL), while unreacted OG eluted much later (4.5 – 20 mL) (Figure 6.5). Figure 6.5b-d shows typical elution profiles obtained for OG-labelled PLA_2, OG-labelled dextrin and OG-labelled dextrin-PLA_2 conjugates, before and after purification by PD-10 column. The OG-labelled PLA_2 still had 11.3 % free OG after the first pass through the PD-10 column, therefore it was necessary to repeat the purification step with this conjugate to achieve 0.83 % free OG content. All conjugates used in these experiments contained < 1.51 % free OG. The characteristics of the OG-labelled conjugates synthesised are summarised in Table 6.1. All OG-labelled conjugates had similar specific activities (3.15 – 4.96 μg OG/ mg OG-labelled conjugate).

The fluorescence absorption and emission spectra of OG can be seen in Figure 6.6 (λ_{ex} = 488 nm and λ_{em} = 520 nm). The fluorescence excitation and emission spectra of OG-labelled conjugates are also shown in Figure 6.6, and are not markedly different from those of free OG.

6.3.2 Cell uptake of OG-labelled conjugates

An increase in cell-associated fluorescence was seen for all the OG-labelled conjugates after 1 h at 37 °C, with the increase seen for OG-labelled PLA_2 being the greatest (Figure 6.7). Cell-associated fluorescence was reduced in all cases at 4 °C compared to 37 °C (Figure 6.8). When comparing the percentage of fluorescence which was attributable to the internalised OG-labelled conjugates, dextrin-PLA_2 conjugate showed the highest increase in internalisation after 60 min, with 76 % of total cell-associated fluorescence being internalised (Figure 6.9).

6.3.3 Stability of OG-labelled conjugates *in vitro*

Prior to incubation of OG-labelled conjugates with MCF-7 cells, OG-labelled dextrin, OG-labelled PLA_2 and OG-labelled dextrin-PLA_2 conjugate contained 0.49 %, 0.83 % and 1.51 % of free OG, respectively. After 1 h incubation with MCF-7 cells, free OG levels were estimated as 8.41 %, 15.88 % and 9.36 %, respectively (Figure 6.10a-c, Table 6.2).

FPLC of OG-labelled dextrin-PLA_2 conjugate containing cell culture media

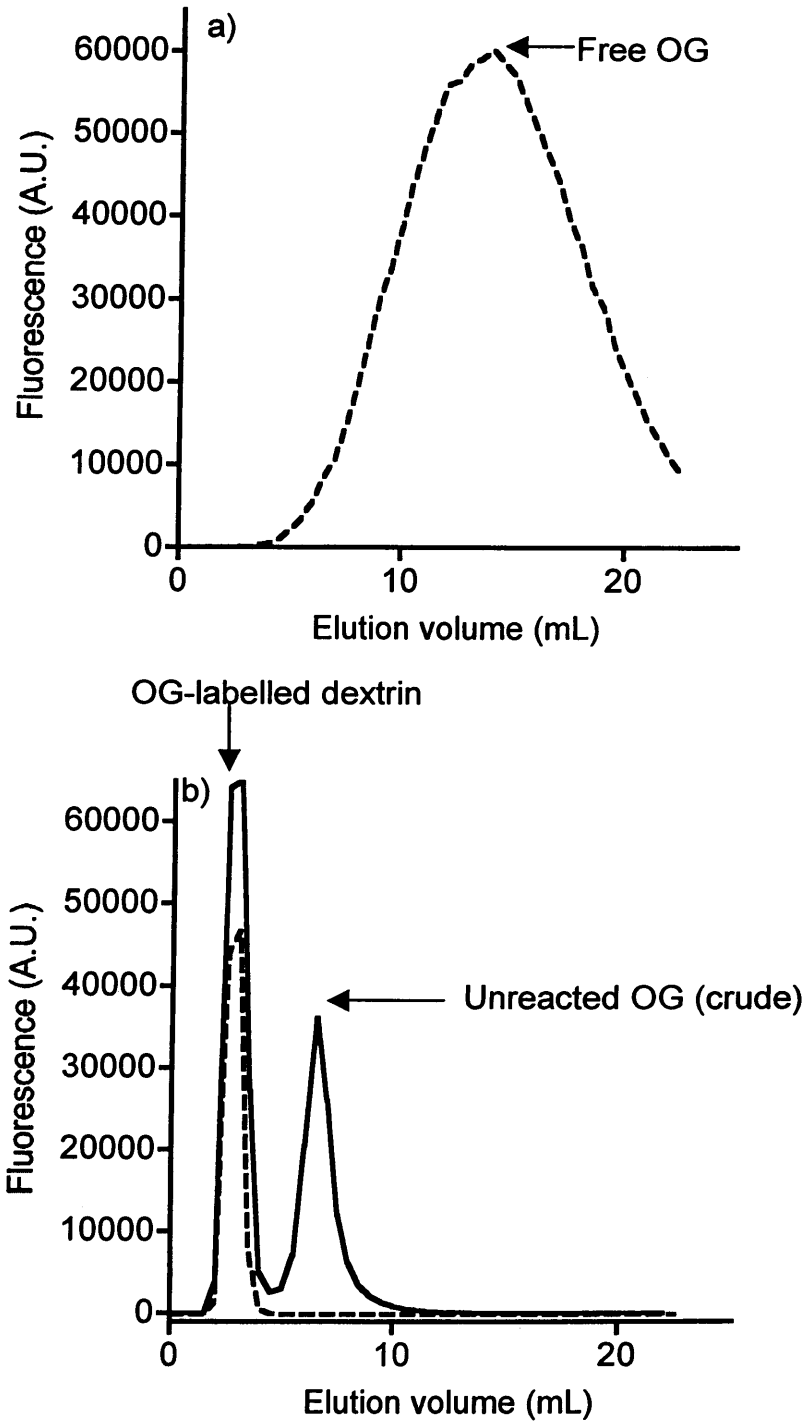

Figure 6.5 Evaluation of reaction yield and purity of OG-labelled conjugates using a PD-10 column. Panel a) shows the elution profile of free OG in PBS. Panels b-d show the elution profile of the crude and purified (b) OG-labelled dextrin, (c) OG-labelled PLA_2, (d) OG-labelled dextrin-PLA_2 conjugate. PD-10 columns eluted with PBS. (Cont. overleaf)

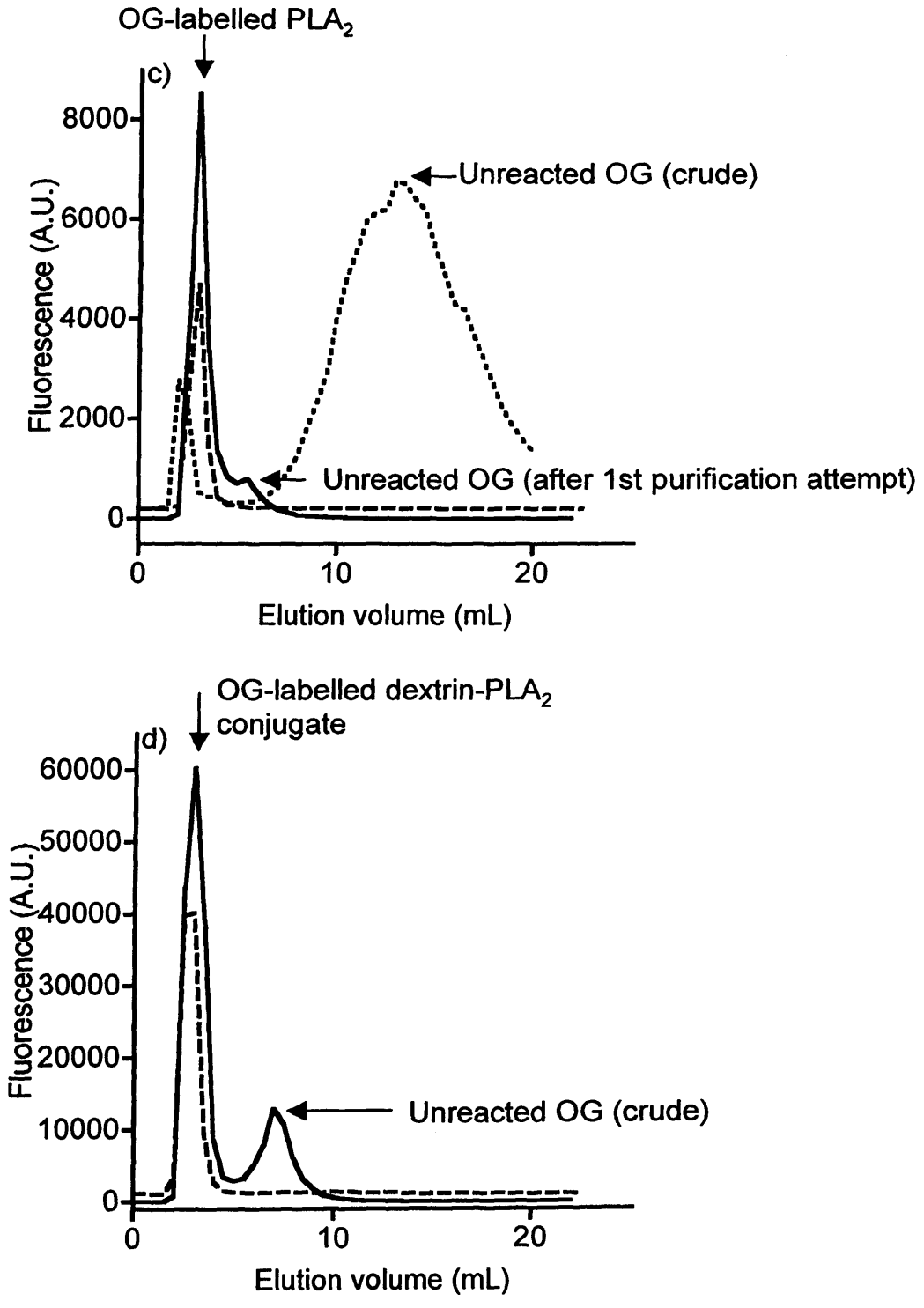

Figure 6.5 Evaluation of reaction yield and purity of OG-labelled conjugates using PD-10 column. (Cont. from overleaf)

Table 6.1 Characteristics of OG-labelled conjugates.

Name	Molar ratio (OG: dextrin or PLA_2)	Labelling efficiency (μg OG/mg conjugate)	Free OG (%)
Dextrin-OG	0.51	4.96	0.03
PLA_2-OG	0.11	3.37	0.83
Dextrin-PLA_2-OG	0.34 (dex: OG) 1.93 (PLA_2: OG)	3.15	1.51

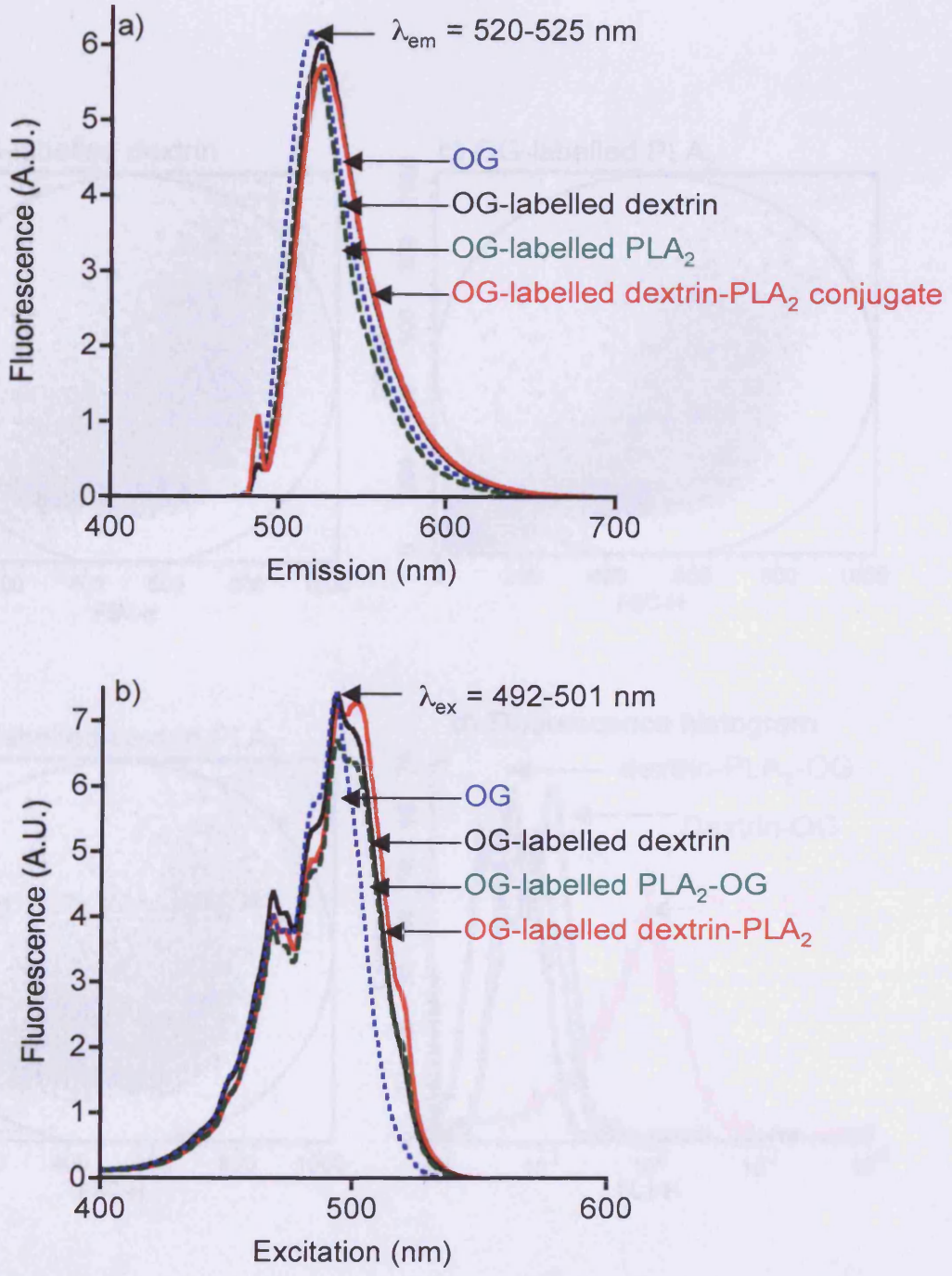

Figure 6.6 Fluorescence excitation and emission spectra of OG (100 ng/mL) and evaluation of the effect of conjugation on the fluorescence spectrum. Panel a) shows the fluorescence emission spectra, and panel b) shows the fluorescence excitation spectra. OG and OG-labelled conjugates were studied in ddH_2O.

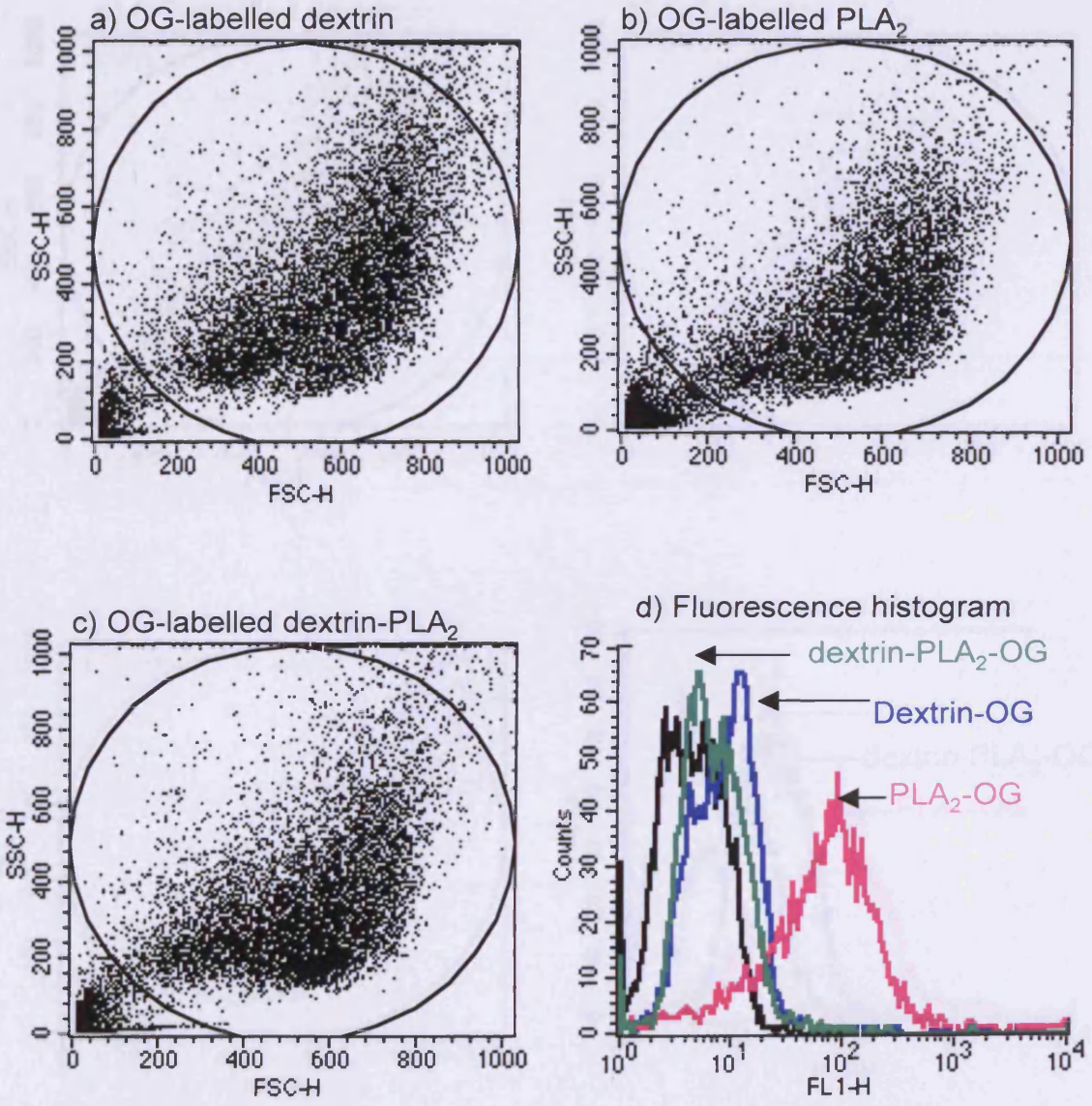

Figure 6.7 Uptake of OG-conjugates conjugates by MCF-7 cells at 4 °C. Panels a-c show scatter plots for cell associated fluorescence at 4 °C after incubation (1 h) with a) OG-labelled dextrin, b) OG-labelled PLA_2 and c) OG-labelled dextrin-PLA_2 conjugate. Panel d) shows a histogram to compare cell associated fluorescence of OG-labelled conjugates, compared to control cells. Control cells (incubated only with medium) are shown in black.

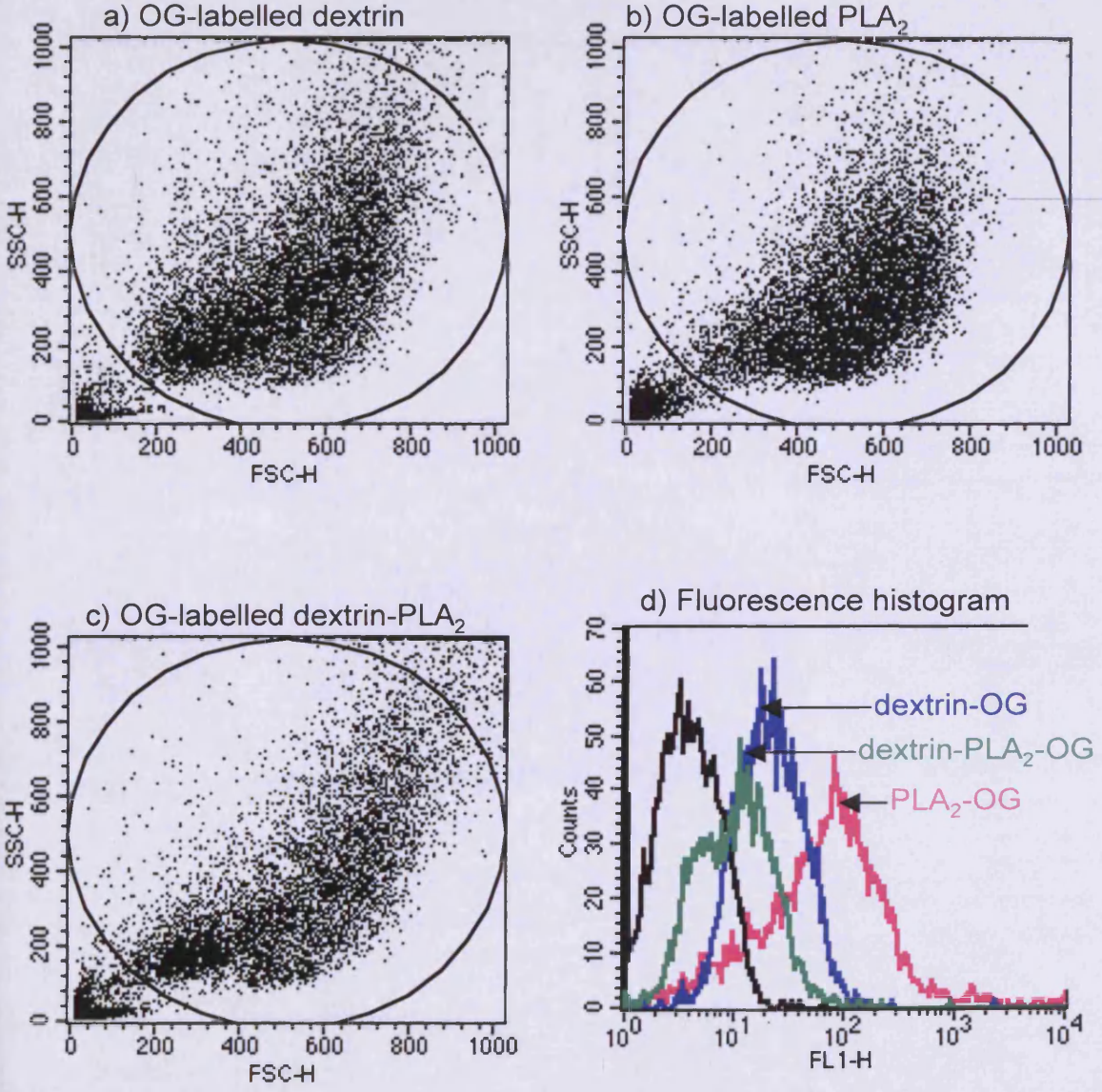

Figure 6.8 Uptake of OG-labelled conjugates by MCF-7 cells at 37 °C. Panels a-c show scatter plots for cell associated fluorescence at 37 °C after incubation (1 h) with a) OG-labelled dextrin b) OG-labelled PLA_2 and c) OG-labelled dextrin-PLA_2 conjugate. Panel d) shows a histogram to compare cell associated fluorescence of OG-labelled conjugates, compared to control cells. Control cells (incubated only with medium) are shown in black.

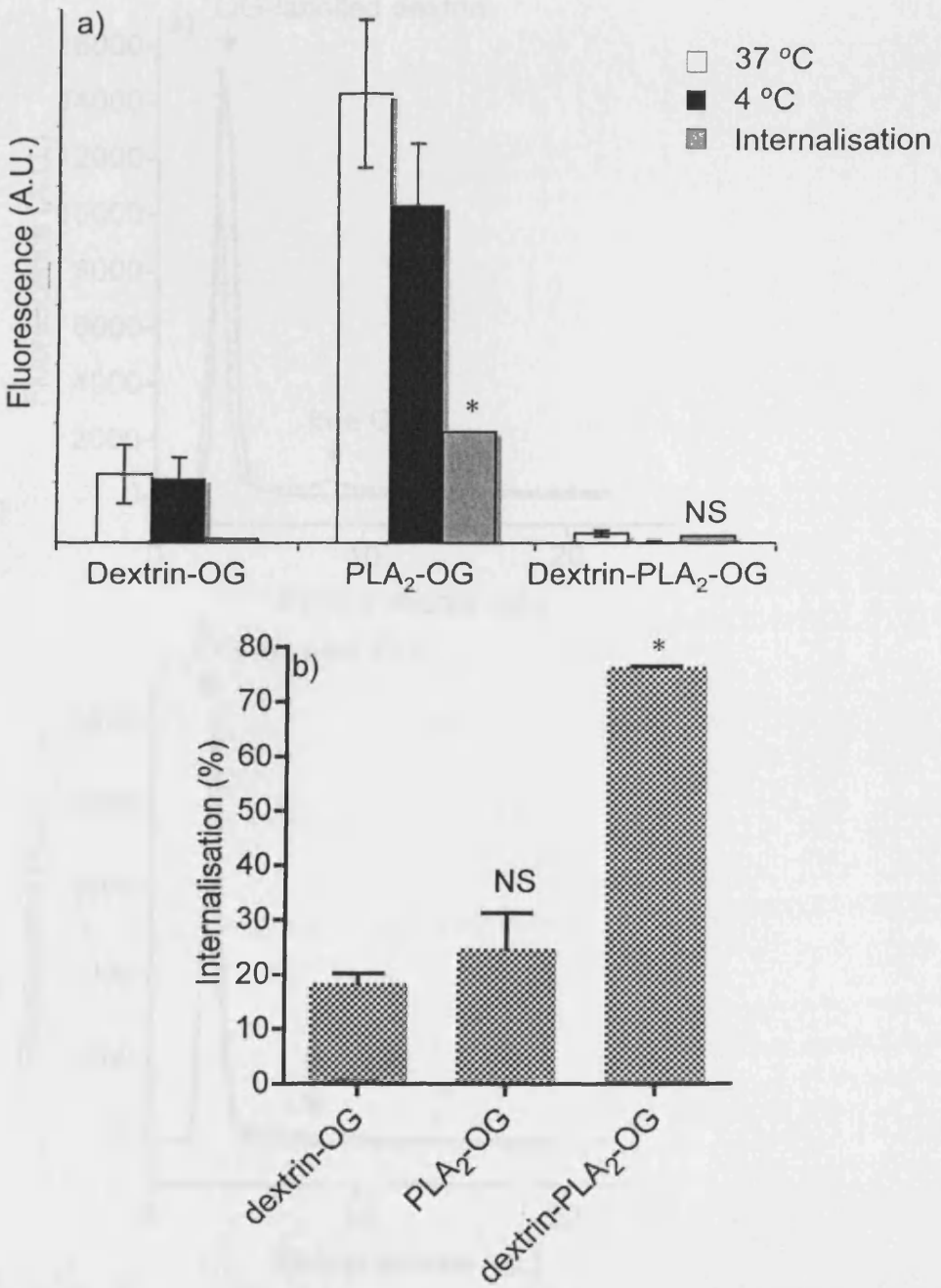

Figure 6.9 Cell associated fluorescence of OG-labelled dextrin, OG-labelled PLA_2 and OG-labelled dextrin-PLA_2 conjugate by MCF-7 cells. Panel a) shows uptake of OG-labelled dextrin, OG-labelled PLA_2 and OG-labelled dextrin-PLA_2 conjugate at 37 °C and 4 °C, and the calculated internalisation. Panel b) shows % of cell-associated fluorescence that represented by internalisation $(((FL_{37\ C}-FL_{4\ C})/FL_{37\ C}) \times 100)$. Data represents mean ± SD, n = 3. * indicates signigficance compared to OG-labelled dextrin control, where $p<0.05$ (ANOVA and Bonferroni post hoc test). NS defines no significant difference, where $p>0.05$, (calculated using ANOVA).

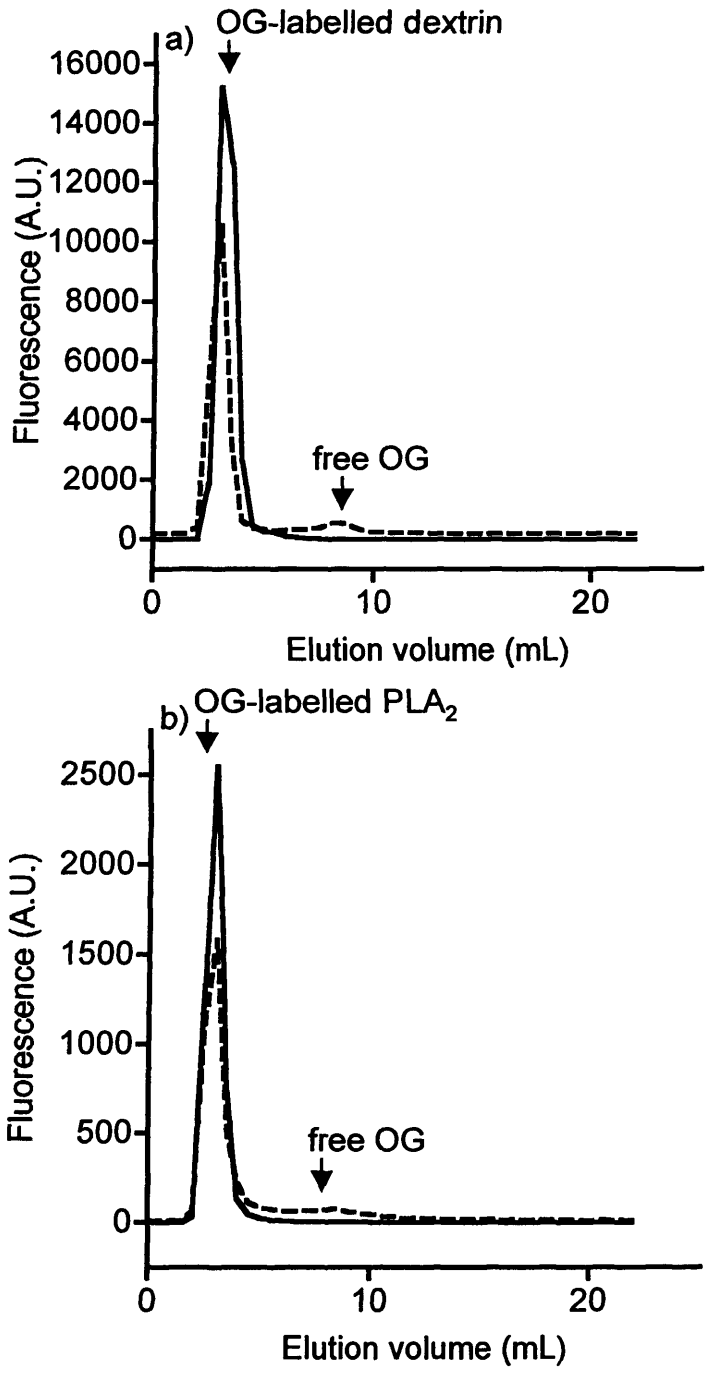

Figure 6.10 Evaluation of cell culture medium after incubation of MCF-7 cells with OG-labelled conjugates (1 h, 37 °C). Panels a-c show the PD-10 column elution profile of (a) OG-labelled dextrin, (b) OG-labelled PLA_2, and (c) OG-labelled dextrin-PLA_2 conjugate. PD-10 columns eluted with PBS. (Cont. overleaf)

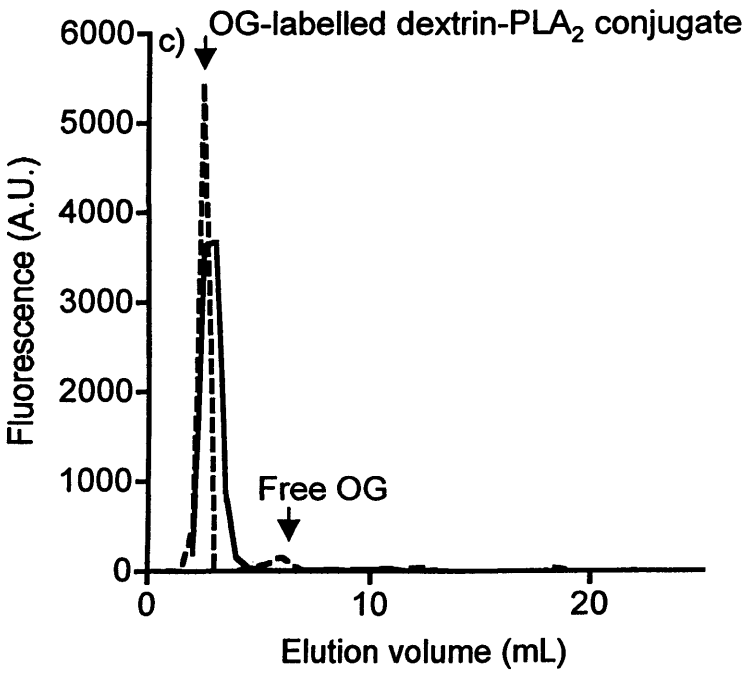

Figure 6.10 Evaluation of cell culture medium after incubation of MCF-7 cells with OG-labelled conjugates (1 h, 37 °C). (Cont. from overleaf)

Table 6.2 Summary of free OG released from OG-labelled conjugates during a 1 h incubation with MCF-7 cells.

Name	Before incubation (%)	After incubation (%)
Dextrin-OG	0.49	8.41
PLA_2-OG	11.3 (1st purification)	15.88
	0.83 (2nd purification)	
Dextrin-PLA_2-OG	1.51	9.36

showed the presence of a number of extra peaks following incubation with MCF-7 cells (Figure 6.11). These peaks corresponded to the elution volumes of free PLA_2, free OG, and some additional peaks probably corresponding to smaller breakdown products.

6.3.4 Confocal microscopy

In parallel experiments, OG-labelled dextrin, OG-labelled PLA_2 and OG-labelled dextrin-PLA_2 were incubated with MCF-7 cells and the subcellular localisation was visualised using fluorescence microscopy (N.B. all fluorescent images are also presented in an electronic format to aid visualisation and the CD can be found at the back of the thesis, in Appendix II).

When incubated with MCF-7 cells (Figure 6.12b), BSA-TR was not detectable within EEA1 positive early endocytic compartments. Not surprisingly, after the 16 h chase it was found exclusively within LAMP-1 positive LE/L compartments (Figure 6.12c). When cells were incubated with OG-labelled dextrin, after the 16 h chase clear vesicular labelling was seen in the perinuclear region and no apparent surface binding (Figure 6.12a). Moreover, the OG-labelled dextrin conjugate was exclusively co-localised to the BSA-TR containing vesicles. It was thus concluded that OG-labelled dextrin was also solely located within these LE/L structures.

When cells were incubated with OG-labelled PLA_2 (1 h pulse, 4 h chase at 37 °C) clear plasma membrane labelling was seen. There was negligible vesicular labelling at this shorter incubation time (Figure 6.13). OG-labelled dextrin-PLA_2 conjugate (1 h pulse, 4 h chase at 37 °C) also showed marked labelling of the plasma membrane, but in this case there was a small degree of vesicular labelling (Figure 6.14). Imaging of EEA1 and LAMP-1 positive structures in these cells showed marked changes in vesicle distribution (Figure 6.13 and 6.14). The staining was seen predominantly around the edge of those cells treated with OG-labelled PLA_2 and OG-labelled dextrin-PLA_2 conjugate. There was no co-localisation of EEA1 or LAMP-1 probes with OG-labelled conjugates in any instance.

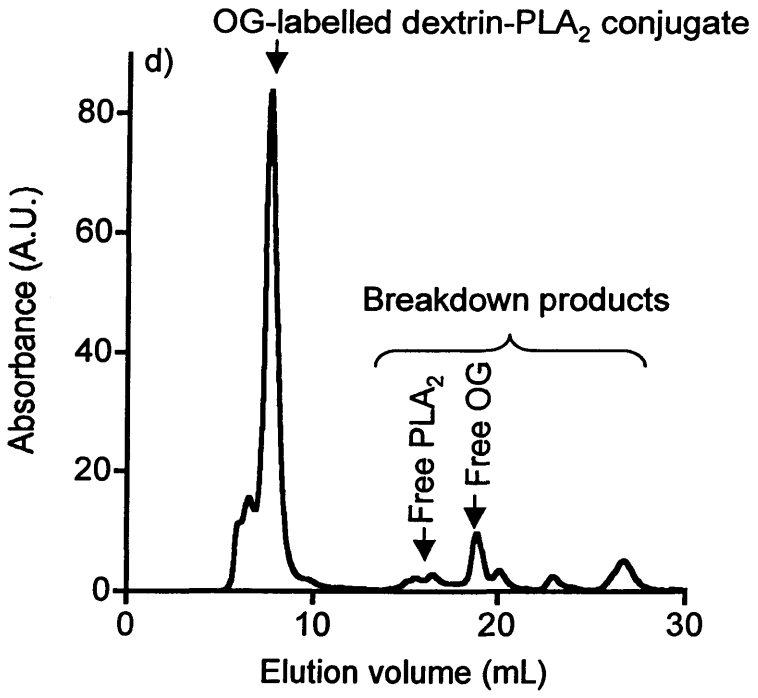

Figure 6.11 FPLC characterisation of cell culture medium after incubation of MCF-7 cells with OG-labelled conjugates (1 h, 37 °C). Figure shows FPLC analysis of OG-labelled dextrin-PLA_2 conjugate. FPLC column eluted with PBS. (Cont. overleaf)

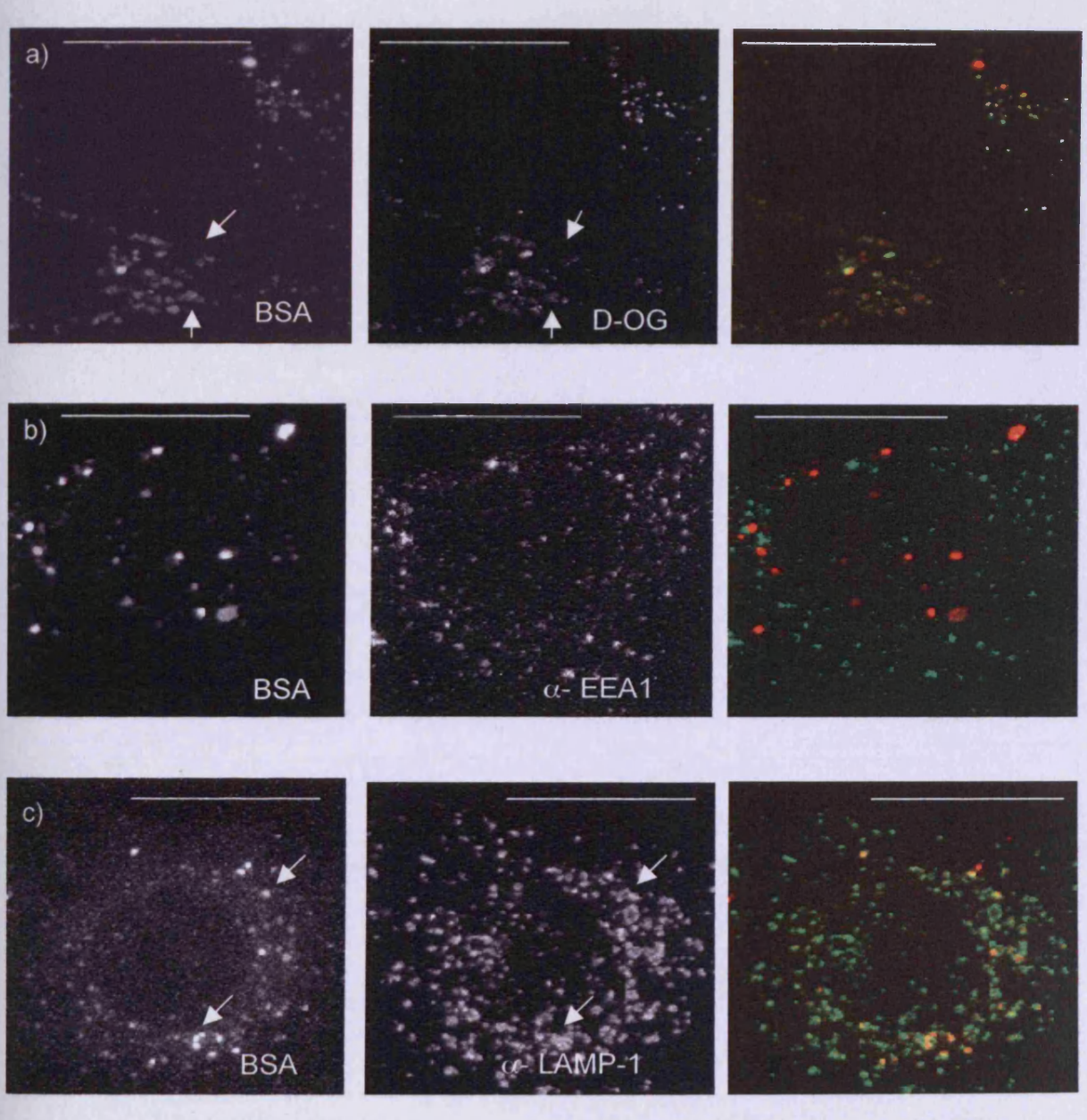

Figure 6.12 Representative confocal images of fixed MCF-7 cells showing cellular localisation of BSA-TR and OG-labelled dextrin. Cells were incubated with OG-labelled dextrin (4 h pulse and 16 h chase at 37 °C) and co-labelled with endosomal (EEA1) and lysosomal (LAMP-1) markers. Cells were seeded at a density of 1 x 10^4 cells/mL. Size bar = 10 μm. Arrows indicate co-localisation of probes.

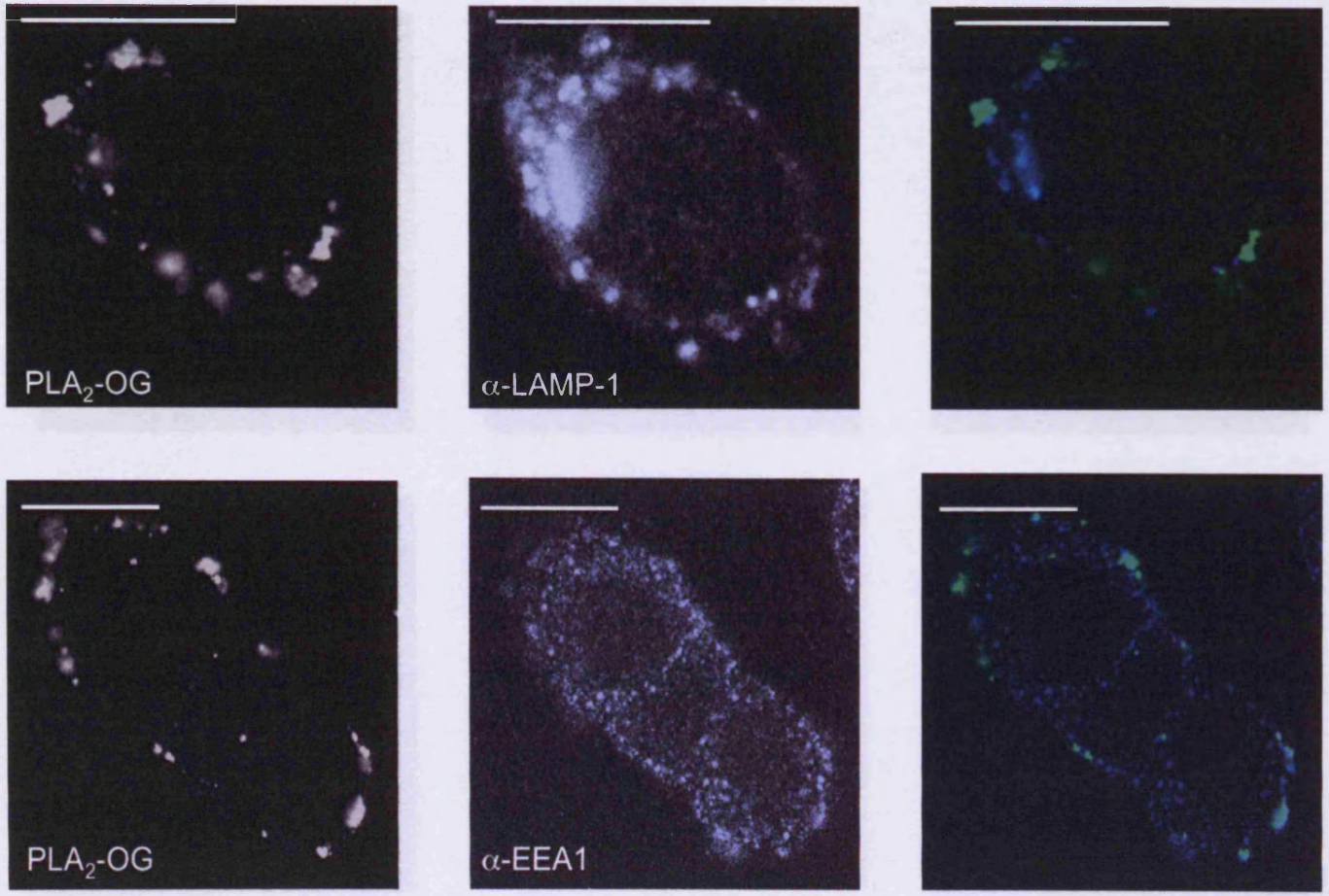

Figure 6.13 Representative confocal images of fixed MCF-7 cells showing cellular localisation of OG-labelled PLA_2. Cells were incubated with OG-labelled PLA_2 (1 h pulse and 4 h chase at 37 °C) and co-labelled with endosomal (EEA1) and lysosomal (LAMP-1) markers. Cells were seeded at a density of 1 x 10^4 cells/mL. Size bar = 10 μm.

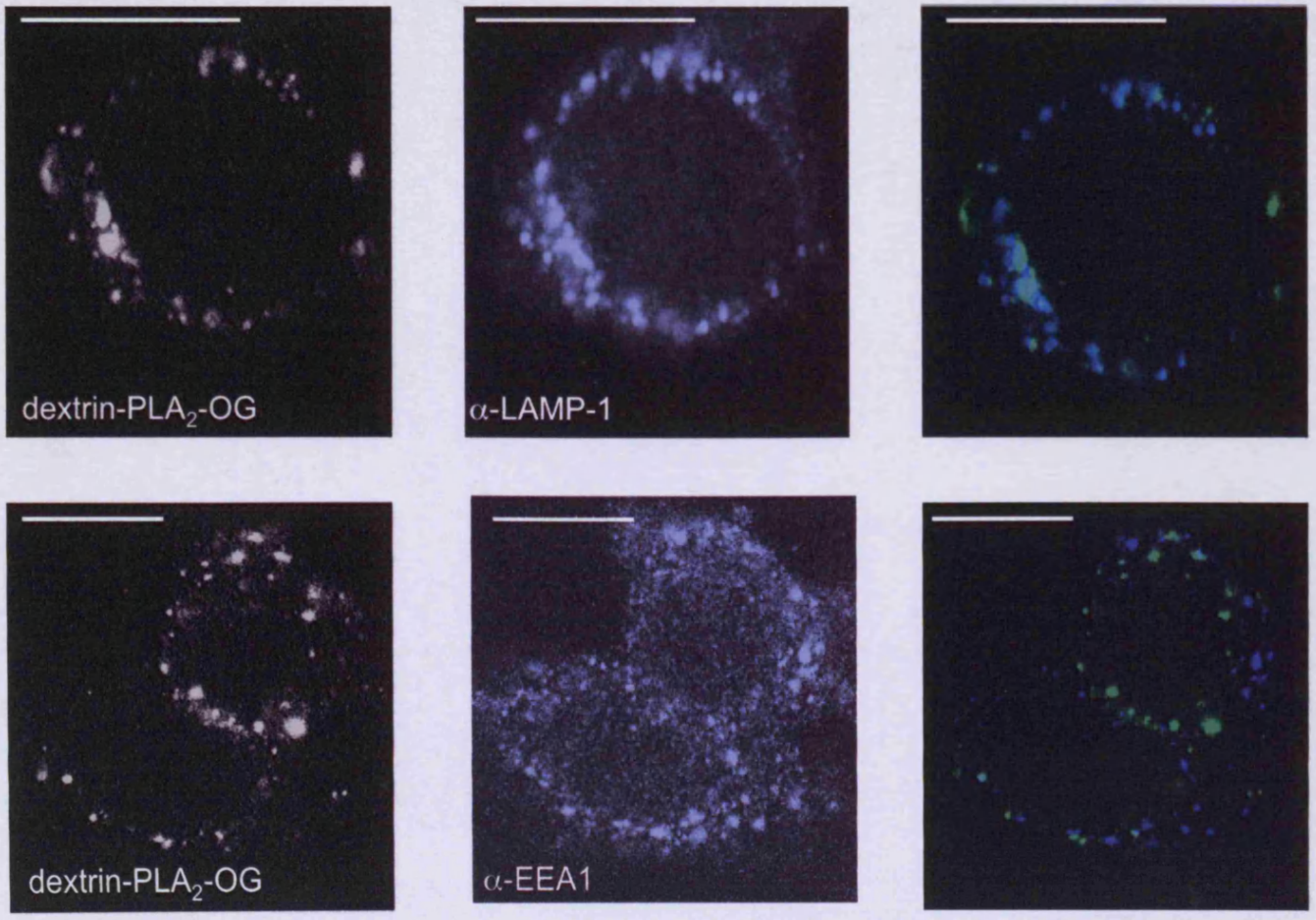

Figure 6.14 Representative confocal images of fixed MCF-7 cells showing cellular localisation of OG-labelled dextrin-PLA_2 conjugate. Cells were incubated with OG-labelled dextrin-PLA_2 conjugate (1 h pulse and 4 h chase at 37 °C) and co-labelled with endosomal (EEA1) and lysosomal (LAMP-1) markers. Cells were seeded at a density of 1 x 10^4 cells/mL. Size bar = 10 μm.

6.4 Discussion

Since neither dextrin nor PLA_2 have inherent fluorescence it was necessary to label them with a fluorescent probe to study cell uptake and intracellular localisation. It was hoped that these studies would give further insight into the site of action of the dextrin-PLA_2 conjugate, identify to what extent it was taken up by cells, and also define its intracellular fate, compared to unconjugated PLA_2 and dextrin.

Synthesis of the OG-labelled conjugates was performed by reacting OG with the carboxylic acid groups of succinoylated dextrin or PLA_2 (glutamic acid, aspartic acid residues and terminal COOH). A 5 h reaction time was chosen as TLC showed successful conjugation at this time. The conjugates prepared contained 3-5 μg OG/ mg conjugate and in all cases, purification by PD-10 column successfully removed free OG from reaction mixtures, producing conjugates with < 1.51 % free OG as was also seen in the OG-labelled conjugates synthesised here. Ideally, OG-labelled conjugates should contain minimal free OG. A number of other OG-labelled polymer conjugates have been described in the literature (Table 6.3). Despite using different reaction conditions to conjugate OG to architecturally different polymers, similar molar ratios were achieved with dextrin in these studies.

OG conjugation to the probes studied here showed no change in the fluorescent profile of OG. This was particularly important to verify since previous studies have shown that the fluorescence of doxorubicin was quenched after conjugation to HPMA copolymers and yields were different in conjugates containing more than one drug (Greco *et al*, 2007).

6.4.1 Cellular uptake of dextrin-PLA_2 conjugate

While low molecular weight drugs can easily enter cells by passive diffusion, macromolecules are usually excluded from this route. Uptake is therefore limited to the endocytic route. The studies presented here confirmed internalisation of OG-labelled dextrin, OG-labelled PLA_2 and OG-labelled dextrin-PLA_2 conjugate by MCF-7 cells. However, the pattern of cell-associated fluorescence differed among the conjugates. OG-labelled PLA_2 showed highest cell-associated fluorescence after

Table 6.3 Characteristics of some polymer-OG conjugates described in the literature.

Polymer	Reaction conditions	Molar ratio (OG/polymer)	Labelling efficiency (μg OG/ mg polymer)	Free OG (% total)	Reference
PEI	2 h, RT	NS	NS	NS	(Godbey, 1999)
G5 PAMAM dendrimer	3 h, RT, pH 8.5	4.0	68.2	NS	(Yoo and Juliano, 2000)
		1.75	30.1	NS	(Yoo and Juliano, 2000)
		0.8	13.8	NS	(Yoo and Juliano, 2000)
PEI (branched)	MeOH, pH 8.5,	0.80	16.4	0.6	(Seib *et al* 2007)
PEI (linear)	2h, RT	0.73	15.0	0.7	(Seib *et al*, 2007)
G2 PAMAM dendrimer		0.50	78.6	0.1	(Seib *et al*, 2007)
G3 PAMAM dendrimer		0.56	41.5	0.2	(Seib *et al*, 2007)
G4 PAMAM dendrimer		0.71	25.6	0.6	(Seib *et al*, 2007)
HPMA copolymer	DMSO, 16 h, RT	0.91	2.5	0.6	(Richardson *et al*, 2008)
mPEG-NH_2	$NaHCO_3$ buffer pH 9, 4 h, RT	0.04	4.2	2.9	(Richardson *et al*, 2008)
Hyaluronic acid	ddH_2O, pH 8, 20 h, RT	0.9	3.4	0.1	(Gilbert, 2007)
Dextrin	PBS buffer, pH 8 EDC/sulfo-NHS, 5 h, RT	0.51	4.96	0.03	(Richardson *et al*, 2008)

NS = not stated

1 h at both 37 °C and 4 °C, while OG-labelled dextrin and OG-labelled dextrin-PLA_2 conjugate showed much lower rates of internalisation or extracellular binding. As PLA_2 is known to act at the cell membrane it is not surprising that there was a high degree of extracellular binding for OG-labelled PLA_2. As the extracellular binding of OG-labelled dextrin-PLA_2 conjugate was so low, it would seem that dextrin conjugation has sterically masked the enzyme and reduced membrane binding. However, since the conjugate showed equivalent cytotoxicity to free PLA_2 after 72 h (Chapter 5) it is proposed that sufficient time for unmasking is required for full enzyme activity, and this is not achieved within the 1 h incubation used here.

In order to standardise the flow cytometry experiments, OG concentration was kept the same for all conjugates (1.5 μg/mL). However, it is worth bearing in mind that the concentration of dextrin and PLA_2 differed among the OG-labelled conjugates in order to keep OG concentration constant. Table 6.4 summarises the concentrations of OG components applied to cells for flow cytometry studies. Given that OG-labelled dextrin-PLA_2 conjugates contained 5.2 % protein, it is not surprising that PLA_2 concentration in this study was low. This difference could affect the cellular uptake and localisation of the conjugated PLA_2, compared to free enzyme, however it was felt that it was more important to standardise the OG content for these studies.

It was important to know if the probe used was stable during such cell culture experiments designed to study trafficking of the probes to confirm that internalisation was of the OG-conjugate, and not simply the free probe. Here, it was shown that some free OG was liberated from all the probes after a 1 h incubation with MCF-7 cells. This could have been due to enzymatic degradation of dextrin and PLA_2, or hydrolysis of the amide bond to OG. The amide bond formed between OG and dextrin and PLA_2 might be expected to be biologically stable (Banks and Paquette, 1995) but of course both dextrin and PLA_2 are potentially biodegradable. Seib *et al* (2007) also observed some OG liberation and they speculated that there may be a degree of reversible complexation between OG and the polymers.

Table 6.4 Comparison of the concentrations of OG, dextrin or PLA_2 applied to cells during the flow cytometry experiments.

Name	OG		Dextrin		PLA_2	
	μg/mL	mM	μg/mL	mM	μg/mL	mM
Dextrin-OG	1.5	0.0030	302	1.664	-	-
PLA_2-OG	1.5	0.0030	-	-	408	0.0282
Dextrin-PLA_2-OG	1.5	0.0030	451	2.485	24.8	0.0016

All OG-labelled conjugates showed evidence of internalisation, and a higher uptake was seen for OG-labelled PLA_2. While OG-labelled dextrin and OG-labelled dextrin-PLA_2 conjugate showed only 8-9 % free OG release over a 1 h incubation, the amount of OG released from OG-labelled PLA_2 was double in the same time frame. Still, the amount of free OG in these studies was not high and previous studies have shown that while cells can readily take up free fluorophore, this could be easily removed during normal cell washing and should not significantly affect uptake observations (Seib *et al*, 2007).

6.4.2 Cellular localisation of dextrin-PLA_2 conjugate

Visualisation of the subcellular localisation of OG-labelled dextrin uptake by confocal microscopy showed fluorescence in vesicular compartments which was consistent with an endocytic uptake and correlates with the internalisation seen with flow cytometry. Since cells were subjected to 4 h pulse and 16 h chase for the microscopy studies, it is not surprising that cellular uptake of OG-labelled dextrin appeared higher than seen in the flow cytometry experiments which were only conducted for 1 h.

It is also worth mentioning the different pulse-chase times used for confocal microscropy experiments. 4 h pulse with 16 h chase was first used for OG-labelled dextrin, however there were concerns that incubating cells with PLA_2 or dextrin-PLA_2 conjugate for this length of time could kill the cells. Richardson *et al* (2008) have shown that a 1 h pulse followed by a 4 h chase is sufficient time for trafficking to the lysosomes, therefore cellular localisation of the OG-labelled conjugates can still be compared. In the MTT assay, 55 % and 90 % viability was see when MCF-7 cells were incubated for 72 h with PLA_2 (408 μg/mL) and dextrin-PLA_2 conjugate (24.8 μg/mL), respectively.

It is often assumed that PLA_2 induces cell lysis by disruption of the cell membrane, however recent studies have shown it to be more complicated. Normally, after injury to the cell membrane, rapid resealing occurs with little loss of intracellular contents. However, studies undertaken by Steinhardt *et al* (1994) revealed that botulinum neurotoxins A and B are capable of blocking membrane

resealing. Given that PLA_2 acts by hydrolysing phospholipids, this effect could also result in inhibition of membrane repair.

When cells were incubated with OG-labelled PLA_2 and OG-labelled dextrin-PLA_2 conjugate, migration of endosomal and lysosomal vesicles towards the plasma membrane was observed (Figure 6.13 and 6.14). Direction of secretory vesicles to the cell membrane is well documented as a means of repairing damage to cell membranes (Reddy *et al*, 2001). Reddy *et al* (2001) showed that after cells were subjected to wounding by scratching the cell surface with a single-edge surgical blade, plasma membrane repair was mediated by Ca^{2+} regulated vesicle trafficking to the membrane. The authors hypothesised that fusion of lysosomes with the plasma membrane was triggered by elevated intracellular Ca^{2+} concentrations. Further studies by Jaiswal *et al* (2002) observed that many organelles, including the endoplasmic reticulum, post-Golgi vesicles, early endosomes, late endosomes, and lysosomes, were located within 100 nm of the plasma membrane after incubation with Ca^{2+} and they suggested that this could also be implicated in repair of membrane damage.

Similarly, transmission electron microscopy (TEM) and scanning electron microscopy (SEM) have also been used to visualise the effect of PLA_2 on OVCAR-3 cell membranes (Newman *et al*, 1996). SEM studies demonstrated cell separation, membrane damage and blebbing after 3 h treatment with PLA_2, while longer periods of exposure revealed 'holes' in the membrane associated with severe disruption of the cell membrane. TEM also showed the formation of small lipid-containing vesicles inside the cells, which increased in number as PLA_2 exposure time was extended.

The evidence here supports the hypothesis that PLA_2 and dextrin-PLA_2 conjugate does indeed act at the level of the cell membrane causing damage by hydrolysis of phospholipids. This agrees with previous studies where cells that were incubated in the presence of 20 mM ammonium chloride or 0.5 mM quinacrine, (inhibitors of receptor-mediated endocytosis), did not appear to internalise PLA_2 (Alicea, 1998). Alicea (1998) also observed release of lactase dehydrogenase (LDH) into the medium, an increase in concentration of free palmitic acid in cell membranes

and a concentration-dependant increased staining with trypan blue, all of which are consistent with membrane damage.

Considerations for confocal microscopy interpretation

A number of technical issues can limit the usefulness of confocal microscopy. These include limited optical resolution, the small number of cells that can be viewed relative to the entire population, artefacts produced during fixation, and incorrect interpretation of the data (North, 2006; Pearson, 2007). In these studies, OG was selected as the fluorescent probe to reduce the likelihood of artefacts, since it is less susceptible to photobleaching and both concentration- and pH-dependent fluorescence quenching. Careful loading of OG also ensured that cellular uptake and subsequent trafficking was due solely to dextrin, PLA_2 or dextrin-PLA_2 conjugate, and not simply probe-driven effects. Here, the intracellular localisation of OG-labelled conjugates was observed relative to both endocytosed physiological markers and indirect immuno-fluorescent labelling, in an effort to reduce making incorrect assumptions as to the compartments occupied by OG-labelled conjugates.

6.5 Conclusions

Fluorescent probes were synthesised using OG, with free OG content of < 1.51 % of total OG content after purification by PD-10 column and specific activity was similar (specific activity = 3.15 – 4.96 μg OG/ mg OG-labelled conjugate) for all OG-conjugates synthesised. The fluorescence characteristics of free and bound OG and OG-labelled conjugates were similar.

It was concluded that PLA_2, and OG-labelled dextrin-PLA_2 conjugate to a lesser extent, interact with cells extracellularly, resulting in the migration of early and late endosomal vesicles to the cell periphery as a means of repairing membrane damage. It was also noted that dextrin conjugation reduced extracellular binding of PLA_2.

Chapter Seven

Investigating Dextrin-PLA_2 Conjugates as a Trigger for Polymer Enzyme Liposome Therapy (PELT)

7.1 Introduction

The evaluation of dextrin-PLA_2 conjugate in the preceding chapters has demonstrated its potential as a novel therapeutic agent against cancer in it's own right. However, there is also the possibility of using dextrin-PLA_2 conjugates as a trigger for the release of drug encapsulated within liposomes. This concept has previously been named 'Polymer Enzyme Liposome Therapy' (PELT) (Duncan *et al*, 2001). The concept of PELT has been previously introduced in detail in Chapter 1 (section 1.5.2). Previous preliminary experiments have demonstrated proof of concept using HPMA copolymer-PLC with Doxil® and DaunoXome® (Satchi-Fainaro and Duncan, unpublished). Therefore the aim of this study was to establish whether a dextrin-PLA_2 conjugate would also be capable of accelerating the rate of drug release from liposomes.

7.1.1 Recent progress in controlling liposomal drug release

Despite the many advantages of clinically used liposomal anticancer drugs, i.e. prolonging drug circulation time, and tumour targeting by EPR (reviewed in Torchilin, 2005), there remain some drawbacks to their use (described more fully in section 1.5.2). A major limitation is the relatively slow release of encapsulated drug at the target site. Therefore, research has been undertaken to try and enhance the drug release rate. Examples of currently used liposome formulations and the novel methods being explored to enhance active and tumour-specific drug release are shown in Figure 7.1.

Antibody-PLC conjugates

One approach has been the use of antibody-PLC conjugates to try and improve the release of daunorubicin from DaunoXome® (Carter *et al*, 1998) (Figure 7.1d). This two-step method uses IV administration of an anti-carcinoembryonic antigen (CEA)/ EGFR antibody-PLC conjugate. Time is allowed for clearance and tumour targeting of the immunoconjugates, before the liposome-encapsulated daunorubicin is administered. It is postulated that the liposomes are specifically lysed in the tumour interstitium by the pre-targeted PLC, resulting in localised release of cytotoxic drug in the tumour. Results from fluorescence studies *in vitro* revealed an

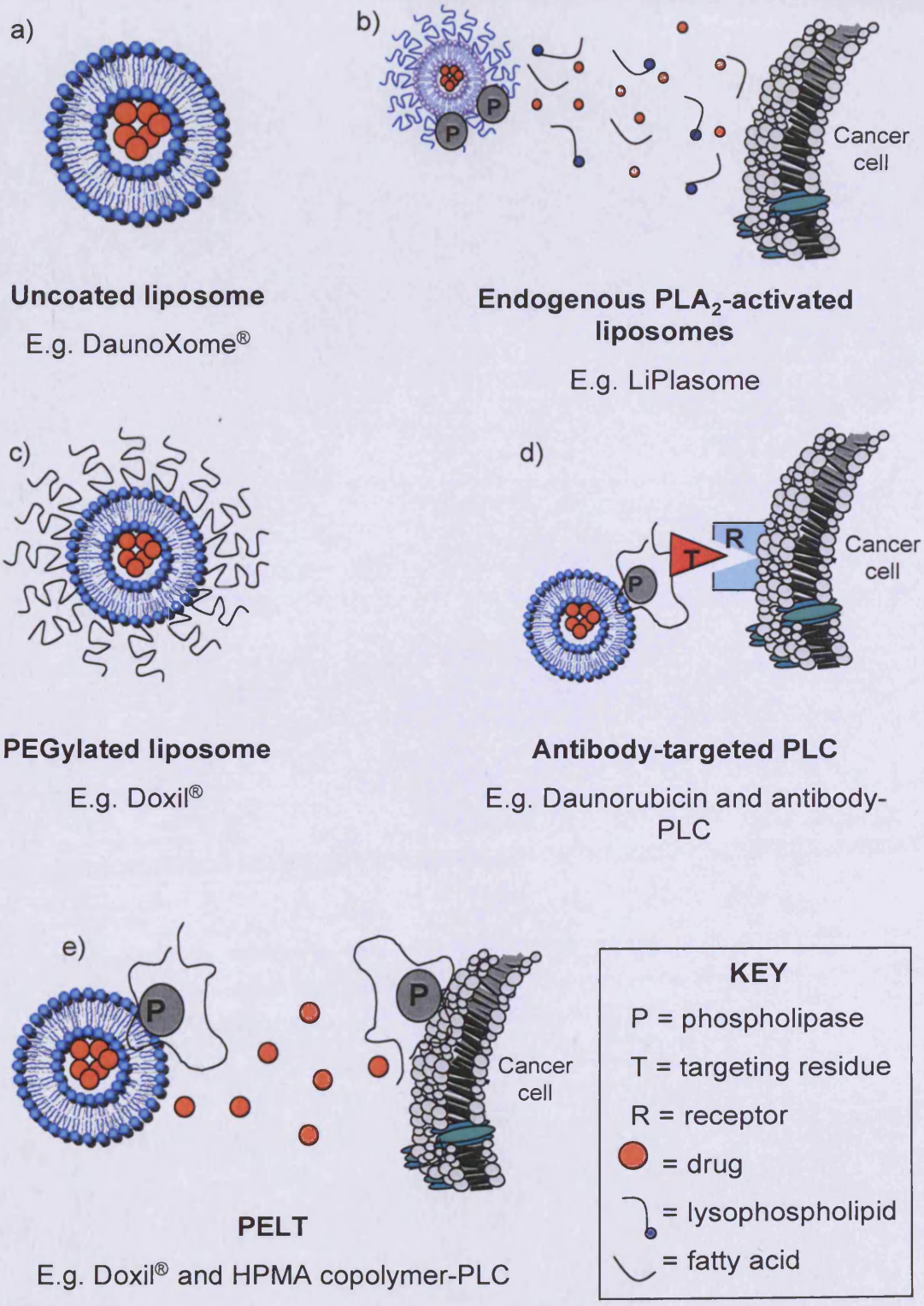

Figure 7.1 Schematics of liposomal formulations in clinical use and in development.

increase in free daunorubicin in the medium of HeLa cells previously treated with anti-EGFR antibody-PLC conjugates. This group also looked at the effect of anti-EGFR antibody-PLC conjugates and DaunoXome® on A431 tumour xenografts in mice. They found that 50 days after the two-step treatment was administered, tumour growth was inhibited in 5 out of 6 mice compared with no effect in the 13 control mice treated with DaunoXome® alone or the anti-EGFR antibody (without PLC) and DaunoXome® (Carter *et al*, 1998).

LiPlasomes

Many solid tumours appear have a high concentration of $sPLA_2$ in the tumour interstitium, with $sPLA_2$ concentrations in the region of 9 to 188 ng/mL (Cupillard *et al*, 1999). Moreover, $sPLA_2$ concentration is said to increase with tumour grade (Graff *et al*, 2001; Jiang *et al*, 2002). LiPlasomes, a form of liposomal drug carrier, which exploit the high concentration of intratumoural PLA_2, have been developed to capitalise on this observation (Figure 7.1c). These novel lipidic systems are based on PEG-coated liposomes, and they contain phospholipids specially designed to be hydrolysed by the $sPLA_2$ found in cancer tissues. It is postulated that this results in a site-specific release of encapsulated drug. Moreover, the phospholipids used to encapsulate the drug are 'permeability proenhancer lipids' that are converted to 'permeability enhancers' after enzyme hydrolysis, which can further enhance drug diffusion across target cell membranes (Andresen *et al*, 2004a).

In vitro experiments have been undertaken with Liplasomes encapsulating doxorubicin, which show release of drug within 2-4 h in the presence of $sPLA_2$-secreting colon cancer cells. Greater cytotoxicity was seen than for free drug. Doxil® alone showed only slow doxorubicin release and significantly less cytotoxicity after 6 h treatment (Andresen *et al*, 2004b). Further *in vitro* studies using HT29 cells compared LiPlasome-encapsulated cisplatin with a clinically tested Stealth liposomal formulation. In this case the LiPlasome formulation had an IC_{50} value of 10 μM (ten-fold lower than for free cisplatin) while the stealth liposomal platinate had an IC_{50} value that was > 1000 μM (24 h incubation) (Andresen *et al*, 2004c).

The *in vitro* experiments using LiPlasomes have mainly used a group II PLA_2

extracted from snake venom (*Agkistrodon piscivorus piscivorus)*. It is composed of a 121 amino acids, eight of which are lysine residues (Han *et al*, 1997). In contrast, the human group IIA $sPLA_2$ found endogenously in tumour tissues contains 124 amino acids, six of which are lysine residues. Human group IIA $sPLA_2$'s expression and secretion is induced by pro-inflammatory agents (e.g. IL-2, TNF and particularly IL-6) and is inhibited by glucocorticoids (Diez *et al*, 1992). Studies by Cupillard *et al* (1999) showed that mouse group IIA $sPLA_2$s have a high affinity to the mouse M-type membrane receptor (1-10 nM range), but much lower affinity to receptors from other animal species, including human.

These observations could mean that the LiPlasome may not be degraded in the same way *in vivo* as it has *in vitro* due to the use of snake venom PLA_2 from a different species to the cells. Furthermore, studies comparing the activity of bee venom and bovine pancreas PLA_2 described in section 4.3.1 showed a significant difference in *in vitro* cytotoxicity towards MCF-7 cells, with the mammalian PLA_2 being far less toxic. This is a potential limitation for LiPlasomes, which rely on human, intratumoural PLA_2 for activation.

7.1.2 Choice of liposomal drug formulation: DaunoXome®

DaunoXome® was selected here as the model liposomal drug formulation. Doxil® and Myocet® have been previously described in detail in section 1.5.2 and Table 7.1 lists the characteristics of some liposomal drug formulations on the market.

DaunoXome® is commonly used as a first-line chemotherapy agent for advanced AIDS-related Kaposi's sarcoma (Rosenthal *et al*, 2002). It is usually administered IV over 60 min at a dose of 40 mg/m^2, with doses repeated every two weeks. DaunoXome® contains daunorubicin citrate (Figure 7.2) encapsulated in small unilamellar vesicles (SUV) dispersed in an aqueous medium containing sucrose, glycine and calcium chloride dihydrate (2 mg/mL, pH 4.9-6.0). DaunoXome® was selected since the liposomes are not PEGylated (unlike Doxil®). The PEG coat could sterically hinder access of the dextrin-PLA_2 conjugate, decreasing phospholipid hydrolysis. Furthermore, studies on the body distribution of Doxil® suggests that drug clearance occurs in two phases, with a relatively short first phase ($t_{1/2}$

Table 7.1 Examples of liposomal drugs currently on the market.

Product name *Drug*	Indication	Phospholipids (Drug/lipid ratio)	Liposome type	Particle diameter
Membrane incorporated drug				
Abelcet®	Invasive fungal infections in	DMPC: DMPG 7:3	MLV	< 5 μm
Amphotericin B	immuno-compromised patients	(1:1 molar ratio)		
AmBisome®	Visceral leishmaniasis	HSPC 213 mg; DSPG 84 mg;	SUV	< 100 nm
Amphotericin B	Cryptococcal meningitis in HIV-infected patients	cholesterol 52 mg; α-tocopherol 0.64 mg		
	Aspergillus, Candida and/or Cryptococcus infections	(1:6 w/w ratio)		
Visudyne™	Age-related macular	DMPC: EPG	SUV	< 100 nm
Verteporfin	degeneration (AMD)	(1: 7.5-15)		
Encapsulated drug				
DaunoXome®	Advanced HIV-related Kaposi's	DSPC: cholesterol 2:1	SUV	~ 45 nm
Daunorubicin	Sarcoma	(18.7:1 w/w ratio)		
Doxil®	Ovarian Cancer	mPEG-DSPE: HSPE:	LUV	100 nm
Doxorubicin		cholesterol 1: 3: 1		
		(1:6 w/w ratio)		
Myocet®	Advanced HIV-related Kaposi's	EPC: cholesterol 1:1	OLV	180 nm
Doxorubicin	Sarcoma, Ovarian cancer, Advanced breast Cancer	(1:4 molar ratio)		

DMPC- dimyristoyl phosphatidylcholine; DMPG- dimyristoyl phosphatidylglycerol; HSPC- hydrogenated soy phosphatidylcholine; DSPG-distearoyl phosphatidylglycerol; EPG- egg phosphatidylglycerol; mPEG-DSPE- N-(carbonyl-methoxypolyethylene glycol 2000)-1,2-distearoyl-sn-glycero-3-phosphoethanolamine sodium salt; EPC- egg phosphatidylcholine; MLV- multilamellar vesicle; SUV- small unilamellar vesicle ; LUV- large unilamellar vesicle ; OLV-Oligolamellar vesicle

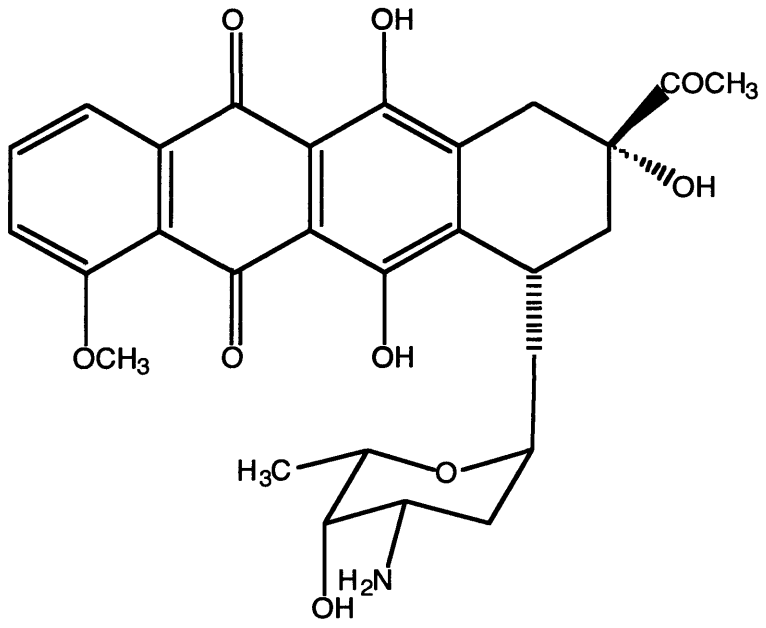

Figure 7.2 Chemical structure of daunorubicin, MWW = 563.99.

≈ 5 h) and a prolonged second phase ($t_{1/2}$ = 45 h) (Janknegt, 1996). This biphasic drug clearance is not seen with DaunoXome®, which has a $t_{1/2}$ of ~ 5 h (Bellott *et al*, 2001), and so it was decided that DaunoXome® would give a simpler drug release profile for these initial proof of concept studies than a PEGylated formulation.

When administered as free drug, daunorubicin has a $t_{1/2}$ of 0.77 h. Its use is associated with severe acute toxicities including myelosuppression, alopecia, necrosis of tissue following extravasation and cumulative dose-limiting cardiotoxicity (maximum tolerated cumulative dose (MTD) = 550 mg/m^2) (reviewed in Hortobagyi, 1997). Moreover, since daunorubicin is inherently fluorescent, monitoring drug release from the liposomes can be undertaken simply using a fluorescent platereader. Daunorubicin produces a three-peak fluorescence emission spectra (520 – 700 nm) corresponding to its triple helical complexes. It is well known that the shape of the fluorescence spectrum of daunorubicin is markedly changed by factors such as hydrophobicity of the solvent and intercalating with DNA (Goldman *et al*, 1978; Laigle *et al*, 1996).

7.1.3 PLA_2 as a trigger for PELT

Although proof of concept studies for PELT used PLC to rupture liposomes, it was interesting to determine whether PLA_2 could also be used. A number of studies have shown that $sPLA_2$ can degrade liposomes (including bee venom PLA_2) (Ghomashchi *et al*, 1998; Jorgensen *et al*, 1999a) and also it was shown here that dextrin-PLA_2 conjugate retained activity in the cytotoxicity assays and the egg yolk emulsion assay (Chapters 4 and 5). An additional benefit of using a dextrin-PLA_2 conjugate as a component of PELT would be the option to combine its individual activity at the cell surface with improved liposomal action (Figure 7.1e).

Moreover, while PLC and HPMA copolymer have a similar molecular weight (~ 30,000 g/mol) (HPMA copolymer was used as a polymer carrier for PLC (Satchi-Fanairo and Duncan, unpublished)) the dextrin used here (MW ~ 51,000 g/mol) is approximately 3 times larger than PLA_2. This should allow greater protein masking as well as a better pharmacokinetic profile able to promote better tumour targeting by the EPR effect. As dextrin-PLA_2 conjugate can be activated by α-amylase (the

PUMPT concept (Chapter 4) this might enhance the slow unveiling of PLA_2 to be able to release liposomally-entrapped drug.

7.1.4 Aims of these studies

To summarise, the aims of this study were:

- To evaluate the ability of free PLA_2 and the dextrin-PLA_2 conjugate to trigger the release of daunorubicin from DaunoXome®.
- To assess the effect of incubation of DaunoXome® with free PLA_2 and dextrin-PLA_2 conjugate on liposome size by photon correlation spectroscopy (PCS).
- To test the cytotoxicity of daunorubicin and DaunoXome® incubated with free PLA_2 and the dextrin-PLA_2 conjugate in MCF-7 cells.

7.2 Methods

Succinoylated dextrin was prepared as described in section 3.2.2. EFdex5 (20.9 mol % succinoylation) was used for these studies. Dextrin-PLA_2 conjugates were synthesised and characterised according to methods described in Chapter 4. DexPLA7 (MW ~ 195,000 g/mol; PLA_2 content 9.4 wt. %) was used in these studies.

7.2.1 Fluorescence properties of free daunorubicin and DaunoXome®- effect of Triton X-100

First, the fluorescence emission spectrum of DaunoXome® was determined in PBS (pH 7.6) and a Triton X-100 solution (1 % v/v) (to solubilise liposomes and release daunorubicin). DaunoXome® was diluted in PBS (20 μg/mL), placed in a polystyrene cuvette (3 mL), and the emission was measured in the interval 500-700 nm with the excitation wavelength set at λ_{ex} = 485 nm. For comparison, DaunoXome®, diluted in Triton X-100 solution (20 μg/mL in 1 % v/v Triton X-100 solution), was monitored for fluorescence in the same way.

The effect of Triton X-100 concentration on the fluorescence of free daunorubicin was studied in various concentrations of Triton X-100. A stock solution of Triton X-100 was prepared in ddH_2O (1 % v/v) and serial dilutions were made to

produce a range of concentrations (0 - 1 % v/v). A stock solution of daunorubicin (1 mg/mL) was then diluted using Triton X-100 solutions to a final concentration of 20 μg/mL. Daunorubicin + Triton X-100 solutions (3 mL) were transferred to a polystyrene cuvette and their fluorescence emission was measured in the interval 500-700 nm and the excitation wavelength was set at λ_{ex} = 485 nm.

7.2.2 Stability testing of liposomes

PCS was used to measure mean diameter and polydispersity of DaunoXome® following incubation with dextrin-PLA_2 conjugate, PLA_2, Triton X-100 and in PBS. DaunoXome® (2 mg/mL) was diluted fresh on the day of experiment to 1:100 in PBS (pH 7.6) and stored at 4 °C prior to use. Dextrin-PLA_2 conjugate and PLA_2 were dissolved in PBS (pH 7.6, 100 μg/mL) and equilibrated at 37 °C. DaunoXome® solution (1 mL) was added to a polystyrene cuvette and allowed to equilibrate to 37 °C in the PCS machine (30 min). Dextrin-PLA_2 conjugate, PLA_2 or Triton X-100 (2 %) solution (1 mL) was added immediately before initiating the first measurement. The stability of the liposomes was followed for 3 h at 37 °C (n = 3). Data is presented as mean liposome diameter over 3 h.

7.2.3 Daunorubicin release from DaunoXome® in the presence of PLA_2 and dextrin-PLA_2 conjugate

DaunoXome® (2 mg/mL) was diluted fresh on the day of experiment (1:100) in PBS (pH 7.6) and was always stored at 4 °C between experiments on the day of use. Then PLA_2 or dextrin-PLA_2 conjugate (100 μg/mL PLA_2 eq.; final experiment concentration of 50 μg/mL) (100 μL) was added to each well of a black 96-well microfluor plate and the plate was incubated at 37 °C for 30 min prior to starting the experiment to preserve enzyme activity. Triton X-100 (2 % v/v; final experiment concentration of 1 % v/v) was used to give 100 % drug release value while PBS was used as a negative control.

A countdown of 60 min was started upon addition of 100 μL of DaunoXome® solution to the first column (6 replicates) and the plate incubated at 37 °C to ensure PLA_2 activity was preserved. Subsequently, DaunoXome® solution was added at 50, 40, 30, 20, 10, 5 and 0 min time points. Fluorescence was measured using a

fluorescent plate reader ((λ_{ex} = 485 nm and λ_{em} = 520 nm) and results presented as percentage of 100 % drug release by Triton X-100 (corrected for background fluorescence of intact DaunoXome®).

7.2.4 Unmasking of dextrin-PLA_2 conjugates by incubation with α-amylase

To study the effects of α-amylase on the ability of the dextrin-PLA_2 conjugates to release daunorubicin from DaunoXome®, dextrin-PLA_2 conjugates (0.5 mg/mL) were first incubated with α-amylase (2 mg/mL, 200 SU/mL) for 16 h at 37 °C in Tris buffer (1.5 mL, pH 8.2). The release of daunorubicin from DaunoXome® was then followed as described in section 7.2.3.

7.2.5 Cytotoxicity assessment in MCF-7 cells

For determination of cytotoxicity against MCF-7 treatments were tested by MTT assay (section 2.4.7.5) using media supplemented as detailed in below.

To compare the cytotoxicity of daunorubicin and DaunoXome®, complete media was supplemented with a range of concentrations of daunorubicin or DaunoXome®.

To study the effect of PLA_2 or dextrin-PLA_2 conjugate on the cytotoxicity of daunorubicin or DaunoXome®, complete media was used. A PLA_2 or dextrin-PLA_2 conjugate concentration of 50 μg/mL PLA_2 eq. was used and the daunorubicin or DaunoXome® concentration varied.

7.3 Results

7.3.1 Fluorescence properties of free daunorubicin and DaunoXome®- effect of Triton X-100

The fluorescence emission spectra of daunorubicin exhibited peaks at 560, 590 and 620 nm. When the liposomes were incubated with Triton X-100, fluorescence was noticeably increased. The fluorescence of DaunoXome® in PBS was ~ 12-13 times lower than when they were incubated in the presence of Triton X-100 (Figure 7.3).

Overall, the general shape of the fluorescence emission spectrum of free daunorubicin was unchanged by the addition of Triton X-100, up to 1 % v/v and

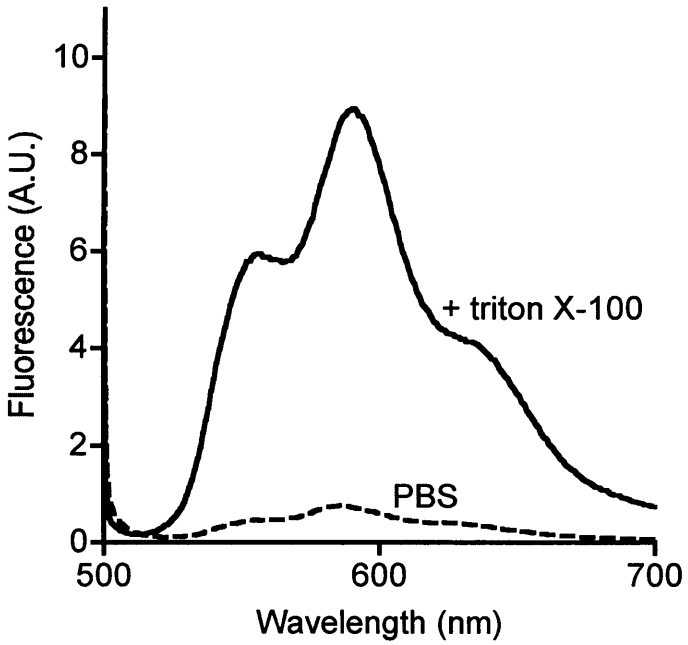

Figure 7.3 Fluorescence emission spectra of DaunoXome® before and after release of entrapped daunorubicin using Triton X-100. DaunoXome® (20 μg/mL) was suspended in PBS or Triton X-100 (1 % v/v) solution.

there was no obvious fluorescence quenching (Figure 7.4).

7.3.2 Stability testing of DaunoXome®

DaunoXome® showed a classical unimodal distribution of size (Figure 7.5a). The mean diameter was 49.8 nm and this remained the same over a 3 h incubation period (Figure 7.5b). When Triton X-100 was added the vesicle diameter dropped rapidly to < 20 nm within 1 min. In contrast, when DaunoXome® was incubated with free PLA_2 the liposomes appeared to get larger over time, reaching a maximum diameter of ~ 120 nm after 3 h. When liposomes were incubated with the dextrin-PLA_2 conjugate, the mean diameter remained unchanged over the course of the 3 h experiment. However, when the dextrin-PLA_2 conjugate was unmasked using α-amylase, a slight increase in size of the liposomes was seen (~ 60 nm).

7.3.3 Daunorubicin release from DaunoXome®

When DaunoXome® was incubated with various concentrations of native PLA_2 complete release of daunorubicin was achieved after 1 h incubation with 50 and 100 μg/mL PLA_2 (Figure 7.6). Incubation of DaunoXome® with 25 μg/mL achieved only partial drug release, which appeared to plateau at ~ 60 %. As expected, Triton X-100 caused immediate release of 100 % daunorubicin, while PBS caused < 5 % daunorubicin release during the 1 h incubation.

A concentration of 50 μg/mL PLA_2 eq. was subsequently selected for assessing the drug release from DaunoXome® by the dextrin-PLA_2 conjugate. Dextrin conjugation reduced daunorubicin release by PLA_2 to ~ 20 % of the free PLA_2 level (Figure 7.7) Addition of α-amylase led to a faster initial rate of drug release, however free daunorubicin detected after 1 h was statistically equal to that of masked dextrin-PLA_2 conjugate.

7.3.4 Cytotoxicity of DaunoXome® in MCF-7 cells

First, the cytotoxiticity of free daunorubicin towards MCF-7 cells was compared to that of DaunoXome® (Figure 7.8). The results showed very similar effects on cell viability, such that free drug had an IC_{50} of 125.0 ± 35 μg/mL, and DaunoXome® had an IC_{50} value of 83.6 ± 10.7 μg/mL. These results were not significantly different.

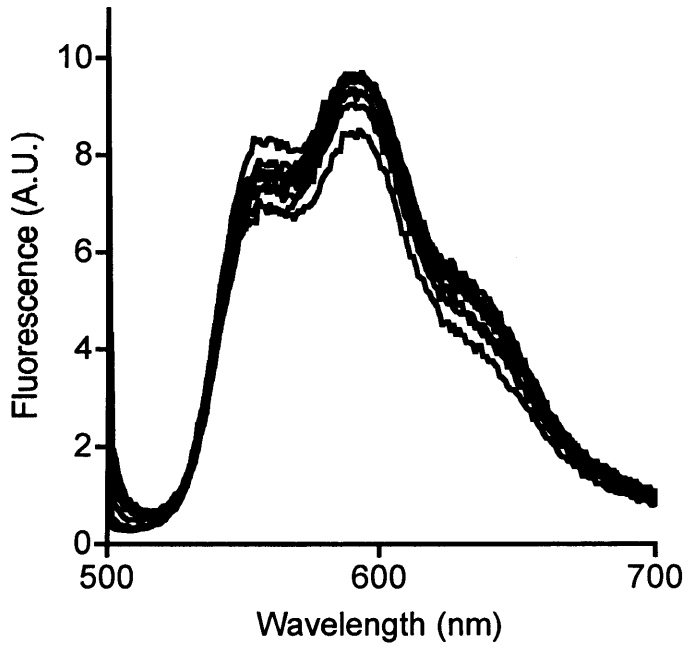

Figure 7.4 Fluorescence emission spectra of Daunorubicin in varying concentrations of Triton X-100. Daunorubicin (20 μg/mL) was suspended in Triton X-100 (0-1 % v/v) solution.

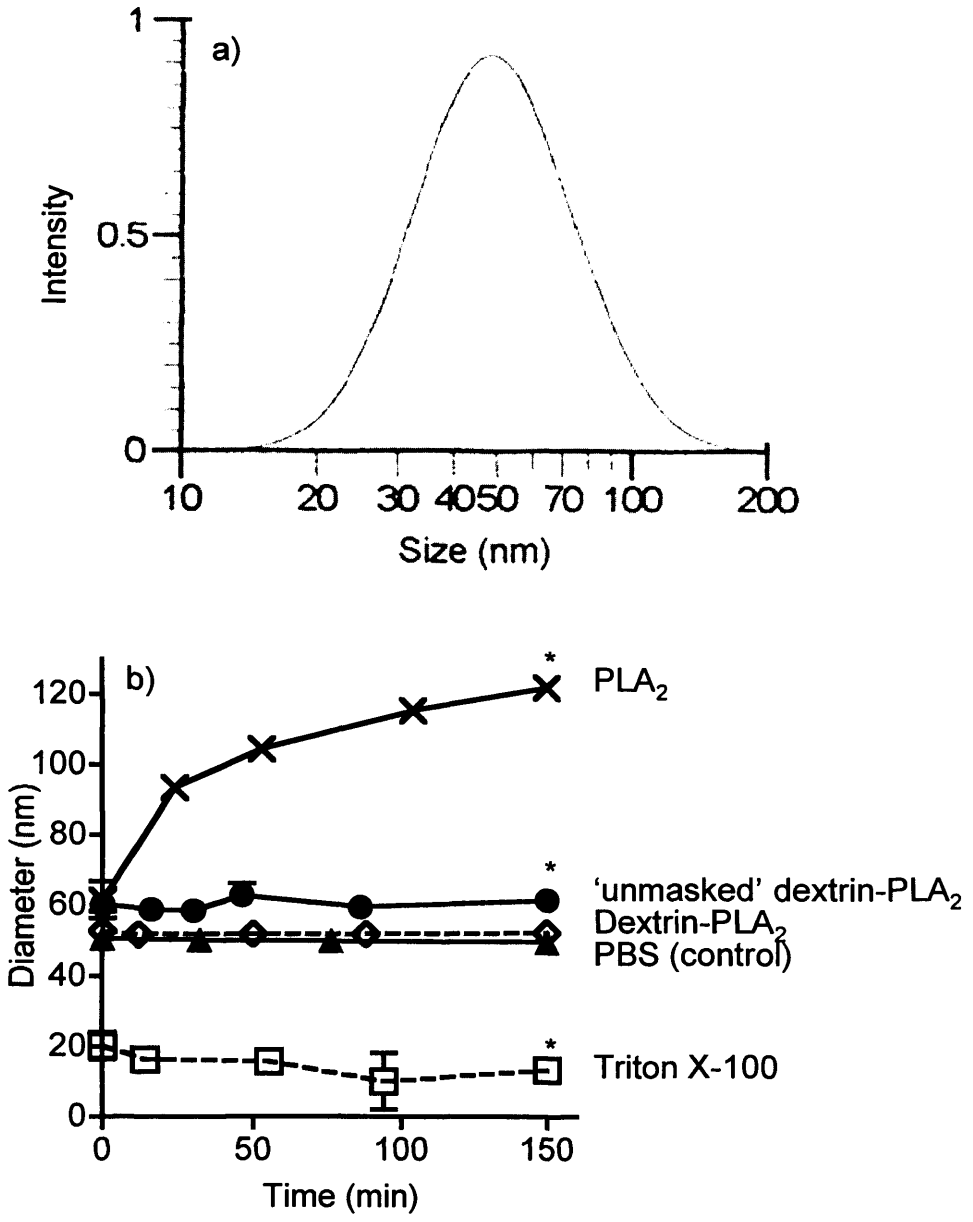

Figure 7.5 Measurements of liposome diameter for stability testing of DaunoXome® +/- PLA_2 and dextrin-PLA_2 conjugate (50 μg/mL PLA_2 eq.) over 3 h. Panel (a) shows a typical unimodal calibration curve of DaunoXome® in PBS. Panel (b) shows variation over time of DaunoXome® diameter. Data represents diameter (nm) ± SD, (n = 6; except DaunoXome® n =3). Where error bars are invisible they are within size of data points. * indicates significance compared to PBS control, where $p<0.05$ (ANOVA and Bonferroni *post hoc* test).

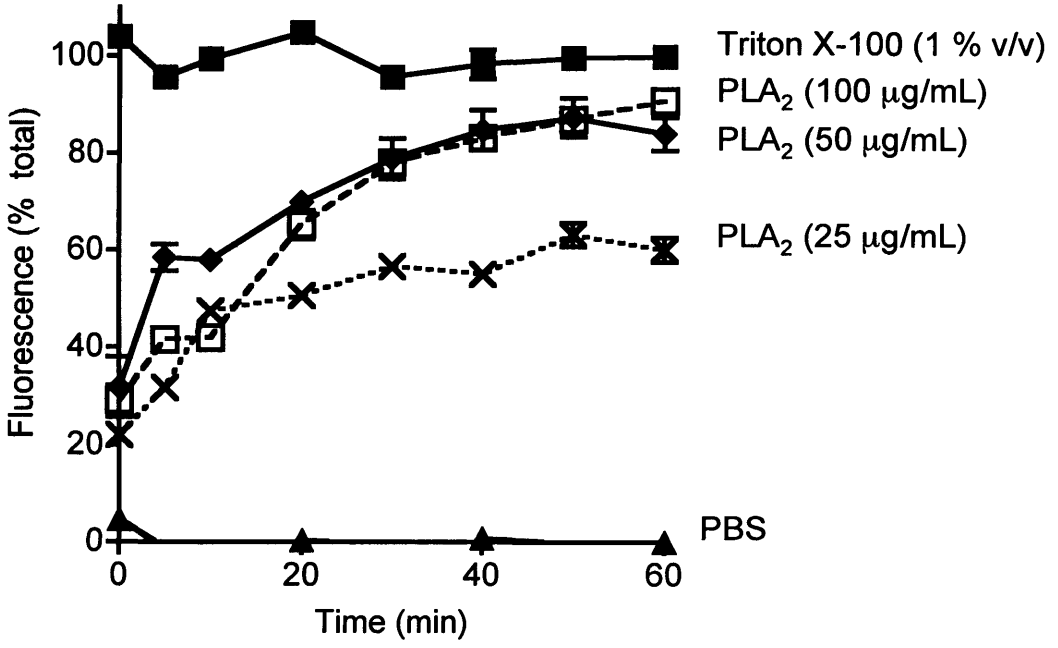

Figure 7.6 Release of daunorubicin from DaunoXome® in the presence of different PLA_2 concentrations over 60 min. DaunoXome® in the absence of enzyme is included as a control. Triton X-100 (1 % v/v) was used for 100 % drug release. Data represents % fluorescence compared to Triton X-100 (1 % v/v) solution ± SEM, (n = 6). Where error bars are invisible they are within size of data points.

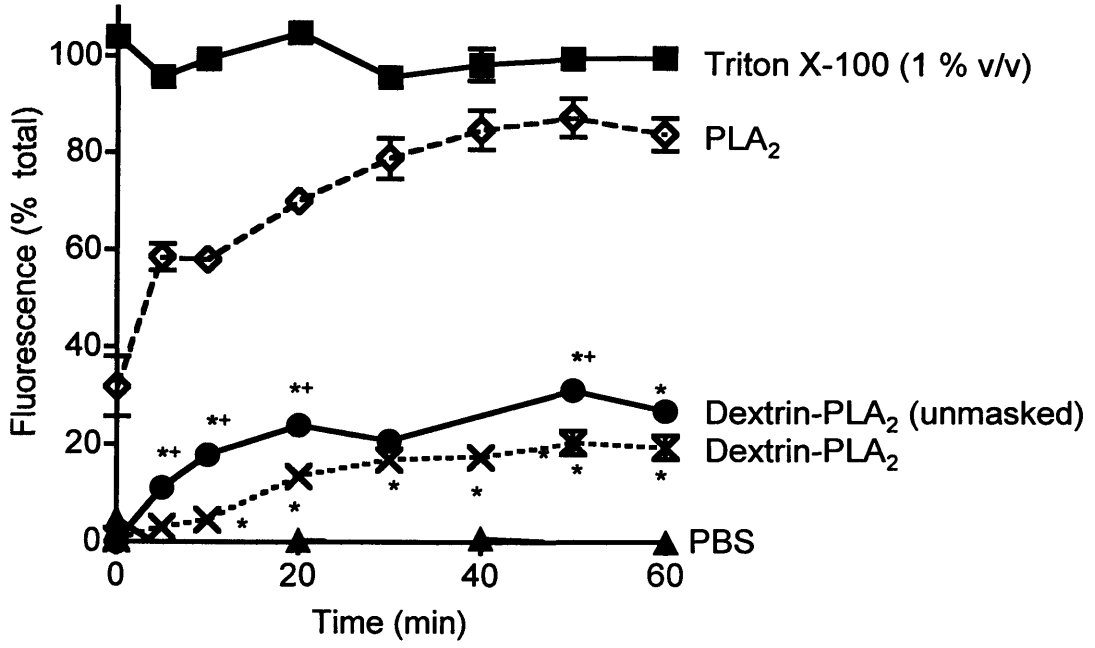

Figure 7.7 Release of daunorubicin from DaunoXome® in the presence of PLA_2, dextrin-PLA_2, unmasked dextrin-PLA_2 conjugate (50 μg/mL PLA_2 eq.) over 60 min. DaunoXome® in the absence of enzyme is included as a control. Triton X-100 (1 % v/v) was used for 100 % drug release. Data represents % fluorescence compared to Triton X-100 (1 % v/v) solution ± SEM, (n = 6). Where error bars are invisible they are within size of data points. * indicates significance compared to PLA_2 control, where $p<0.05$ (ANOVA and Bonferroni *post hoc* test). $^+$ indicates significance compared to dextrin-PLA_2 control, where $p<0.05$ (ANOVA and Bonferroni *post hoc* test).

Next, the cell viability of MCF-7 cells incubated with free daunorubicin (Figure 7.9) or DaunoXome® (Figure 7.10) +/- PLA_2 or dextrin-PLA_2 conjugate was assessed. The IC_{50} values obtained are summarised in Table 7.2. When free daunorubicin was combined with PLA_2, it was found to be as cytotoxic as the daunorubicin + dextrin-PLA_2 conjugate combination (IC_{50} values = 10.0 μg/mL and 16.7 μg/mL, respectively). However, when DaunoXome® was combined with the dextrin-PLA_2 conjugate it was more cytotoxic than DaunoXome® with free PLA_2 (IC_{50} values = 33.6 μg/mL compared to 4.3 μg/mL, respectively).

7.4 Discussion

Since Triton X-100 was to be used to achieve complete drug release, it was first considered important to (i) confirm that encapsulation of daunorubicin in DaunoXome® quenched its fluorescence, and (ii) that Triton X-100 would not greatly alter the spectral shape or fluorescence output of daunorubicin. As expected, encapsulation decreased the fluorescence output of daunorubicin. However, addition of Triton X-100 to the DaunoXome® solution greatly increased the fluorescence, and the intensity and shape of the fluorescence spectrum was the same as that of free daunorubicin.

The results here showed that PLA_2 caused a surprising increase in liposome diameter, which is likely to be accompanied by a striking change in vesicle volume. The liposomes in the absence of PLA_2, however, were stable for 3 h, suggesting that the morphological changes must be attributable to hydrolysis of phospholipids. It was expected that lysophospholipids and fatty acid hydrolysis products would desorb as monomers, micelles or smaller vesicles (Speijer *et al*, 1996). It has been reported that higher membrane curvature allows tighter packing of the wedge-shaped lysophospholipids in the outer monolayer (Haydon and Taylor, 1963). It is, therefore, surprising that incubation of DaunoXome® with PLA_2, and to a lesser extent, unmasked dextrin-PLA_2 conjugate, induced growth of liposomes, rather than shrinkage. However, this trend has also been reported when liposomes were incubated with PLC (Basanez *et al*, 1997). Initially, vesicle aggregation was seen by TEM, followed by PLC-induced vesicle fusion, and ultimately, the formation of

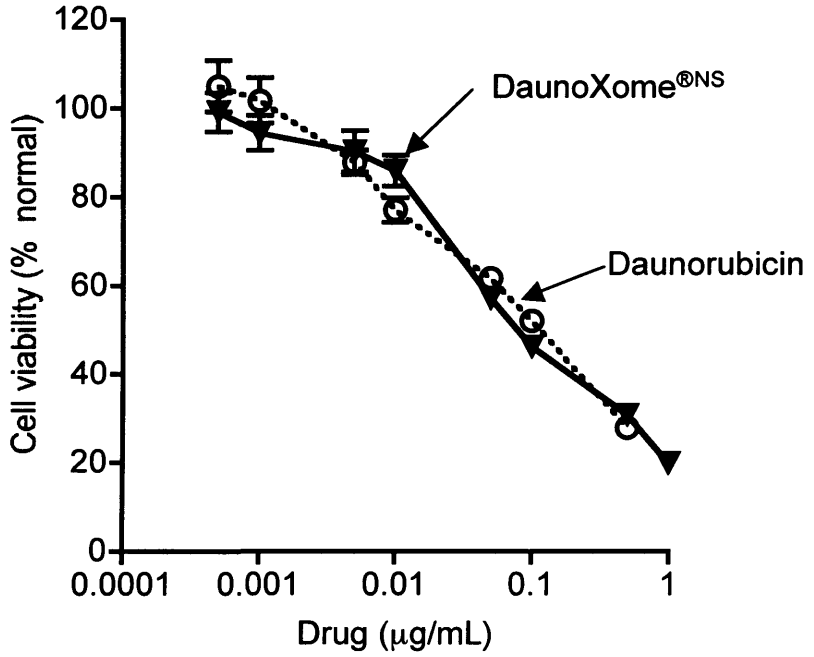

Figure 7.8 Cell viability of MCF-7 cells incubated with daunorubicin and DaunoXome® for 72 h. Graph compares the effect of daunorubicin and DaunoXome® concentration on cell viability. Data represents % normal growth of control cells ± SEM, (n =18). Where error bars are invisible they are within size of data points. NS defines no significant difference ($p>0.05$), calculated using paired students t-test.

Table 7.2 IC_{50} values of daunorubicin and DaunoXome® +/- PLA_2 and dextrin-PLA_2 conjugate following cell viability assessment using the MTT assay (72 h).

Drug	IC_{50} (ng/mL)				
	Drug	Drug + PLA_2	*% change*	Drug + dextrin-PLA_2	*% change*
Daunorubicin	125.0 ± 35	10.0 ± 2.5	*↓ 92*	16.7 ± 3.3	*↓ 87*
DaunoXome®	83.6 ± 10.7	33.6 ± 4.3	*↓ 60*	4.3 ± 0.7	*↓ 95*

Data represents % normal growth of control cells ± SEM, (n = 18).

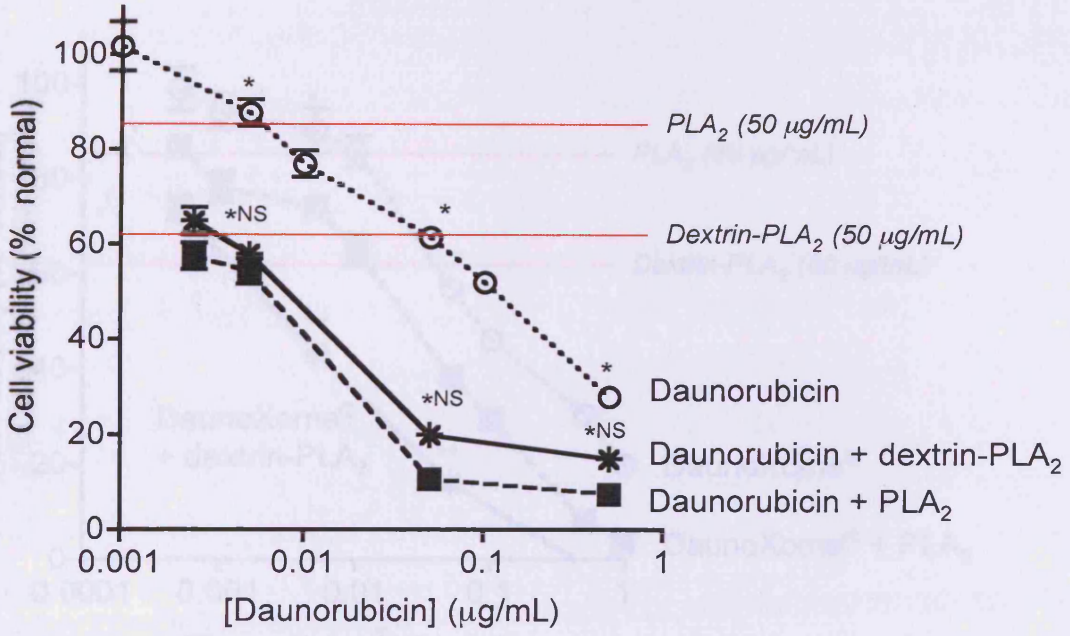

Figure 7.9 Cell viability of MCF-7 cells incubated with daunorubicin +/- PLA_2 and dextrin-PLA_2 conjugate (50 μg/mL PLA_2 eq.) for 72 h. Graph shows effect of daunorubicin concentration on cell viability. Data represents % normal growth of control cells ± SEM, (n = 6; except daunorubicin n =18). Where error bars are invisible they are within size of data points. * indicates significance compared to daunorubicin control, where $p<0.05$ (ANOVA and Bonferroni *post hoc* test). NS defines no significant difference ($p>0.05$) from daunorubicin + PLA_2 control (ANOVA and Bonferroni *post hoc* test).

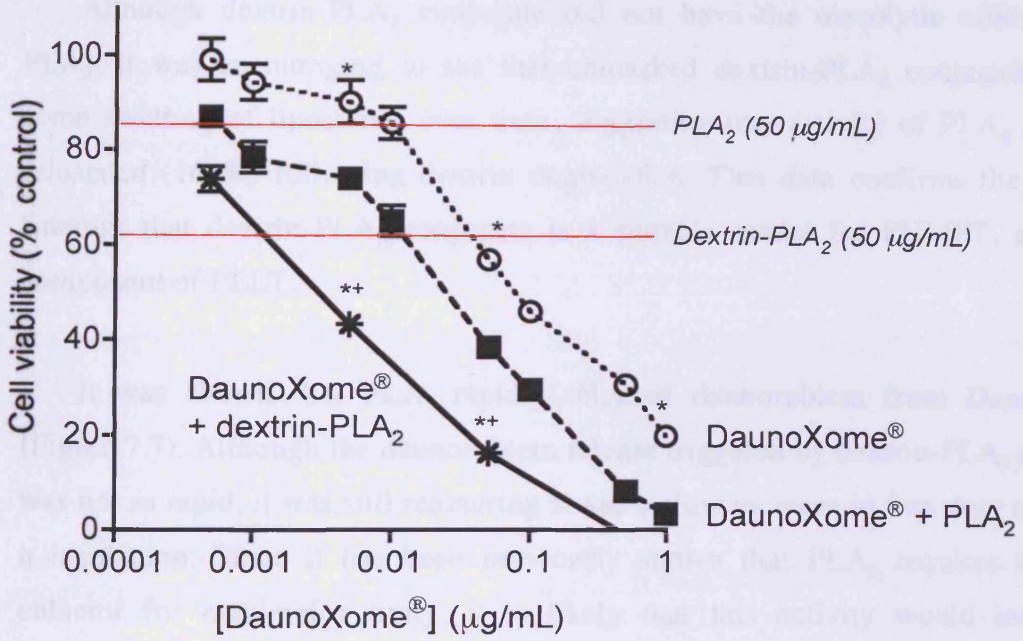

Figure 7.10 Cell viability of MCF-7 cells incubated with DaunoXome® +/- PLA_2 and dextrin-PLA_2 conjugate (50 μg/mL PLA_2 eq.) for 72 h. Graph shows effect of DaunoXome® concentration on cell viability. Data represents % normal growth of control cells ± SEM, (n = 6; except DaunoXome® n =18). Where error bars are invisible they are within size of data points. * indicates significance compared to DaunoXome® control, where $p<0.05$ (ANOVA and Bonferroni *post hoc* test). $^+$ indicates significance compared to DaunoXome® + PLA_2 control, where $p<0.05$ (ANOVA and Bonferroni *post hoc* test).

large spherical vesicles.

Studies have also described the action of PLA_2 on phospholipid vesicles (Lehtonen and Kinnunon, 1995; Wilschut *et al*, 1979). Here, they hypothesised that accumulation of lysophospholipids and fatty acids can alter the permeability of the membrane, rendering them more prone to osmolytic swelling. This osmotic stretching of the lipid bilayer can further modulate its susceptibility to PLA_2 activity. It therefore seems likely that osmolytic swelling is the reason behind the liposome growth seen with DaunoXome®, and to a lesser extent, unmasked dextrin-PLA_2 conjugate.

Although dextrin-PLA_2 conjugate did not have the osmolytic effect of free PLA_2, it was encouraging to see that unmasked dextrin-PLA_2 conjugate showed some swelling of liposomes over time, suggesting that activity of PLA_2 had been reinstated (16 %) following dextrin degradation. This data confirms the previous findings that dextrin-PLA_2 conjugate is a suitable model for PUMPT, even as a component of PELT.

It was shown that PLA_2 rapidly released daunorubicin from DaunoXome® (Figure 7.7). Although the daunorubicin release triggered by dextrin-PLA_2 conjugate was not as rapid, it was still reassuring to see a slow increase in free drug over the 1 h incubation. Since it has been previously shown that PLA_2 requires Ca^{2+} as a cofactor for maximal activity, it is likely that this activity would increase in physiological conditions, where Ca^{2+} is present. It would have been interesting here to undertake these experiments in PBS +/- Ca^{2+}, but this was not done.

It was apparent that α-amylase treated dextrin-PLA_2 conjugate was able to release drug from DaunoXome® faster than the masked conjugates. Again, physiological conditions, where α-amylase is present, would be expected to trigger this unmasking of the dextrin-PLA_2 conjugate.

When Carter *et al* (1998) incubated DaunoXome® with PLC for 1 h, they observed maximal release of daunorubicin at 1 nM enzyme. However, the authors did not report the drug release from liposomes using their anti-CEA antibody-PLC conjugate, so it is difficult to assess whether conjugation of the antibody reduced the

ability of PLC to burst liposomes. They did, however, report a 16-18 fold increase in free daunorubicin in tissue medium following 1 h pre-treatment of HeLa cells with anti-CEA antibody-PLC conjugate and 3 h treatment with DaunoXome®, compared to free PLC with DaunoXome®. In the experiments reported here, maximal drug release after 1 h was achieved using 50 μg/mL (3.16 μM) PLA_2. This is much higher than the concentration of PLC required for 100 % daunorubicin release. The superior ability of PLC to release encapsulated drug was also seen by Satchi-Fainaro and Duncan (unpublished), and supports the theory that PLC may be more active towards DaunoXome® than PLA_2. Since DaunoXome® contains PC and both PLC and PLA_2 are reported to preferentially hydrolyse PC, they should both hydrolyse DaunoXome® readily. However, DaunoXome® also contain cholesterol (2 PC: 1 cholesterol), which has been shown to enhance PLC's activity (Ruiz-Arguello *et al*, 1998). This enhancement could further explain the higher activity seen with PLC conjugates.

Drug release studies by Satchi-Fainaro and Duncan (unpublished) used the same fluorescence methods as in these experiments. However, they showed complete release of daunorubicin from DaunoXome® during incubation with HPMA copolymer-PLC conjugate. Perhaps since PLC and PLA_2 have different phospholipid specificities (PI and PC compared to PC, PE and SM, respectively), the composition of liposomes could also influence the rate of drug release from the vesicles.

7.4.1 Cytotoxicity of DaunoXome®

The IC_{50} values obtained in previous cytotoxicity studies investigating DaunoXome® in a number of tumour cell lines are summarised in Table 7.3 for comparison with those obtained for MCF-7 in these studies. In all cases, DaunoXome® appeared to be more cytotoxic to the cells than free daunorubicin, though there was a broad variation between IC_{50} values. In these studies, the cytotoxicity of free and liposomal daunorubicin was not significantly different, although DaunoXome® had an IC_{50} value of 84 ± 10.7 ng/mL, while free daunorubicin had an IC_{50} value of 125 ± 35 ng/mL.

Table 7.3 IC_{50} values reported in the literature of daunorubicin and liposomal daunorubicin towards various cell lines.

Cell line	Tumour origin	IC_{50} (ng/mL) Daunorubicin	DaunoXome	Reference
KSC-10	AIDS-related Kaposi's sarcoma	78	7.2	(Masood *et al*, 1996)
Colo-320 DM	Human colorectal adenocarcinoma	333	64	(Masood *et al*, 1996)
P1798	Murine lymphosarcoma	43	12.8	(Masood *et al*, 1996)
ME180	Human ovarian carcinoma	30	11	(Masood *et al*, 1996)
K562	Human chronic myeloid leukaemia	5000	10000	(Liu *et al*, 2002)
CEM	Human T-lymphoblastic leukaemia	53	77	(Liu *et al*, 2002)

Jorgensen *et al* (1999a, 1999b) have also studied PLA_2-triggered drug release from liposomes, although they used PEG-covered liposomes, while the liposomes used these studies were uncoated. In fact, the authors reported that $sPLA_2$ was unable to hydrolyse DaunoXome® or Doxil® due to their high cholesterol content and inability to activate PLA_2 by electrostatic attractions. They concluded that PLA_2 is more active towards PEGylated liposomes and that the enzyme activity increased with increasing degree of PEGylation (Jorgensen *et al*, 1999b). This effect is believed to be attributed to an electrostatic interaction between the cationic PLA_2 and the anionic phosphate head groups of the lipopolymers (reviewed in Jorgensen *et al*, 2002). This observation does not correlate with the results obtained in these studies, where PLA_2 induced 100 % daunorubicin release from non-PEGylated liposomes at 50 μg/mL after 1 h.

If, as Davidsen *et al* (2003) suggested, the phospholipid hydrolysis products, lysophospholipids and free fatty acids, enhance drug permeation across the target membrane and destabilise the liposomal carriers, then cytotoxicity of DaunoXome® with PLA_2 or the dextrin-PLA_2 conjugate would be expected to be higher than for free drug. However, this was not the case in these studies, where there was little difference seen between free drug and the liposomal formulation with PLA_2 or dextrin-PLA_2 conjugate. Similarly, Wilschut *et al* (1979) also noted that, despite PLA_2 hydrolysis of 60 % of the outer membrane phospholipids, the liposomes still maintained barrier properties. The authors suggested that, although lysophospholipids and fatty aids are known to have a destabilising effect on membranes, this could be controlled so long as the membrane curvature was high and hydrolysis products were located only in one half of the bilayer.

Clostridium novyi-NT has previously been used to enhance the release and efficacy of liposomal doxorubicin (Cheong *et al*, 2006). Since *C. novyi-NT* is haemolytic and can selectively infect and kill tumours by exploiting their hypoxic environment (Barbe *et al*, 2006; Ryan *et al*, 2006), it was hypothesised that these properties could be utilised to improve tumour-selective drug release from liposomes. In these studies, mice bearing large, established tumours were treated with *C. novyi-NT* and a single dose of Doxil®. This combination led to complete

tumour regression in 100 % of mice and 65 % of the mice were still alive after 90 days. Interestingly, when mice were treated with free doxorubicin and *C. novyi-NT*, 100 % died within 2 weeks, showing the importance of liposomal encapsulation for limiting systemic toxicity. The authors concluded that an enzyme, liposomase, was responsible for liposome disruption and associated enhancement of intratumoural release of liposomal doxorubicin. However, based the findings of the studies reported here, and the work of Carter *et al* (1998) using PLC, it is possible that the enzyme responsible for the lipolytic affects was actually PLC, since this enzyme is secreted from *C. novyi-NT* (Bettegowda *et al*, 2006). Nevertheless, this supports the potential of enzyme-triggered intratumoural liposomal drug release.

7.5 Conclusions

Having shown that a dextrin-PLA_2 conjugate has potential as a novel treatment of breast cancer, these studies have also proven its applicability as a means of triggering drug release from liposomes. It has been shown that the PUMPT concept demonstrated previously, is also applicable to PELT, and unmasked dextrin-PLA_2 has higher activity towards liposomes than the masked enzyme. This work showed that it possible to trigger the release of liposomally encapsulated drug using PLA_2 and dextrin-PLA_2 conjugate, and that these conjugates were able to enhance cytotoxicity towards MCF-7 cells. Morphological changes were observed in liposomes incubated with PLA_2 and unmasked dextrin-PLA_2 conjugate, suggestive of osmolytic swelling of the vesicles.

Chapter Eight

General Discussion

8.1 General comments: Dextrin-PLA_2 conjugate as an anticancer agent

Previous clinical studies demonstrated the exciting anticancer potential of PLA_2 (Costa *et al*, 1998; Cura *et al*, 2002). The first aim of this thesis was to ascertain whether PLA_2 conjugates could be synthesised that would display reduced cytotoxicity and anticancer activity in cell lines (e.g. breast cancer) with high expression of EGFR. From Chapter 3 to 6, the research has evolved from synthesis and characterisation of dextrin-PLA_2 to mechanistic studies.

8.1.1 Recent developments in the field: polymer-protein conjugates and other breast cancer treatments

It is important to consider how the field of nanomedicine and cancer therapy has evolved since the commencement of these studies in 2004. Although recent statistics show that two thirds of women newly diagnosed with breast cancer are likely to survive for over 20 years (Cancer Research UK), the incidence and mortality rates of advanced metastatic breast cancer remain high, and the disease is still a major health priority. Consequently, the National Institute for Health and Clinical Excellence (NICE) plans to publish clinical guidelines for early and advanced breast cancer treatment in January 2009, giving evidence-based recommendations for good practice.

Breast cancer treatment has advanced dramatically since the introduction of radical mastectomy in 1882 (Figure 8.1). Chemotherapy has evolved from nitrogen mustards, discovered in the 1940s during World War Two (reviewed in Benderly, 2002), to tamoxifen, an endocrine agent initially developed as a contraceptive (reviewed in Jordan, 2008). More recently, treatments with improved specificity have become the main focus of research. Cancer therapy using proteins and peptides such as L-lysine-α-oxidase (Kusakabe *et al*, 1980) and phosphoglycerate kinase (Lay *et al*, 2000), and the development of a number of molecular targeted compounds such as trastuzumab and bevacizumab, have demonstrated the ongoing research in the field of novel breast cancer therapies. Enhanced tumour specificity has also been demonstrated by new polymer-protein conjugates entering clinical trials for cancer (reviewed in Pasut *et al*, 2008). For example, PEG-methioninase acts to deplete

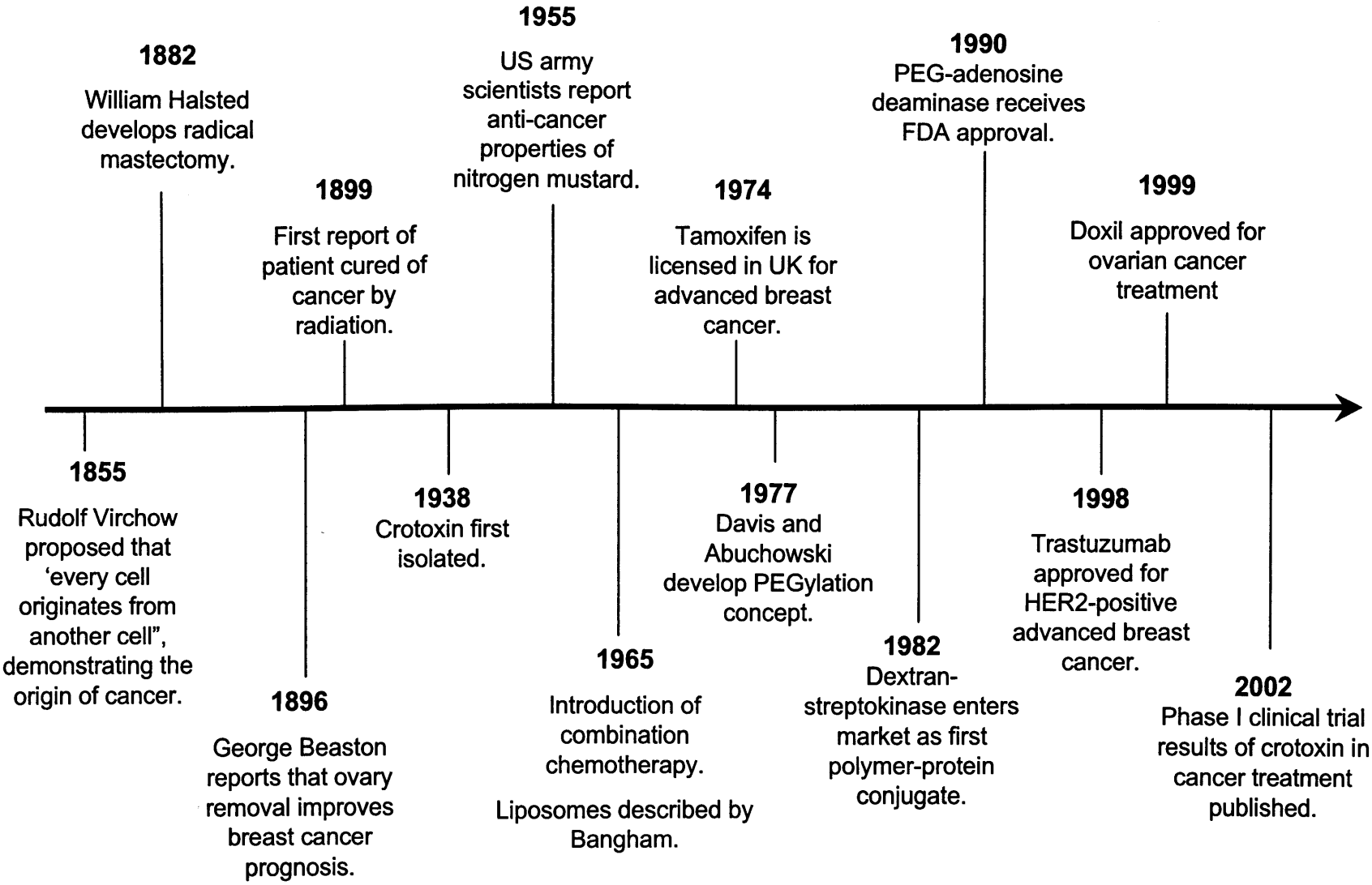

Figure 8.1 Milestones in the areas relating to these studies.

methionine stores in tumour cells, which are often auxotrophic for this protein. Conjugation of methioninase to PEG (3-7 molecules of PEG per protein) increased its half-life 36-fold and reduced anti-methioninase antibodies 100-1000-fold after repeated administration, compared to those elicited by the native enzyme (Yang *et al*, 2004). All of these conjugates, however, contain PEG, a non-biodegradable polymer, despite the well-known limitations associated with it (section 1.2.1). PEGylation chemistry is frequently being reviewed and improved (Brocchini *et al*, 2007; Fontana *et al*, 2007), and therefore remains a key area in the developing field of nanomedicine.

In parallel, a study of PubMed citations since 1975 in the field of phospholipase in cancer revealed rising interest in this area (Figure 8.2). However, after a peak around 1995, publications appear to have decreased- possibly owing to toxicity issues and drug delivery problems (Cura *et al*, 2002; Freitas and Frezard, 1997). This trend highlights once more the importance of developing novel methods for delivery of therapeutic proteins for cancer treatment.

8.1.2 Current status of crotoxin

Given that the rationale for dextrin-PLA_2 conjugate stemmed, in part, from the PLA_2, crotoxin (reviewed in section 1.1) (Cura *et al*, 2002), it is important to review the most recent developments in this product.

Consideration has been made to using drug delivery systems to reduce crotoxin's toxicity. As mentioned previously (section 1.3), PLA_2 has been conjugated to PEG (Bianco *et al*, 2002). Liposomal formulations encapsulating crotoxin have also been described (Freitas and Frezard, 1997; Magalhaes *et al*, 2001). Here, Freitas and Frezard (1997) encapsulated crotoxin into liposomes made from SM and cholesterol. No toxicity was seen when mice were administered (IV) liposomal crotoxin at a dose of up to 91 times as high as its LD_{50}. Magalhaes *et al* (2001) investigated the stability of liposomes having different membrane compositions (non-phospholipid amphiphile, polyoxyethylene 2-cetyl ether, dicetyl phosphate and cholesterol). All liposome formulations retained > 75 % encapsulated crotoxin after 1

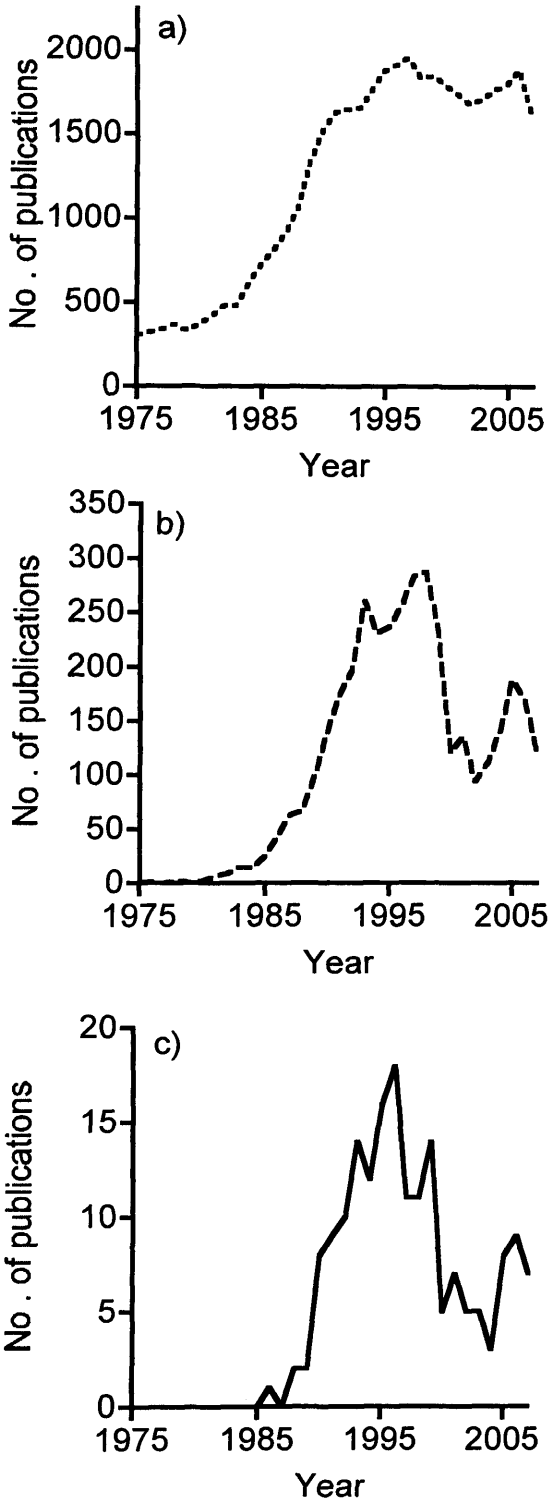

Figure 8.2 Results published in Pubmed database during the period 1975-2007. Panels a-c represent the number of publications cited in PubMed since 1975, where the search terms were: a) phospholipase, b) PLA_2, and c) PLA_2 + cancer.

week incubation at 37 °C. As expected, toxicity in mice was dependant on the membrane composition, such that liposomes composed of PLA_2-resistant phospholipids were less toxic. These studies demonstrate the interest in utilising novel drug delivery techniques for delivery of PLA_2.

Major advances with crotoxin have also been made by Celtic Biotech, who are developing it for the treatment of cancer, pain and viral infections (e.g. HIV) (Celtic Biotech Ltd., 2005). Recent publications have described mechanistic studies of the cytotoxic effects of crotoxin in human breast cancer cells (Yan *et al*, 2006; Yan *et al*, 2007), but interest is also growing in its analgesic properties (Zhang *et al*, 2006; Zhu *et al*, 2007). The pain relieving properties of crotoxin were discovered when it was noticed that patients receiving crotoxin required less analgesic medications (Giorgi *et al*, 1993). Zhang *et al* (2006) have since discovered that the analgesic effects are mediated through an action on the central nervous system, but do not involve the muscarinic and opioid receptors, which are responsible for the analgesic effects of neostigmine and morphine, respectively. More recently, Zhu *et al* (2007) showed that crotoxtin mediates its analgesic effects, at least in part, by the central serotonergic system, like amitriptyline.

Since PLA_2 from other snake and bee venoms has also shown analgesic activity (Chen and Robinson, 1990; Pu *et al*, 1995), it is possible that PLA_2 from bee venom could also have this effect, adding a further therapeutic opportunity to a dextrin-PLA_2 conjugate. However, while studies have shown that bee venom does have analgesic properties, it is the water-soluble fraction (<10,000 g/mol) that is responsible for this effect (Kwon *et al*, 2005).

8.1.3 Critical evaluation of the present study

The choice of dextrin as polymeric carrier for PLA_2 was appropriate for the reasons outlined in sections 1.3.1 and 4.1.2. Moreover, as outlined by Duncan *et al* (2008), an ideal conjugate for PUMPT should be capable of fully masking the enzyme's activity after polymer conjugation, but be capable of reinstating maximal activity after unmasking by polymer degradation. While the range of masked-unmasked activity described in the literature for dextrin conjugates is varied (see

Table 4.4), the dextrin-PLA_2 conjugates synthesised here demonstrated 80 % greater activity of the conjugate after unmasking by α-amylase. Furthermore, while the development of novel polymer-protein conjugates containing non-biodegradable polymers (e.g. PEG) is limited by their molecular weight and slow clearance from the body after longer-term clinical use, dextrin's biodegradability means that conjugates above the renal threshold (40,000 g/mol) can still be of clinical value.

Selection of bee venom PLA_2 was made after comparison with bovine PLA_2, since these were the only two commercially and readily available PLA_2s. However, with the growing success of crotoxin, it would be interesting to synthesise and characterise a dextrin-crotoxin conjugate for comparison to the bee venom PLA_2 conjugates.

To fully assess the clinical efficacy of dextrin-PLA_2 conjugates as anti-cancer agents the most important experiments relate to *in vivo* assessment of pharmacokinetics and anti-tumour activity. Since these kinds of experiments have been used to test the PDEPT combinations in mice bearing subcutaneous B16F10 melanoma (Satchi *et al*, 2001; Satchi-Fainaro *et al*, 2003), as well as a number of other anti-cancer polymer conjugates (Ulbrich *et al*, 2003), these experiments would be relatively easy to perform. Although *in vitro* model systems are useful for evaluating cytotoxicity, it is important to note that this technique represents a gross simplification of the *in vivo* scenario. Data obtained from *in vitro* studies can only give a possible indication of what could happen *in vivo,* since it lacks the complexity of the multicomponent physiological processes of a living model. Nevertheless, *in vitro* studies were still considered to be essential for investigating the potential of dextrin-PLA_2 conjugates as novel anti-cancer agents.

8.1.4 Options for future development of dextrin-PLA_2 conjugates

The results presented in this thesis underline the possibilities of a polymer-phospholipase conjugate. However, some questions remain unanswered. Therefore, first, the most important outstanding experiments in developing dextrin-PLA_2 as a novel anti-cancer agent are described, and then a broader perspective of future research areas that could be explored is given.

In future studies, it would be interesting to study the physicochemical characteristics of the dextrin-PLA_2 conjugates. The size and shape of the conjugates, with respect to their composition, protein loading and following unmasking, could be investigated using small-angle neutron scattering (SANS). This technique has previously been used to study the size, conformation and solution behaviour of unconjugated polymers (poly(amidoamine) (Khayat *et al*, 2006)), micelle components (DSPE-PEG(2000)-CCK8 peptide (Tesauro *et al*, 2007)) and polymer-drug conjugates (HPMA copolymer-doxorubicin (Paul *et al*, 2007)). SANS would be a valuable tool to determine conformation-activity relationships for dextrin-PLA_2 conjugates under physiologically relevant conditions.

Circular dichroism (CD) spectroscopy would also be a valuable tool for studying the effect of dextrin-conjugation on the folding of PLA_2. This technique uses differential absorption of left- and right-handed polarised light to determine the structure of macromolecules. PEG-GCSF conjugate has been analysed using CD spectroscopy, which showed that the secondary structure of GCSF was not altered by site-specific conjugation to PEG (Paul *et al*, 2007). CD spectroscopy would be useful to assess the conformational changes of PLA_2 when conjugated to dextrin, but also after unmasking of the conjugate by incubation with α-amylase.

Considering the results obtained in these studies from a broader point of view, as well as the recent developments of polymer conjugates described in the literature, there are a number of potential avenues for extending these studies. Figure 8.3 (panels a-b) shows a schematic representation of some future possibilities for dextrin-PLA_2 conjugates as novel anticancer agents. First, since dextrin-PLA_2 and doxorubicin showed enhanced cytotoxicity in MCF-7 cells (Figure 5.10) and recent studies have shown enhanced activity of HPMA copolymer-aminoglutethimide (AGM)-doxorubicin, compared to HPMA copolymer-doxorubicin with HPMA copolymer-AGM (Greco *et al*, 2005), it would be interesting to investigate dextrin-PLA_2-doxorubicin conjugates.

Secondly, a targeting agent, such as EGF, could be added to the dextrin-PLA_2 conjugate to enhance tumour specificity, since EGFR is commonly overexpressed on cancer cells. However, while a number of tumour-targeting methods have been

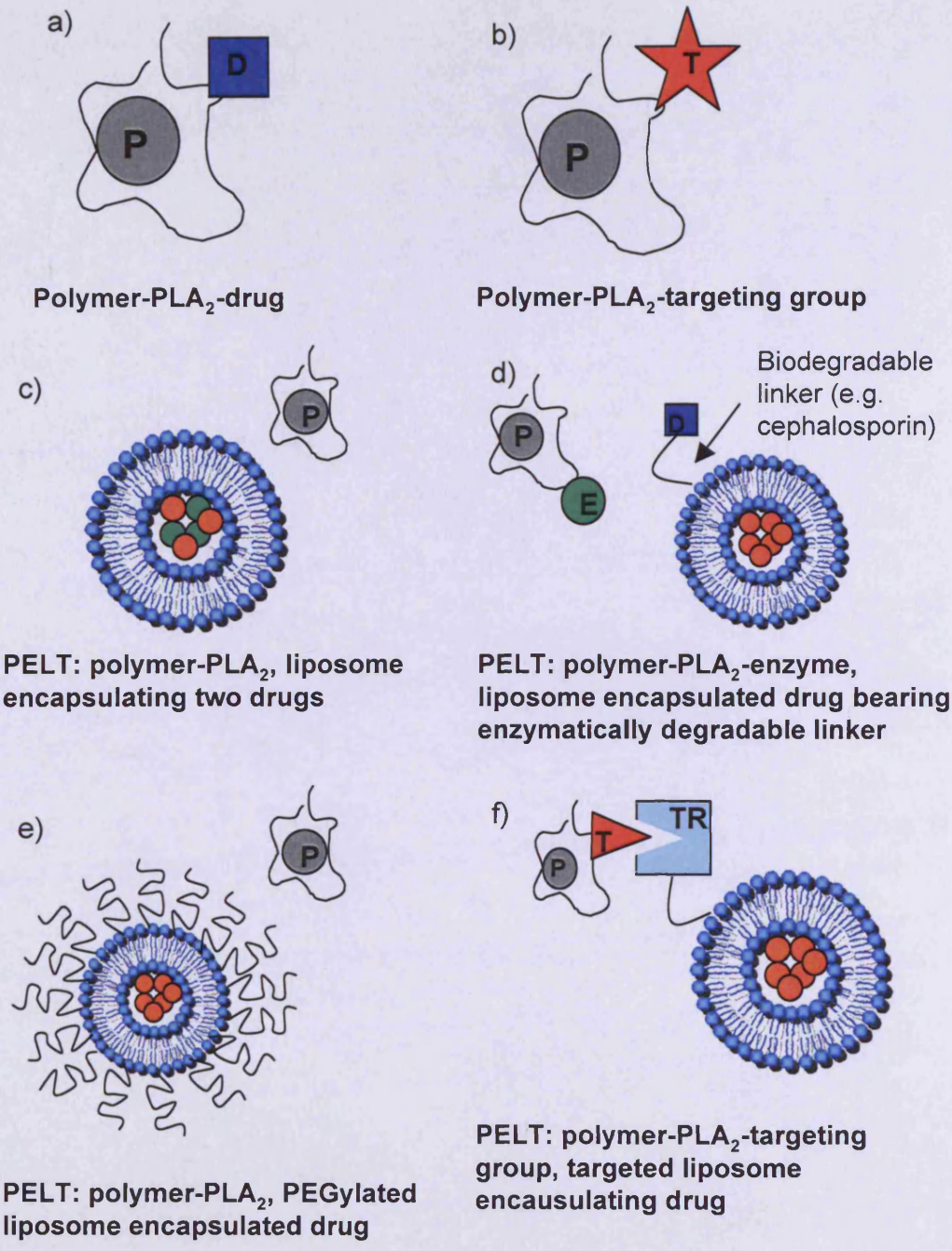

Figure 8.3 Schematic representation of the future possibilities for the use of dextrin-PLA_2 conjugates as novel anticancer treatments. Where P = PLA_2, D = drug (e.g. doxorubicin), T = targeting residue (e.g. EGF), E = enzyme (e.g. β-lactamase), and TR = target receptor (e.g. EGFR).

described (e.g. antibodies, peptides, and folate) (reviewed in Duncan, 2005), only PK2 (HPMA copolymer-doxorubicin-galactosamine) has been evaluated clinically.

8.2 General comments: Dextrin-PLA_2 conjugate as a trigger for PELT

Previous studies have demonstrated the possibility of using HPMA copolymer-Gly-Gly-PLC as a trigger for drug release from liposomes. Therefore, Chapter 7 of this thesis aimed to provide proof of concept data for the use of dextrin-PLA_2 conjugate as a trigger for PELT.

8.2.1 Current status of LiPlasome development

Given that the rationale for using dextrin-PLA_2 conjugate as a trigger for PELT stemmed, in part, from LiPlasome (reviewed in section 7.1.1) (Jorgensen *et al*, 2002), the recent developments in this product are interesting to review.

Since the initial studies provided proof of principle for LiPlasome, ongoing research has investigated further the expression and activity of $sPLA_2$ in tumour tissue (Tribler *et al*, 2007). Further studies have explored the molecular basis of phospholipid hydrolysis (Linderoth *et al*, 2008; Peters *et al*, 2007) and optimised phospholipid functionalisation and structure for PLA_2 degradation (Linderoth *et al*, 2007). At the end of 2007, LiPlasome Pharma reported successful completion of its preclinical studies, which demonstrated proof of principle of tumour-activation and integrated prodrug and drug delivery platform (LiPlasome Pharma A/S, 2008). Therefore, Phase I studies of LiPlasome encapsulating doxorubicin, cisplatin (LiPlaCis) and methotrexate (LiPloxa), as well as novel prodrug lipids that are specifically converted to active anticancer lipids by tumoural PLA_2, are due to commence early in 2008.

8.2.2 Critical evaluation of the present study

The data presented here were only preliminary to demonstrate proof of concept, and further investigations are necessary for optimisation of the concept.

Initial proof of concept studies for the PELT concept used HPMA copolymer-

Gly-Gly-PLC (Satchi-Fainaro and Duncan, unpublished). These non-biodegradable conjugates contained ~ 60 wt. % PLC, compared to 5-9 wt. % PLA_2 in dextrin-PLA_2 conjugates. These differences make it difficult to compare the efficiency of HPMA copolymer-PLC conjugate and dextrin-PLA_2 conjugate to trigger drug release from liposomes. The value of using a biodegradable polymer has already been reviewed in sections 1.3.1 and 4.1.2. It is unknown whether the biodegradability of dextrin improves the ability of PLA_2 to trigger drug release from liposomes, so it would be interesting to compare dextrin-PLA_2 conjugates with HPMA copolymer- or PEG-PLA_2 conjugates. The benefits of these polymers have been outlined in sections 1.2.1 and 1.3.1.

Although these studies used the commercially available formulation, DaunoXome®, improved activity and selectivity could be achieved by designing the liposome specifically for the PELT concept. Literature shows that PLA_2 preferentially hydrolyses PC, SM and PE (Diez *et al*, 1994; Monteggia *et al*, 2000), and has a preference for curved, tightly packed membranes (Best *et al*, 2002). The hydrolytic activity of the dextrin-PLA_2 conjugate could be assessed using phospholipid monolayers in Langmuir troughs. These systems allow the preparation of stable model membranes in different molecular environments while simultaneously assessing their influence on the rate of phospholipid hydrolysis. Grainger *et al* (1990) have used this method to study phospholipid hydrolysis by PLA_2. By studying the activity of dextrin-PLA_2 towards a variety of phospholipid monolayers, it would be possible to select the best composition for the drug-loaded liposomes.

These studies also reported morphological changes in DaunoXome® during incubation with PLA_2. TEM would be a valuable tool to further investigate the effects of dextrin-PLA_2 conjugate to the liposomal surface. This technique would also elucidate the mechanism of action of dextrin-PLA_2.

8.2.3 Options for future development of PELT

Since PELT is part of a whole new field of two-step processes and combination therapies using polymers as carriers Figure 8.3 (panels c-f) also shows several polymer combinations based on this model for development in the future.

Briefly, panel (c) represents a liposome encapsulating two different drugs to act synergistically on cancer cells. Panel (d) describes a drug-loaded liposome bearing an anti-cancer drug conjugated to the surface via an enzymatically degradable linker. This model uses a polymer-PLA_2-enzyme conjugate to simultaneously trigger drug liberation from inside liposome and release the drug bound to the liposome surface after enzymatic cleavage of the degradable linker. Panel (e) represents the PELT concept using PEGylated liposomes, since some literature has suggested that PLA_2 is more active on these surfaces (reviewed in section 7.4.3). Finally, panel (f) demonstrates polymer-PLA_2 bearing a targeting residue which co-localises with drug-loaded liposomes labelled with the corresponding target receptor. This concept has the potential to increase specificity, though relies heavily on the efficacy of the EPR effect.

8.3 Contribution of this thesis to nanotechnological medicine

The work undertaken in this thesis has demonstrated two ways in which dextrin-PLA_2 conjugates can be used as anticancer agents.

These studies have shown the ability to mask and unmask enzyme activity by triggered degradation of dextrin (Ferguson *et al*, 2006a; Ferguson *et al*, 2006b). The underlying mechanism of dextrin-PLA_2's anticancer activity with respect to EGFR has been demonstrated (Ferguson and Duncan, 2008; Ferguson *et al*, 2007) and its intracellular fate followed (Richardson *et al*, 2008). Results from the PELT studies have proven that dextrin-PLA_2 conjugates are suitable triggers for drug release from liposomes (Ferguson and Duncan, 2008).

In conclusion, bioresponsive conjugates of PLA_2 have shown exciting anticancer activity. Not only has its inherent anticancer activity been demonstrated, but also dextrin-PLA_2's ability to trigger drug release from liposomes in the PELT model offers an additional opportunity for research.

Bibliography

Abuchowski A, McCoy JR, Palczuk NC, van Es T, Davis FF (1977) Effect of covalent attachment of polyethylene glycol on immunogenicity and circulating life of bovine liver catalase. *Journal of Biological Chemistry* **252:** 3582-3586

Alicea E. (1998) Crotoxin: Membrane Damage and Cell Injury in Ovarian Cancer Cells. MD thesis, University of Texas (Houston, USA)

Alley MC, Scudiero DA, Monks A, Hursey ML, Czerwinski MJ, Fine DL, Abbott BJ, Mayo JG, Shoemaker RH, Boyd MR (1988) Feasibility of drug screening with panels of human tumor cell lines using a microculture tetrazolium assay. *Cancer Research* **48:** 589-601

Alscher DM, Mettang T, Kuhlmann U (2001) Cure of lifelong fatigue by calcium supplementation. *Lancet* **358:** 888

Amirghofran Z, Bahmani M, Azadmehr A, Javidnia K (2007) Immunomodulatory and apoptotic effects of *Stachys obtusicrena* on proliferative lymphocytes. *Medical Science Monitor* **13:** BR145-150

Andresen TL, Davidsen J, Begtrup M, Mouritsen OG, Jorgensen K (2004a) Enzymatic release of antitumor ether lipids by specific phospholipase A_2 activation of liposome-forming prodrugs. *Journal of Medicinal Chemistry* **47:** 1694-1703

Andresen TL, Jensen SS, Jensen LT, Kaasgaard T, Jorgensen K (2004b) Triggered Liposomal Drug Release in Cancer Tissue by Secretory Phospholipase A_2. *Proceedings of the 31st Annual Meeting of the Controlled Release Society*, 134

Andresen TL, Jensen SS, Jorgensen K (2004c) Active and Tumour Specific Drug Release Using Targeted Liposomal Drug Carriers. *Company report: LiPlasome,* Technical University of Denmark (Lyngby, Denmark)

Andresen TL, Jensen SS, Jorgensen K (2005) Advanced strategies in liposomal cancer therapy: problems and prospects of active and tumor specific drug release. *Progress in Lipid Research* **44:** 68-97

Annand RR, Kontoyianni M, Penzotti JE, Dudler T, Lybrand TP, Gelb MH (1996) Active site of bee venom phospholipase A_2: the role of histidine-34, aspartate-64 and tyrosine-87. *Biochemistry* **35:** 4591-4601

Araki N, Egami Y, Watanabe Y, Hatae T (2007) Phosphoinositide metabolism during membrane ruffling and macropinosome formation in EGF-stimulated A431 cells. *Experimental Cell Research* **313:** 1496-1507

AstraZeneca (2003) Information on the use of ZD1839 ('IRESSA') for non-clinical studies

Astsaturov I, Cohen RB, Harari PM (2006) EGFR-targeting monoclonal antibodies

in head and neck cancer. *Current Cancer Drug Targets* **6:** 691-710

Bakina E, Farquhar D (1999) Intensely cytotoxic anthracycline prodrugs: galactosides. *Anticancer Drug Design* **14:** 507-515

Balan S, Choi JW, Godwin A, Teo I, Laborde CM, Heidelberger S, Zloh M, Shaunak S, Brocchini S (2007) Site-specific PEGylation of protein disulfide bonds using a three-carbon bridge. *Bioconjugate Chemistry* **18:** 61-76

Bangham AD, Standish MM, Watkins JC (1965) Diffusion of univalent ions across the lamellae of swollen phospholipids. *Journal of Molecular Biology* **13:** 238-252

Banks PR, Paquette DM (1995) Comparison of three common amine reactive fluorescent probes used for conjugation to biomolecules by capillary zone electrophoresis. *Bioconjugate Chemistry* **6:** 447-458

Barbe S, Van Mellaert L, Anne J (2006) The use of clostridial spores for cancer treatment. *Journal of Applied Microbiology* **101:** 571-578

Basanez G, Ruiz-Arguello MB, Alonso A, Goni FM, Karlsson G, Edwards K (1997) Morphological changes induced by phospholipase C and by sphingomyelinase on large unilamellar vesicles: a cryo-transmission electron microscopy study of liposome fusion. *Biophysical Journal* **72:** 2630-2637

Bellott R, Auvrignon A, Leblanc T, Perel Y, Gandemer V, Bertrand Y, Mechinaud F, Bellenger P, Vernois J, Leverger G, Baruchel A, Robert J (2001) Pharmacokinetics of liposomal daunorubicin (DaunoXome) during a phase I-II study in children with relapsed acute lymphoblastic leukaemia. *Cancer Chemotherapy and Pharmacology* **47:** 15-21

Bendele A, Seely J, Richey C, Sennello G, Shopp G (1998) Short communication: renal tubular vacuolation in animals treated with polyethylene-glycol-conjugated proteins. *Toxicological Sciences* **42:** 152-157

Benderly BL (2002) From poison gas to wonder drug. *American Heritage of Invention and Technology* **18:** 48-54

Best KB, Ohran AJ, Hawes AC, Hazlett TL, Gratton E, Judd AM, Bell JD (2002) Relationship between erythrocyte membrane phase properties and susceptibility to secretory phospholipase A_2. *Biochemistry* **41:** 13982-13988

Bettegowda C, Huang X, Lin J, Cheong I, Kohli M, Szabo SA, Zhang X, Diaz LA, Jr., Velculescu VE, Parmigiani G, Kinzler KW, Vogelstein B, Zhou S (2006) The genome and transcriptomes of the anti-tumor agent Clostridium novyi-NT. *Nature Biotechnology* **24:** 1573-1580

Bianco ID, Daniele JJ, Delgado C, Fisher D, Francis GE, Fidelio GD (2002) Coupling reaction and properties of poly(ethylene glycol)-linked phospholipases

A_2. *Bioscience Biotechnology and Biochemistry* **66:** 722-729

Bier H, Hoffmann T, Haas I, van Lierop A (1998) Anti-(epidermal growth factor) receptor monoclonal antibodies for the induction of antibody-dependent cell-mediated cytotoxicity against squamous cell carcinoma lines of the head and neck. *Cancer Immunology Immunotherapy* **46:** 167-173

Bisaccia E, Lugo A, Torres O, Johnson B, Scarborough D (2007) Persistent inflammatory reaction to hyaluronic acid gel: a case report. *Cutis* **79:** 388-389

Bollinger JG, Diraviyam K, Ghomashchi F, Murray D, Gelb MH (2004) Interfacial binding of bee venom secreted phospholipase A_2 to membranes occurs predominantly by a nonelectrostatic mechanism. *Biochemistry* **43:** 13293-13304

Briggs GE, Haldane JB (1925) A Note on the Kinetics of Enzyme Action. *Biochemical Journal* **19:** 338-339

Brocchini S, Godwin A, Balan S, Choi JW, Zloh M, Shaunak S (2007) Disulfide bridge based PEGylation of proteins. *Advanced Drug Delivery Reviews* **60:** 3-12

Brockhoff G, Hofstaedter F, Knuechel R (1994) Flow cytometric detection and quantitation of the epidermal growth factor receptor in comparison to Scatchard analysis in human bladder carcinoma cell lines. *Cytometry* **17:** 75-83

Brown MD, Schatzlein AG, Uchegbu IF (2001) Gene delivery with synthetic (non viral) carriers. *International Journal of Pharmaceutics* **229:** 1-21

Bruneel D, Schacht E (1993a) Chemical Modification of Pullulan: 1. Periodate Oxidation. *Polymer* **34:** 2628-2632

Bruneel D, Schacht E (1993b) Chemical Modification of Pullulan: 2. Chloroformate Activation. *Polymer* **34:** 2633-2658

Bruneel D, Schacht E (1994) Chemical Modification of Pullulan: 3. Succinoylation. *Polymer* **35:** 2656-2658

Buck FF, Vithayathil AJ, Bier M, Nord FF (1962) On the mechanism of enzyme action. 73. Studies on trypsins from beef, sheep and pig pancreas. *Archives of Biochemistry and Biophysics* **97:** 417-424

Burack WR, Biltonen RL (1994) Lipid bilayer heterogeneities and modulation of phospholipase A_2 activity. *Chemistry and Physics of Lipids* **73:** 209-222

Campbell CT, Prince M, Landry GM, Kha V, Kleiner HE (2007) Pro-apoptotic effects of 1'-acetoxychavicol acetate in human breast carcinoma cells. *Toxicological Letters* **173:** 151-160

Cancer Research UK (2005) Reduce the Risk Vol. 2005.

Carter G, White P, Fernie M, King S, McLean G, Titball R, Carr FJ (1998) Enhanced antitumour effect of liposomal daunorubicin using antibody-phospholipase C conjugates or fusion protein. *International Journal of Oncology* **13:** 819-825

Celtic Biotech Ltd. (2005) Novel Cancer Therapy & Pain Treatment Drug Discovery. Dublin, Ireland. *http://www.celticbiotech.com*, accessed on Jan 14 2008

Chaffee S, Mary A, Stiehm ER, Girault D, Fischer A, Hershfield MS (1992) IgG antibody response to polyethylene glycol-modified adenosine deaminase in patients with adenosine deaminase deficiency. *Journal of Clinical Investigation* **89:** 1643-1651

Chen RZ, Robinson SE (1990) The effect of cholinergic manipulations on the analgesic response to cobrotoxin in mice. *Life Sciences* **47:** 1949-1954

Cheong I, Huang X, Bettegowda C, Diaz LA, Jr., Kinzler KW, Zhou S, Vogelstein B (2006) A bacterial protein enhances the release and efficacy of liposomal cancer drugs. *Science* **314:** 1308-1311

Chi CC, Wang SH, Kuo TT (2006) Localized cutaneous polyvinylpyrrolidone storage disease mimicking cheilitis granulomatosa. *Journal of Cutaneous Pathology* **33:** 454-457

Chiu HC, Hsiue GH, Lee YP, Huang LW (1999) Synthesis and characterization of pH-sensitive dextran hydrogels as a potential colon-specific drug delivery system. *Journal of Biomaterials Science* **10:** 591-608

Choumet V, Lafaye P, Mazie JC, Bon C (1998) A monoclonal antibody directed against the non-toxic subunit of a dimeric phospholipase A_2 neurotoxin, crotoxin, neutralizes its toxicity. *Biological Chemistry* **379:** 899-906

Chwetzoff S, Tsunasawa S, Sakiyama F, Menez A (1989) Nigexine, a phospholipase A_2 from cobra venom with cytotoxic properties not related to esterase activity. Purification, amino acid sequence, and biological properties. *Journal of Biological Chemistry* **264:** 13289-13297

Chytry V, Kopecek J (1982) A convenient model system for the study of the influence of water-soluble polymer carrier on the interaction between proteins. *Makromolekulare Chemie, Rapid Communications* **3:** 11-15

Cohen S (1987) Epidermal growth factor. *In Vitro Cellular and Developmental Biology* **23:** 239-246

Conner SD, Schmid SL (2003) Regulated portals of entry into the cell. *Nature* **422:** 37-44

Corin RE, Viskatis LJ, Vidal JC, Etcheverry MA (1993) Cytotoxicity of crotoxin on murine erythroleukemia cells *in vitro*. *Investigational New Drugs* **11:** 11-15

Cornish-Bowden A (2004) Fundamentals of enzyme kinetics. Portland Press (London, UK)

Costa LA, Miles H, Araujo CE, Gonzalez S, Villarrubia VG (1998) Tumor regression of advanced carcinomas following intra- and/or peri-tumoral inoculation with VRCTC-310 in humans: preliminary report of two cases. *Immunopharmacology and Immunotoxicology* **20:** 15-25

Costa SA, Reis RL (2004) Immobilisation of catalase on the surface of biodegradable starch-based polymers as a way to change its surface characteristics. *Journal of Materials Science* **15:** 335-342

Cupillard L, Mulherkar R, Gomez N, Kadam S, Valentin E, Lazdunski M, Lambeau G (1999) Both group IB and group IIA secreted phospholipases A2 are natural ligands of the mouse 180-kDa M-type receptor. *Journal of Biological Chemistry* **274:** 7043-7051

Cura JE, Blanzaco DP, Brisson C, Cura MA, Cabrol R, Larrateguy L, Mendez C, Sechi JC, Silveira JS, Theiller E, de Roodt AR, Vidal JC (2002) Phase I and pharmacokinetics study of crotoxin (cytotoxic $PLA_{(2)}$, NSC-624244) in patients with advanced cancer. *Clinical Cancer Research* **8:** 1033-1041

Davidsen J, Jorgensen K, Andresen TL, Mouritsen OG (2003) Secreted phospholipase $A_{(2)}$ as a new enzymatic trigger mechanism for localised liposomal drug release and absorption in diseased tissue. *Biochimica et Biophysica Acta* **1609:** 95-101

Davis FF (2002) The origin of PEGnology. *Advanced Drug Delivery Reviews* **54:** 457-458

Dennis EA (1997) The growing phospholipase A_2 superfamily of signal transduction enzymes. *Trends in Biochemical Sciences* **22:** 1-2

Devakumar J, Mookambeswaran V (2007) A Novel Affinity-Based Controlled Release System Involving Derivatives of Dextran with Enhanced Osmotic Activity. *Bioconjugate Chemistry* **18:** 477-483

Devleeschouwer N, Body JJ, Legros N, Muquardt C, Donnay I, Wouters P, Leclercq G (1992) Growth factor-like activity of phenol red preparations in the MCF-7 breast cancer cell line. *Anticancer Research* **12:** 789-794

Diez E, Chilton FH, Stroup G, Mayer RJ, Winkler JD, Fonteh AN (1994) Fatty acid and phospholipid selectivity of different phospholipase A_2 enzymes studied by using a mammalian membrane as substrate. *The Biochemical Journal* **301(3):** 721-726

Diez E, Louis-Flamberg P, Hall RH, Mayer RJ (1992) Substrate specificities and properties of human phospholipases A_2 in a mixed vesicle model. *Journal of Biological Chemistry* **267:** 18342-18348

Donato NJ, Martin CA, Perez M, Newman RA, Vidal JC, Etcheverry M (1996) Regulation of epidermal growth factor receptor activity by crotoxin, a snake venom phospholipase A_2 toxin. A novel growth inhibitory mechanism. *Biochemical Pharmacology* **51:** 1535-1543

Dordal MS, Ho AC, Jackson-Stone M, Fu YF, Goolsby CL, Winter JN (1995) Flow cytometric assessment of the cellular pharmacokinetics of fluorescent drugs. *Cytometry* **20:** 307-314

Drenth J, Enzing CM, Kalk KH, Vessies JC (1976) Structure of porcine pancreatic prephospholipase A_2. *Nature* **264:** 373-377

Duncan R (2003) The dawning era of polymer therapeutics. *Nature Reviews Drug Discovery* **2:** 347-360

Duncan R (2005) N-(2-Hydroxypropyl)methacrylamide Copolymer Conjugates. *Polymeric Drug Delivery Systems*, Kwon GS (ed) Marcel Dekker, Inc. (New York, USA), 1-92

Duncan R (2006) Polymer conjugates as anticancer nanomedicines. *Nature Reviews Cancer* **6:** 688-701

Duncan R (2007) Designing polymer conjugates as lysosomotropic nanomedicines. *Biochemical Society Transactions* **35:** 56-60

Duncan R, Ferruti P, Sgouras D, Tuboku-Metzger A, Ranucci E, Bignotti F (1994) A polymer-Triton X-100 conjugate capable of pH-dependent red blood cell lysis: a model system illustrating the possibility of drug delivery within acidic intracellular compartments. *Journal of Drug Targeting* **2:** 341-7

Duncan R, Gac-Breton S, Keane R, Musila R, Sat YN, Satchi R, Searle F (2001) Polymer-drug conjugates, PDEPT and PELT: basic principles for design and transfer from the laboratory to clinic. *Journal of Controlled Release* **74:** 135-146

Duncan R, Gilbert HRP, Carbajo RJ, Vicent MJ (2008) Polymer Masked-Unmasked Protein Therapy (PUMPT) 1. Bioresponsive dextrin-trypsin and -MSH conjugates designed for α-amylase activation. *Biomacromolecules*: In Press

Early Breast Cancer Trialists' Collaborative Group (1998) Polychemotherapy for early breast cancer: an overview of the randomised trials. Early Breast Cancer Trialists' Collaborative Group. *Lancet* **352:** 930-942

Early Breast Cancer Trialists' Collaborative Group (2005) Effects of chemotherapy

and hormonal therapy for early breast cancer on recurrence and 15-year survival: an overview of the randomised trials. *Lancet* **365:** 1687-1717

Eisenthal R, Danson MJ (1998) Enzyme Assays: A Practical Approach. Oxford University Press (Oxford, UK)

El-Rayes BF, LoRusso PM (2004) Targeting the epidermal growth factor receptor. *British Journal of Cancer* **91:** 418-424

Barman, T. E. (ed) (1969) Enzyme Handbook, Vol. II Springer-Verlag (New York, USA), 618-619, 819

Etrych T, Mrkvan T, Rihova B, Ulbrich K (2007) Star-shaped immunoglobulin-containing HPMA-based conjugates with doxorubicin for cancer therapy. *Journal of Controlled Release* **122:** 31-38

European Bioinformatics Institute PDBsum Vol. 2004. *http://www.ebi.ac.uk/thornton-srv/databases/cgi-bin/pdbsum*, accessed Nov 11 2004

European Science Foundation (2005) ESF: European Medical Research Councils (EMRC) Forward Look report. http://www.esf.org, accessed on Jun 22 2006

Evans WH, Hardison WG (1985) Phospholipid, cholesterol, polypeptide and glycoprotein composition of hepatic endosome subfractions. *The Biochemical Journal* **232:** 33-36

Evrard A, Cuq P, Ciccolini J, Vian L, Cano JP (1999) Increased cytotoxicity and bystander effect of 5-fluorouracil and 5-deoxy-5-fluorouridine in human colorectal cancer cells transfected with thymidine phosphorylase. *British Journal of Cancer* **80:** 1726-1733

ExPASy (2004) Trypsin; porcine pancreas. In *ExPASy protein database:* http://www.expasy.org/uniprot/P00761

ExPASy (2004) Phospholipase A_2; Apis mellifera (honeybee). In *ExPASy Protein Database:* http://www.expasy.org/uniprot/P00630

ExPASy (2005) Phospholipase A_2; Porcine. In *ExPASy Protein Database:* http://www.expasy.org/uniprot/P00593

Ferguson EL, Duncan R (2007) Investigating the cytotoxicity and mechanism of action of dextrin-phospholipase A_2 conjugates as novel anti-tumour agents. *Proceedings of the 34th Annual Meeting & Exposition of the Controlled Release Society* (Long Beach, USA), 100

Ferguson EL, Duncan R (2008) Investigating a dextrin-phospholipase A_2 conjugate as a trigger for polymer enzyme liposome therapy (PELT). *Proceedings of the*

International Symposium on Polymer Therapeutics (Valencia, Spain), in press

Ferguson EL, Schmaljohann D, Duncan R (2006). Polymer-phospholipase conjugates as novel anti-cancer agents: dextrin-phospholipase A_2. *Proceedings of 33rd Annual Meeting & Exposition of the Controlled Release Society,* Vol. 33 (Vienna, Austria), 660

Ferguson EL, Schmaljohann D, Duncan R (2006) Polymer-phospholipases as novel anti-cancer nanomedicines. *SET for Britain & Britain's Top Younger Scientists, Engineers and Technologists* (London, UK), L2-30

Ferguson EL, Schmaljohann D, Duncan R (2007) Dextrin-phospholipase A_2 conjugates as enzyme-triggered anti-cancer agents. *Proceedings of the 13th United Kingdom and Ireland Controlled Release Society's Annual Symposium* (London, UK)

Fitzpatrick SL, Brightwell J, Wittliff JL, Barrows GH, Schultz GS (1984a) Epidermal growth factor binding by breast tumor biopsies and relationship to estrogen receptor and progestin receptor levels. *Cancer Research* **44:** 3448-3453

Fitzpatrick SL, LaChance MP, Schultz GS (1984b) Characterization of epidermal growth factor receptor and action on human breast cancer cells in culture. *Cancer Research* **44:** 3442-3447

Fontana A, Spolaore B, Mero A, Veronese FM (2007) Site-specific modification and PEGylation of pharmaceutical proteins mediated by transglutaminase. *Advanced Drug Delivery Reviews* **60:** 13-28

Freitas TV, Frezard F (1997) Encapsulation of native crotoxin in liposomes: a safe approach for the production of antivenom and vaccination against *Crotalus durissus terrificus* venom. *Toxicon* **35:** 91-100

Ghomashchi F, Lin Y, Hixon MS, Yu BZ, Annand R, Jain MK, Gelb MH (1998) Interfacial recognition by bee venom phospholipase A_2: insights into nonelectrostatic molecular determinants by charge reversal mutagenesis. *Biochemistry* **37:** 6697-6710

Gilbert HRP. (2007) Bioresponsive Polymer-Protein Conjugates as a Unimolecular Drug Delivery System. PhD thesis, Cardiff University (Cardiff, UK)

Gilbert HRP, Vicent MJ, Duncan R (2005) Polymer-Protein Conjugates : Optimising Design For Triggered Activation. *Proceedings of the 32nd Annual Meeting of the Controlled Release Society* (Miami, USA), 455

Gill GN, Kawamoto T, Cochet C, Le A, Sato JD, Masui H, McLeod C, Mendelsohn J (1984) Monoclonal anti-epidermal growth factor receptor antibodies which are inhibitors of epidermal growth factor binding and antagonists of epidermal growth factor binding and antagonists of epidermal growth factor-stimulated tyrosine

protein kinase activity. *Journal of Biological Chemistry* **259:** 7755-7760

Giorgi R, Bernardi MM, Cury Y (1993) Analgesic effect evoked by low molecular weight substances extracted from *Crotalus durissus terrificus* venom. *Toxicon* **31:** 1257-1265

Godbey WT, Wu KK, Mikos AG (1999) Tracking the intracellular path of poly(ethylenimine)/DNA complexes for gene delivery. *Proceedings of the National Academy of Sciences of the United States of America* **96:** 5177-5181

Goldberg HJ, Viegas MM, Margolis BL, Schlessinger J, Skorecki KL (1990) The tyrosine kinase activity of the epidermal-growth-factor receptor is necessary for phospholipase A_2 activation. *The Biochemical Journal* **267:** 461-465

Goldkorn T, Balaban N, Shannon M, Matsukuma K (1997) EGF receptor phosphorylation is affected by ionizing radiation. *Biochimica et Biophysica Acta* **1358:** 289-299

Goldman R, Facchinetti T, Bach D, Raz A, Shinitzky M (1978) A differential interaction of daunomycin, adriamycin and their derivatives with human erythrocytes and phospholipid bilayers. *Biochimica et Biophysica Acta* **512:** 254-269

Good MJ, Hage WJ, Mummery CL, De Laat SW, Boonstra J (1992) Localization and quantification of epidermal growth factor receptors on single cells by confocal laser scanning microscopy. *Journal of Histochemistry and Cytochemistry* **40:** 1353-1361

Grace M, Youngster S, Gitlin G, Sydor W, Xie L, Westreich L, Jacobs S, Brassard D, Bausch J, Bordens R (2001) Structural and biologic characterization of PEGylated recombinant IFN-alpha2b. *Journal of Interferon and Cytokine Research* **21:** 1103-1115

Graff JR, Konicek BW, Deddens JA, Chedid M, Hurst BM, Colligan B, Neubauer BL, Carter HW, Carter JH (2001) Expression of group IIa secretory phospholipase A_2 increases with prostate tumor grade. *Clinical Cancer Research* **7:** 3857-3861

Grainger DW, Reichert A, Ringsdorf H, Salesse C, Davies DE, Lloyd JB (1990) Mixed monolayers of natural and polymeric phospholipids: structural characterization by physical and enzymatic methods. *Biochimica et Biophysica Acta* **1022:** 146-154

Grant JW, Smyth TP (2004) Toward the development of a cephalosporin-based dual-release prodrug for use in ADEPT. *Journal of Organic Chemistry* **69:** 7965-7970

Greco F, Vicent MJ, Gee S, Jones AT, Gee J, Nicholson RI, Duncan R (2007) Investigating the mechanism of enhanced cytotoxicity of HPMA copolymer-Dox-

AGM in breast cancer cells. *Journal of Controlled Release* **117:** 28-39

Greco F, Vicent MJ, Penning NA, Nicholson RI, Duncan R (2005) HPMA copolymer-aminoglutethimide conjugates inhibit aromatase in MCF-7 cell lines. *Journal of Drug Targeting* **13:** 459-470

Gruenberg J (2001) The endocytic pathway: a mosaic of domains. *Nature Reviews Molecular Cell Biology* **2:** 721-730

Haag R, Kratz F (2006) Polymer therapeutics: concepts and applications. *Angewandte Chemie* **45:** 1198-1215

Hack N, Margolis B, Schlessinger J, Skorecki K (1991) Interaction of epidermal growth factor with vasoactive hormones in the regulation of phospholipase A_2. *Journal of Basic and Clinical Physiology and Pharmacology* **2:** 161-182

Hambek M, Solbach C, Schnuerch HG, Roller M, Stegmueller M, Sterner-Kock A, Kiefer J, Knecht R (2001) Tumor necrosis factor alpha sensitizes low epidermal growth factor receptor (EGFR)-expressing carcinomas for anti-EGFR therapy. *Cancer Research* **61:** 1045-1049

Hamstra DA, Rice DJ, Fahmy S, Ross BD, Rehemtulla A (1999) Enzyme/prodrug therapy for head and neck cancer using a catalytically superior cytosine deaminase. *Human Gene Therapy* **10:** 1993-2003

Han SK, Yoon ET, Scott DL, Sigler PB, Cho W (1997) Structural aspects of interfacial adsorption. A crystallographic and site-directed mutagenesis study of the phospholipase A_2 from the venom of Agkistrodon piscivorus piscivorus. *Journal of Biological Chemistry* **272:** 3573-3582

Hanley MR (1979) Conformation of the neurotoxin crotoxin complex and its subunits. *Biochemistry* **18:** 1681-1688

Harari PM, Huang SM (2004) Combining EGFR inhibitors with radiation or chemotherapy: will preclinical studies predict clinical results? *International Journal of Radiation, Oncology, Biology, Physics* **58:** 976-983

Hardwicke J, Ferguson EL, Moseley R, Stephens P, Thomas D, Duncan R Dextrin-rhEGF conjugates as bioresponsive nanomedicines for wound repair. *Nature Nanotechnology*: Submitted

Harris JM, Chess RB (2003) Effect of PEGylation on pharmaceuticals. *Nature Reviews Drug Discovery* **2:** 214-221

Harush-Frenkel O, Debotton N, Benita S, Altschuler Y (2007) Targeting of nanoparticles to the clathrin-mediated endocytic pathway. *Biochemical and Biophysical Research Communications* **353:** 26-32

Hashizume H, Baluk P, Morikawa S, McLean JW, Thurston G, Roberge S, Jain RK, McDonald DM (2000) Openings between defective endothelial cells explain tumor vessel leakiness. *American Journal Pathology* **156:** 1363-1380

Haydon DA, Taylor J (1963) The stability and properties of bimolecular lipid leaflets in aqueous solutions. *Journal of Theoretical Biology* **4:** 281-296

Heimbrook DC, Stirdivant SM, Ahern JD, Balishin NL, Patrick DR, Edwards GM, Defeo-Jones D, FitzGerald DJ, Pastan I, Oliff A (1990) Transforming growth factor alpha-Pseudomonas exotoxin fusion protein prolongs survival of nude mice bearing tumor xenografts. *Proceedings of the National Academy of Sciences of the United States of America* **87:** 4697-4701

Hershfield MS, Buckley RH, Greenberg ML, Melton AL, Schiff R, Hatem C, Kurtzberg J, Markert ML, Kobayashi RH, Kobayashi AL, *et al* (1987) Treatment of adenosine deaminase deficiency with polyethylene glycol-modified adenosine deaminase. *New England Journal of Medicine* **316:** 589-596

Hewlett LJ, Prescott AR, Watts C (1994) The coated pit and macropinocytic pathways serve distinct endosome populations. *Journal of Cell Biology* **124:** 689-703

Hortobagyi GN (1997) Anthracyclines in the treatment of cancer. An overview. *Drugs* **54 Suppl 4:** 1-7

Hreczuk-Hirst D, Chicco D, German L, Duncan R (2001a) Dextrins as potential carriers for drug targeting: tailored rates of dextrin degradation by introduction of pendant groups. *International Journal of Pharmaceutics* **230:** 57-66

Hreczuk-Hirst D, German L, Duncan R (2001b) Dextrins as Carriers for Drug Targeting: Reproducible Succinoylation as a Means to Introduce Pendant Groups. *Journal of Bioactive and Compatible Polymers* **16:** 353-365

Imai Y, Leung CK, Friesen HG, Shiu RP (1982) Epidermal growth factor receptors and effect of epidermal growth factor on growth of human breast cancer cells in long-term tissue culture. *Cancer Research* **42:** 4394-4398

Inaji H, Koyama H, Higashiyama M, Noguchi S, Yamamoto H, Ishikawa O, Omichi K, Iwanaga T, Wada A (1991) Immunohistochemical, ultrastructural and biochemical studies of an amylase-producing breast carcinoma. *Virchows Archive A: Pathological Anatomy and Histopathology* **419:** 29-33

Invitrogen Molecular Technologies (2004) Molecular Probes Vol. 2004.

Invitrogen Molecular Technologies (2006). A Guide to Fluorescent Probes and Labeling Technologies. *http://probes.invitrogen.com/handbook,* accessed on Jan 26 2006

Jaiswal JK, Andrews NW, Simon SM (2002) Membrane proximal lysosomes are the major vesicles responsible for calcium-dependent exocytosis in nonsecretory cells. *Journal of Cell Biology* **159:** 625-635

Janknegt R (1996) Liposomal formulations of cytotoxic drugs. *Support Care Cancer* **4:** 298-304

Jiang J, Neubauer BL, Graff JR, Chedid M, Thomas JE, Roehm NW, Zhang S, Eckert GJ, Koch MO, Eble JN, Cheng L (2002) Expression of group IIA secretory phospholipase A_2 is elevated in prostatic intraepithelial neoplasia and adenocarcinoma. *American Journal of Pathology* **160:** 667-671

Johannes L, Lamaze C (2002) Clathrin-dependent or not: is it still the question? *Traffic* **3:** 443-451

Johnson KD, Clark A, Marshall S (2002) A functional comparison of ovine and porcine trypsins. *Comparative Biochemistry and Physiology Part B* **131:** 423-431

Jones AT (2007) Macropinocytosis: searching for an endocytic identity and role in the uptake of cell penetrating peptides. *Journal of Cell and Molecular Medicine* **11:** 670-684

Jones AT, Gumbleton M, Duncan R (2003) Understanding endocytic pathways and intracellular trafficking: a prerequisite for effective design of advanced drug delivery systems. *Advanced Drug Delivery Reviews* **55:** 1353-1357

Jordan VC (2008) Tamoxifen: Catalyst for the change to targeted therapy. *European Journal of Cancer* **44:** 30-38

Jorgensen K, Davidsen J, Mouritsen OG (2002) Biophysical mechanisms of phospholipase A_2 activation and their use in liposome-based drug delivery. *FEBS Letters* **531:** 23-27

Jorgensen K, Kiebler T, Hylander I, Vermehren C (1999a) Interaction of a lipid-membrane destabilizing enzyme with PEG-liposomes. *International Journal of Pharmaceutics* **183:** 21-24

Jorgensen K, Vermehren C, Mouritsen OG (1999b) Enhancement of phospholipase A_2 catalyzed degradation of polymer grafted PEG-liposomes: effects of lipopolymer-concentration and chain-length. *Pharmaceutical Research* **16:** 1491-1493

Journe F, Dumon JC, Kheddoumi N, Fox J, Laios I, Leclercq G, Body JJ (2004) Extracellular calcium downregulates estrogen receptor alpha and increases its transcriptional activity through calcium-sensing receptor in breast cancer cells. *Bone* **35:** 479-488

Kano-Sueoka T, King DM, Fisk HA, Klug SJ (1990) Binding of epidermal growth

factor to its receptor is affected by membrane phospholipid environment. *Journal of Cell Physiology* **145:** 543-548

Kato Y, Onishi H, Machida Y (2004) N-succinyl-chitosan as a drug carrier: water-insoluble and water-soluble conjugates. *Biomaterials* **25:** 907-915

Kell B (1971) In The Enzymes, Vol. III (3rd edn). Boyer PD (ed), Academic Press (New York, USA), 250-275

Kerr DJ, Young AM, Neoptolemos JP, Sherman M, Van-Geene P, Stanley A, Ferry D, Dobbie JW, Vincke B, Gilbert J, el Eini D, Dombros N, Fountzilas G (1996) Prolonged intraperitoneal infusion of 5-fluorouracil using a novel carrier solution. *British Journal of Cancer* **74:** 2032-2035

Khayat Z, Griffiths PC, Grillo I, Heenan RK, King SM, Duncan R (2006) Characterising the size and shape of polyamidoamines in solution as a function of pH using neutron scattering and pulsed-gradient spin-echo NMR. *International Journal of Pharmaceutics* **317:** 175-186

Kingma RL, Snijder HJ, Dijkstra BW, Dekker N, Egmond MR (2002) Functional importance of calcium binding sites in outer membrane phospholipase A. *Biochimica et Biophysica Acta* **1561:** 230-237

Kini RM (2003) Excitement ahead: structure, function and mechanism of snake venom phospholipase A_2 enzymes. *Toxicon* **42:** 827-840

Kirby CJ, Gregoriadis G (1999) Liposomes. In *Encyclopedia of Controlled Drug Delivery*, Vol. 1. Mathiowitz E (ed), John Wiley & Sons, Inc. (New York, USA), 461-492

Kohn DB, Sadelain M, Glorioso JC (2003) Occurrence of leukaemia following gene therapy of X-linked SCID. *Nature Reviews Cancer* **3:** 477-488

Kollmannsberger C, Schittenhelm M, Honecker F, Tillner J, Weber D, Oechsle K, Kanz L, Bokemeyer C (2006) A phase I study of the humanized monoclonal anti-epidermal growth factor receptor (EGFR) antibody EMD 72000 (matuzumab) in combination with paclitaxel in patients with EGFR-positive advanced non-small-cell lung cancer (NSCLC). *Annals of Oncology* **17:** 1007-1013

Kopecek J (1984) Controlled biodegradability of polymers- a key to drug delivery systems. *Biomaterials* **5:** 19-25

Kopecek J, Rejmanova P, Duncan R, Lloyd JB (1985a) Controlled release of drug model from N-(2-hydroxypropyl)-methacrylamide copolymers. *Annals of the New York Academy of Sciences* **446:** 93-104

Kopecek J, Rejmanova P, Strohalm J, Ulbrich K, Rihova B, Chytry V, Lloyd JB, Duncan R (1985b) Synthetic polymeric Drugs. *European patent application*

85309560.2, EP0187547

Kopecek J, Sprincl L, Lim D (1973) New types of synthetic infusion solutions. I. Investigation of the effect of solutions of some hydrophilic polymers on blood. *Journal of Biomedical Materials Research* **7:** 179-191

Kremer M, Judd J, Rifkin B, Auszmann J, Oursler MJ (1995) Estrogen modulation of osteoclast lysosomal enzyme secretion. *Journal of Cell Biochemistry* **57:** 271-279

Kudo I, Murakami M (2002) Phospholipase A_2 enzymes. *Prostaglandins and Other Lipid Mediators* **68-69:** 3-58

Kumar RR, Meenakshi A, Sivakumar N (2001) Enzyme immunoassay of human epidermal growth factor receptor (hEGFR). *Human Antibodies* **10:** 143-147

Kusakabe H, Kodama K, Kuninaka A, Yoshino H, Misono H, Soda K (1980) A new antitumor enzyme, L-lysine alpha-oxidase from *Trichoderma viride*. Purification and enzymological properties. *Journal of Biological Chemistry* **255:** 976-981

Kwon YB, Ham TW, Kim HW, Roh DH, Yoon SY, Han HJ, Yang IS, Kim KW, Beitz AJ, Lee JH (2005) Water soluble fraction (<10 kDa) from bee venom reduces visceral pain behavior through spinal alpha 2-adrenergic activity in mice. *Pharmacology Biochemistry and Behavior* **80:** 181-187

Laemmli UK (1970) Cleavage of structural proteins during the assembly of the head of bacteriophage T4. *Nature* **227:** 680-685

Laigle A, Fiallo MM, Garnier-Suillerot A (1996) Spectral shape modifications of anthracyclines bound to cell nuclei: a microspectrofluorometric study. *Chemico-Biological Interactions* **101:** 49-58

Lambeau G, Ancian P, Nicolas JP, Beiboer SH, Moinier D, Verheij H, Lazdunski M (1995) Structural elements of secretory phospholipases A_2 involved in the binding to M-type receptors. *Journal of Biological Chemistry* **270:** 5534-5540

Lambeau G, Lazdunski M (1999) Receptors for a growing family of secreted phospholipases A_2. *Trends in Pharmacological Sciences* **20:** 162-170

Lanz E, Gregor M, Slavik J, Kotyk A (1997) Use of FITC as a Fluorescent Probe for Intracellular pH Measurement. *Journal of Fluorescence* **7:** 1573-4994

Lavignac N, Lazenby M, Franchini J, Ferruti P, Duncan R (2005) Synthesis and preliminary evaluation of poly(amidoamine)-melittin conjugates as endosomolytic polymers and/or potential anticancer therapeutics. *International Journal of Pharmaceutics* **300:** 102-112

Lawal OS (2004) Succinyl and acetyl starch derivatives of a hybrid maize:

physicochemical characteristics and retrogradation properties monitored by differential scanning calorimetry. *Carbohydrate Research* **339:** 2673-2682

Lay AJ, Jiang XM, Kisker O, Flynn E, Underwood A, Condron R, Hogg PJ (2000) Phosphoglycerate kinase acts in tumour angiogenesis as a disulphide reductase. *Nature* **408:** 869-873

Lee C, Park DW, Lee J, Lee TI, Kim YJ, Lee YS, Baek SH (2006) Secretory phospholipase A_2 induces apoptosis through TNF-alpha and cytochrome c-mediated caspase cascade in murine macrophage RAW 264.7 cells. *European Journal of Pharmacology* **536:** 47-53

Lehtonen JY, Kinnunen PK (1995) Phospholipase A_2 as a mechanosensor. *Biophysical Journal* **68:** 1888-94

Lin WW, Chang PL, Lee CY, Joubert FJ (1987) Pharmacological study on phospholipases A_2 isolated from *Naja mossambica mossambica* venom. *Proceedings of the National Science Council, Republic of China Part B, Life Sciences* **11:** 155-163

Linderoth L, Andresen TL, Jorgensen K, Madsen R, Peters GH (2008) Molecular basis of phospholipase A_2 activity toward phospholipids with sn-1 substitutions. *Biophysical Journal* **94:** 14-26

Linderoth L, Peters GH, Jorgensen K, Madsen R, Andresen TL (2007) Synthesis of sn-1 functionalized phospholipids as substrates for secretory phospholipase A_2. *Chemistry and Physics of Lipids* **146:** 54-66

Line BR, Mitra A, Nan A, Ghandehari H (2005) Targeting tumor angiogenesis: comparison of peptide and polymer-peptide conjugates. *Journal of Nuclear Medicine* **46:** 1552-1560

LiPlasome Pharma A/S (2008) LiPlasome. (Lyngby, Denmark) *http://liplasome.com,* accessed on Jan 14 2008

Liu FT, Kelsey SM, Newland AC, Jia L (2002) Liposomal encapsulation diminishes daunorubicin-induced generation of reactive oxygen species, depletion of ATP and necrotic cell death in human leukaemic cells. *British Journal of Haematology* **117:** 333-342

Livneh E, Benveniste M, Prywes R, Felder S, Kam Z, Schlessinger J (1986) Large deletions in the cytoplasmic kinase domain of the epidermal growth factor receptor do not affect its laternal mobility. *Journal of Cell Biology* **103:** 327-331

Lostumbo A, Mehta D, Setty S, Nunez R (2006) Flow cytometry: a new approach for the molecular profiling of breast cancer. *Experimental and Molecular Pathology* **80:** 46-53

Luzio JP, Mullock BM, Pryor PR, Lindsay MR, James DE, Piper RC (2001) Relationship between endosomes and lysosomes. *Biochemical Society Transactions* **29:** 476-480

Maeda H, Matsumura Y (1989) Tumoritropic and lymphotropic principles of macromolecular drugs. *Critical Reviews in Therapeutic Drug Carrier Systems* **6:** 193-210

Maeda H, Oda T, Matsumura Y, Kimura M (1988) Improvement of pharmacological properties of protein-drugs by tailoring with synthetic polymers. *Journal of Bioactive and Compatible Polymers* **3:** 27-43

Magalhaes T, Viotti AP, Gomes RT, de Freitas TV (2001) Effect of membrane composition and of co-encapsulation of immunostimulants in a liposome-entrapped crotoxin. *Biotechnology and Applied Biochemistry* **33:** 61-64

Magne N, Fischel JL, Dubreuil A, Formento P, Poupon MF, Laurent-Puig P, Milano G (2002) Influence of epidermal growth factor receptor (EGFR), p53 and intrinsic MAP kinase pathway status of tumour cells on the antiproliferative effect of ZD1839 ("Iressa"). *British Journal of Cancer* **86:** 1518-1523

Maity G, Mandal S, Chatterjee A, Bhattacharyya D (2007) Purification and characterization of a low molecular weight multifunctional cytotoxic phospholipase A_2 from Russell's viper venom. *Journal of Chromatography B* **845:** 232-243

Malamud D, Drysdale JW (1978) Isoelectric Points of Proteins. *Analytical Biochemistry* **86:** 620-647

Margolis BL, Holub BJ, Troyer DA, Skorecki KL (1988) Epidermal growth factor stimulates phospholipase A2 in vasopressin-treated rat glomerular mesangial cells. *Biochemical Journal* **256:** 469-474

Marinetti GV (1965) The action of phospholipase A on lipoproteins. *Biochimica et Biophysica Acta* **98:** 554-565

Martikainen P, Nyman K, Nevalainen TJ (1993) Toxic effects of human pancreatic and snake and bee venom phospholipases A_2 on MCF-7 cells in culture. *Toxicon* **31:** 835-843

Masood R, Lee MJ, Espina BM, Adler-Moore JP, Gill PS (1996) Liposomal daunorubicin (DaunoXome) has enhanced cytotoxicity in an AIDS-related Kaposi's sarcoma cell line. *Proceedings of the 11th International Conference on AIDS* (Vancouver, Canada), 99

Mathur RS, Mathur SP, Young RC (2000) Up-regulation of epidermal growth factor-receptors (EGF-R) by nicotine in cervical cancer cell lines: this effect may be mediated by EGF. *American Journal of Reproductive Immunology* **44:** 114-120

Matsumura Y, Maeda H (1986) A new concept for macromolecular therapeutics in cancer chemotherapy: mechanism of tumoritropic accumulation of proteins and the antitumor agent SMANCS. *Cancer Research* **46:** 6387-92

Maxfield FR, McGraw TE (2004) Endocytic recycling. *Nature Reviews Molecular Cell Biology* **5:** 121-132

Melamed MR, Mullaney PF, Shapiro HM (1990) An Historical Review of the Development of Flow Cytometers and Sorters. In *Flow Cytometry and Sorting*, Melamed MR, Lindmo T, Mendelsohn ML (eds), 2nd edn. Wiley-Liss, Inc. (New York, USA) 1-9

Mero A, Pasut G, Dalla Via L, Fijten MW, Schubert US, Hoogenboom R, Veronese FM (2008) Synthesis and characterization of poly(2-ethyl 2-oxazoline)-conjugates with proteins and drugs: suitable alternatives to PEG-conjugates? *Journal of Controlled Release* **125:** 87-95

McArdle CS, Kerr DJ, O'Gorman P, Wotherspoon HA, Warren H, Watson D, Vinke BJ, Dobbie JW, el Eini DI (1994) Pharmacokinetic study of 5-fluorouracil in a novel dialysate solution: a long-term intraperitoneal treatment approach for advanced colorectal carcinoma. *British Journal of Cancer* **70:** 762-766

McDonald DM, Foss AJ (2000) Endothelial cells of tumor vessels: abnormal but not absent. *Cancer and Metastasis Reviews* **19:** 109-120

Mills IG, Jones AT, Clague MJ (1999) Regulation of endosome fusion. *Molecular Membrane Biology* **16:** 73-79

Mitra A, Nan A, Papadimitriou JC, Ghandehari H, Line BR (2006) Polymer-peptide conjugates for angiogenesis targeted tumor radiotherapy. *Nuclear Medicine and Biology* **33:** 43-52

Miyasaki K (1975) Experimental polymer storage disease in rabbits. An approach to the histogenesis of sphingolipidoses. *Virchows Archive A: Pathological Anatomy and Histology* **365:** 351-365

Mlcochova P, Bystricky S, Steiner B, Machova E, Koos M, Velebny V, Krcmar M (2006) Synthesis and characterization of new biodegradable hyaluronan alkyl derivatives. *Biopolymers* **82:** 74-79

Mokrasch LC (1967) Use of 2.4.6-trinitrobenzenesulfonic acid for the coestimation of amines, amino acids and proteins in mixtures. *Analytical Biochemistry* **18:** 64-71

Monteggia E, Colombo I, Guerra A, Berra B (2000) Phospholipid distribution in murine mammary adenocarcinomas induced by activated neu oncogene. *Cancer Detection and Prevention* **24:** 207-211

Moore A (2007) Breast-cancer therapy--looking back to the future. *New England Journal of Medicine* **357:** 1547-1549

Mosmann T (1983) Rapid colorimetric assay for cellular growth and survival: application to proliferation and cytotoxicity assays. *Journal of Immunological Methods* **65:** 55-63

Mukherjee A, Dhadda AS, Shehata M, Chan S (2007) Lapatinib: a tyrosine kinase inhibitor with a clinical role in breast cancer. *Expert Opinion in Pharmacotherapy* **8:** 2189-2204

Murakami M, Kudo I (2002) Phospholipase A_2. *Journal of Biochemistry* **131:** 285-292

Murakami M, Kudo I (2004) Secretory phospholipase A_2. *Biological and Pharmaceutical Bulletin* **27:** 1158-1164

Mustonen P, Kinnunen PK (1991) Activation of phospholipase A_2 by adriamycin *in vitro*. Role of drug-lipid interactions. *The Journal of Biological Chemistry* **266:** 6302-6307

Nan A, Ghandehari H, Hebert C, Siavash H, Nikitakis N, Reynolds M, Sauk JJ (2005) Water-soluble polymers for targeted drug delivery to human squamous carcinoma of head and neck. *Journal of Drug Targeting* **13:** 189-197

National Cancer Institute (2005) Dictionary of Cancer Terms. *http://www.cancer.gov/dictionary*, accessed Oct 30 2005

Nemunaitis J, Cunningham C, Senzer N, Gray M, Oldham F, Pippen J, Mennel R, Eisenfeld A (2005) Phase I study of CT-2103, a polymer-conjugated paclitaxel, and carboplatin in patients with advanced solid tumors. *Cancer Investigation* **23:** 671-676

Newman RA, Yu YH, Xu FJ, Thomton A, Bast RC, Von Hoff DD, Vidal JC, AEtcheverry MA (1996) Cellular pharmacology and cytotoxicity of crotoxin, a phospholipase A_2 toxin, against human breast, colon and ovarian cancer cell lines. *Proceedings of the American Association for Cancer Research* Vol. 37, 393

Nichols B (2003) Caveosomes and endocytosis of lipid rafts. *Journal of Cell Science* **116:** 4707-4714

Nicolas JP, Lin Y, Lambeau G, Ghomashchi F, Lazdunski M, Gelb MH (1997) Localization of structural elements of bee venom phospholipase A_2 involved in N-type receptor binding and neurotoxicity. *The Journal of Biological Chemistry* **272:** 7173-7181

North AJ (2006) Seeing is believing? A beginners' guide to practical pitfalls in image

acquisition. *Journal of Cell Biology* **172:** 9-18

Nyati MK, Morgan MA, Feng FY, Lawrence TS (2006) Integration of EGFR inhibitors with radiochemotherapy. *Nature Reviews Cancer* **6:** 876-885

Office for National Statistics (2004) National Statistics: Cancer. *http://www.statistics.gov.uk*, accessed Sep 30 2004

Oliveira S, van Bergen en Henegouwen PM, Storm G, Schiffelers RM (2006) Molecular biology of epidermal growth factor receptor inhibition for cancer therapy. *Expert Opinion in Biological Therapy* **6:** 605-617

Op den Kamp JA, de Gier J, van Deenen LL (1974) Hydrolysis of phosphatidylcholine liposomes by pancreatic phospholipase A_2 at the transition temperature. *Biochimica et Biophysica Acta* **345:** 253-256

Oupicky D, Konak C, Ulbrich K, Wolfert MA, Seymour LW (2000) DNA delivery systems based on complexes of DNA with synthetic polycations and their copolymers. *Journal of Controlled Release* **65:** 149-171

Oupicky D, Ulbrich K (1999) Conjugates of Semitelechelic Poly[N-2-hydroxypropyl)methacrylamide] with Enzymes for Protein Delivery. *Journal of Bioactive and Compatible Polymers* **14:** 213-231

Pan H, Kopeckova P, Wang D, Yang J, Miller S, Kopecek J (2006) Water-soluble HPMA copolymer--prostaglandin E1 conjugates containing a cathepsin K sensitive spacer. *Journal of Drug Targeting* **14:** 425-435

Pasut G, Sergi M, Veronese FM (2008) Anti-cancer PEG-enzymes: 30 years old, but still a current approach. *Advanced Drug Delivery Reviews* **60:** 69-78

Paul A, Vicent MJ, Duncan R (2007) Using small-angle neutron scattering to study the solution conformation of N-(2-hydroxypropyl)methacrylamide copolymer-doxorubicin conjugates. *Biomacromolecules* **8:** 1573-1579

Pearson H (2007) The good, the bad and the ugly. *Nature* **447:** 138-140

Peers E, Gokal R (1998) Icodextrin provides long dwell peritoneal dialysis and maintenance of intraperitoneal volume. *Artificial Organs* **22:** 8-12

Peters AR, Dekker N, van den Berg L, Boelens R, Kaptein R, Slotboom AJ, de Haas GH (1992) Conformational changes in phospholipase A_2 upon binding to micellar interfaces in the absence and presence of competitive inhibitors. A ^{1}H and ^{15}N NMR study. *Biochemistry* **31:** 10024-10030

Peters GH, Moller MS, Jorgensen K, Ronnholm P, Mikkelsen M, Andresen TL (2007) Secretory phospholipase A_2 hydrolysis of phospholipid analogues is dependent on water accessibility to the active site. *Journal of the American*

Chemical Society **129:** 5451-5461

Pierce Chemical Technical Library (2002) Assays: protein. Pierce Chemical Technical Library (Rockford, USA)

Pimm MV, Perkins AC, Duncan R, Ulbrich K (1993) Targeting of N-(2-hydroxypropyl)methacrylamide copolymer-doxorubicin conjugate to the hepatocyte galactose-receptor in mice: visualisation and quantification by gamma scintigraphy as a basis for clinical targeting studies. *Journal of Drug Targeting* **1:** 125-131

Plummer DT (1978) *An Introduction to Practical Biochemistry* (2nd edn). McGraw-Hill Book Company Limited (London, UK)

Pouckova P, Zadinova M, Hlouskova D, Strohalm J, Plocova D, Spunda M, Olejar T, Zitko M, Matousek J, Ulbrich K, Soucek J (2004) Polymer-conjugated bovine pancreatic and seminal ribonucleases inhibit growth of human tumors in nude mice. *Journal of Controlled Release* **95:** 83-92

Pu XC, Wong PT, Gopalakrishnakone P (1995) A novel analgesic toxin (hannalgesin) from the venom of king cobra (*Ophiophagus hannah*). *Toxicon* **33:** 1425-1431

Puijk WC, Verheij HM, De Haas GH (1977) The primary structure of phospholipase A_2 from porcine pancreas. A reinvestigation. *Biochimica et Biophysica Acta* **492:** 254-259

Punnonen K, Hietanen E, Auvinen O, Punnonen R (1989) Phospholipids and fatty acids in breast cancer tissue. *Journal of Cancer Research and Clinical Oncology* **115:** 575-578

Ramanathan M (1997) Flow cytometry applications in pharmacodynamics and drug delivery. *Pharmaceutical Research* **14:** 1106-1114

Ramirez HL, Valdivia A, Cao R, Torres-Labandeira JJ, Fragoso A, Villalonga R (2006) Cyclodextrin-grafted polysaccharides as supramolecular carrier systems for naproxen. *Bioorganic and Medicinal Chemistry Letters* **16:** 1499-1501

Ramon J, Saez V, Baez R, Aldana R, Hardy E (2005) PEGylated interferon-alpha2b: a branched 40K polyethylene glycol derivative. *Pharmaceutical Research* **22:** 1374-1386

Reddy A, Caler EV, Andrews NW (2001) Plasma membrane repair is mediated by $Ca^{(2+)}$-regulated exocytosis of lysosomes. *Cell* **106:** 157-169

Reddy LH (2005) Drug delivery to tumours: recent strategies. *Journal of Pharmacy and Pharmacology* **57:** 1231-1242

Reynolds LJ, Washburn WN, Deems RA, Dennis EA (1991) Assay strategies and methods for phospholipases. *Methods in Enzymology* **197:** 3-23

Richardson SCW, Wallom K-L, Ferguson EL, Deacon SP, Davies MW, Powell AJ, Piper RC, Duncan R (2008) The use of fluorescence microscopy to define polymer conjugate localisation to late endocytic compartments in fixed and live target cells *Journal of Controlled Release*: In Press

Ringsdorf H (1975) Structure and properties of pharmacologically active polymers. *Journal of Polymer Science- Polymer Symposia* **51:** 135-153

Roberts MJ, Bentley MD, Harris JM (2002) Chemistry for peptide and protein PEGylation. *Advanced Drug Delivery Reviews* **54:** 459-476

Rodeck U, Melber K, Kath R, Menssen HD, Varello M, Atkinson B, Herlyn M (1991) Constitutive expression of multiple growth factor genes by melanoma cells but not normal melanocytes. *Journal of Investigational Dermatology* **97:** 20-26

Romond EH, Perez EA, Bryant J, Suman VJ, Geyer CE, Jr., Davidson NE, Tan-Chiu E, Martino S, Paik S, Kaufman PA, Swain SM, Pisansky TM, Fehrenbacher L, Kutteh LA, Vogel VG, Visscher DW, Yothers G, Jenkins RB, Brown AM, Dakhil SR, Mamounas EP, Lingle WL, Klein PM, Ingle JN, Wolmark N (2005) Trastuzumab plus adjuvant chemotherapy for operable HER2-positive breast cancer. *New England Journal of Medicine* **353:** 1673-1684

Rosenberg P (1990) Phospholipases. In *Handbook of Toxinology*. Shier WT, Mebs D (eds), CRC Press (Boca Raton, USA), 88

Rosenthal E, Poizot-Martin I, Saint-Marc T, Spano JP, Cacoub P (2002) Phase IV study of liposomal daunorubicin (DaunoXome) in AIDS-related Kaposi sarcoma. *American Journal of Clinical Oncology* **25:** 57-59

Rowinsky EK, Schwartz GH, Gollob JA, Thompson JA, Vogelzang NJ, Figlin R, Bukowski R, Haas N, Lockbaum P, Li YP, Arends R, Foon KA, Schwab G, Dutcher J (2004) Safety, pharmacokinetics, and activity of ABX-EGF, a fully human anti-epidermal growth factor receptor monoclonal antibody in patients with metastatic renal cell cancer. *Journal of Clinical Oncology* **22:** 3003-3015

Ruiz-Arguello MB, Goni FM, Alonso A (1998) Phospholipase C hydrolysis of phospholipids in bilayers of mixed lipid compositions. *Biochemistry* **37:** 11621-11628

Rupprich C, Becker M, Buttner W, Boeden HF, Schroder KL, Hansicke A, Konnecke A (1990) Biospecific adsorbents on the basis of chloroformate-activated bead cellulose. *Biomaterials, Artificial Cells, and Artificial Organs* **18:** 665-670

Samoshina NM, Samoshin VV (2005) The Michaelis constants ratio for two

substrates with a series of fungal (mould and yeast) beta-galactosidases. *Enzyme and Microbial Technology* **36:** 239-251

Satchi R. (1999) PDEPT: Polymer Directed Enzyme Prodrug Therapy. PhD thesis, University of London (London, UK)

Satchi R, Connors TA, Duncan R (2001) PDEPT: polymer-directed enzyme prodrug therapy. I. HPMA copolymer-cathepsin B and PK1 as a model combination. *British Journal of Cancer* **85:** 1070-1076

Satchi-Fainaro R, Duncan R (2008) PELT: Polymer enzyme liposome therapy. HPMA copolymer-phospholipase C and Doxil/ Daunoxomes as a novel combination. Unpublished

Satchi-Fainaro R, Hailu H, Davies JW, Summerford C, Duncan R (2003) PDEPT: polymer-directed enzyme prodrug therapy. 2. HPMA copolymer-beta-lactamase and HPMA copolymer-C-Dox as a model combination. *Bioconjugate Chemistry* **14:** 797-804

Satchi-Fainaro R, Wrasidlo W, Lode HN, Shabat D (2002) Synthesis and characterization of a catalytic antibody-HPMA copolymer-Conjugate as a tool for tumor selective prodrug activation. *Bioorganic and Medicinal Chemistry* **10:** 3023-3029

Sato H (2002) Enzymatic procedure for site-specific PEGylation of proteins. *Advanced Drug Delivery Reviews* **54:** 487-504

Sato JD, Kawamoto T, Le AD, Mendelsohn J, Polikoff J, Sato GH (1983) Biological effects in vitro of monoclonal antibodies to human epidermal growth factor receptors. *Molecular Biology and Medicine* **1:** 511-529

Schacht E, Vandoorne F, Vermeersch J, Duncan R (1987) Polysaccharides as drug carriers- Activation procedures and biodegradation studies. *American Chemical Society Symposium Series* **348:** 188-200

Scott DL, White SP, Otwinowski Z, Yuan W, Gelb MH, Sigler PB (1990) Interfacial catalysis: the mechanism of phospholipase A_2. *Science* **250:** 1541-1546

Seib FP, Jones AT, Duncan R (2007) Comparison of the endocytic properties of linear and branched PEIs, and cationic PAMAM dendrimers in B16F10 melanoma cells. *Journal of Controlled Release* **117:** 291-300

Seymour LW, Ferry DR, Anderson D, Hesslewood S, Julyan PJ, Poyner R, Doran J, Young AM, Burtles S, Kerr DJ (2002) Hepatic drug targeting: phase I evaluation of polymer-bound doxorubicin. *Journal of Clinical Oncology* **20:** 1668-1676

Sgouras D, Duncan R (1990) Methods for the evaluation of biocompatibility of soluble synthetic polymers which have potential for biomedical use: 1 — Use of

the tetrazolium-based colorimetric assay (MTT) as a preliminary screen for evaluation of *in vitro* cytotoxicity. *Journal of Materials Science: Materials in Medicine* **1:** 61-68

Shipolini RA, Callewaert GL, Cottrell RC, Doonan S, Vernon CA, Banks BE (1971) Phospholipase A from bee venom. *European Journal of Biochemistry* **20:** 459-468

Shipolini RA, Doonan S, Vernon CA (1974) The disulphide bridges of phospholipase A_2 from bee venom. *European Journal of Biochemistry* **48:** 477-483

Shukla R, Thomas TP, Peters JL, Desai AM, Kukowska-Latallo J, Patri AK, Kotlyar A, Baker JR, Jr. (2006) HER2 specific tumor targeting with dendrimer conjugated anti-HER2 mAb. *Bioconjugate Chemistry* **17:** 1109-1115

Sigismund S, Woelk T, Puri C, Maspero E, Tacchetti C, Transidico P, Di Fiore PP, Polo S (2005) Clathrin-independent endocytosis of ubiquitinated cargos. *Proceedings of the National Academy of Sciences of the United States of America* **102:** 2760-2765

Singer JW, Baker B, De Vries P, Kumar A, Shaffer S, Vawter E, Bolton M, Garzone P (2003) Poly-(L)-glutamic acid-paclitaxel (CT-2103) [XYOTAX], a biodegradable polymeric drug conjugate: characterization, preclinical pharmacology, and preliminary clinical data. *Advances in Experimental Medicine and Biology* **519:** 81-99

Sirova M, Strohalm J, Subr V, Plocova D, Rossmann P, Mrkvan T, Ulbrich K, Rihova B (2007) Treatment with HPMA copolymer-based doxorubicin conjugate containing human immunoglobulin induces long-lasting systemic anti-tumour immunity in mice. *Cancer Immunology, Immunotherapy* **56:** 35-47

Six DA, Dennis EA (2000) The expanding superfamily of phospholipase $A_{(2)}$ enzymes: classification and characterization. *Biochimica et Biophysica Acta* **1488:** 1-19

Sky-Peck HH, Thuvasethakul P (1977) Human pancreatic alpha-amylase. II. Effects of pH, substrate and ions on the activity of the enzyme. *Annals of Clinical and Laboratory Science* **7:** 310-317

Smith J (2005) Erlotinib: small-molecule targeted therapy in the treatment of non-small-cell lung cancer. *Clinical Therapeutics* **27:** 1513-1534

Smith PK, Krohn RI, Hermanson GT, Mallia AK, Gartner FH, Provenzano MD, Fujimoto EK, Goeke NM, Olson BJ, Klenk DC (1985) Measurement of protein using bicinchoninic acid. *Analytical Biochemistry* **150:** 76-85

Sorkin A (2000) The endocytosis machinery. *Journal of Cell Science* **113 Pt 24:**

4375-4376

Sorkina T, Huang F, Beguinot L, Sorkin A (2002) Effect of tyrosine kinase inhibitors on clathrin-coated pit recruitment and internalization of epidermal growth factor receptor. *The Journal of Biological Chemistry* **277:** 27433-27441

Speijer H, Giesen PL, Zwaal RF, Hack CE, Hermens WT (1996) Critical micelle concentrations and stirring are rate limiting in the loss of lipid mass during membrane degradation by phospholipase A_2. *Biophysical Journal* **70:** 2239-2247

Steinhardt RA, Bi G, Alderton JM (1994) Cell membrane resealing by a vesicular mechanism similar to neurotransmitter release. *Science* **263:** 390-393

Sterin M, Cohen JS, Ringel I (2004) Hormone sensitivity is reflected in the phospholipid profiles of breast cancer cell lines. *Breast Cancer Research and Treatment* **87:** 1-11

Swift L, McHowat J, Sarvazyan N (2003) Inhibition of membrane-associated calcium-independent phospholipase A_2 as a potential culprit of anthracycline cardiotoxicity. *Cancer Research* **63:** 5992-5998

Swift L, McHowat J, Sarvazyan N (2007) Anthracycline-induced phospholipase A_2 inhibition. *Cardiovascular Toxicology* **7:** 86-91

Syrigos KN, Rowlinson-Busza G, Epenetos AA (1998) *In vitro* cytotoxicity following specific activation of amygdalin by beta-glucosidase conjugated to a bladder cancer-associated monoclonal antibody. *International Journal of Cancer* **78:** 712-719

Talsma H. (1991) Preparation, Characterisation and Stabilization of Liposomes. Utrecht University (Utrecht, Netherlands)

Tesauro D, Accardo A, Gianolio E, Paduano L, Teixeira J, Schillen K, Aime S, Morelli G (2007) Peptide derivatized lamellar aggregates as target-specific MRI contrast agents. *Chembiochem* **8:** 950-955

Thornton M, Barkley L, Mason JC, Shaunak S (1999) Anti-Kaposi's sarcoma and antiangiogenic activities of sulfated dextrins. *Antimicrobial Agents and Chemotherapy* **43:** 2528-2533

Torchilin VP (2005) Recent advances with liposomes as pharmaceutical carriers. *Nature Reviews Drug Discovery* **4:** 145-160

Torchilin VP, Voronkov JI, Mazoev AV (1982) The use of immobilised streptokinase (Streptodekaza) for the therapy of thromboses. *Therapeutic Archives Russia* **54:** 21-25

Treetharnmathurot B, Ovartlarnporn C, Wungsintaweekul J, Duncan R,

Wiwattanapatapee R (2008) Effect of PEG molecular weight and linking chemistry on the biological activity and thermal stability of PEGylated trypsin. *International Journal of Pharmaceutics*: In Press

Treetharnmathurot B, Ferguson EL, Dieudonné L, Schmaljohann D, Wiwattanapatapee R, Duncan R. (2008) Dextrin-RNase A and ST-HPMA-RNase A Conjugates: Effect of polymer on anti-tumor activity. For *International Journal of Pharmaceutics*: in preparation

Tribler L, Jensen LT, Jorgensen K, Brunner N, Gelb MH, Nielsen HJ, Jensen SS (2007) Increased expression and activity of group IIA and X secretory phospholipase A_2 in peritumoral versus central colon carcinoma tissue. *Anti-cancer Research* **27:** 3179-3185

Ulbrich K, Etrych T, Chytil P, Jelinkova M, Rihova B (2003) HPMA copolymers with pH-controlled release of doxorubicin: in vitro cytotoxicity and in vivo antitumor activity. *Journal of Controlled Release* **87:** 33-47

Urade R, Hayashi Y, Kito M (1988) Endosomes differ from plasma membranes in the phospholipid molecular species composition. *Biochimica et Biophysica Acta* **946:** 151-163

Valentin E, Lambeau G (2000) Increasing molecular diversity of secreted phospholipases $A_{(2)}$ and their receptors and binding proteins. *Biochimica et Biophysica Acta* **1488:** 59-70

van den Berg B, Tessari M, Boelens R, Dijkman R, de Haas GH, Kaptein R, Verheij HM (1995) NMR structures of phospholipase A_2 reveal conformational changes during interfacial activation. *Nature Structural Biology* **2:** 402-406

van der Aa MA, Huth US, Hafele SY, Schubert R, Oosting RS, Mastrobattista E, Hennink WE, Peschka-Suss R, Koning GA, Crommelin DJ (2007) Cellular Uptake of Cationic Polymer-DNA Complexes Via Caveolae Plays a Pivotal Role in Gene Transfection in COS-7 Cells. *Pharmaceutical Research* **24:** 1590-1598

Van Winden E. Freeze-drying of Liposomes. Utrecht University, Utrecht, 1996

Vasey PA, Kaye SB, Morrison R, Twelves C, Wilson P, Duncan R, Thomson AH, Murray LS, Hilditch TE, Murray T, Burtles S, Fraier D, Frigerio E, Cassidy J (1999) Phase I clinical and pharmacokinetic study of PK1 [N-(2-hydroxypropyl)methacrylamide copolymer doxorubicin]: first member of a new class of chemotherapeutic agents-drug-polymer conjugates. Cancer Research Campaign Phase I/II Committee. *Clinical Cancer Research* **5:** 83-94

Ventech Research Inc. (1995) Overview of Crotoxin, a new anticancer agent. Ventech Research Inc. (Cambridge, USA)

Vercauteren R, Bruneel D, Schacht E, Duncan R (1990) Effect of the chemical

modification of dextran on the degradation by dextranase. *Journal of Bioactive and Compatible Polymers* **5:** 346-357

Vercauteren R, Schacht E, Duncan R (1992) Effect of the chemical modification of dextran on the degradation by rat liver lysosomal enzymes. *Journal of Bioactive and Compatible Polymers* **5:** 4-15

Vicent MJ, Manzanaro S, de la Fuente JA, Duncan R (2004) HPMA copolymer-1,5-diazaanthraquinone conjugates as novel anticancer therapeutics. *Journal of Drug Targeting* **12:** 503-515

Villalonga ML, Fernandez M, Fragoso A, Cao R, Villalonga R (2003a) Functional stabilization of trypsin by conjugation with beta-cyclodextrin-modified carboxymethylcellulose. *Preparative Biochemistry and Biotechnology* **33:** 53-66

Villalonga ML, Reyes G, Fragoso A, Cao R, Fernandez L, Villalonga R (2005) Chemical glycosidation of trypsin with O-carboxymethyl-poly-beta-cyclodextrin: catalytic and stability properties. *Biotechnology and Applied Biochemistry* **41:** 217-223

Villalonga R, Fernandez M, Fragoso A, Cao R, Di Pierro P, Mariniello L, Porta R (2003b) Transglutaminase-catalyzed synthesis of trypsin-cyclodextrin conjugates: kinetics and stability properties. *Biotechnology and Bioengineering* **81:** 732-737

Villalonga R, Fernandez M, Fragoso A, Cao R, Mariniello L, Porta R (2003c) Thermal stabilization of trypsin by enzymic modification with beta-cyclodextrin derivatives. *Biotechnology and Applied Biochemistry* **38:** 53-59

Wallom K-L. HPMA copolymer-mannose conjugates for intracellular delivery of anti-leishmanial compounds to macrophages. PhD thesis, Cardiff University, Cardiff, UK, 2008

Watala C, Kowalczyk JK (1990) Hemolytic potency and phospholipase activity of some bee and wasp venoms. *Comparative Biochemistry and Physiology* **97:** 187-194

Weedon SJ, Green NK, McNeish IA, Gilligan MG, Mautner V, Wrighton CJ, Mountain A, Young LS, Kerr DJ, Searle PF (2000) Sensitisation of human carcinoma cells to the prodrug CB1954 by adenovirus vector-mediated expression of *E. coli* nitroreductase. *International Journal of Cancer* **86:** 848-854

Weitzel JN, Pooler PA, Mohammed R, Levitt MD, Eckfeldt JH (1988) A unique case of breast carcinoma producing pancreatic-type isoamylase. *Gastroenterology* **94:** 519-520

Werle M, Bernkop-Schnurch A (2006) Strategies to improve plasma half life time of peptide and protein drugs. *Amino Acids* **30:** 351-367

West MA, Bretscher MS, Watts C (1989) Distinct endocytotic pathways in epidermal growth factor-stimulated human carcinoma A431 cells. *Journal of Cell Biology* **109:** 2731-2739

Wiegant FA, Blok FJ, Defize LH, Linnemans WA, Verkley AJ, Boonstra J (1986) Epidermal growth factor receptors associated to cytoskeletal elements of epidermoid carcinoma (A431) cells. *Journal of Cell Biology* **103:** 87-94

Wilschut JC, Regts J, Scherphof G (1979) Action of phospholipase A_2 on phospholipid vesicles. Preservation of the membrane permeability barrier during asymmetric bilayer degradation. *FEBS Letters* **98:** 181-186

Yan CH, Liang ZQ, Gu ZL, Yang YP, Reid P, Qin ZH (2006) Contributions of autophagic and apoptotic mechanisms to CrTX-induced death of K562 cells. *Toxicon* **47:** 521-530

Yan CH, Yang YP, Qin ZH, Gu ZL, Reid P, Liang ZQ (2007) Autophagy is involved in cytotoxic effects of crotoxin in human breast cancer cell line MCF-7 cells. *Acta Pharmacologica Sinica* **28:** 540-548

Yang Z, Wang J, Lu Q, Xu J, Kobayashi Y, Takakura T, Takimoto A, Yoshioka T, Lian C, Chen C, Zhang D, Zhang Y, Li S, Sun X, Tan Y, Yagi S, Frenkel EP, Hoffman RM (2004) PEGylation confers greatly extended half-life and attenuated immunogenicity to recombinant methioninase in primates. *Cancer Research* **64:** 6673-6678

Yarden Y (2001) The EGFR family and its ligands in human cancer. signaling mechanisms and therapeutic opportunities. *European Journal of Cancer* **37 Suppl 4:** S3-8

Yoo H, Juliano RL (2000) Enhanced delivery of antisense oligonucleotides with fluorophore-conjugated PAMAM dendrimers. *Nucleic Acids Research* **28:** 4225-4231

Zhang HL, Han R, Chen ZX, Chen BW, Gu ZL, Reid PF, Raymond LN, Qin ZH (2006) Opiate and acetylcholine-independent analgesic actions of crotoxin isolated from *crotalus durissus terrificus* venom. *Toxicon* **48:** 175-182

Zhao S, Du XY, Chen JS, Zhou YC, Song JG (2002) Secretory phospholipase $A_{(2)}$ inhibits epidermal growth factor-induced receptor activation. *Experimental Cell Research* **279:** 354-364

Zhu Q, Wu DC, Zhou XP, Gong S, Cheng BC, Qin ZH, Reid PF, Yin QZ, Jiang XH (2007) Inhibitory effect of crotoxin on the pain-evoked discharge of neurons in thalamic parafascicular nucleus in rats. *Toxicon* **51:** 102-111

APPENDIX I

Publications

Papers

1. Richardson, S., Wallom, K-L., **Ferguson, E.L.,** Deacon, S.P., Davies, M.W., Powell, A.J., Piper, R.C., and Duncan, R. (2008) The use of fluorescence microscopy to define polymer localisation to the late endocytic compartments in cells that are targets for drug delivery. *Journal of Controlled Release*. In Press.

2. Hardwicke, J., **Ferguson, E.L.,** Moseley, R., Stephens, P., Thomas, D. and Duncan, R. Dextrin-rhEGF conjugates as bioresponsive nanomedicines for wound repair. *Nature Nanotechnology,* submitted

3. **Ferguson, E.L.** and Duncan, R. (2008) Dextrin-phospholipase A_2 Conjugates as Novel Anticancer Agents. Journal of Controlled Release, in preparation

4. **Ferguson, E.L.** and Duncan, R. (2008) Dextrin-phospholipase A_2 Conjugates as a trigger for Polymer Enzyme Liposome Therapy (PELT).

Abstracts

1. **Ferguson, E.L.,** Schmaljohann, D. and Duncan, R., (2006). Polymer-Phospholipase Conjugates As Novel Anti-Cancer Agents: Dextrin-Phospholipase A_2. *Proceedings of 33rd Annual Meeting & Exposition of the Controlled Release Society,* **33**, # 660 ***Oral Presentation and Poster***

2. **Ferguson E.L.,** Schmaljohann D. and Duncan R., (2006). Polymer-Phospholipases as Novel Anti-Cancer Nanomedicines. *SET for Britain & Britain's Top Younger Scientists, Engineers and Technologists* (House of Commons, London), L2-30 ***Poster Presentation***

3. Duncan R., Vicent M., Greco F. and **Ferguson E.L.** (2006). Polymer Anti-Cancer Conjugates and their use in Combination Therapy. *Proceedings of 33rd Annual Meeting & Exposition of the Controlled Release Society,* **33,** # 25.

4. Duncan, R., M. J. Vicent, M.J., Greco, F., Gilbert, H.R.P., Schmaljohann, D. and

Ferguson, E.L. (2006). Novel Anticancer Polymer Conjugates Designed to Treat Hormone-Dependant Cancers and Circumvent Resistance. *Proceedings of 7th Spanish-Portugese Conference on Controlled Drug Delivery*, p6

5. **Ferguson, E.L.** and Duncan, R., (2007). Investigating the Cytotoxicity and Mechanism of Action of Dextrin-Phospholipase A_2 Conjugates as Novel Anti-Tumour Agents. *Proceedings of 34th Annual Meeting & Exposition of the Controlled Release Society,* **34**, # 100 ***Oral Presentation***

6. Ferguson, E.L., Schmaljohann, D. and Duncan, R., (2007). Dextrin-phospholipase A_2 Conjugates as Enzyme-triggered Anti-cancer Agents. *United Kingdom and Ireland Controlled Release Society's Annual Symposium,* **13, *Oral Presentation***

7. **Ferguson, E.L.,** Schmaljohann, D. and Duncan, R., (2007). Dextrin-Phospholipase A_2 Conjugates as an Enzyme-Triggered Anti-Cancer Agent: Mode of Action. *ESF Summer School in Nanomedicine,* Cardiff, UK ***Poster Presentation***

8. **Ferguson, E.L.** and Duncan, R., (2007). Investigating the Cytotoxicity and Mechanism of Action of Dextrin-Phospholipase A_2 Conjugates as Novel Anti-Tumour Agents. *Merck Academic Partnerships Symposium,* London, UK ***Poster Presentation***

9. Duncan, R., **Ferguson, E.L.**, Gilbert, H.R.P., Hardwicke, J., Schmaljohann, D., Moseley, R., Stephens, P. and Thomas, D.W. (2007). Polymer Therapeutics - Towards New Nanomedicines. *Symposium for Frontiers in Biomedical Polymers, Ghent*

10. Treetharnmathurot, B., **Ferguson, E.L.,** Dieudonné, L., Schmaljohann, D., Wiwattanapatapee, R. and Duncan, R. (2008). Effect of Polymer and its Molecular Weight on the *in vitro* Cytotoxicity of Ribonuclease Conjugates. *Proceedings of 35th Annual Meeting & Exposition of the Controlled Release Society,* submitted

11. **Ferguson, E.L.** and Duncan, R. (2008). Investigating a Dextrin-Phospholipase A_2 Conjugate as a Trigger for Polymer Enzyme Liposome Therapy (PELT). *Proceedings of the International Symposium on Polymer Therapeutics*, submitted

12. Izzo, L., Nilmini, R., Wallom, K-L., **Ferguson, E.L.,** Griffiths, P. and Duncan, R. (2008). Does Polymer Stereochemistry Effect the Physico-chemical and Biological Behaviour of Polymer Therapeutics? *Proceedings of the International Symposium on Polymer Therapeutics*, submitted

13. Hardwicke, J., **Ferguson, E.L.**, Moseley, R., Stephens, P., Thomas, D. and Duncan, R. (2008). Designing Polymer Therapeutics to Promote Tissue Repair. *Proceedings of the International Symposium on Polymer Therapeutics*, submitted

14. Treetharnmathurot, B., **Ferguson, E.L.,** Dieudonné, L., Schmaljohann, D., Wiwattanapatapee, R. and Duncan, R. (2008). Effect of Polymer and its Molecular Weight on the Thermasl Stability of Bound Protein. *Proceedings of the International Symposium on Polymer Therapeutics*, submitted